ESTABLISHING THE ENVIRONMENTAL RISK OF METAL
CONTAMINATED RIVER BANK SEDIMENTS

By

SARAH FRANCESCA LYNN LYNCH

A thesis submitted to the University of Birmingham for the degree of
DOCTOR OF PHILOSOPHY

School of Geography, Earth and Environmental Sciences

College of Life and Environmental Sciences

University of Birmingham

March 2015

ABSTRACT

Climate change predictions indicate an increase in the frequency and duration of flood events along with longer dry antecedent conditions, which could alter patterns of trace metal release from contaminated river bank sediments.

This study took a laboratory mesocosm approach. Chemical analysis of water and sediment samples allowed the patterns of Pb and Zn release and key mechanisms controlling Pb and Zn mobility to be determined.

Trace metal contaminants Pb and Zn were released throughout flooded periods. The highest concentrations of dissolved Pb were observed at the end of the longest flood period and high concentrations of dissolved Zn were released at the start of a flood. These concentrations were found to exceed environmental quality standards. Key mechanisms controlling mobility were (i) evaporation, precipitation and dissolution of Zn sulphate salts, (ii) anglesite solubility control of dissolved Pb, (iii) oxidation of galena and sphalerite, (iv) reductive dissolution of Mn/Fe hydroxides and co-precipitation/adsorption with Zn.

In light of climate change predictions these results indicate future scenarios may include larger or more frequent transient 'pulses' of dissolved Pb and Zn released to river systems. These short lived pollution episodes could act as a significant barrier to achieving the EU Water Framework Directive objectives.

DEDICATION


TO MY HUSBAND AND CHILDREN

# ACKNOWLEDGEMENTS

**TABLE OF CONTENTS**

# LIST OF ILLUSTRATIONS

# LIST OF TABLES

# 1.  INTRODUCTION

In England and Wales metal mining activities can be dated back to the Bronze
Age (Ixer and Budd, 1998) with peak extraction during the mid 19th century, when
the UK was, for a time, the world's largest producer of Cu, Sn and Pb (Lewin and
Macklin, 1987). Due to falling metal prices and the discovery of large metalliferous
deposits outside of the UK, in the early 20th Century many of these mines closed
(Byrne et al., 2010) and there are now over 3000 abandoned metal mines in the
UK. However even though active mining and dumping of waste into rivers has
ceased, mining pollution arising from impacted catchments still contributes
thousands of tonnes of trace metals to river systems annually (Environment
Agency, 2008a). Unlike the Coal Authority for coal mines, there is no national body
legally responsible for dealing with pollution from abandoned metal mines
(Environment Agency, 2008a; Johnston and Rolley, 2008), although the Coal
Authority is now assisting with the management and remediation of impacted
catchments alongside the Environment Agency funded by the Department for
Environment Food and Rural Affairs and the Welsh government funds similar work
carried out by Natural Resources Wales through the metal mines strategy for
Wales framework (Environment Agency, 2008a; Environment Agency, 2014).

A traditional approach to the management and remediation of pollution arising
from abandoned mines was to focus on point sources of pollution arising from
adits and shafts (Younger, 1998; Laine, 1999; Younger, 2000). However, there is
now greater emphasis on dealing with diffuse sources of pollution, the regulatory
driver being the EU Water Framework Directive 2000/60/EC that requires
management of water quality at a catchment scale delivered through the River

Basin Management Plans (Collins et al*., 2012). Diffuse sources of pollution can contribute high trace metal loads and acidity to rivers potentially damaging the health of ecosystems (Environment Agency, 2008a; Banks and Palumbo-Roe, 2010; Gozzard et al., 2011; Palumbo Roe et al*., 2012) with over half of the 226 water bodies known to be impacted by non-coal mine water pollution showing evidence of diffuse sources of pollution (Environment Agency, 2012a). That could serve as a significant barrier to achieving the EU Water Framework Directive's target of achieving 'good' ecological and chemical status for all surface and groundwater by 2015 (Environment Agency, 2008b).

Diffuse sources of pollution can arise from (i) the runoff and seepage from waste piles and tailings heaps (Merrington and Alloway, 1994; Macklin et al., 2006; Hofmann and Schuwirth, 2008; Lu and Wang, 2012) (ii) the remobilisation of previously deposited contaminated overbank sediment (Environment Agency 2008b ; Gozzard *et al.,* 2011) and (iii) through inputs of contaminated sub-surface water via the hyporheic zone (Gandy et al., 2007; Krause et al., 2010; Palumbo-Roe *et al.,* 2012).

## 1.1 Transport and Deposition of Contaminant Trace metals

Streams and rivers are the main routes by which contaminants are dispersed through river systems. Metal contaminants may be transported in dissolved form as free aqueous ions, metal sulphates, carbonates or hydroxides (vanLoon and Duffy, 2011) or in particulate form, partitioned with primary sulphide minerals, or sorbed to sediment particles consisting of clay, carbonates, Fe or Mn hydroxides or organics, depending on the geology and mineralogy of the site and the chemical properties of the metal (Bradley and Lewin, 1982; Merrington and

Alloway, 1994; Palumbo-Roe et al., 2009; Byrne et al., 2009). Reports indicate that under circum-neutral pH conditions over 90% of contaminants travel in particulate form and so follow the natural transport pathways of sediment loads (Macklin *et al.,* 2006).

Patterns of deposition can be complex and depend on a number of factors, for example larger grains may be deposited nearer to the active channel through gravitational sorting (Macklin and Dowsett, 1989; Matsuda, 2004) whereas finer grain sizes (< 2 mm) may travel further, sometimes tens of km downstream as suspended load (Bradley 1995, Coulthard and Macklin, 2003) and can be dispersed throughout the catchment. During severe flooding, contaminated sediment can be deposited overbank on floodplains as vertical accretion deposits (Macklin and Lewin 1989; Dennis et al., 2003; Young et al., 2007; Foulds et al., 2014).

Where flood embankments are in place, floodplain land is limited or flood magnitude is low, fine grained contaminated sediment may remain closer to the active channel as lateral accretion deposits (figure 1.1) (Wolfenden and Lewin, 1977; Environment Agency, 2008b, Hudson-Edwards et al, 1999a).
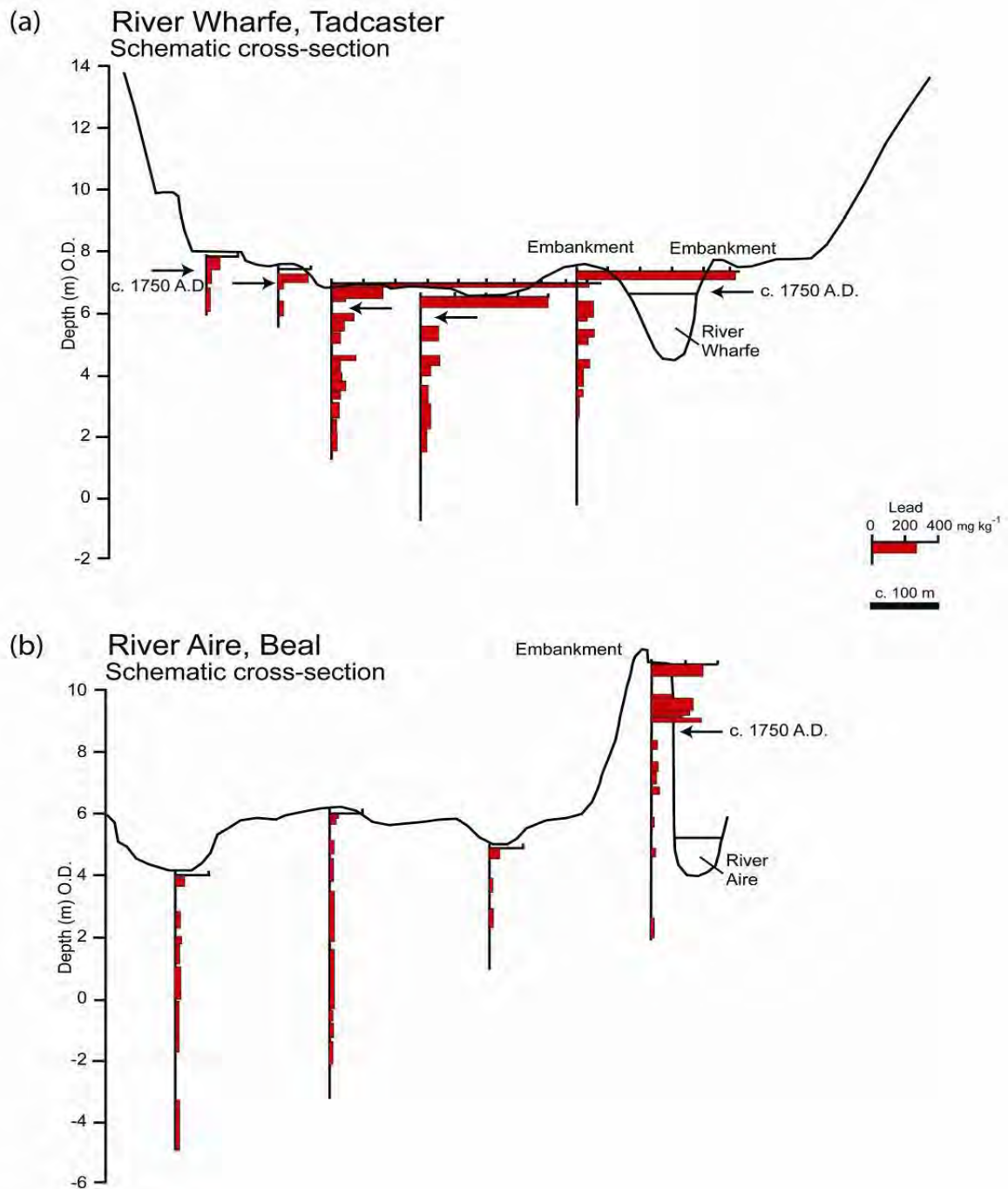


**Figure 1.1 Lead concentrations in overbank sediments from (a) River Wharfe, Tadcaster and (b) River Aire, Beal (Hudson-Edwards *et al.,*1999a).**

Here the active reworking of contaminated sediment can result in a general decrease in contamination from the source (Wolfenden and Lewin, 1977) although complex patterns of deposition can arise along river reaches due to inputs from clean and contaminated sources (Walling *et al.,* 2003; Dennis *et al.,* 2009). The highest trace metal concentrations are often reported as present in the clay and silt size fraction of the sediment due to the larger reactive surface area (Horowitz and Elrick, 1987; Stone and Droppo, 1996; Environment Agency, 2008b; Byrne et al., 2010), although higher concentrations have been associated with the coarse grained fraction, for example spoil material that may be entrained during high flow (Gozzard *et al.,* 2011; Zhao and Marriott, 2013).

Hot spots of contamination may arise in areas of preferential deposition at the base of hillslopes in alluvial fans, on the valley floor as continuous alluvial fill (figure 1.2) (Macklin and Lewin, 1989; Coulthard and Macklin, 2003; Dennis et al., 2009), where natural wetland habitats develop (Yeh, 2008; Batty, 2003), in point bars where the river channel meanders or in pools and back waters (figure 1.3) (Jeffries and Mills, 1990; Lewin and Macklin, 1987). These hot spots can serve as secondary sources of contamination to the river system, the extent of which depends on the depositional environment (Coulthard and Macklin, 2003).
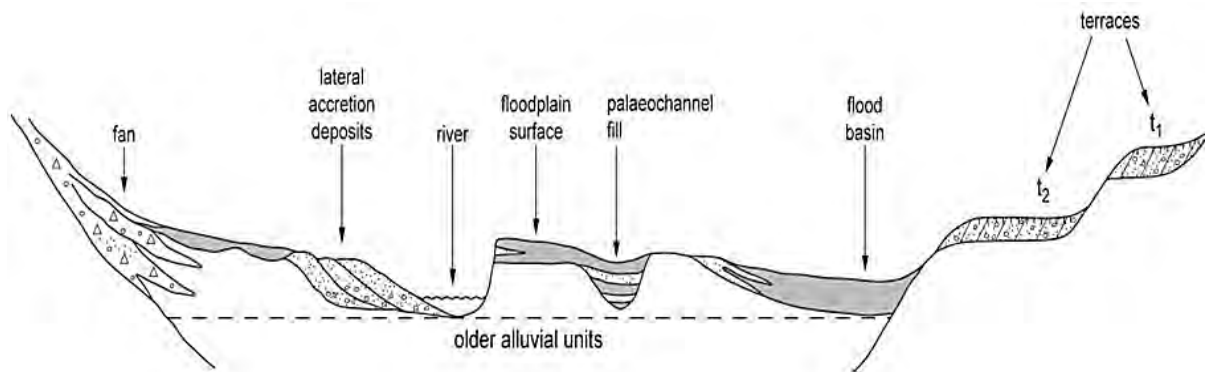
**Figure 1.2 Schematic valley section showing alluvial units of contemporary sedimentation. Older fluvial units may be preserved in terraces (t1, t2) or buried at levels beyond the zone of active reworking by the river (Macklin and Lewin, 2008).**
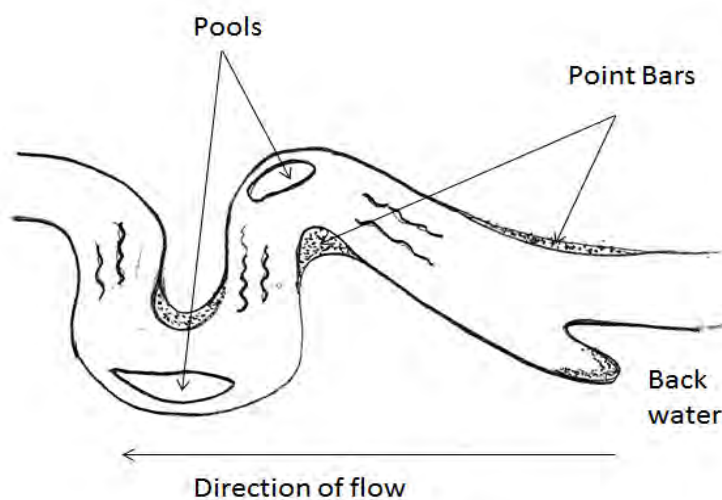


**Figure 1.3 Depositional environments within or beside the active channel (source original).**

**1.2 Storage, Remobilisation and chemical perturbation of contaminated sediment**

On the floodplain surface away from the active channel, sediment associated metal contaminants may be consigned to long term storage. Thousands of tonnes of metals such as Pb and Zn are estimated to be buried deep within the floodplains of mining impacted catchments (Walling et al., 2003; Dennis et al., 2009). Predictions using catchment sediment models such as TRACER suggest that 70% of the stored contaminants may remain within the river systems more than 200 years after mine closure (Coulthard and Macklin et al., 2003). The elevated levels of sediment associated metals deposited and stored on floodplains can have serious environmental implications with regards to uptake by plants and ingestion by grazing animals (Dennis et al., 2003; Young et al., 2007; Foulds et al., 2014). Moreover, during severe flood episodes, contaminated sediment can be remobilised and re-introduced back into the river channel in the lower reaches of the catchment (Dennis et al., 2003; Young et al., 2007; Hurkamp et al., 2009).

Closer to the active channel, dynamic environmental perturbations may occur in the sediment that cause changes in reduction-oxidation (redox) potential and drying for example where:

(i) Storm events (Dennis et al., 2003; Caruso and Bishop, 2009; Byrne et al., 2013), dredging or bioturbation (Eggleton and Thomas, 2004; Linge, 2008) remobilise and expose previously buried reduced sediments to oxygen.

(ii)     Upwelling reduced groundwater and downwelling oxidised surface water interface in saturated transitional regions of the hyporheic zone (Gandy et al., 2007; Krause et al., 2010; Byrne et al., 2013).

(iii)    Inundation and draining episodes result in the submergence and exposure of contaminated river bank sediment (Du Laing et al., 2009) (figure 1.4).

All of these processes could serve to increase the bioavailability of sediment associated trace metal contaminants.
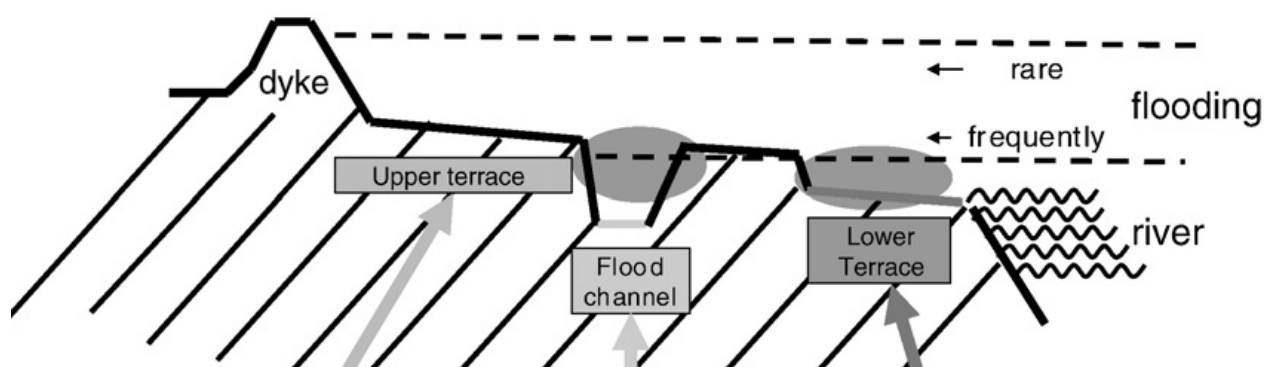


**Figure 1.4 Characteristic topographical scheme of relief in floodplain ecosystems, including water regime. Modified from (Du Laing et al., 2009).**

**1.3 Geochemical partitioning and contaminant trace metal mobility**

Trace metal contaminants can become associated with various geochemical phases in the sediment depending on the geology and mineralogy of the site and the chemical environmental conditions. Patterns of geochemical partitioning have been found to change spatially with depth (Hurkamp et al., 2009), transversely across the floodplain (Bradley, 1995) and along river channels (Evans, 1991; Byrne et al., 2010). Contaminants associated with residual mineral forms are

generally impervious to environmental changes and may remain unavailable for uptake. However, where trace metal contaminants are associated with other geochemical phases for example, clays (Evans, 1991), carbonates (Cravotta, 2008), detrital organic matter (Bradley, 1995; Linge, 2008), Fe and Mn hydroxide minerals (Palumbo-Roe et al., 2009; Wang et al., 2010), metal sulphides (Billon, 2001; Morse et al., 2002; Du Laing et al., 2007; Ku et al., 2008) and metal sulphate salts (Hudson-Edwards et al., 1999b; Alastuey et al., 1999; Buckby et al., 2003; Taylor and Hudson-Edwards, 2008; Byrne et al., 2009) changes in environmental conditions could potentially increase trace metal bioavailability. In metal mining impacted catchments trace metals such as Pb and Zn are often partitioned with Fe and Mn hydroxides and sulphur minerals in the sediment (Bradley and Lewin, 1982; Tripole et al., 2006; Buekers et al., 2008; Zakir and Shikazono, 2011). These minerals can undergo dissolution and precipitation reactions in response to changes in redox potential and drying and as a result sediment can become a source of contamination to river systems (Charlatchka and Cambier, 2000; Lesven et al., 2010; Torres et al., 2013). Moreover freshly precipitated Fe, Mn hydroxides (Shuman, 1977; Ford et al., 1997) and sulphur minerals (Buckby et al., 2003; Nordstrom, 2009; Merinero et al., 2009) are generally more reactive so where dynamic changes in redox potential and drying occur these more labile minerals could build up over time (Lynch et al. 2014).

## 1.4 Sediment Quality Guidelines

In the UK and Europe there are currently no mandatory threshold values for trace metal contaminants in river sediments, mainly due to the challenges of setting fixed standards in river systems where contamination is spatially highly variable

and where limited toxicological data are available (Environment Agency, 2008b). Catchments with a long history of mining are often naturally highly mineralised and difficulties can arise when assessing the precise environmental risk contaminated soils and sediment may pose (Dennis et al., 2003). There are however interim sediment quality guideline values developed by the Environment Agency (Environment Agency, 2008b) that are used to trigger further investigation. Threshold effect level (TEL) is the concentration below which sediment associated contaminants are not considered to represent a significant hazard to aquatic organisms where as predicted effect level (PEL) is the level above which adverse biological effects are expected to occur.

**Table 1.1 Total Effect Level and Predicted Effect Level sediment guideline values (Environment Agency, 2008b).**

| Guideline Concentrations | Pb mg/kg | Zn mg/kg |
|---|---|---|
| Threshold Effect Level (TEL) (EA Draft Sediment Quality Guidelines) | 35 | 123 |
| Environment Agency draft sediment quality guidelines: Predicted Effect Level (PEL) (EA Draft Sediment Quality Guidelines) | 91.3 | 315 |
| | | |

In June 2012 after severe flooding, freshly deposited sediment in 4 catchment areas in Wales, UK was found to contain trace metal concentration values that exceeded PEL guidelines, in some cases by an order of magnitude indicating that severe biological effects would be likely to occur. Three examples of the 4

catchments are the Clarach catchment found to contain 5,000 – 30,000 mg/kg Pb, and the Ystwyth and Rheidol catchments that contained 1,000 – 5,000 mg/kg Pb and > 1,000 mg/kg Zn (Foulds et al., 2014). These concentrations are similar to soil and sediment values from severely polluted mining systems worldwide such as the Bunker Hill mining and metallurgical superfund site, Coeur d'Alene River Valley, Idaho, USA containing 1,000 – 30,000 mg/kg Pb (USGS, 2001) and the abandoned Pb-Zn mine, Kabwe, Zambia containing up to 51,188 mg/kg Pb, although Zn concentrations were considerably higher (up to 91,595 mg/kg) (Nakayama et al., 2011). The results are particularly concerning in light of recent studies that have attributed Pb contaminated silage from flood affected fields in Wales, UK, as the cause of cattle poisoning and mortality (Foulds et al., 2014).

## 1.5 Predicted effects of future climate change

Future climate change predictions in West Wales and North West England based on UKCP09 river basin regions include a shift towards aridity along with a decline in river flow (Q95) (DEFRA, 2012a). Furthermore it is predicted the occurrence of localized heavy rainfall events will rise and that could result in an increase in the frequency and duration of river flooding (DEFRA, 2012b).

Longer dryer antecedent conditions along with more frequent/longer duration flood events could alter patterns of submergence and exposure of river bank sediment. Flow data from a typical year (2012) were selected to show how variable patterns of daily flow can be, with periods of high flow and low flow lasting from a week to almost a month (Figure 1.5).

Effects such as these observed in year 2012 expose river bank sediments to variable regimes of water saturation, resulting in river bank sediment remaining inundated for periods of less than a week to greater than three weeks and similarly for periods of drainage. If climate change predictions materialise, such events may become more prevalent and/or extreme.

Although flow patterns follow no regular pattern, figure 1.5 shows inundation periods are commonly followed by periods of drainage. Moreover during different periods of the year there is a tendency for longer periods of low flow e.g. March – June. This could result in sediment remaining drained for long periods of time. Other times of the year e.g. Sept – Dec the frequencies of high and low flow increase and this could result in a higher frequency of inundation and drainage of river bank sediment. If predictions of future climate change are to be taken into account and there is to be an increase in aridity and longer/more frequent flood events, patterns of inundation and drainage such as those described for 2012 could become more pronounced.

Changes in wetting and drying are likely to alter redox potential conditions and drying of the sediment and influence trace metal bioavailability. How these changes could alter key geochemical processes, control mineral form and influence contaminant trace metal mobility over various temporal and spatial scales in response to wet and dry sequences is currently unknown. Therefore when evaluating the risk of trace metal contaminated sediment in the context of changing patterns of inundation and drainage of river bank sediment, the experimental wetting and drying of sediment should include sequences of longer

wet periods, sequences of longer dry periods and sequences that include higher frequency inundation periods.
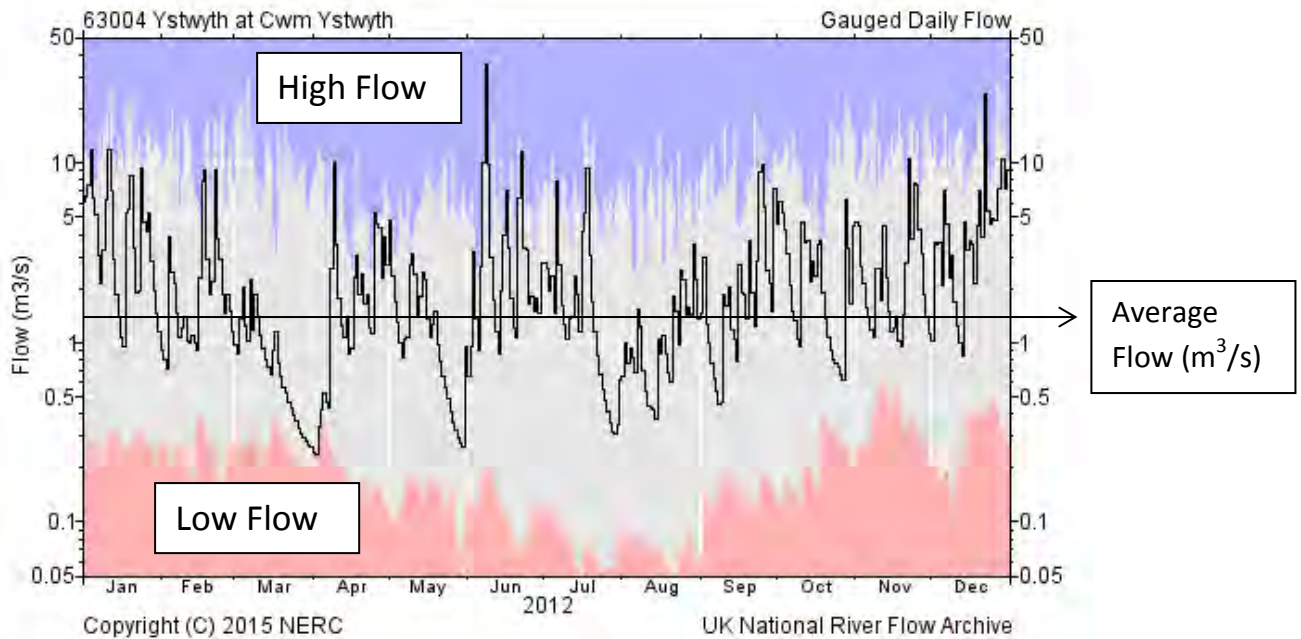


**Figure 1.5 Gauged daily flow at Cwmystwyth SN790737, in 2012 (CEH, 2014). Daily flow (black line), Red and blue envelopes represent lowest and highest flows on each day over the period of record.**

## 1.6 Terminology

Although it is accepted that the dictionary definition of 'sediments' refers to material that has settled to the bottom of the river most of literature throughout the thesis has made reference to river bank 'sediments'. Furthermore a key paper, very relevant to the study, 'Assessment of metal mining contaminated river sediments in England and Wales' (Environment Agency, 2008b) discusses the issues of contaminated sediment deposited by rivers overbank and on floodplains. The current chapter discusses the movement of contaminated sediment and deposition of this sediment on river banks and floodplains in detail. The sediment used in chapter 5 was close to the river channel and it could be argued that material collected for the study included sediments that had been deposited during periods of high flow. The material collected for chapter 3 is likely to have been predominantly mine tailings (rather than soil). For continuity and in keeping with the literature the term 'sediments' rather than 'soil' has been used throughout the thesis.

**1.7 Conclusion**

Diffuse sources of trace metal pollution arising from metal mining contaminated sediments are a known source of contamination to river systems. Contaminant loads have been found to increase in response to storm events. These hydrological events are likely to increase in duration and frequency in response to future climate change. How diffuse sources of contamination contribute to trace metal loads as a result of these environmental perturbations over time is currently not understood. There are no mandatory standards for sediment and the partitioning of trace metal contaminants with different fractions of the sediment is not considered. However the sediment environment is likely to change in redox potential and drying in response to flood events and antecedent dry periods that could increase the bioavailability of trace metal contaminants associated with minerals sensitive to these environmental perturbations. Understanding how mining polluted sediment can become a source of diffuse trace metal pollution in response to wet and dry episodes is essential for effective management and remediation.

## 1.8 Project aim and objectives

The primary aim of this project was to establish the environmental risk metal mining contaminated river bank sediments pose in response to various wet/dry sequences.

Within this overall aim, there are several key objectives:

- Identify the key geochemical processes that occur in sediments in response to a) changing antecedent conditions and b) duration/frequency of flooding
- Determine the link between changes in geochemical processes, metal speciation and bioavailability
- Determine the primary properties of river sediments that control metal bioavailability under a) changing antecedent conditions and b) duration of flooding

Focussed aims and objectives are provided within chapters 3, 4 and 5.

# 2. METHODOLOGY

## 2.1 Sample site

### 2.1.1 Justification of Sample Site

Cwmystwyth is a Pb and Zn mine abandoned in 1921 (Bick, 1976). The Afon Ystwyth runs through the Cwmystwyth mine and has been identified as a top 30 priority mining 'impacted' water body in the western Wales river basin district (Environment Agency, 2012b). Owing to the large trace metal loads of the river, particularly Zn, the Afon Ystwyth has been found to contribute significantly to chemical and biological water quality objective failures in Wales (Natural Resources Wales, 2004).

Although mining has ceased, previous field studies at Cwmystwyth found trace metal concentrations in the river bed sediments to be high (7870±5730 and 2620±1930 mg/kg) compared to upstream sites (50±60 and 640±640 mg/kg) for Pb and Zn respectively (Montserrat, 2010). It is possible that these sediments could act as a source of trace metal pollution to the Afon Ystwyth. This was indicated in a recent study that found high concentrations of dissolved Zn in the river water at the site (410±318 µg/L) compared to upstream sites (6.25±9.46 µg/L) although Pb was below detection (Montserrat, 2010). Historical field studies of the Cwmystwyth site however have found high concentrations of both Zn (307 µg/L) and Pb (68 µg/L) half a km below the Cwmystwyth mine area, with concentrations remaining high for Zn (168 µg/L) and Pb (58 µg/L) up to 7.5 km downstream (Fuge et al.,1991). Moreover, the annual flux of Pb and Zn through

the Ystwyth catchment has been found to be disproportionately large for its small catchment size (32.1 km$^2$) (Mayes et al., 2013). The presence of metals within sediments and waters therefore enables the use of this site as an example of metal contamination and it can be used to determine whether the sediments are acting as a source of trace metal pollution to the river and to understand the key mechanisms responsible for the release of these contaminants.

## 2.1.2 Site Description

The sample site at Cwmystwyth (SN799743) is located on the north bank of the Afon Ystwyth and is 250 m above sea level. The river runs from east to west (figure 2.1), and drains into the Irish sea via Aberystwyth (figure 2.2). The north side of the river is marked by spoil heaps rising to 500 m and on the south side grass banks, used primarily for grazing, rise steeply to 450 m (plates 2.1, 2.2).
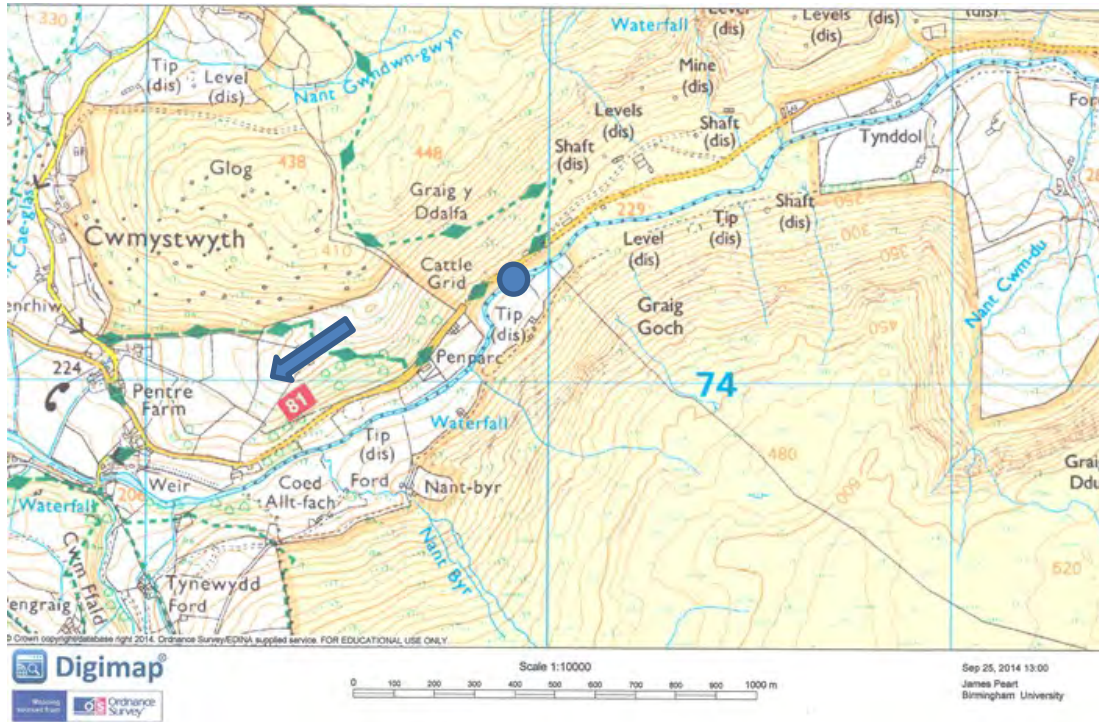
**Figure 2.1 Location of sample site, grid reference SN799743 (blue dot denotes sampling location, blue arrow the direction of flow). Crown copyright database 2012.**
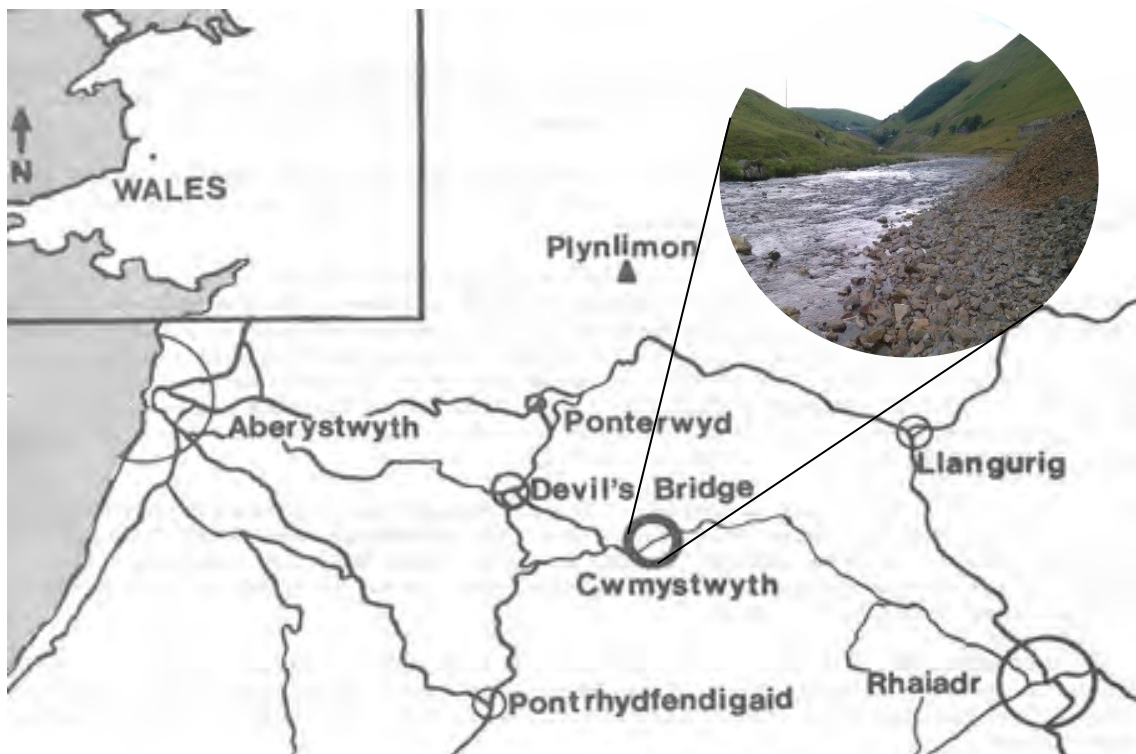


**Figure 2.2 Map showing location of the Cwmystwyth mine.**

**Plate 2.1 Upstream of sample site (source original).**



**Plate 2.2 Downstream of sample site (source original).**

## 2.1.3 Topography

The country rock in the region of the mine dates from the Silurian Period with alternating bedrock of hard coarse sandstones and shales that form the upper Llandovery Series (BGS, 2007). This bedrock is impermeable, generally without groundwater, except at shallow depth (CEH, 2014). Shallow sub-surface river flow was observed at this site on the second sampling visit 11th December 2014. Superficial deposits, along the river are flints, sand and silt (CEH, 2014). Rivers that rise on this type of geology (low in limestone) have been described as 'base poor' (Natural Resources Wales, 2004). Having a low alkalinity makes them more susceptible to acidic inputs brought about through metal pollution (Natural Resources Wales, 2004).

## 2.1.4 Mineralogy in and around the mine site

The main metalliferous vein runs parallel with the river to the north of the sample site with many old mining adits and shafts located to the east (Hughes, 1981). The main ores mined were galena (PbS), sphalerite (ZnS) and chalcopyrite ($CuFeS_2$) although no chalcopyrite is recorded as having been raised since 1845 and very little trace of chalcopyrite has been found in waste heaps (Hughes, 1981). Mined minerals were primarily in a gangue (non-commercial product mixed in with the ore) of quartz. Other primary and secondary minerals identified in the mine and around the mine site are pyrite ($FeS_2$), Fe oxides (limonite ($FeO(OH).nH_2O$) and goethite ($FeO(OH)$)) (Hughes, 1981), anglesite ($PbSO_4$), hemimorphite ($Zn_4Si_2O_7(OH)_2.H_2O$) and leadhillite ($Pb_4(CO_3)_2(SO_4)(OH)_2$) (Mintdat.org, 2014).

## 2.1.5 Rainfall and river flow characteristics

Standard-period average annual rainfall (SAAR) for years, 1996 – 1991, is 1994 mm for catchment area 32.1 km$^2$ (station grid reference SN790737) (figure 2.3) (CEH, 2014). This is high, compared to catchments in other localities around the UK, e.g. Mersey, Ashton Weir, 1129 mm  catchment area 660 km$^2$, South Tyne, Alston 1523 mm catchment area 118.5 km$^2$, Thames, Reading, 680 mm catchment area  4633.7 km$^2$ (CEH, 2014).
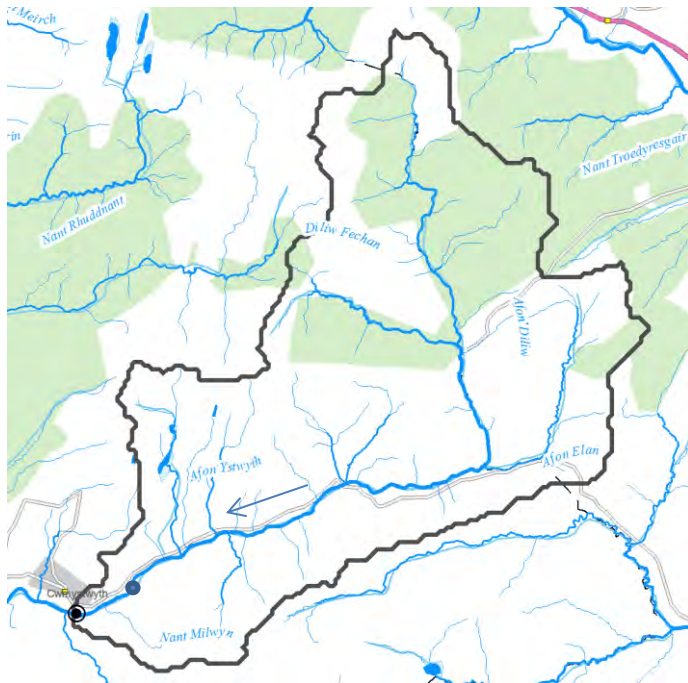


**Scale 1 cm – 1 km**

**Figure 2.3 The Ystwyth Catchment (black line), gauging station (black dot), sample site (blue dot). Blue arrow shows direction of flow (CEH, 2014).**

Daily flow shows a highly variable pattern at the gauging station just under 1 km downstream from the sample site (figures 2.4 and 2.5). Readings often fall far below or above the mean value (1.989 m$^3$/s) and flow remains low or high for periods greater than a week. Changes in river flow are known to cause a rise and

fall in river water stage and that has been found to influence patterns of hyporheic exchange flow (vertical, lateral and longitudinal) (Byrne et al., 2013). The inundation of river bank sediments brought about through a rise in river stage can introduce nutrients into the sediment (Byrne et al., 2010) and create dynamic redox potential conditions (Gandy et al., 2007, Krause et al., 2010). That, coupled to long dry antecedent conditions could alter the form of redox sensitive elements, such as sulphur and Fe, associated with trace metal pollutants such as Pb and Zn potentially increasing their bioavailability.
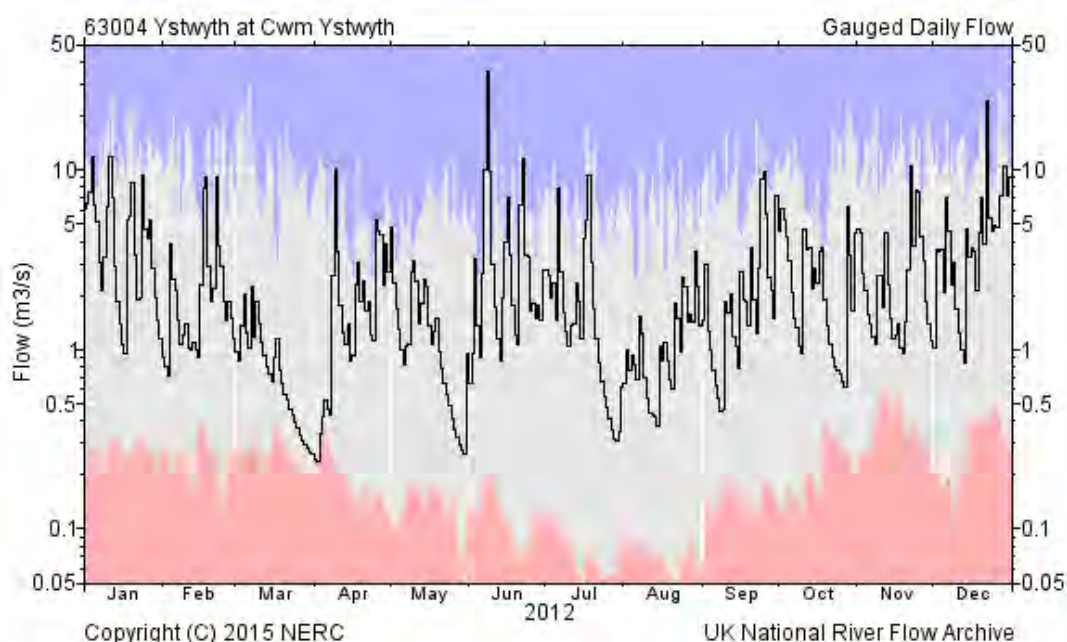


**Figure 2.4 Gauged daily flow at Cwmystwyth SN790737, in 2012 (CEH, 2014). Daily flow (black line), Red and blue envelopes represent lowest and highest flows on each day over the period of record.**
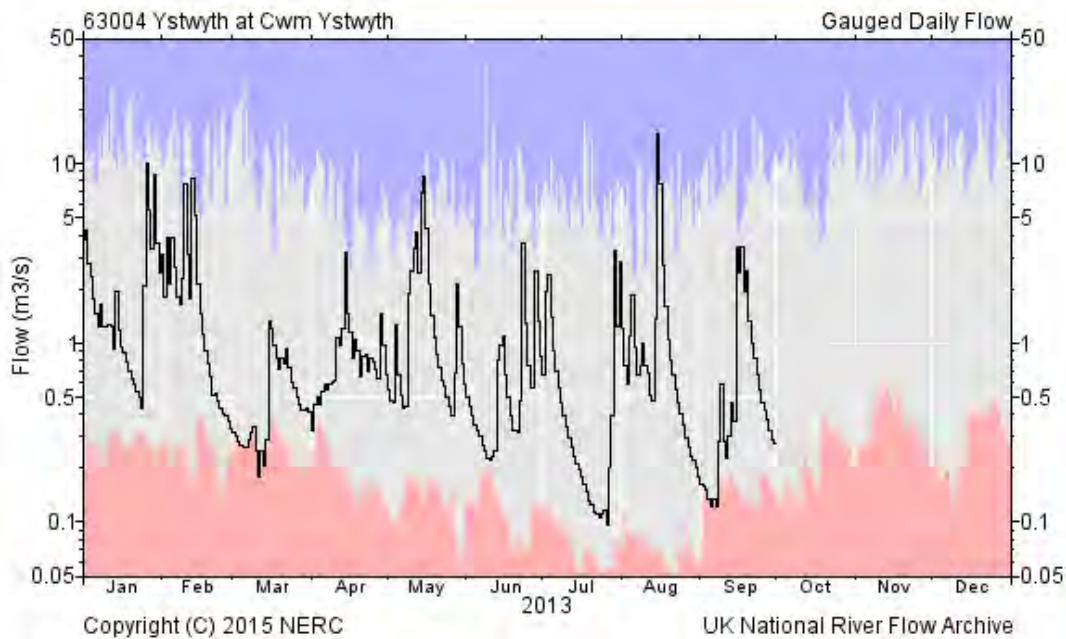
**Figure 2.5 Gauged daily flow at Cwmystwyth SN790737, in 2013 (CEH, 2014). Daily flow (black line), Red and blue envelopes represent lowest and highest flows on each day over the period of record.**

## 2.1.6 Sediment collection

Visual inspection of the northern river bank indicated that sediment was made up of predominantly sandy gravel interspersed with some finer silt particles and larger pebbles and boulders.

The sediment samples were collected from different locations in chapters 3 and 5. Further information is provided in each chapter. A stainless steel shovel was used to collect sediment from the top 10 cm. Quantity of sediment required was calculated based on number and size of columns to fill, multiplied by 3 (to allow for spare).

## 2.2 Laboratory Analysis

## 2.2.1 Mesocosm Experiments

In chapters 3 and 5 sediment collected from the sample site was homogenised by hand using a plastic trowel, added to mesocosms and treated to variable wet/dry runs over 12 weeks in order to simulate the river bank environment, in a highly simplified fashion, in order to investigate the influence of different wet/dry runs on mobility of trace metal pollutants Pb and Zn - the primary contaminants in river water (Mayes et al., 2013, Fuge et al., 1991) and sediment (Montserrat, 2010) at the site.

Mesocosms were created using uPVC (unplasticized polyvinyl chloride) drain-pipe. Plain end caps (Clarks Drain) were fitted to the bottom and holes (2.5 cm diameter) were drilled into the side of the drain pipe, at the middle (10 cm below sediment surface) and bottom (24 cm below sediment surface). Siphon tube taps were attached to PTFE (polytetrafluoroethylene) tubes and fitted into the holes. Evo-Stik waterproof sealant was added around the joints on the outside only (figure 2.6).

**Figure 2.6 Mesocosm setup.**

Artificial Rainwater (ARW) was created based on Plynlimon rainwater chemistry (table 2.1) (pH 4.9-5.2), found in the uplands of mid-Wales (Neal et al., 2001).

**Table 2.1 Artificial Rainwater Chemistry**

| Salt | (mg/L) |
|---|---|
| $K_2SO_4$ | 0.2 |
| $CaSO_4.2H_2O$ | 0.74 |
| $MgSO_4.7H_2O$ | 0.56 |
| NaCl | 4.47 |
| $MgCl_2.6H_2O$ | 1.36 |
| $NH_4NO_3$ | 0.726 |
| $(NH_4)2SO_4$ | 0.18 |

All mesocosms were kept at field capacity for three weeks. Twice a week 500 ml ARW was added via the top of the mesocosm until water percolated through the bottom tap. This was carried out to allow the sediment to equilibrate.

Mesocosms were divided into 7 wet and dry runs (figure 2.7). As noted (section 2.1.5) the Cwmystwyth gauged daily flow (grid reference SN790737, taken from the UK National River Flow Archive (CEH, 2014), provided guidance regarding the length of time river bank sediment may be exposed or submerged (figures 2.4 and 2.5).

| Run # | Sampling: | A | B | C | D | E | F | G | H | I | J | K | L | |
|---|---|---|---|---|---|---|---|---|---|---|---|---|---|---|
| 1 | 1 week wet 1 week dry | | | | | | | | | | | | | |
| 2 | 1 week wet 2 weeks dry | | | | | | | | | | | | | |
| 3 | 1 week wet 3 weeks dry | | | | | | | | | | | | | |
| 4 | 2 weeks wet 1 week dry | | | | | | | | | | | | | |
| 5 | 3 weeks wet 1 week dry | | | | | | | | | | | | | |
| 6 | Constant flood (control) | | | | | | | | | | | | | |
| 7 | Field Capacity (control) | | | | | | | | | | | | | |

**Figure 2.7 – Wet and dry runs, weeks A – L (12 weeks)**

Key:

| | |
|---|---|
| Dry | (orange) |
| Wet | (blue) |

Variable runs were designed to include :

a) longer wet runs

b) longer dry runs

c) wet and dry run of same duration and frequency.

Control runs were non-variable and either constant wet (flood) or unsaturated and oxidised (field capacity). This allowed a comparison between variable and non-

variable wet and dry runs. Constant flood and field capacity were sampled every week. Variable run samples were taken only at the start and end of a wet period. An extended experimental timeframe for each column of 20 days at field capacity followed by 12 weeks treatment period promoted the removal of any artefacts and allowed time for systems to settle into a steady pattern.

At the start of a flood, ARW was added to the columns up to 5 cm above the sediment level to simulate flood conditions (Du Laing et al., 2007). Water was left for 2 - 3 hours to allow for contact time between sediment and pore water. Water samples were then taken from the top using a plastic syringe and from the middle and bottom via the taps, in that order to avoid mixing between levels. Using a Hanna Combo pH/EC and temperature hand held stick meter model No 98129, the pH, conductivity and temperature were recorded for each sample.

Each sample was filtered through a 0.45 µm PTFE syringe filter into two metal-free 60ml centrifuge tubes. One sample was acidified with nitric acid ($HNO_3$) to below pH 2.5 for metal analysis by flame atomic absorption Spectroscopy (FAAS) (section 2.2.3) or Inductively Coupled Plasma with Optical Emission Spectroscopy (ICP/OES) (section 5.2.8). The other was frozen (-20 °C) for subsequent anion analysis by IC2000 Anion Dionex (section 2.2.4). After sampling, flood levels were kept at 5cm above sediment level by topping up with ARW. Mesocosms were then left *'in flood'*, with the taps closed, for the allotted timeframe.

At the end of a wet period the above sample methodology was repeated and any pore water remaining in the mesocosm after sampling was drained out via the bottom tap into a bucket and discarded. Mesocosms were then left '*dry*' for the allotted timeframe.

For the constant flood, samples were taken weekly at the same time as the variable runs. After sampling flood levels were kept at 5cm above sediment level by topping up with ARW. For field capacity ARW was allowed to percolate though the mesocosm and collected at the bottom sampling point. Field capacity samples were collected at the same time as the flood samples.

At the end of each treatment period (after 12 weeks), sediment was collected using a plastic spatula from the top, middle and bottom of the mesocosm. Sediment was freeze-dried to preserve mineral state to allow for characterisation of the sediment through sequential extraction analysis (SEQ), (section 2.2.5) Scanning Electron Microscopy/Energy Dispersive Spectroscopy (SEM/EDS) (section 2.2.10) and X-ray Diffraction (section 2.2.11).

## 2.2.2 Trace metal and anion analysis

Pore water sampled from mesocosm runs in chapters 3 and 5 and sequential extraction samples from chapters 4 and 5 were filtered to measure 'dissolved' analyte concentrations.

For pore water analysis, the concentration of dissolved analyte was used as a proxy to indicate the potential bioavailability of trace metal pollutants Pb and Zn. Uptake of a pollutant by an organism occurs after the metal has passed from the aqueous phase through the biological membrane into the organism (Twardowska et al., 2006). One model developed to try to describe how the uptake mechanism occurs - the Biotic Ligand Model (BLM) theorises that the cell wall acts in a similar way to a ligand, in that it binds the metal prior to uptake. For the cell wall to bind to the metal it may need to compete with any ligand the metal is already bound to.

Therefore the BLM predicts that the bioavailability of a metal is based on the concentration of free (uncomplexed) metal ions. Although a number of exceptions exist the BLM has shown good correlation in relating free metal-ion concentrations to metal uptake by fish and invertebrates (Chapman et al., 2003).

Samples were filtered through a 0.45 µm PTFE syringe filter. Using filtered metal concentration as a proxy for bioavailability of metal ions has its limitations. The BLM predicts bioavailability is liked to uncomplexed metal ions however it is likely that in the presence of high concentrations of ligands such as dissolved organic carbon that can readily complex with 'free' metal ions (vanLoon and Duffy., 2011, Du Laing et al., 2009) the use of filtered concentrations as a proxy for bioavailability would be unsuccessful. Historical data however indicated that dissolved organic carbon is low at the Cwmystwyth site (Montserrat, 2010) and therefore this method was deemed as acceptable.

The choice of filter size 0.45 µm as a cut-off point for dissolved analytes is arbitrary. Environment Agency quality standards for Pb required to achieve 'good' status for river water define 'dissolved' as 'filtered through a 0.45 µm' filter (Environment Agency, 2010a). This filter size was therefore chosen to allow for an accurate assessment of the environmental risk releases of dissolved Pb posed. Furthermore studies commonly use 0.45 µm as the cut-off point between dissolved and particulate (Gao et al., 2006; Banks and Palumbo-Roe, 2010; Byrne et al., 2013) and in order to compare concentrations of dissolved elements with findings from other studies this filter size was chosen.

Prior to analysis filtered water samples were preserved for cation analysis by acidifying to pH $\leq$ 2 using nitric acid ($HNO_3$) to keep metals in solution and for anion analysis filtered water samples were placed in the freezer at 20°C.

## 2.2.3 Flame Atomic Absorption Spectroscopy

Flame Atomic Absorption Spectroscopy (FAAS) (Perkin Elmer Analyst 300) was used to measure Fe, Mn, Zn, Pb, Ca, Ni, Cu (mg/L) for pore water samples (chapter 3) and Fe, Mn, Zn and Pb in sequential extraction solutions (chapter 4). For FAAS a pore water sample is introduced as an aerosol, into an atomised 'cell', usually an air-acetylene flame. The flame ionises the atoms in the sample which absorb energy at specific wavelengths from a light beam that passes through the flame. The light beam is specific to the element of interest. The excited atoms re-emit the same wavelengths, but in random directions, that results in a net attenuation of beam intensity along the beam path. The attenuation of the beam at the specific wavelength, that a monochromator is tuned to, is reflective of the number of atoms of the measured analyte and so provides a measure of concentration of that analyte in the pore water sample (Gill, 1997). Only one element can be measured at a time, therefore measurement of many elements can be highly time consuming. However, it is cost effective, sensitive and offers freedom from spectral interference (Gill, 1997). Independent check (quality) standards were used to measure accuracy at the start, middle, and end of the run. The run was considered acceptable if the data were within 5% of the expected concentration e.g. 1 ppm (0.95-1.05 ppm). Where Zn, Pb, Fe and Mn exceeded maximum concentration (table 2.2) samples were diluted 1 in 10 or 1 in 20. This correction was taken into account when calculating actual concentration.

**Table 2.2 Cation detection limit, maximum concentration, standard range and independent check standard value (ppm) for FAAS analysis**

| Cation | Detection Limit (ppm) | Maximum concentration (ppm) | Calibration standard range (ppm) | Independent check (quality) standard (ppm) |
|--------|----------------------|-----------------------------|----------------------------------|--------------------------------------------|
| Ca | 0.06 | 5 | 1 - 5 | 2 or 5 |
| Fe | 0.03 | 10 | 1 - 10 | 5 |
| Cu | 0.01 | 5 | 1 – 5 | 2 |
| Mn | 0.01 | 5 | 0.5 - 5 | 1 or 2 |
| Zn | 0.02 | 1 | 0.1 – 1 | 1 |
| Ni | 0.01 | 10 | 1 – 7.5 | 2.5 |
| Pb | 0.04 | 20 | 1 - 20 | 2 or 5 |

## 2.2.4 Ion Chromatography

Dissolved sulphate, nitrate, chloride and phosphate were measured in pore water samples in chapters 3 and 5 using ion chromatography (Dionex ICS2000).

Ion chromatography works by injecting a water sample into a mobile phase that transports the sample through a chromatography column. In the column ionic analytes compete for exchange sites and separate based on size and ionic charge. Analytes are detected on elution from the column and identified based on their retention time.

Standards of 1, 2, 5, 10, 50, 100 ppm were used. Where sulphate concentrations exceeded 100 ppm, samples were diluted. Independent check standards of 5 and10 ppm were used to check for drift. The run was considered acceptable if within 5% of the expected concentration. Fresh batches of ARW were always analysed as a blank. Anion detection limits are detailed below (table 2.3).

**Table 2.3 Anion detection limits (ppm)**

| Anion | Detection Limit (ppm) |
|---|---|
| **Sulphate** | 0.07 |
| **Nitrate** | 0.04 |
| **Chloride** | 0.06 |
| **Phosphate** | 0.06 |

## 2.2.5 Sequential Extraction

Different Fe phases may display a wide range of reactivity (adsorption capacity and susceptibility to reduction). It is generally agreed that the most reactive forms of Fe are freshly precipitated forms (Shuman, 1977; Younger, 1995; Ford et al., 1997; Nordstrom and Alpers, 1999; Cravotta and Bilger, 2001; Burton et al., 2005). In order to determine whether the mesocosm runs had altered the form of Fe and Mn hydroxides in the sediment resulting in a build-up of more reactive forms of Fe and Mn in the sediment and whether that had subsequently influenced the mobility of pollutant trace metals Pb and Zn, a sequential extraction procedure that focused primarily on Fe and Mn minerals was designed (chapters 4 and 5). The first three extraction steps (table 2.4) were taken from two research papers (Lovley and Phillips 1986, Poulton and Cranfield 2005). These steps were run sequentially (from most reactive to least reactive) and were intended to extract different forms of Fe and Mn in the sediment at the end of each wet and dry run along with partitioned trace metals Pb and Zn. The forth step was an aqua regia digestion designed to remove metals partitioned with residual minerals (unlikely to alter form in response to wetting and drying sequences) (Montserrat 2012, Linge 2008, Wilson and Pyatt 2007).

Extraction step 1 (table 2.4) was taken from Lovley and Phillips, (1986). Over prolonged flood periods oxidised Fe and Mn hydroxides can undergo reductive dissolution (Charlatchka and Cambier 2000, Davis and Kent 1990) and reduced Fe (II) can form a mono layer on sediment surfaces (Lovley and Phillips, 1986). This first extraction step was intended to determine whether there had been a build-up of reduced Fe(II) and Mn(II) loosely sorbed to the surface of sediment for certain wet and dry runs along with any loosely sorbed trace metals Pb and Zn. Lovely and Phillips (1986) had reported that this extraction step did not change the oxidation state of Fe. The extraction was therefore chosen as the first step in the sequence as it would not alter the oxidation state of other Fe mineral forms in the sediment and it would extract (only) reduced Fe(II) loosely sorbed to the surface of sediment. Measuring the concentration of reduced Fe and Mn loosely sorbed to the sediment for each wet and dry run was intended to help understand the extent to which certain runs had altered the form of Fe and Mn hydroxides in the sediment. Quantifying reduced Fe and Mn was important because this form of Fe (and Mn) could quickly oxidise when exposed to atmospheric conditions (i.e. where flood waters subside). Freshly precipitated Fe and Mn hydroxides are more reactive and can scavenge high concentrations of trace metals Pb and Zn (Du Laing et al. 2009, Lovley and Phillips 1987).

Extraction steps 2 and 3 (table 2.4) were run sequentially following the methodology of Poulton and Cranfield (2005). Step 2 was a hydroxylamine hydrochloride extraction intended to extract (only) the easily reducible (reactive) Fe and Mn hydroxides (along with partitioned Pb and Zn) (Poulton and Cranfield (2005). It was hoped that this would help to determine whether certain wet and dry

runs resulted in a build-up of 'reactive' Fe and Mn hydroxides. Freshly precipitated Fe and Mn has an adsorption capacity ten times that of aged oxides (Shuman, 1977) and has been found to sorb high concentrations of contaminant trace metals such as Pb and Zn (Evans, 1991). Where sediment is exposed to flood conditions reactive Fe and Mn hydroxides could quickly undergo reductive dissolution and release contaminant trace metals Pb and Zn back into the river (Lynch et al., 2014).

Step 3 (table 2.4) was a more stringent dithionite extraction intended to extract more residual, less reactive forms of Fe (goethite and hematite) and Mn hydroxide (along with partitioned Pb and Zn). This form of Fe and Mn hydroxide has been reported to reduce more slowly (Lovley and Phillips, 1987) and has a lower sorption capacity (Shuman, 1977) than freshly precipitated Fe and Mn hydroxide. It is anticipated that this form of Fe and Mn hydroxide would be less likely to transform in response to wet and dry runs.

Extraction step 4 was an aqua regia digestion. This form of extraction is used as the final step in many extractions (Montserrat 2012, Linge 2008, Pueyo et al., 2008, Wilson and Pyatt 2007). It was intended to measure more residual Fe and Mn hydroxides along with associated trace metals Pb and Zn. This allowed the quantification of minerals that were unreactive and unlikely to release contaminant trace metals as a result of the wet and dry runs.

Approximately 1 gram of sediment was collected from the top (0 - 1 cm deep) and bottom (24 cm deep) of each mesocosm using a plastic spatula and added to a small polyethylene zip bag. All collected sediment was frozen at

-20$^{\circ}$C immediately after sampling and once frozen was then freeze dried (-70°C) for storage in order to preserve redox state.

Prior to extraction, samples were divided into size fractions $\leq$ 63 µm (clay/silt) and 64-2000 µm (fine – coarse sand) by dry sieving in order to investigate differences in metal concentration and geochemical partitioning between these two size fractions.

The sediment was weighed (as close as possible to 0.1 g) and the weight was noted for back calculation and then added to a 15 ml polyethylene centrifuge tube. Each sample was run in triplicate.

A modified four step sequential extraction procedure was run to identify 4 Fe phases (table 2.4), along with any partitioned Mn, Pb and Zn.

For steps 1 and 2, the extractant (5 ml) was added to the sediment sample and mixed using a rotational shaker for 1 hour. The sample was then centrifuged and the supernatant was filtered through a 0.45 µm PTFE syringe filter. This filtered supernatant was added to a 50 ml glass volumetric and made up with deionised water.

Step 3 and 4 were carried out in a fume cupboard. For step 3 the extractant was made up immediately before use: 5 g dithionite, 5.88 g sodium citrate, 2 ml acetic acid made up to 100 ml with deionised water in a glass volumetric. This extractant (5 ml) was added to the sediment remaining from the previous two extractions. The sample was mixed using a rotational shaker for 2 hours. The samples were then centrifuged and filtered through a Whatman Membrane (nylon) 0.45 µm filter.

This filtered supernatant was added to a 50 ml glass volumetric and made up with deionised water.

For step 4 (aqua regia) cHCl and $cHNO_3$ were pipetted in a 3:1 ratio to a centrifuge tube containing the sediment remaining from the previous three extractions. The tubes were agitated gently and left in a fume cupboard overnight. The following day the tubes were heated at $80^oC$ for two hours. The supernatant was then filtered through a Whatman no 42 filter and 0.5 ml of 0.14 M KCl was added as an ionisation suppressant. This mix was then added to a 50 ml glass volumetric and made up with deionised water. All samples were added to labelled tubes for analysis of metals (Fe, Mn, Pb and Zn), via Flame AAS (chapter 3) or ICP/OES (chapter 5).

**Table 2.4 Sequential extraction steps**

| Step # | Extractant | Purpose | References |
|---|---|---|---|
| 1 | 0.5M HCl | To measure reduced Fe(II) and Mn (II) loosely sorbed to the surfaces of minerals in sediment. This procedure may also be applicable to other di-valent metals (i.e. Pb and Zn). | Lovley and Phillips (1986) |
| 2 | 0.25M Hydroxylamine hydrochloride in 0.25M HCl | To reduce, labile, easily reducible forms of Fe – likely to be ferrihydrite and Lepidocrocite. | Lovley and Phillips (1987) Poulton and Canfield (2005) |
| 3 | 50g/L sodium dithionite with 0.2M in 0.35M acetic acid | To reduce, reducible forms of iron – ferrihydrite, lepidocrocite and also more crystalline forms of Fe goethite, hematite and akaganeite. | Poulton and Canfield (2005) |
| 4 | Aqua Regia | Considered effective for the extraction of most metals in sediment and soil. A measure of pseudo-total metals | Wilson and Pyatt (2007) Montserrat (2012) |

## 2.2.6 Total 'Dissolved' Carbon (TC) and Non Purgeable Organic Carbon (NPOC)

The microbially mediated oxidation of carbon, coupled to the reduction of redox sensitive elements is known to influence the bioavailability of trace metals (van-Loon and Duffy, 2011). These processes can also change the physico-chemical characteristics of the water that can, in turn, also influence trace metal mobility. Therefore in chapters 3 and 5 measurement of dissolved organic and inorganic components in pore water samples and sediment was carried out.

For pore water samples TC and NPOC (dissolved organic carbon DOC) were measured using a carbon analyser (Shimadzu TOC-V CSN).

A) For TC measurement a water sample was taken up by the carbon analyser and heated to 680°C in the machine. The $CO_2$ generated by oxidation was detected using a non-dispersive infrared (NDIR) detector.

B) For NPOC, the sample was first acidified to pH 2 to transform any inorganic carbon to $CO_2$. The $CO_2$ was removed via sparging with a carrier gas. The remaining (acidified) water sample was then taken up by the carbon analyser and NPOC measured using the TC method A (above) (Shimadzu Scientific Instruments, 2014).

For both TC and NPOC the area under the curve was compared to a standard calibration curve to determine concentrations. The instrument was calibrated in range 0 – 10 ppm, a working standard of 10 ppm was prepared and diluted automatically by the instrument and included (0, 2, 4, 5.882, 10 ppm). Quality control standards and blanks were poured into vials and measured every 15

samples. The run was considered acceptable and accurate if within 5% of the expected concentration. All pore water samples were filtered (0.45 µm) prior to analysis.

Using the above results the inorganic carbon concentration of the pore water was calculated as:

Inorganic Carbon = Total Carbon – Non Purgeable Organic carbon

## 2.2.7 Total organic carbon (TOC) and Inorganic Carbon (IC) (sediments)

For TOC and IC determination in sediments a separate solid sample module of the Shimadzu instrument (SSM 5000A) was used. A sub sample of sieved (2 mm) sediment was weighed (no greater than 50 mg), and oven dried at $140^{o}$C for 24 hours.

A) For determination of total carbon (TC) the prepared sediment sample was combusted at $900^{o}$C in a stream of oxygen to ensure complete conversion to $CO_2$. The $CO_2$ generated was detected using a non-dispersive infrared (NDIR) detector.

B) For inorganic carbon (IC) determination a separate sub sample of the sediment sample was treated inside the Shimadzu instrument with phosphoric acid to produce $CO_2$ that was purged at $200^{o}$C and detected using a non-dispersive infrared (NDIR) detector (Shimadzu Scientific Instruments, 2014).

The $CO_2$ released for both methods was measured through a calibration curve. Calibration was performed using different weights of a solid with known carbon content, for TOC glucose was used that contained 40% carbon and for IC sodium carbonate was used that contained 11.3 % carbon.

The results provided information regarding % TC and % TIC that allowed % TOC to be calculated:

TOC = TC – TIC

## 2.2.8 Alkalinity

Alkalinity measured as calcium carbonate can provide an indication of the buffering capacity of the water. Alkalinity analysis was carried out on samples in chapter 3 and 5. Unfiltered samples were analysed using the standard operating procedure for GLNPO (Great Lakes National Program office) total alkalinity titration method (Palmer, 1992) to measure mg/L of alkalinity as calcium carbonate.

## 2.2.9 Grain size analysis

Metals can often be concentrated in fine sediment due to the resulting large surface area, although this is not always the case. To determine the grain size of the sediment collected for the mesocosm runs in chapters 3 and 5 a series of Endecotts sieves of size fractions (> 8 mm, 2 – 8 mm, 2 – 1 mm, 1 – 0.5 mm, 0.5 – 0.25 mm, 0.25 – 0.125 mm, 0.125 mm – 63 µm, < 63 µm) were used. Size fraction > 8 mm was only used for chapter 3 as larger pebbles were removed from the sediment for chapter 5. Larger pebbles were kept in the sediment for chapter 3 because this was found to aid drainage through the mesocosm and that helped during weekly sampling. That was not needed in chapter 5 as the drainage was sufficient for sampling.

A representative sample of the sediment for each of the experimental runs was analysed after homogenisation. Sample size was approximately 2.5 kg.

After sieving on a vibration platform (Fritsch), each size fraction was weighed and then divided into the following Wentworth size classes: pebbles > 8 mm, granules and fine pebbles 2-8 mm, very coarse to very fine sand 63 μm – 2 mm, silt/clay < 63 μm.

## 2.2.10 Scanning Electron Microscopy with Energy Dispersive Spectroscopy (SEM/EDS)

A combination of SEM/EDS was carried out in chapters 4 and 5 to create images of, and identify, map and quantify elements at the surface of the sediment samples for areas at micron scale. Freeze dried sediment was dusted lightly onto carbon stubs and either coated in carbon or platinum to encourage conductivity. A working distance of 10 mm was used.

SEM/EDS Instruments were:

Philips XL30 FEG ESEM fitted with an Oxford Instruments X-Sight EDS ATW X-Ray detector (University of Birmingham, UOB) (chapter 4 only)

FEI Quanta 200 ESEM (Liverpool John Moores, LJMU) (chapters 4 & 5)

EDS software used for both machines was Oxford Instruments INCA

For SEM/EDS, electrons generated from a heated tungsten filament are fired from a gun and travel through a series of lenses before coming into contact with the sediment surface. Energy is dissipated as a variety of signals that are used for imaging and element identification:

**Back scattered images** of sediment samples were taken for chapters 4 and 5. For this a SEM image of the sediment surface was created by an electron beam rastered across the sample surface.

Back scattered electrons are the result of elastic collisions that involve no energy loss, just the deflection of electrons that do not contribute to X-ray generation. These electrons escape from just below the sample surface. The proportion of electrons generated in this way increases with mean atomic number of the element. This produces an image where high atomic number elements such as Pb are much brighter components than low atomic number elements (figure 2.8) (Oxford Instruments, 2008).
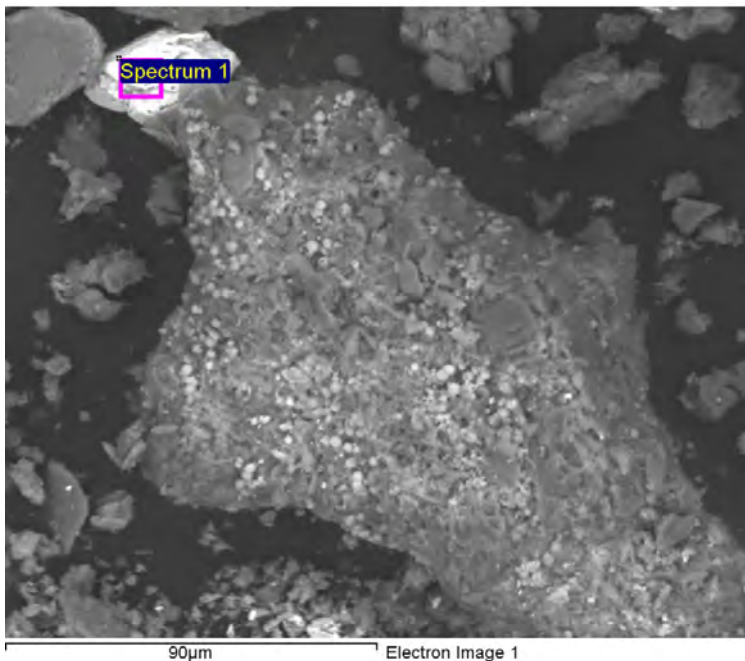


**Figure 2.8 Back scattered electron image. The bright material is Pb sulphide (PbS) (spectrum 1) (Source original, 2014) (UOB)**
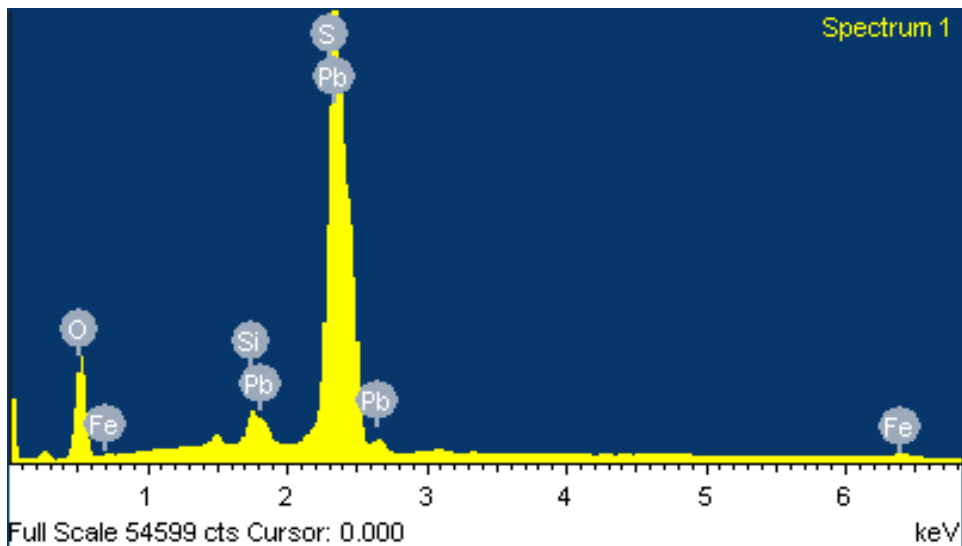
**Figure 2.9 EDS spectrum (histogram) for 'spectrum 1' see figure 2.8 (source original, 2014) (UOB)**

EDS analysis was carried out on sediment samples in chapters 4 and 5 in order to identify the elements present at the sediment surface through x-ray generation.

**For x-ray generation** a high energy incident electron beam excites an atom in the sample and results in the ejection of an electron from the inner shell of that atom. The resulting vacancy in the electron shell is filled by an electron from a higher energy outer shell. The energy excess is released as x-ray radiation that is characteristic of the element from which it was generated. X-rays from different elements result in different pulse heights that are proportional to the x-ray energy. The instrument processes the pulse and places it into a fixed energy channel. An EDS is produced (figure 2.9). This is a histogram, the 'x' axis measures the energy in keV and the 'y' axis is the intensity. X-ray lines are named based on the shell of the ejected electron e.g. K, L, M, and the outer shell of the electron that filled the vacancy e.g. alpha if one shell out, beta if two shells out etc. (Oxford Instruments, 2008).

The energy of the incident electron beam dictates which x-ray lines are excited. An accelerating voltage of 20 keV was used, as recommended, because at least one series of X-rays from every element would be excited (Oxford Instruments, 2008).

**A quant specification** was reported for selected 'spectrums' in chapters 4 and 5. The acquisition of atomic % of particular elements on the sediment surface can allow stoichiometric relationships to be postulated and help in the identification of minerals. For example where the atomic% of Pb and sulphur are similar (table 2.5) the 1:1 molar relationship could indicate the presence of galena (PbS). A processing speed of 5 was used as recommended for an unknown sample this lowered noise and optimised resolution (Oxford Instruments, 2008).

A Quant specification calculation was carried out automatically through the INCA software using the following methodology: A 'top-hat' filtering method was used to suppress background emission. Accurate intensity measurements were obtained through the use of a quant optimization standard that produced known peaks. The peak intensity was derived using a least squares fitting routine for standard peaks of known composition. Matrix corrections used an correction method (XPP, developed by Pouchou and Pichoir) where apparent concentrations are used to calculate correction factors for precise estimates of concentrations and an iterative procedure was used to achieve concentrations within 0.01% (Oxford Instruments, 2008).

Apparent concentration = (intensity of sample / intensity of the standard) * wt %
std

Weight  %  = Apparent concentration / intensity correction

Atomic % = Weight % / Atomic weight (the sum of atomic weights for all elements
in the sample were normalized to 100%)

**Table 2.5 Quant specification, Element weight% and atomic% for 'spectrum 1' (see figures 2.8 and 2.9), oxygen (O), silicon (Si), Sulphur (S), Fe and Pb (source original 2014) (UOB).**

| Element | Weight% | Atomic% |
|---------|---------|---------|
| O K     | 39.07   | 80.96   |
| Si K    | 1.50    | 1.78    |
| S K     | 8.53    | **8.82** |
| Fe K    | 0.69    | 0.41    |
| Pb M    | 50.20   | **8.03** |
| Totals  | 100.00  |         |

A smart map function was used in chapters 4 and 5 to produce a 2D map of elements using acquired x-ray data. This was intended to show the association of different elements on (or near to) the sediment surface using a processing speed of 2.

## 2.2.11 X-ray Diffraction (XRD)

XRD was carried out in combination with SEM/EDS in chapters 4 and 5 to identify unknown crystalline solids in the sediment samples using a Rigaku Miniflex XRD with Cu anode (Liverpool John Moores University).

Freeze dried sediment was ground into a fine powder and smoothed into a mount (figure 2.10). The fine powder ensured crystals were randomly oriented and had uniform intensity. For a reproducible intensity, powder should be < 10 μm, preferably 1 μm (I.C.D.D., 2008).
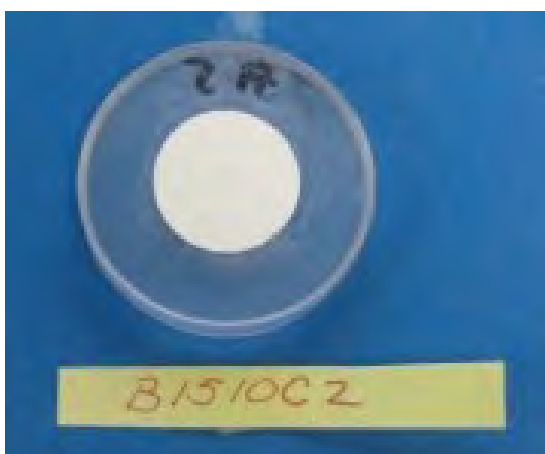


**Figure 2.10 Fine powder in a mount for XRD analysis (I.C.D.D., 2008)**

During XRD an X-ray of known wavelength (λ) is incident upon a crystal. The x-ray causes the atoms in the crystal to oscillate and electrons 'scatter' x-rays of the same frequency as the incident wave. In this way each atom in each crystal plane produces a diffraction pattern.

XRD works on the principle of constructive interference (figure 2.11) e.g. Wave number 3 is incident on a lower crystal plane than wave number 2 so it would need to travel twice the distance of incident wave 2. If that extra travelling distance

is an integer the reflected waves from each plane will be 'in phase' and that will

intensify the signal received by the defractometer.

In that case Bragg's condition is satisfied:    $n\lambda = 2d_{(h,k,l)} \sin\Theta$

Where :

d = the spacing between planes,
$\lambda$ = the wavelength of the incident and reflected wave,
n = the number of additional wavelengths the reflected wave has travelled,
$\Theta$ = the angle between the incident wave and the crystal plane
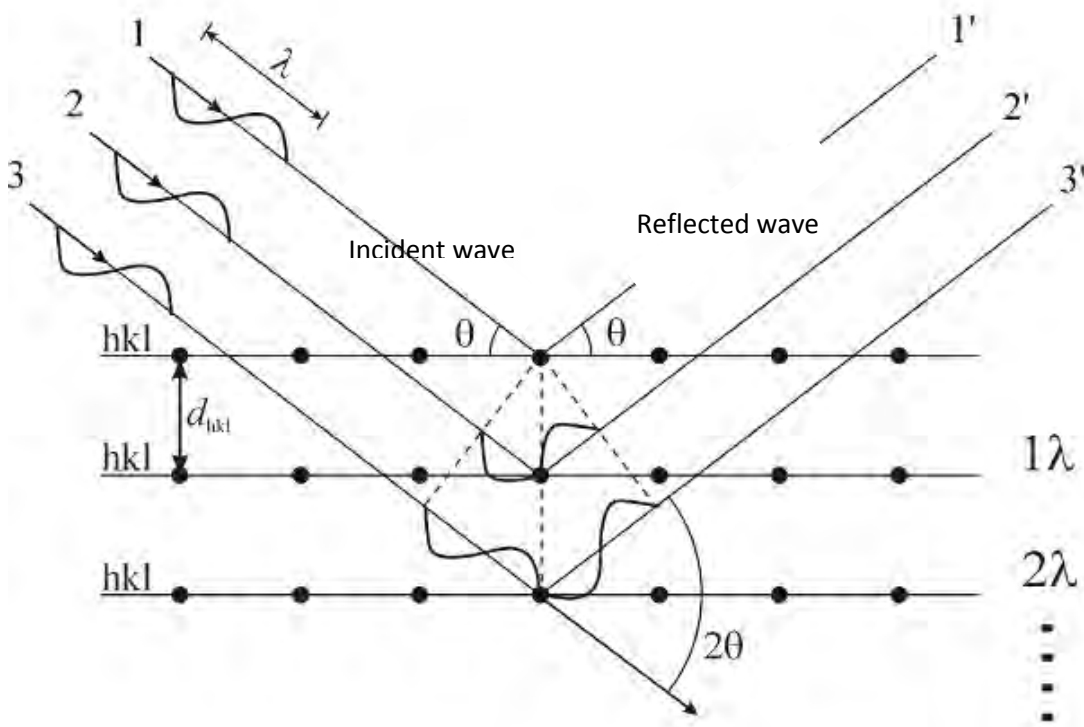


**Figure 2.11 Diffraction of waves incident on a crystal solid. Horizontal lines represent crystal planes, black dots atoms on each plane, h, k, I are Miller Indices (appendix 2.2.11) (modified from Ku Leuven, 2010)**

A diffractometer can be used to determine the interatomic spacing and the arrangement of atoms in a crystal. The XRD device rotates at different $\Theta$ angles and the intensity of the reflected waves will vary depending on the angle (as a result of constructive interference as discussed above). The intensity of the reflected waves is measured as a function of the $2\Theta$ angle (figure 2.12).
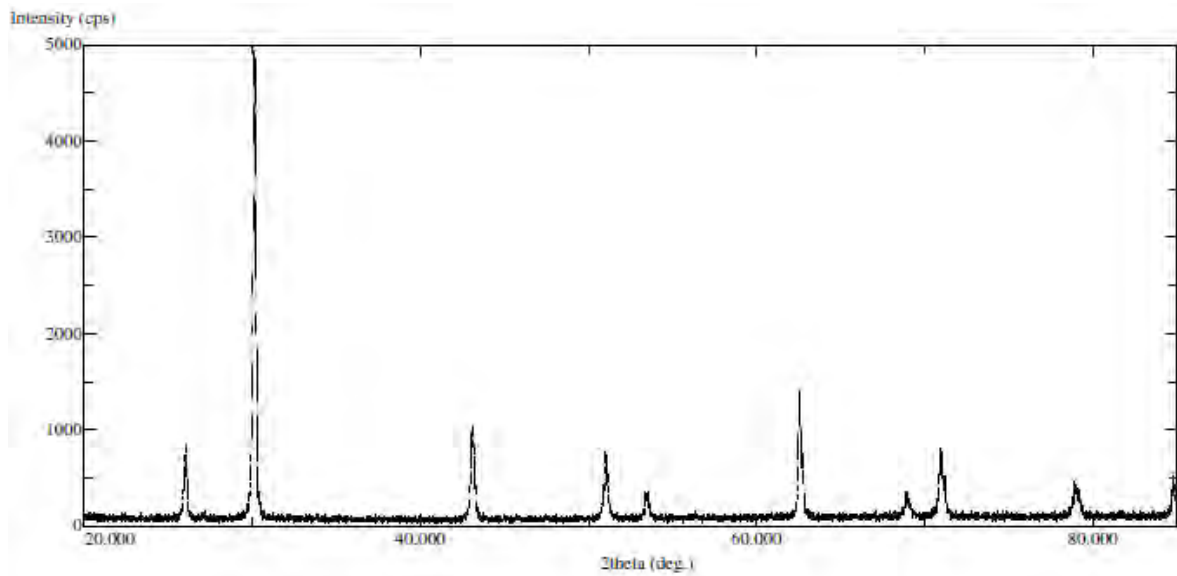


**Figure 2.12 X-ray diffraction pattern for a crystal standard of Galena (PbS) showing intensity maxima as a function of $2\Theta$ angle. Maxima occur where Bragg's conditions is satisfied (source original, 2014).**

Intensity peaks measured by the diffractometer can be interpreted by using the $2\Theta$ angle to calculate 'd' the spacing between crystal planes (table 2.5).

Bragg's condition can be re-arranged to give:     $d = \lambda / 2 \operatorname{Sin}\Theta$

**Table 2.6 Miller indices, first three 2Θ 'maxima' and Θ angles for galena (PbS) (as per figure 2.12) for incident wave length (λ) copper Kα (1.542 Å), with calculated 'd' and 'a' values (a is the lattice constant).**

| *Miller indices h, k, l | 2Θ angle | Θ angle | **d** | a |
|---|---|---|---|---|
| 1, 1, 1 | 25.96 | 12.98 | **3.43** | 5.94 |
| 2, 0, 0 | 30.07 | 15.035 | **2.97** | 5.94 |
| 2, 2, 0 | 43.05 | 21.525 | **2.1** | 5.94 |

*An explanation of Miller indices and calculation of the lattice constant is provided in appendix 2.2.11. The lattice constant for galena is 5.94 Å (I.C.D.D., 2008) as can be seen in table 2.6 that corresponds with the calculated 'a' value.

The calculations are provided for information only. For the current project software package SIeve for PDF2 was used to identify minerals.

In chapters 4 and 5 a powdered sample was placed in the XRD instrument and an X-ray diffraction pattern was acquired. An output file was produced with automatically calculated 'd' values. SIeve software was used to identify minerals from the extensive list of 'd' values acquired during analysis. The data was imported as a txt file into data processing software package SIeve for PDF2. PDF2 through I.C.D.D.'s SIeve option (I.C.D.D., 2008) treated the data to remove background x-rays, normalise intensities and identify peaks. These peaks were then matched by 2Θ angle to a database of minerals. Many minerals have characteristic peaks at high 'd' spacings (low Θ angles). Therefore intensity overlaps are common at low angles. For this reason intensity 'maxima' were obtained over a wide angle range (5 – 90 degrees).

This technique was for qualitative purposes only and was used in combination with SEM/EDS and sequential extraction to identify unknown crystalline solids in the sediment samples.

## 2.2.12 Statistical analysis non-parametric tests

In chapters 3 and 5 the Wilcoxon rank sum test was carried out to identify significant differences in pore water data. Calculations were performed using SPSS 20.0. Data for the independent t-test was visually inspected (histograms and p-p plots) and numerically assessed for skewness and kurtosis. It was found that even after transformation some data sets showed a significant skew and/or kurtosis. Additionally, Levene's tests revealed that for some data groups the variances were significantly different even after several transformations. Therefore the non-parametric Wilcoxon rank sum test was applied.

Wilcoxon rank sum test can be used to test the differences between two conditions by comparing the medians of each group. All observations for two groups are ranked together and the sum of the ranks for each of the two groups is calculated. The test statistic 'W' for this test is the sum of ranks in the group that either contains the fewest observations or if both groups are the same, the smaller ranked sum. The $mean_W$ and standard error of this statistic $SE_W$ are calculated from the sample sizes of each group. The test statistic W, the $mean_W$ and $SE_W$ are used to calculate the z-score if the z score is >1.96 or <-1.96 there is a significant difference between the two groups at the α 0.05 level, a z score >2.58 or <-2.58 is significant at α 0.01 level and a z score >3.29 or <-3.29 is significant at α 0.001 level (Fields, 2009).

In chapters 3 and 5 Wilcoxon rank sum tests were used to highlight differences in a) dissolved Pb and Zn concentrations at the start and end of a flood b) the release of dissolved Pb and Zn over a flood between the top and bottom of the mesocosm.

Spearman's rho a non – parametric version of Pearson correlation was used to test for relationships between Pb and pore water variables and Zn and pore water variables in chapters 3 and 5. As the nature of the relationship between Zn/Pb and other variables was unknown the 2-tailed (non-directional) test was selected. Calculations were performed using SPSS 20.0.

## 2.2.13 Principal Component Analysis (PCA)

PCA was carried out in chapters 3 and 5 to determine key factors linked to the mobility of dissolved Zn and Pb for selected variable runs at the bottom of the mesocosms.

PCA is a variable reduction technique that decomposes the original data into linear components or factors. A matrix representing the relationship between variables is used to calculate linear components by determining eigenvalues. Eigenvectors are calculated from these eigenvalues and provide the loadings of a variable on a factor (Field, 2009).

The importance of a factor with regards to explaining the percentage variance of the data can be assessed from the eigenvalue. Generally factors with eigenvalues over Kaiser's criterion of '1' are recommended for selection (Field, 2009). For selected factors eigenvectors, (the loadings of a variable on a factor), can indicate

what underlying variables are highly associated with that factor, allowing an assumption to be made as to what that factor may represent.

Sampling adequacy is necessary to ensure reliability of factor analysis. Recommendation of sample size varies (Field, 2009), however the Kaiser-Meyer-Olkin (KMO) measure of sampling adequacy was used. A KMO statistic between 0.5 – 0.7 is mediocre, 0.7 – 0.8 is good, 0.8 – 0.9 is great >0.9 is superb (Field, 2009).

Underlying variables within a factor should correlate. For that reason, Bartlett's test of sphericity was run to test this assumption by comparing the data correlation matrix with an identity matrix (where no variables correlate).  Bartlett's test was significant where the data's correlation matrix was significantly different to an identity matrix. A significant result indicated the variables within a factor correlated (Field, 2009).

Factor rotation was chosen based on whether the factors were thought to be unrelated (orthogonal) or related (oblique).
Orthogonal factors are rotated and kept independent of each other.
Oblique factors are allowed to correlate (Field, 2009).

A score was calculated for each observation and for each factor. The scores were mapped on a scatter plot where the two selected factors were the 'x' and 'y' axis. High variable loadings on each factor were also indicated on this plot. This allowed some indication as to what each factor might represent, how that linked to the sediment conditions created through wetting and drying and ultimately how that influenced dissolved Zn and Pb concentrations.

## 2.2.14 PHREEQC (Ph-Redox-Equilibrium in "C")

For this study the geochemical computer program PHREEQC was used for speciation and saturation index (SI) calculations using the WATEQ4F.dat database distributed with the PHREEQC program. The log K's and reaction enthalpies can be different for different databases and that can affect solubility calculations. However the WATEQ4F.dat is the PHREEQC.dat database extended with many heavy metals (Appelo and Postma, 2010) and was chosen for use as it was found to hold data for a wider mineral selection than PHREEQC.dat.

In chapters 3 and 5 the WATEQ4F database was used to calculate the saturation state of various minerals, using input data derived from pore water measurements for selected runs.

Data was considered acceptable if charge balance ($\leq$ 5%).

Electrical charge balance (%) = (cations + (-anions))/ (cations –(-anions)) * 100

Data was charge balanced by altering Na ($\pm$6 mg/L) for selected runs. Altering Na slightly did not alter the SI for minerals displayed.

Saturation state $\Omega$ can be expressed as the ratio between ion activity product (IAP) and solubility product (K) and is generally expressed on a logarithmic scale to allow for comparison against a SI. Using the mineral anglesite ($PbSO_4$) as an example:

$\Omega$ = IAP/K    or SI = log ($IAP_{anglesite}$ / $K_{anglesite}$)

$IAP_{anglesite}$ = $[Pb^{2+}][SO_4^{2-}]$ (activities in pore water sample)

$K_{anglesite}$ = $[Pb^{2+}]$ $[SO4^{2-}]$ (activities at equilibrium)   (Appelo and Postma, 2010)

SI = < 0 undersaturation, SI = 0 ($\pm$ 0.2) saturation, SI > 0 supersaturation

For undersaturation, dissolution would be expected and supersaturation suggests precipitation (Appelo and Postma, 2010).

## 2.2.15 DET analysis

In addition to pore water and sediment analysis DET analysis was carried out in chapter 5. The aim of using DET was to measure the interaction of solutes at a higher spatial resolution (cm scale) than could be achieved through bulk pore water analysis. It was hoped this would (i) further corroborate the results obtained through pore water analysis, (ii) minimise oxidation, precipitation and sorption of redox sensitive solutes that could occur due to exposure to atmospheric conditions, (iii) provide information regarding the co-distribution of solutes at a higher spatial scale to identify the mechanisms of dissolved Pb and Zn release that may have been missed through bulk pore water analysis.

To allow time for the wet and dry sequences to become established and so measure differences in element release as a result of that wet and dry sequence the flood period chosen for analysis was towards the end of each treatment period.

DET probes supplied by (DGT Ltd) were kept in a sealed plastic bag with a few drops of 0.01M NaCl in the fridge until use. Instructions for use were supplied with the probes by DGT Ltd.

The DET probe consisted of a high porosity polyacrylamide gel made of 95% water. The gel was under and overlain with a 0.45 µm filter membrane and

secured in a plastic casing with a window opening of 15 cm length and 1.8 cm width (figure 2.12). The window allowed direct contact with pore water once deployed (Ullah et al., 2012).
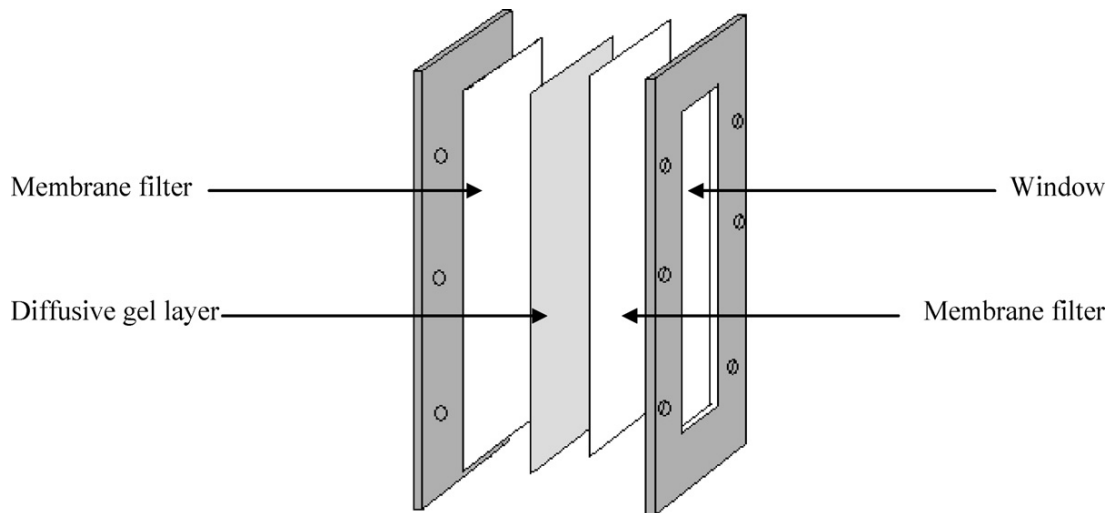


**Figure 2.13 DET gel assembly (Ullah et al., 2012)**

Prior to deployment the probes were deoxygenated. DET probes were immersed in 0.01 mol NaCl solution (recommended by DGT Ltd for freshwater analysis) in an acid washed wide necked conical flask. The flask was capped and bubbled under nitrogen gas in a fume cupboard for 24 hours. Deoxygenation was intended to prevent precipitation of reduced Fe and Mn on deployment of the probe (Davison et al., 2000).

At the start of a flood a stainless steel trowel was used to create a hole in the sediment in order to deploy the probe vertically into the mesocosm. The deoxygenated DET probe was transferred from the conical flask to the mesocosm allowing only a few seconds for the transfer (to minimise contact with the air).

The probe remained deployed until equilibration was reached (concentration of the solutes in the gel equalled concentration of the solutes in the pore water). Diffusion of solutes into the gel depletes concentrations in the pore water adjacent to the sampler window. Harper et al. (1997) noted that deployment times required for equilibration depends on re-supply of solutes (through desorption or dissolution) from the sediment in addition to gel thickness. These authors calculated that it would take 18 minutes to 36 hours for 99% equilibration of a 0.4 mm thick gel where resupply of solutes from the sediment was consistent (fully buffered) but where no resupply of solutes occurred (diffusion only) 99% equilibration took 78 hours. Their experimental observations however showed that deployment times for equilibration fell between the modelled buffered and diffusive case and were consistent with a modelled partial re-supply case. Therefore the author's experimental data indicated that a partial re-supply case was most likely to occur in natural sediment and an equilibration time falling between 36 hours and 78 hours would be a sufficient deployment time for full equilibration.

For the current DET analysis carried out on coarse grain sediment (rather than the fine grained sediment used in the studies above) the sample methodology used by Ullah et al. (2013) and Byrne et al. (2014), field studies carried out on coarse grain sediment, was used. These authors found that full equilibration occurred over a 72 hour deployment time. A recommendation to use this deployment time was also given by DGT Ltd. Research had found that this deployment time would be sufficient for sediment to collapse around the probe, redox potential conditions to become re-established and for full equilibration to be achieved (Ullah et al., 2013).

Probes were inserted for 72 hours at the start of a flood and 72 hours prior to the end of a flood.

After deployment the DET probes were carefully removed from the sediment and, using a Teflon coated razor blade, the gel and the filter membranes were cut from the window. The top filter membrane was removed but the base filter membrane was kept in place. The gel and filter membrane were placed on the glass tray and using the Teflon razor blade cut into 1 cm slices. Each gel strip was added to a pre-labelled 1.5 ml Eppendorf vial with 1 ml nitric acid (1 mol). Five minutes was allowed for probe removal and gel cutting to minimise peak relaxation due to diffusion of solutes through the gel, although relaxation effects are likely to be minimal for analysis at 1 cm resolution (Byrne et al., 2014). Strips were kept in the vial with nitric acid in the fridge until analysis (as advised by DGT Ltd). A blank DET probe underwent all analysis except deployment.

Prior to analysis the Eppendorf vials were shaken on a reciprocating shaker for 24 hours to allow for back equilibration of Fe, Mn, Pb and Zn from the gel to the nitric acid.

For ICP/OES and IC analysis the samples were diluted 1:10 with DIW so that there was enough sample to analyse all elements. 1 ml of the diluted sample was added to a labelled 1.5 ml vial and stored in the freezer (-20°C) for IC analysis (section 2.2.4) and 9 ml was kept for ICP/OES analysis (see method 5.2.5). The dilution factor based on the volume of DET strip diluted in 1 ml nitric acid (as carried out by Ullah et al., 2012; Ullah et al., 2013) with a further dilution x10 with DIW to allow for subsequent analysis by ICP/OES and IC analysis was (x56).

Concentrations of Fe, Mn, Pb Zn in 10 blank DET samples were below detection.

Analytical accuracy of repeat control standards were < 5% for Fe, Mn, Pb and Zn.

# 3. ESTABLISHING THE IMPORTANCE OF WET AND DRY SEQUENCES ON THE RELEASE OF PB and ZN IN METAL MINING CONTAMINATED RIVER BANK SEDIMENT

## 3.1 Introduction

This chapter investigates the potential for Pb and Zn polluted sediment to become a source of trace metal contamination to river systems under variable wet and dry conditions. The submergence and exposure of contaminated river bank sediment brought about through inundation and draining can promote contaminant trace metal release to pore and surface water and pose a serious environmental risk to river systems. The magnitude of trace metal release can vary as a result of geochemical, mineralogical and environmental factors that may be linked to the length of time metal contaminated sediment is submerged and exposed.

Quantifying, and identifying the key mechanisms of, contaminant trace metal release is necessary to understand the environmental risk metal-contaminated sediment may pose. This is particularly important in light of the longer drier antecedent conditions (DEFRA, 2012a) followed by more frequent, large flood events predicted as a result of future climate change in Northern and Western Britain (Hannaford and Marsh, 2008; DEFRA, 2012b).

Pb and Zn can exist in a variety of forms such as hydroxides, chlorides, sulphates and carbonates in the sediment of mining impacted systems (table 3.1) (Salomons et al., 1987; Desbarats and Dirom, 2007; Du Laing et al., 2009). The partitioning of these trace metals has been found to depend on properties of the metal (Hamilton Taylor et al., 1997; Wen and Allen, 1999; Smith, 1999) and the pH (Boult et al.,

1994; Lee et al., 2002), anion composition (Baltpurvins et al., 1996), the ionic strength (James and MacNaughton, 1977) and redox potential (Wen and Allen, 1999) of the aqueous solution. The partitioning and speciation of trace metals is important because it relates to bioavailability and toxicity (vanLoon and Duffy, 2011).

Often in these systems Zn and Pb are partitioned with redox sensitive minerals such as Fe, Mn hydroxides and sulphur (Wen and Allen, 1999; Li et al., 2001; Du Laing et al., 2009). Therefore where redox potential changes occur at locations along the river bank, precipitation and dissolution of Fe, Mn and sulphur minerals potentially control the release of dissolved Pb and Zn to rivers (Patrick and Delaune, 1972; Eggleton and Thomas, 2004).

**Table 3.1 Pb and Zn partitioning within metal contaminated sediment**

| Metal | Sediment Fraction | pH | Redox Potential | Reference |
|---|---|---|---|---|
| $Pb^{2+}$ | Fe hydroxide | Circum neutral | Oxic | Desbarats & Dirom, 2007 |
| $Pb^{2+}$ | Natural Organic Matter | Circum neutral | Oxic | Hamilton Taylor, 1997 |
| $Pb^{2+}$ | Mn hydroxide | Circum Neutral | Oxic | Eggleton and Thomas, 2004 |
| $Pb^{2+}$ | Sulphate | < 6 | Oxic | Nordstrom and Alpers, 1999 |
| $Pb^{2+}$ | Sulphide | 6.5 | Reduced | Weber et al., 2009 |
| Pb2+ | Carbonate | Circum neutral | Oxic /Reduced | Nordstrom and Alpers, 1999 |
| $Pb^{2+}$ | Oxide | | Oxic | Barrett et al., 2010 |
| $Zn^{2+}$ | Fe Hydroxide | Circum neutral | Oxic | Parkman, 1996; Desbarats & Dirom, 2007; Du Laing et al., 2009 |
| $Zn^{2+}$ | Mn Hydroxide | Circum neutral | Oxic | Du Laing et al., 2009 |
| $Zn^{2+}$ | Sulphide | Circum neutral | reduced | Parkman, 1996; Eggleton and Thomas, 2004 |
| $Zn^{2+}$ | Carbonate | > 7 | Oxic | Khodaverdiloo et al., 2012; Carroll et al., 1998 |
| $Zn^{2+}$ | Oxide | > 7 | Oxic | Carroll et al., 1998 |

Pb and Zn are listed in the European Community (EC) Dangerous Substances Directive (76/464/EEC), because of their known toxic effects. Zn is an essential metal but at high concentrations has toxic effects. Pb has no biological role and is toxic at very low doses. In the UK statutory environmental quality standards (EQS) are set for the protection of surface water (table 3.2). These surface water requirements must be met in order to achieve 'good' standard of rivers and freshwater lakes necessary to meet the EU Water Framework Directive (WFD)

requirements. The influence of water hardness on toxicity of Zn, means that EQS
for Zn are water hardness ($CaCO_3$) banded.

**Table 3.2 EQS for Pb and Zn for the protection of surface water**
**Annual average values (Environment Agency, 2011)**

| Trace metal | EQS µg/L | Description |
|---|---|---|
| **Pb** | 7.2 | Dissolved concentration. |
| **Zn** | 8 | 0 – 50 mg/L $CaCO_3$ (hardness) Total concentration |
| **Zn** | 50 | 50 – 100 mg/L $CaCO_3$ Total concentration |

Previous laboratory studies have investigated (i) the effects of inundation and
prolonged flooding of contaminated soil (Weber et al., 2009) and sediment (Wragg
and Palumbo-Roe, 2011), and (ii) the oxidation of anoxic sediment through batch
studies (Caille et al., 2003) to determine the subsequent mobility of contaminant
trace metals Pb and Zn. Weber et al. (2009) carried out inundation experiments
(52 days) on metal contaminated floodplain soil collected from the river Mulde,
Germany. A microcosm set-up for saturated sediment (9 cm depth) found that Pb
and Zn were initially mobilised due to the reductive dissolution of Fe and Mn
hydroxides, however, as flooding continued, the reduction of sulphate resulted in
the partial sequestration of Pb but not Zn, they concluded that the control of metal
contaminant mobility through sulphide precipitation was dependent on the relative
thermodynamic stability of the respective metal sulphides. Wragg and Palumbo-
Roe (2011) carried out inundation experiments (88 days) on mining contaminated
sediment collected from five locations along Rookhope Burn, in the Northern

Pennine Orefield, UK. Oxidised, surface water measurements were taken from saturated sediment samples (2.5 cm depth). They found that dissolved Pb increased over flood periods where concentrations in the sediment were high and galena and cerussite were detectable through X-ray diffraction. It was suggested that cerussite, formed through the oxidation of galena, may have controlled the pore water concentration of dissolved Pb. These authors noted that dissolved Zn concentrations were often independent of the original concentration in the sediment, with the release of dissolved Zn possibly related to Zn partitioning with Mn hydroxides and subsequent dissolution of this mineral following a decline in redox potential conditions (Wragg and Palumbo-Roe, 2011). Caille et al., (2003) carried out a batch experiment (76 days) to oxidise metal polluted (Zn, Pb, Cu) dredged sediment collected from the Scarpe canal, Northern France. These authors found that during the first few days the release of all metals increased as a result of the oxidation of sulphide minerals and there was an initial fall in pH. However, following that a rapid decline in dissolved Pb and Zn concentration coincided with an increase in pH and a fall in dissolved Fe. Results from geochemical modelling using MINTEQA2 indicated that conditions were near saturation with respect to calcite and these authors suggested that the increase in pH was as a result of buffering effects from calcite dissolution and trace metal attenuation was linked to the oxidation of reduced Fe and precipitation of ferric-hydroxides (Caille et al., 2003).

A few studies have analysed the effects of wetting and drying sequences on metal contaminated soil or sediment. Du Laing et al., (2007) assessed the influence of varying hydrological regimes on the mobility of Zn in a calcareous metal polluted

sediment-derived-soil collected from the Upper Scheldt, Belgium. Mesocosm experiments (96 days) on soil 10 cm deep were found to result in a pulsed release of dissolved Zn over flooded periods, these authors found that for sequences with long dry periods, a correlation between dissolved trace metals and calcium was apparent and proposed Zn mobility was controlled primarily by processes related to release of calcium such as the dissolution of carbonates. However, for sequences with long wet periods, where sufficiently strong reducing conditions were established mobility of Zn may have been affected by the formation and re-oxidation of sulphides (Du Laing et al., 2007). Khodaverdiloo et al. (2010) carried out a series of saturation and evaporation sequences (160 days) on an alkaline soil spiked with Pb nitrate. High concentrations of carbonate and clay minerals were found to immobilize Pb over time and resulted in a decline in dissolved Pb concentrations. These authors noted that during prolonged incubation under wetting and drying sequences Pb was redistributed slowly from soluble, exchangeable and carbonate-bound fractions to more stable residual fractions that reduced the lability of Pb in the soil.

The sediment and soil used in the above studies displayed circum-neutral pH conditions and was generally high in carbonates. Under these conditions any decline in pH could be buffered through the dissolution of carbonate minerals in the sediment (Komarek and Zeman, 2004). Moreover, in systems high in carbonates, where saturation is reached metal mobility may be controlled by the precipitation of metal carbonates such as cerussite ($PbCO_3$) (Wragg and Palumbo-Roe, 2011). Trace metals Pb and Zn may also be exchanged for Ca, Fe and Mn in carbonate minerals (Cravotta, 2008) and that can serve to attenuate

these contaminants. However carbonate minerals are susceptible to a fall in pH and dissolution of metal carbonates can result in the release of trace metal contaminants (Palumbo-Roe et al., 2009). In sediments where sulphide concentrations in the sediment are higher than carbonate concentrations other processes may influence the release of Pb and Zn such as the oxidation of metal sulphides (Hudson-Edwards et al., 2003; Baskerville and Evans, 2006) and the dissolution of metal sulphate salts that have precipitated over long dry periods (Alastuey et al., 1999; Buckby et al., 2003). These are generally acid producing processes and where carbonate concentrations in the sediment are low, a fall in pH may be poorly buffered and that could serve to mobilise trace metals further. Where sediments are high in sulphides, the oxidation of galena and subsequent release of Pb and sulphate may result in mineral saturation and precipitation of anglesite ($PbSO_4$) that can control Pb solubility (Harris et al., 2003; Palumbo-Roe et al., 2013). Alternatively under low redox potential conditions the precipitation of metal sulphides could control the solubility of Pb and Zn (Du Laing et al., 2007). Changes in redox potential brought about through wetting and drying sequences could alter the reactivity of Fe and Mn minerals over time as freshly precipitated minerals are reported to be highly reactive (Shuman, 1977; Gambrell, 1994; Ford et al., 1997; Wen and Allen, 1999; Lee et al., 2002; Hudson-Edwards, 2003) and that could influence contaminant trace metal mobility. Currently there are no known studies that have investigated the influence of wetting and drying sequences on the mobility of Pb and Zn in mining polluted sediment sampled from a low alkalinity 'base-poor' geological environment likely to be high in trace metal sulphides galena and sphalerite.

In light of climate change predictions, if we are to fully understand the environmental risk of metal mining contaminated sediment, research efforts must focus on understanding the magnitude and key mechanisms of release for contaminant trace metals Pb and Zn in response to wet and dry sequences of different duration and frequency.

### 3.1.1 Aim, Objectives and Hypothesis

An experimental approach was used to determine the effect of wetting and drying sequences on the release of metal contaminants, Pb and Zn, from mining polluted sediments collected from 'base poor' geological site. Within the overall aim, several objectives were identified:

To provide evidence for biogeochemical processes controlling Pb and Zn mobility in response to different wet and dry sequences.

To establish the specific combination of wetting and drying that caused the greatest release of dissolved Pb and Zn.

To determine whether wetting and drying sequences resulted in Environmental Quality Standards (EQS) being exceeded for Pb and Zn.

**It is hypothesised that:**

Over flooded periods, where penetration of oxygen is limited, at depth in the sediment, an increase in dissolved Pb and Zn will be observed due to the microbial reductive dissolution of Fe and Mn hydroxides - where Pb and Zn are associated with these minerals (Du Laing et al., 2009, Torres et al., 2013).

Over prolonged flooding, where conditions become sufficiently reducing (Ross, 1989; Gambrell et al., 1991; Bartlett, 1999) and labile organic matter (Morse et al., 2002; Ku et al., 2008) and sulphate concentrations (Lovley and Klug, 1986) are sufficiently high, Pb and Zn may be attenuated through the reduction of sulphate and precipitation of metal sulphides (Nordstrom and Alpers, 1991; Billon et al., 2001).

Where sediment is exposed to atmospheric conditions, oxidation of reduced minerals galena and spalerite may result in the release of sulphate, Pb and Zn to pore water (Eggleton and Thomas, 2004; Wragg and Palumbo-Roe, 2011). The formation of metal sulphate complexes can serve to keep trace metals mobile under hydrologically saturated conditions (Cravotta, 2008). However anglesite is poorly soluble and the precipitation of anglesite could maintain dissolved Pb concentrations at lower levels, where mineral saturation is reached (Nordstrom and Alpers, 1999; Palumbo-Roe et al., 2013).

The oxidation of reduced Fe and Mn may result in a decline in dissolved Pb and Zn where these trace metals co-precipitate with and adsorb to Fe and Mn hydroxides  (Evans 1991, Desbarats and Dirom 2005, Davis and Kent 1990, Charlatchka and Cambier 2000).

Over long dry periods the evaporation of pore water and precipitation of metal sulphate salts could serve to attenuate Pb and Zn in the short term (Buckby et al., 2003; Nordstrom, 2009). When flood conditions return subsequent dissolution of these highly soluble metal sulphates could release high concentrations of Pb and Zn back into pore water (Harris et al., 2003; Byrne et al., 2009).

## 3.2 Methods

### 3.2.1 River water physicochemical conditions

The pH, temperature and conductivity of river water was measured on the day of sediment sampling using a calibrated single multiparameter meter (YSI 556, YSI hydrodata Ltd, Letchworth, UK). On $6^{th}$ July 2012, pH 5.4, temperature 15.5 °C and the conductivity was 18 – 24 µS cm$^{-1}$.

### 3.2.2 Sediment collection

Visual inspection of the northern river bank indicated that sediment was made up of predominantly sandy gravel interspersed with some finer silt particles and larger pebbles and boulders.

In order to achieve a holistic overview of the potential environmental risk the contamination at the site posed, samples were taken from a variety of locations on the north bank of the river (plates 3.1 and 3.2). A shovel was used to collect approximately 0.1 m$^3$ from the top 10 cm of sediment. Quantity of sediment required was calculated based on number and size of columns to fill, multiplied by 3 (to allow for spare).

**Plate 3.1 Site of sediment collection (1) location marked with arrow**



**Plate 3.2 Site of sediment collection (2) location marked with arrow**

### 3.2.3 Laboratory Methods

To try to preserve the sediment characteristics and mineralogical relationships sediment was not treated with chemicals, crushed or sieved. Crushing the sediment would have exposed additional surface areas to pore water changes (in response to the wet and dry runs), potentially increasing the reactivity of minerals in the sediment and altering the experimental results. Sieving the sediment would have reduced the particle size that may have influenced (i) the penetration of oxygen into lower layers altering the redox conditions and therefore influencing the experimental results and (ii) impeded drainage. Adequate drainage was necessary for sampling of pore water.

In order to encourage similar conditions in each mesocosm the sediment was first homogenised by hand using a plastic trowel. Similar particle sized sediment was picked out by hand and added to each mesocosm. Each mesocosm was packed to the same height (24 cm deep) using a plastic trowel. Additionally, as noted in section 2.2.1, each column was then held at field capacity for 20 days prior to the start of wet and dry treatment. That was intended to allowed time for mesocosms to settle into a steady pattern and help to encourage similar conditions.

All sample points were numbered (plate 3.3). Sample points were located at the top (0 deep), middle (10cm deep) and bottom (24 cm deep) for all treatments except field capacity where pore water percolated through the mesocosm and was sampled from the bottom location only. Any un-sampled water was drained into a bucket and discarded. The temperature of the laboratory was approximately 20 °C.

**Plate 3.3 Mesocosm setup x21 (7 runs x 3 replicates)**

Mesocosms were left at field capacity for 3 weeks and then separated into 7 runs with different wet and dry treatments (figure 3.1). As noted in general methods section 2.1.5 the Cwmystwyth gauged daily flow (grid reference SN790737), taken from the UK National River Flow Archive (NERC, 2015), provided guidance regarding the length of time river bank sediment may be exposed or submerged.

| Run # | Sampling: | A | B | C | D | E | F | G | H | I | J | K | L |
|---|---|---|---|---|---|---|---|---|---|---|---|---|---|
| 1 | 1 week wet 1 week dry | Wet | Dry | Wet | Dry | Wet | Dry | Wet | Dry | Wet | Dry | Wet | Dry |
| 2 | 1 week wet 2 weeks dry | Wet | Dry | Dry | Wet | Dry | Dry | Wet | Dry | Dry | Wet | Dry | |
| 3 | 1 week wet 3 weeks dry | Wet | Dry | Dry | Dry | Wet | Dry | Dry | Dry | Wet | Dry | | |
| 4 | 2 weeks wet 1 week dry | Wet | Wet | Dry | Wet | Wet | Dry | Wet | Wet | Dry | Wet | Wet | Dry |
| 5 | 3 weeks wet 1 week dry | Wet | Wet | Dry | Wet | Wet | Wet | Dry | Wet | Wet | Wet | Dry | Dry |
| 6 | Constant flood (control) | Wet | Wet | Wet | Wet | Wet | Wet | Wet | Wet | Wet | Wet | Wet | Wet |
| 7 | Field Capacity (control) | FC | FC | FC | FC | FC | FC | FC | FC | FC | FC | FC | FC |

**Figure 3.1 – Wet and dry runs, weeks A – L (12 weeks)**

**Key:**

| | |
|---|---|
| Dry | (orange) |
| Wet | (blue) |

Each of the 7 runs had three replicate columns (total 21x mesocosms). Each replicate was subjected to the same wet and dry treatment. Pore and surface water was sampled from each replicate. The data was used to check that the patterns, and concentrations, of metal released into pore water in response to the different wet and dry runs were similar for each of the replicates.

Water samples were first taken from the top using a plastic syringe and then from the middle and bottom via the taps, in order to avoid mixing between levels. Using a Hanna Combo pH/EC and temperature hand held stick meter model No 98129, the pH, conductivity and temperature were recorded for each sample.

Each sample was filtered through a 0.45 μm PTFE syringe filter into two metal-free 60 ml centrifuge tubes. One sample was acidified with 4% nitric acid ($HNO_3$) to below pH 2.5 for metals (Fe, Mn, Pb, Zn, Cu, Ni) analysis by flame atomic absorption spectroscopy (FAAS). The other was frozen (-20 °C) for subsequent anion (sulphate, nitrate, phosphate, chloride) analysis by IC2000 Anion Dionex. After sampling, flood levels were kept at 5 cm above sediment level by topping up with artificial rain water that was based on Plynlimon rainwater chemistry (pH 4.9-5.2) (Neal et al., 2001). Mesocosms were then left *'in flood'*, with the taps closed, for the allotted timeframe.

Non purgeable organic carbon (NPOC) was measured using a carbon analyser (TOC-V CSN, Shimadzu). All pore water samples were filtered (0.45 μm) prior to analysis. See general methods section 2.2.6 for full details.

Organic and inorganic carbon in the sediment was measured using a Shimadzu solid module (SSM-5000A). A sub-sample of the initial untreated sediment and

sediment remaining at the end of the wet and dry run was sieved (2 mm) and weighed (no greater than 50 mg), and oven dried at 140$^{o}$C for 24 hours. See general methods section 2.2.7 for full details.

Unfiltered water samples were analysed using the standard operating procedure for Great Lakes National Program office (GLNPO) total alkalinity titration method (Palmer 1992) to measure mg/L of alkalinity as calcium carbonate. See general methods section 2.2.8.

For grain size measurement a vibration platform (Fritsch) and series of Endecotts sieves were used. A sediment sample was taken from the top and bottom of the mesocosm. Size-separated fractions were then divided into the following Wentworth size classes: pebbles >8 mm, granules and fine pebbles 2-8 mm, very coarse to very fine sand 63 μm – 2 mm, silt/clay <63 μm. See general methods section 2.2.9 for details.

### 3.2.4 Non-parametric statistical analysis

As discussed in general methods section 2.2.12 statistical analysis revealed the data was not normally distributed. Therefore non-parametric statistical analysis was conducted.

Wilcoxon rank sum test is a non-parametric version of the independent 't' test (Field, 2009) that can be used to test the differences between two conditions by comparing the medians of each group. In this chapter it was used to highlight differences in a) dissolved Pb and Zn concentrations between the start and end of a flood b) the release of dissolved Pb and Zn over a flood between the top and bottom of the mesocosm. See general methods section 2.2.12.

Spearman's rho a non-parametric version of Pearson correlation was used to test for relationships between Pb, Zn and pore water variables (Fe, Mn, Ca, pH, Sulphate, Nitrate). As the nature of the relationship between Zn, Pb and other variables was unknown the 2-tailed (non-directional) test was selected.

## 3.2.5 Simple Regression Analysis

Simple regression between logged dissolved Zn data and sample week (time) was used to assess whether there was a significant increase in the concentration of dissolved Zn at the end of a flood over treatment periods. The $R^2$ value was used to determine what percentage of the variation in dissolved Zn concentration was explained by time (sample week). An F ratio was used to determine if the regression model was a significantly better predictor of dissolved zinc than the mean concentration. The $\beta_1$ value was used to indicate the week by week increase in dissolved Zn (Field, 2009).

## 3.2.6 Principal Component Analysis (PCA)

PCA is a variable reduction technique that decomposes the original data into linear components or factors. In this chapter PCA was carried out to determine key factors linked to the mobility of dissolved Zn for selected variable runs at the bottom of the mesocosms. See general section 2.2.13 for a detailed description of this process.

## 3.2.7 PHREEQC (Ph-Redox-Equilibrium in "C")

WATEQ4F.dat database (the PHREEQC.dat database extended) was used to calculate the saturation state of various minerals, using input data derived from pore water measurements for selected runs (see general methods section 2.2.14). In some cases the pore water concentrations were found to be super-saturated with respect to anglesite. The 'equilibrium_phases' keyword was used to calculate the concentration of anglesite that would precipitate and subsequent dissolved Pb concentrations in pore water if conditions were brought to equilibrium and reached saturation with respect to anglesite.

**Key to run codes:**

| Run Code | Description |
| --- | --- |
| 1wwet | One week flood, followed by one week dry |
| 2wdry | Two weeks dry, followed by one week flooded |
| 3wdry | Three weeks dry, followed by one week flooded |
| 2wwet | Two weeks flooded, followed by one week dry |
| 3wwet | Three weeks flooded, followed by one week dry |
| Flood | Flooded continuously |
| F/C | Field capacity, unsaturated, water percolates through mesocosm |

## 3.3 Results

### 3.3.1 Summary

Pore water pH remained below neutral (5.3 ± 0.5) throughout the 12 weeks for all runs. Bicarbonate concentrations in the pore water were too low to be measured using the GLNPO total alkalinity titration method (Palmer, 1992). This method is used to measure up to 5000 mg/L as calcium carbonate. Where concentrations of calcium carbonate and bicarbonate are very low poor sensitivity can make determination of an end colour point very difficult. Further solid analysis of the sediment (SSM-5000A, Shimadzu), found inorganic carbon (IC) in the sediment below detection both prior to treatment and at the end of the run.

Average NPOC analysis was 1.4 (+0.14). Based on other literature values (Meybeck, 1982), this range was low – medium.

The sediment was predominantly sandy, interdispersed with larger pebbles. Grain sizes showed similar percentages at the top and bottom of the mesocosm (figure 3.2).
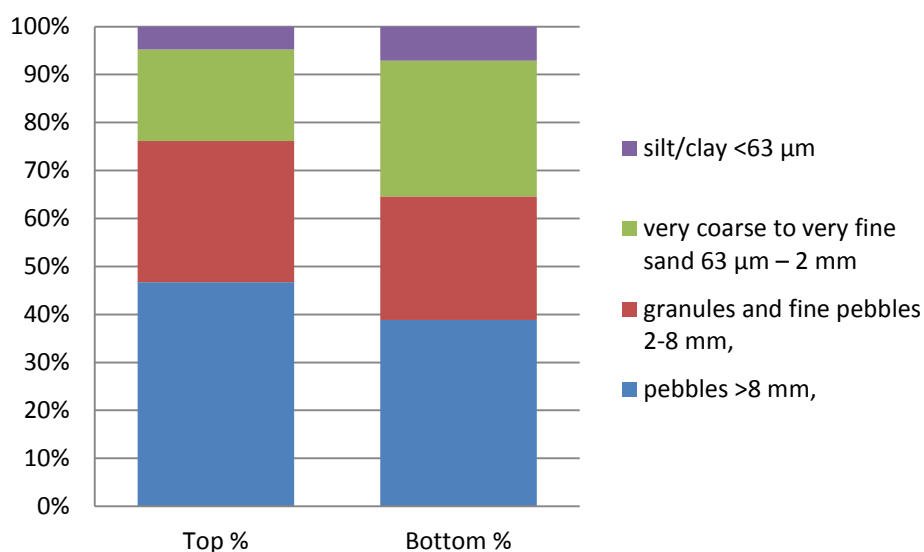
**Figure 3.2. Grain Size % Top and Bottom of the mesocosm**

Pb, Zn, Fe, Mn, Ca, Cl, nitrate and sulphate were detectable in pore water. Pb, Zn and sulphate were the highest dissolved analyte concentrations. Ni and Cu were below detection, in line with previous field study results for river water at the sample location (Montserrat, 2010).

For dissolved Pb, average concentrations were higher in the pore water at the top (T) of the mesocosms compared to the bottom (B) for all runs. The highest average concentration was measured for the three week wet run at the top of the mesocosm (21.5 $\pm$1.6 mg/L). The lowest average concentrations were for the flood run at the bottom of the mesocosm (10.9 $\pm$1 mg/L) and field capacity run (10.1 $\pm$0.9).

For dissolved Zn, average concentrations were higher in the pore water at the bottom of the mesocosms for all runs. The highest average concentration was measured for the three week dry run at the bottom (26.8 $\pm$2.9 mg/L). The lowest average concentration was for the field capacity run (7.7 $\pm$0.4 mg/L).

**Table 3.3: Mean and range (in parenthesis) of dissolved (<0.45μm) metals (mg/L), pH, Conductivity (μS/cm), Temperature (°C) at the end of a flood, by run, Top (T) and Bottom (B) of the mesocosm, key average values (bold and underlined), n=#[1]**

| Run Location | 1wwet (T) n=18 | 1wwet (B) n=18 | 2wdry (T) n=12 | 2wdry (B) n=12 | 3wdry (T) n=9 | 3wdry (B) n=9 | 2wwet (T) n=12 | 2wwet (B) n=12 | 3wwet (T) n=9 | 3wwet (B) n=9 | Flood (T) n=33 | Flood (B) n=33 | F/C (B) n=33 |
|---|---|---|---|---|---|---|---|---|---|---|---|---|---|
| pH | 5.2 | 5.3 | 5.1 | 5.2 | 5.1 | 5.2 | 5.1 | 5.3 | 5.2 | 5.4 | 5.3 | 5.5 | 5.2 |
| (Range) | (5 - 5.6) | (5.1 - 5.5) | (5 - 5.3) | (5.1 - 5.5) | (4.8 - 5.3) | (5 - 5.3) | (4.9 - 5.4) | (5.1 - 5.5) | (4.9 - 5.7) | (5.2 – 5.7) | (5 - 5.8) | (5 – 5.7) | (5.1 - 5.4) |
| Temp 0C | 22.3 | 23.1 | 22.3 | 23.0 | 23.0 | 23.8 | 22.6 | 23.3 | 22.0 | 22.7 | 22.4 | 23.1 | 22.9 |
| (Range) | (20.9 - 24.2) | (21.9 - 24.8) | (21.2 - 23.3) | (21.7 - 23.9) | (21.4 - 24.4) | (22.3 - 25.1) | (20.4 - 24.5) | (20.9 - 25.1) | (21.4 - 22.6) | (22.1 - 23.2) | (19.9 - 24.5) | (29.9 - 25) | (21 - 25) |
| Cond μS/cm | 110.6 | 183.2 | 100.2 | 188.4 | 110.9 | 208.3 | 134.2 | 208.1 | 156.4 | 230.4 | 105.8 | 248.6 | 77.9 |
| (Range) | (87 - 144) | (155 - 204) | (88 - 116) | (152 - 214) | (94 - 136) | (164 - 250) | (107 - 156) | (188 - 224) | (146 - 169) | (218 - 264) | (46 - 126) | (140 - 339) | (50 - 130) |
| Fe | 0.0 | 0.4 | 0.0 | 0.6 | 0.0 | 0.2 | 0.0 | 3.0 | 0.0 | 6.0 | 0.0 | 8.9 | 0.0 |
| (Range) | 0.0 | (0 - 1.7) | 0.0 | (0 - 1.6) | 0.0 | (0 - 0.8) | 0.0 | (2.2 - 3.9) | 0.0 | (3.6 - 10) | 0.0 | (0 - 27.7) | (0 - 0.5) |
| Mn | 0.2 | 1.6 | 0.2 | 1.6 | 0.2 | 1.4 | 0.3 | 5.3 | 1.5 | 7.7 | 0.5 | 9.6 | 0.4 |
| (Range) | (0.1 - 0.4) | (1.2 - 1.8) | (0.1 - 0.2) | (1.1 - 2.2) | (0.1 - 0.3) | (0.6 - 2.9) | (0 - 0.7) | (3.5 - 6.4) | (0.7 - 3.1) | (6.7 - 9.6) | (0 - 1.3) | (0.4 - 16.6) | (0 - 1) |
| Pb | 17.1 | 14.1 | 15.4 | 13.9 | 14.3 | 12.6 | 18.5 | 13.2 | <u>**21.5**</u> | 14.4 | 16.2 | <u>**10.9**</u> | 10.1 |
| (Range) | (9.8 - 22.3) | (8.6 - 24.3) | (13.2 - 17.2) | (12.5 - 15.2) | (10.8 - 16.8) | (10.6 - 16.1) | (14.7 - 24.4) | (10.1 - 13.2) | (16.7 - 30.6) | (9.7 - 24.7) | (5.2 - 27.2) | (3.9 - 28.5) | (4.2 - 23.7) |
| Zn | 11.2 | 20.7 | 8.3 | 21.8 | 11.2 | <u>**26.8**</u> | 15.8 | 21.4 | 15.5 | 18.8 | 10.0 | 17.5 | <u>**7.7**</u> |
| (Range) | (3.8 - 20.4) | (13.8 - 25.2) | (4.3 - 12.9) | (13.3 - 29.8) | (6.2 - 18.2) | (15.2 - 40.5) | (8.3 - 23.8) | (14.9 - 24.9) | (10.6 - 18.6) | (15.5 - 22.6) | (1.5 - 15.8) | (14.2 - 21.4) | (3.3 - 13.3) |
| Ca | 2.4 | 3.9 | 1.7 | 3.4 | 2.1 | 4.1 | 2.3 | 3.9 | 3.3 | 4.2 | 2.6 | 4.5 | 1.9 |
| (Range) | (1.7 - 3.4) | (2.6 - 5) | (1.4 - 2.1) | (2.1 - 4.5) | (1.9 - 2.9) | (2.7 - 5.9) | (1.6 - 2.6) | (2.6 - 5) | (2.8 - 3.8) | (3.9 - 4.7) | (1.5 - 3.6) | (2.8 - 6.8) | (1.3 - 2.8) |
| NO₃⁻ | 2.3 | 0.5 | 3.3 | 2.6 | 4.1 | 2.5 | 1.9 | 0.0 | 1.5 | 0.0 | 1.4 | 0.6 | 2.3 |
| (Range) | (0 - 5.7) | (0 - 1.5) | (2 - 4.9) | (0 - 4.8) | (2.6 - 5.7) | (0 - 6) | (0.9 - 3) | 0.0 | (0 - 3.2) | 0.0 | (0 - 4.2) | (0 - 8.7) | (0.7 - 4.2) |
| Cl- | 1.5 | 1.2 | 1.5 | 1.3 | 2.3 | 1.9 | 2.0 | 1.3 | 2.0 | 1.3 | 2.0 | 2.0 | 1.8 |
| (Range) | (0.3 - 2.9) | (0 - 2.5) | (0.9 - 2.8) | (0.8 - 2.4) | (1.6 - 3.2) | (1.3 - 2.7) | (0.9 - 3.1) | (0.5 - 2.2) | (0.9 - 2.5) | (0.7 - 1.9) | (1.1 - 3) | (0.8 - 3.9) | (0 - 17.8) |
| SO₄²⁻ | 38.9 | 71.2 | 44.5 | 84.1 | 42.7 | 87.9 | 48.6 | 82.9 | 61.8 | 95.0 | 46.5 | 119.7 | 36.2 |
| (Range) | (10.8 - 65) | (60.2 - 100.8) | (25.3 - 90.9) | (57.3 - 142.8) | (25.4 - 63.3) | (61.2-129.5) | (34.7 - 63.4) | (65.3 - 94.2) | (47.2 - 85) | (79.6 - 121.2) | (13.5 - 106.4) | (47.6 - 277.7) | (16.9 - 90.5) |

[1] Note: 'n' relates to number of samples taken at the end of a flood period. The 'n' varied between runs because certain runs had more flood periods than others over the treatment period. Includes replicates.

### 3.3.2 Release of dissolved Pb over a flood period

The concentration of Pb (mg/L) at the start of a flood was compared to the concentration at the end to determine whether individual wet and dry treatments resulted in a significant increase in dissolved Pb over a flood.

All variable  wet and dry runs at the top of the mesocosm were found to release significantly higher concentrations of Pb at the end of a flood compared to the start of a flood ($z = > -1.96$, $p = < .05$). That was not the case at the bottom of the mesocosm for the 2 week dry, 3 week dry and 2 week wet runs ($z =  < -1.96$, $p = > .05$) and nor was it the case for the control runs, the constant flood at the top ($z = -1.424$, $p =  .155$) and bottom ($z = -0.316$, $p =  .752$) or the field capacity run ($z = -0.838$, $p = .402$) (see Wilcoxon rank sum test summary table, appendix 3.3a for full details).

It can be seen (figure 3.3) that average concentrations of dissolved Pb released between the start and end of a flood was $> 5$ mg/L over flooded periods for all variable wet and dry runs at the top of the mesocosm, whereas concentrations of dissolved Pb tended to decline over all runs at the bottom of the mesocosm. The average concentration of dissolved Pb released over a flood period was significantly higher at the top of the mesocosm compared to the bottom ($z = -7.325$, $p = < .001$). The highest release of dissolved Pb was for the 3 week wet run (13.58 mg/L, $n = 9$) and 1 week wet run (11.82 mg/L, $n = 18$) at the top of the mesocosm (figure 3.3).
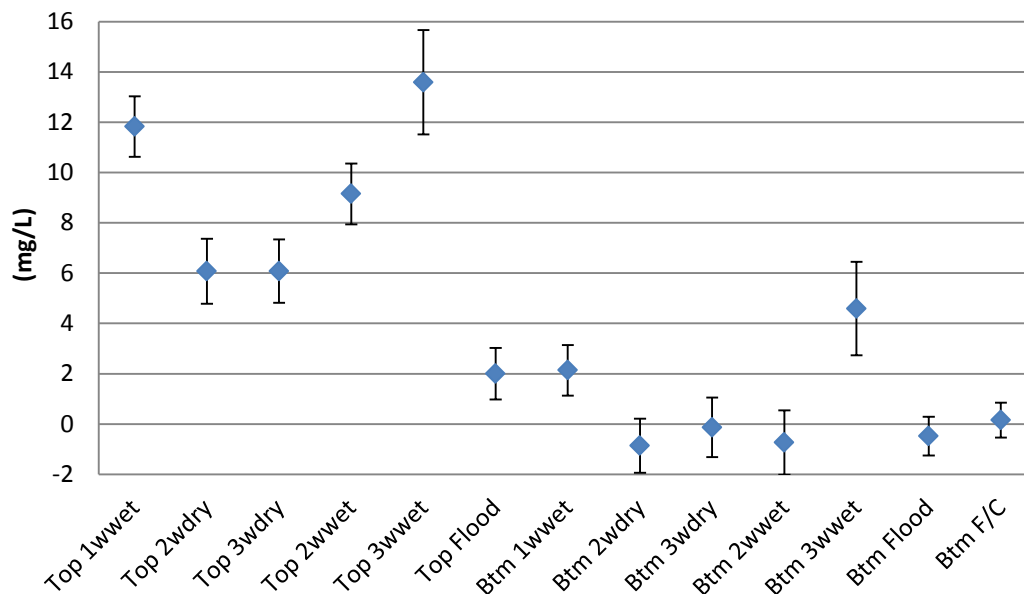
**Figure 3.3: Average concentration of dissolved Pb released over a flood period (mg/L) (concentration at the end of a flood minus concentration at the start) for all runs, top and bottom of the mesocosm. Bars indicate standard error (n = 9 for 3 week wet and 3 week dry, n = 12 for 2 week wet and 2 week dry, n = 18 for 1 week wet, flood and field capacity)**

### 3.3.3 Release of dissolved Zn over a flood

Significantly high concentrations of dissolved Zn were released between the start and end of a flood period for all variable runs at the top and bottom of the mesocosm ($z = > -1.96$, $p = < .01$) except for the 3 week dry run at the bottom of the mesocosm ($z = -1.280$, $p = .2$) (appendix 3.3a). There was no significant increase in dissolved Zn, for the control runs: constant flood at the top ($z = -0.616$, $p = .486$) and bottom ($z = -0.364$, $p = .716$) of the mesocosm and for the field capacity run ($z = -1.677$, $p = .94$).

Average concentrations of dissolved Zn (mg/L) at the end of a flood were found to be higher for all runs at the bottom of the mesocosm compared to the top (table 3.3), (figure 3.4).
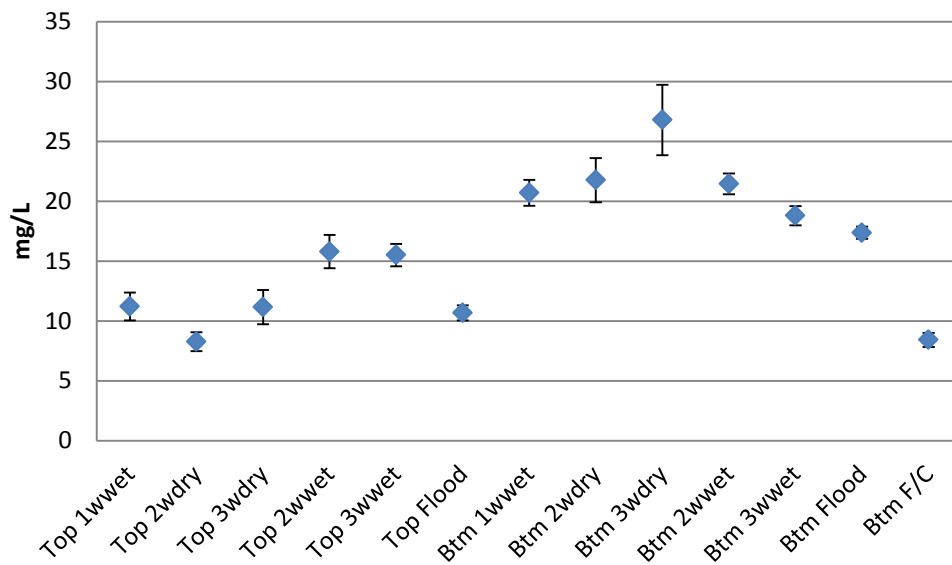
**Figure 3.4: Average dissolved Zn concentrations (mg/L) at the end of a flood period, for all runs, top and bottom of the mesocosm. Bars indicate standard error (n = 9 for 3 week wet and 3 week dry, n = 12 for 2 week wet and 2 week dry, n = 18 for 1 week wet, flood and field capacity)**
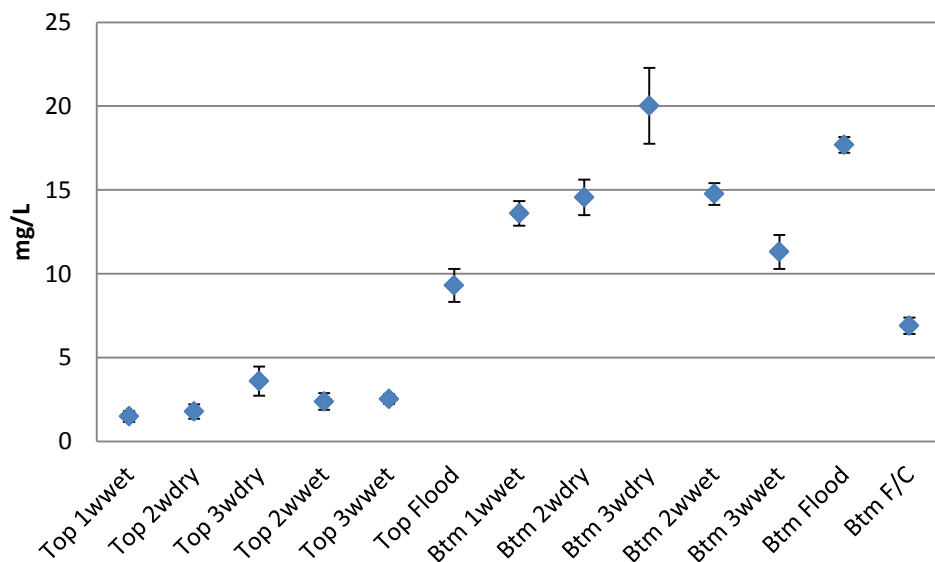


**Figure 3.5: Average Zn concentrations (mg/L) at the start of a flood period, for all runs, top and bottom of the mesocosm. Bars indicate standard error (n = 9 for 3 week wet and 3 week dry, n = 12 for 2 week wet and 2 week dry, n = 18 for 1 week wet, flood and field capacity)**

Average dissolved Zn concentrations at the start of a flood were higher for all runs at the bottom of the mesocosm (figure 3.5). The highest average concentration was observed for the 3 week dry run.

**3.3.4 The relationship between dissolved Pb and variables (Mn, Fe, Ca, pH, sulphate, nitrate and chloride)**

The 3 week wet and 1 week wet run at the top of the mesocosm were selected for analysis due to the high concentration of dissolved Pb released over a flood for these runs (table 3.3). Spearman's rho correlation analysis determined there was a significant negative relationship between dissolved Pb and pH ($r = -.519$, $p = <.05$, 3 week wet run, $r = -.612$, $p = <.01$, 1 week wet run) and a significant positive relationship between dissolved Pb and sulphate ($r = .605$, $p = <.01$, 3 week wet run, $r = .727$, $p = <.01$, 1 week wet run), Mn ($r = .751$, $p = <.01$, 3 week wet run, $r = .754$, $p = <.01$, 1 week wet run) and Ca ($r = .828$, $p = <.01$, 3 week wet run, $r = .796$, $p = <.01$, 1 week wet run). That was not apparent for the constant flood or field capacity run (see appendix 3.3b for Spearman's rho correlation coefficient tables).

The lowest mean concentration of Pb was observed at the bottom of the mesocosm for the constant flooded run (table 3.3). For this run there was a significant negative relationship between dissolved Pb concentration and pH ($r = -.915$, $p = <.01$), sulphate ($r = -.889$, $p = <.01$), Fe ($r = -.885$, $p = <.01$), Mn ($r = -.863$, $p = <.01$) and Ca ($r = -.605$, $p = <.01$) (see appendix 3.3b for Spearman's rho correlation coefficient tables).

### 3.3.5 The relationship between dissolved Zn and variables (Mn, Fe, Ca, pH, sulphate, nitrate and chloride)

A pulsed pattern of release was observed for Zn at the top of the mesocosm (section 3.3.3). Spearman's rho correlation analysis determined there was a significant positive relationship between dissolved Zn and sulphate ($p = <.01$) and Mn ($p = <.01$) and a significant negative relationship between dissolved Zn and pH ($p = < .05$) (except the 2 week dry run) for all runs at the top of the mesocosm.

Pore water data at the bottom of the mesocosm was selected for further statistical analysis of dissolved Zn because this location was found to be the greater source of dissolved Zn contamination (figures 3.4 and 3.5).

At the bottom of the mesocosm trends in the release of dissolved Zn were found to vary for different wet and dry treatments. Spearman's rho correlation analysis found that the relationships between dissolved Zn and other variables (Fe, Mn, Ca, pH, sulphate and nitrate) were different for the longer or more frequent wet runs compared to the 3 week dry run. For the former runs there was a significant positive relationship between dissolved Zn and dissolved iron, manganese, sulphate, calcium and pH and a significant negative relationship between dissolved Zn and nitrate (table 3.4) at the bottom of the mesocosm. However, for the 3 week dry run dissolved Zn correlated positively with only dissolved sulphate, calcium and pH.

**Table 3.4. Spearman's rho correlation of dissolved Zn concentration (mg/L) with dissolved Fe, Mn, Ca, pH, sulphate and nitrate at the bottom of the mesocosm, by run**

| | 1wwet n=36 | 2wdry n=24 | 3wdry n=18 | 2wwet n=24 | 3wwet n=18 | Flood n=36 | F/C n=36 |
|---|---|---|---|---|---|---|---|
| $Fe^{2+}$ | .01 (.699) | .01 (.667) | - | .01 (.754) | .01 (.754) | - | - |
| $Mn^{2+}$ | .01 (.663) | - | - | .01 (.611) | .01 (.808) | .05 (.367) | .01(.599) |
| Nitrate | .01 (-.448) | - | - | .01 (-.747) | .01 (-.724) | - | - |
| Sulphate | .01 (.769) | .01 (.833) | .01 (.849) | .01 (.838) | .01 (.822) | - | .01 (.565) |
| $Ca^{2+}$ | .01 (.727) | .01 (.583) | .01 (.749) | .01 (.566) | .01 (.727) | .05 (.393) | .01 (.488) |
| pH | .01 (.633) | .01 (.594) | .01 (.621) | .01 (.779) | .05 (.509) | - | - |

### 3.3.6 Simple regression analysis of dissolved Zn concentrations at the end of each flood period for all runs at the bottom of the mesocosms

Simple regression analysis of dissolved Zn concentrations at the end of a flood over the treatment period showed a significant linear increase for the 1 week wet, 2 week dry and 3 week dry runs (table 3.5). For these runs the model accounted for > 80% of the variation in dissolved Zn ($R^2$ %) and these runs showed the highest week by week increase in dissolved Zn ($\beta_1$).

**Table 3.5 Simple regression analysis of dissolved Zn concentrations (mg/L) over the treatment period, for each run at the bottom of the mesocosms**

| Run | Logged Y/N | $R^2$ % | Critical F | Sig | $\beta_0$ Intercept | 't' $\beta_0$ | Sig | $\beta_1$ Slope | 't' $\beta_1$ | Sig |
|------|-----|------|-------|--------|-------|--------|--------|------|-------|--------|
| 1wwet | Y | **83.3** | 79.95 | <0.001 | 1.114 | 46.914 | <0.001 | **0.03** | 8.94 | <0.001 |
| 2wdry | Y | **85.4** | 58.71 | <0.001 | 1.089 | 32.145 | <0.001 | **0.04** | 7.66 | <0.001 |
| 3wdry | Y | **91.1** | 71.40 | <0.001 | 1.148 | 33.265 | <0.001 | **0.04** | 8.45 | <0.001 |
| 2wwet | Y | 74.9 | 29.78 | <0.001 | 1.205 | 49.331 | <0.001 | 0.02 | 5.457 | <0.001 |
| 3wwet | Y | 30.2 | 3.028 | 0.125 | 1.200 | 27.184 | <0.001 | 0.01 | 1.740 | 0.125 |
| Flood | Y | 3.6 | 0.6 | 0.449 | 1.217 | 42.208 | <0.001 | 0.01 | 0.776 | 0.449 |
| F/C | Y | 28.1 | 6.244 | 0.024 | 0.766 | 12.25 | <0.001 | 0.02 | 2.499 | 0.024 |

### 3.3.7 Principal components analysis (PCA)

In order to understand what underlying factor(s) may have influenced the mobility of Zn principle components analysis (PCA) was carried out on pore water data for samples at the bottom of the mesocosm.

PCA analysis was split into two parts in order to highlight differences in the mechanisms of Zn release.  These mechanisms were likely to be different for the longer/more frequent wet runs (1 week wet, 2 weeks wet and 3 weeks wet), where conditions could become more reducing, compared to runs with a longer dry period where soluble sulphate salts could potentially build up (3 week dry and 2 week dry) (table 3.4). For this reason PCA analysis was split into two parts:

A. Exploration of underlying factors that may influence the mobility of Zn  for the longer or more frequent wetter runs, 1 week wet, 2 week wet, 3 week wet run. Only the unsaturated field capacity control run was used as a comparison because this run was considered to have more oxidising conditions and so the patterns of Zn release contrasted well. The flood run was not used because this run was more reducing (similar to the longer/more frequent wet runs) and therefore patterns of Zn release in response to prolonged flooding did not contrast so well.

B. Exploration of underlying factors that may influence the mobility of Zn  at the bottom of the mesocosm taking into account the longer dryer runs, 2 week dry, 3 week dry, and (for comparison) the control runs. Both control runs were used because the patterns of Zn release for the longer dryer variable runs contasted well with both control runs. Neither control run had

a long dry period that could allow for a  build up of soluble sulphate salts

that could subsequently be released, along with any zinc, on flood wetting.

Therefore both control runs provided a good contrast to the longer dry runs.


A.  PCA was conducted on 7 items with orthogonal rotation (varimax) as

correlation between factors was low as confirmed by running oblique rotation

(direct oblimin) and checking the component correlation matrix. The Kaiser-

Meyer-Olkin measure verified the sampling adequacy for the analysis, KMO =

0.79 (good, according to Field, 2009) and well above the acceptable limit of 0.5

(Field, 2009). Bartlett's test of sphericity ($\alpha$ = <0.001) indicated that correlations

between variables was sufficiently large for PCA. An analysis was run to obtain

eigenvalues for each factor in the data. Two factors had eigenvalues over

Kaiser's criterion of '1' and in combination these components explained

79.23% of the variance. Table 3.6 shows factor loadings after rotation.

Dissolved Zn, Fe, Mn, sulphate, pH (positive) and nitrate (negative) all loaded

highly onto factor 1. This cluster of variables suggested that factor 1 could

represent redox potential. Factor 2 was more difficult to identify because only

dissolved Pb (positive) and pH (negative) loaded highly onto this factor.

**Table 3.6. Rotated Factor Loadings, Part A (loadings > 0.4 appear in bold)**

|  | Factor1 | Factor2 |
|---|---|---|
| **Sulphate** | **0.93** | -0.14 |
| **Ca** | **0.89** | 0.13 |
| **Mn** | **0.88** | 0.08 |
| **Zn** | **0.86** | 0.08 |
| **nitrate** | **-0.85** | 0.04 |
| **Fe** | **0.80** | 0.04 |
| **pH** | **0.66** | **-0.63** |
| **Pb** | 0.23 | **0.92** |

It's clear from the factor scores for each porewater sample (figure 3.6) that samples for the longer wetter runs  score highly against factor 1 and  pore water samples for the unsaturated field capacity run score negatively for this factor. If factor 1 is, as suggested above, related to redox potential, this could indicate that the wetter runs and field capacity run have very different redox potential conditions. Underlying components associated with factor 1 seem to influence the mobility of Zn.
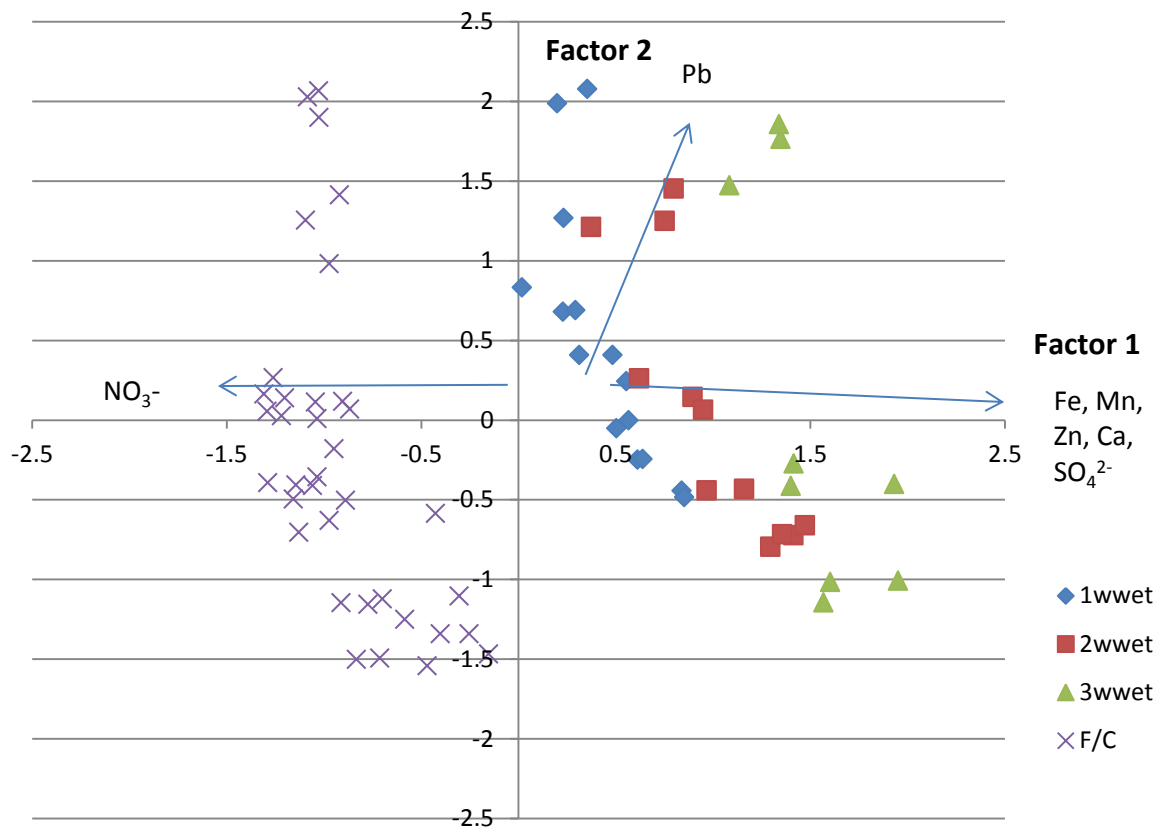
**Figure 3.6. Factor scores for individual pore water samples, grouped by run.**

B. As with part A, PCA was conducted on 7 items with orthogonal rotation
(varimax) as correlation between factors was found to be low. The Kaiser-
Meyer-Olkin measure verified the sampling adequacy for the analysis, KMO =
0.7 (good, according to Field, 2009). Bartlett's test of sphericity ($\alpha$ = <0.001)
indicated that correlations between variables was sufficiently large for PCA. An
analysis was run to obtain eigenvalues for each comonent in the data. Two
components had eigenvalues over Kaiser's criterion of '1' and in combination
these components explained 78.71% of the variance. Table 3.7 shows factor
loadings after rotation. Dissolved Fe, Mn, sulphate, pH (positive) and Pb and
nitrate (negative) all loaded highly onto factor 1. This cluster of variables

suggests that, as for PCA analysis part A, factor 1 could represent redox potential. Contrary to part A however Zn  is now loaded highly onto factor 2 along with calcium and sulphate. This factor only has weak loadings for Fe, and Mn, indicating that these variables are a less importantant contribution to this factor.

**Table 3.7. Rotated Factor Loadings, Part B (loadings > 0.4 appear in bold)**

|  | Factor1 | Factor2 |
|---|---|---|
| Fe | **0.813** | **0.460** |
| Mn | **0.780** | **0.523** |
| pH | **0.778** | **0.420** |
| nitrate | **-0.752** | 0.014 |
| Pb | **-0.668** | 0.121 |
| Zn | -0.234 | **0.919** |
| Ca | 0.316 | **0.915** |
| Sulphate | **0.606** | **0.727** |

The factor scores for each porewater sample (figure 3.7) show that the flood run samples score highly against factor 1. In contrast the pore water samples for the longer dryer runs score negatively for this factor. If factor 1 is, as suggested above, related to redox potential, this could indicate that the longer dryer runs have very different redox potential conditions to the flood run. The longer dryer runs scored highly against factor 2, where Zn, sulphate and Ca were highly loaded. The mobility of Zn  seems to be related to components associated with factor 2 for the longer dryer runs.
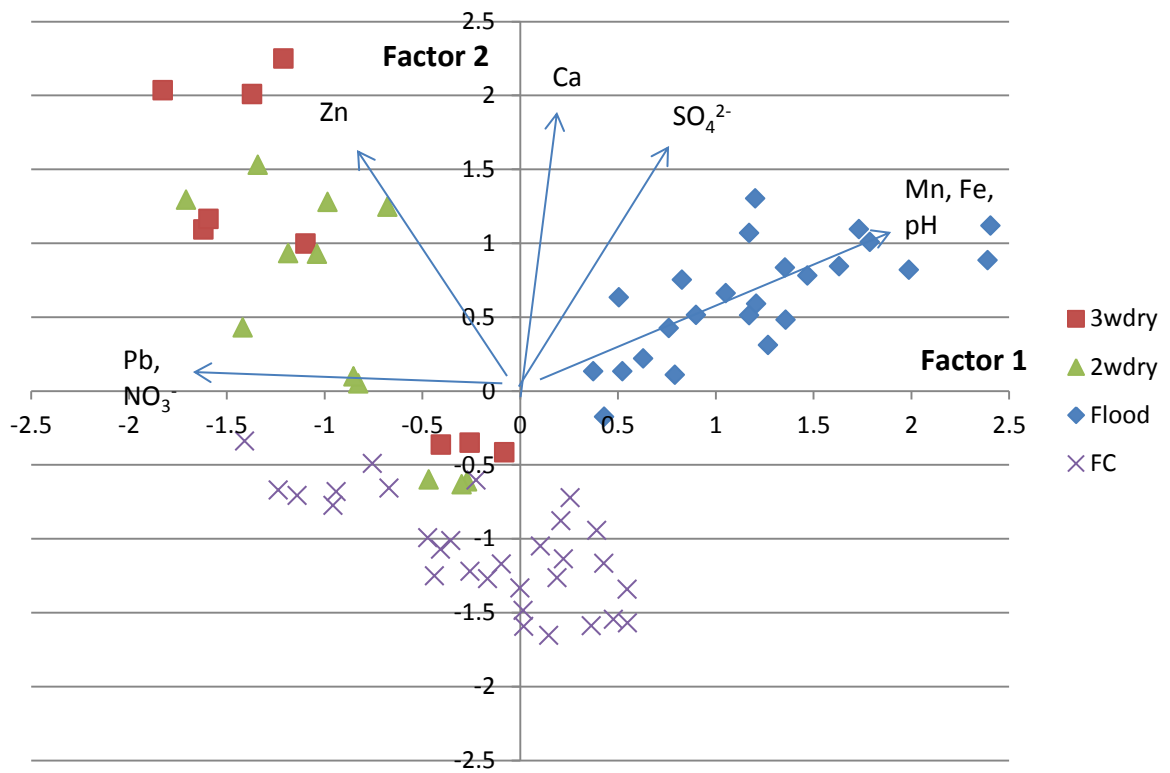
**Figure 3.7. Factor scores for individual pore water samples, grouped by run.**

### 3.3.8 Saturation Indices

To assess how close to saturation the flood water solutions were with respect to mineral phases, particularly anglesite, that may have formed over the treatment period, saturation indices (SI) were calculated using WATEQ4F.dat database (Ball and Nordstrom, 1991).

The three week wet run (top) and flood run (bottom) were selected for analysis because for these runs the highest and lowest mean concentration of dissolved Pb in pore water were observed. Mineral phases and SI's were calculated from input data (table 3.8) and are listed below (table 3.9).

All solution output results were checked for charge balance (within 5%). Small concentrations of Na were added to make up for any charge imbalance. Na was not measured in the pore water, however concentrations measured in previous studies at the sample site (Montserrat, 2010) were similar to the concentrations used to balance charges (7.5 – 32 mg/L).

## Table 3.8. Input data (mg/L) for mineral phases

| Week | D | H | L | D | H | L |
|---|---|---|---|---|---|---|
| Sample | 3wwet | 3wwet | 3wwet | Flood | Flood | Flood |
| Location | Top | Top | Top | Bottom | Bottom | Bottom |
| pH | 5.1 | 5.2 | 5.0 | 5.4 | 5.4 | 5.6 |
| Temp $^0$C | 22.2 | 22.4 | 21.5 | 23.0 | 23.2 | 22.3 |
| Fe | 0.0 | 0.0 | 0.0 | 5.0 | 13.0 | 16.2 |
| Mn | 0.9 | 1.7 | 2.0 | 7.3 | 13.7 | 14.2 |
| Pb | 27.3 | 19.0 | 18.1 | 19.8 | 7.5 | 5.1 |
| Zn | 12.1 | 17.3 | 17.1 | 16.4 | 20.4 | 15.9 |
| Ca | 3.8 | 3.0 | 3.3 | 4.4 | 4.9 | 5.2 |
| $NO_3^-$ | 1.2 | 2.1 | 1.1 | 0.0 | 0.0 | 0.0 |
| $Cl^-$ | 2.4 | 2.4 | 1.4 | 1.5 | 1.8 | 1.7 |
| $SO_4^{2-}$ | 49.3 | 58.3 | 77.7 | 85.0 | 122.3 | 155.1 |
| Na | 7.5 | 9.0 | 18 | 10.5 | 15.8 | 31.6 |

## Table 3.9. Mineral Phases, SI and charge balance (%)

| Week | D | H | L | D | H | L |
|---|---|---|---|---|---|---|
| Sample | 3wwet | 3wwet | 3wwet | Flood | Flood | Flood |
| Location | Top | Top | Top | Bottom | Bottom | Bottom |
| Charge balance % | 0.5 | -0.8 | -0.2 | 0.2 | 0.0 | -0.1 |
| **Anglesite PbSO₄** | **0.36** | **0.25** | **0.32** | **0.37** | **0.04** | **-0.07** |
| Bianchite ZnSO4:6H2O | -5.49 | -5.28 | -5.18 | -5.18 | -4.98 | -5.02 |
| Larnakite PbO:PbSO4 | -1.58 | -1.13 | -1.52 | -0.62 | -1.41 | -0.34 |
| Gypsum CaSO$_4$.2H$_2$O | -2.96 | -3.02 | -2.88 | -2.72 | -2.56 | -2.46 |
| Pb(OH)2 | -2.09 | -2.05 | -2.54 | -1.65 | -2.12 | -1.95 |
| Zincite ZnO | -4.94 | -4.58 | -5.06 | -4.20 | -4.12 | -3.9 |
| ZnO(a) | -4.96 | -4.61 | -5.03 | -4.26 | -4.2 | -3.93 |
| ZnSO4:H2O | -6.76 | -6.54 | -6.47 | -6.43 | -6.22 | -6.28 |

**Key: Weeks and flood durations**

| Run / week | Flood duration | Week number for the run |
|:---:|:---:|:---:|
| 3wwet  D | 3 weeks | 3 |
| 3wwet  H | 3 weeks | 7 |
| 3wwet  L | 3 weeks | 11 |
| Flood  D | 3 weeks | 3 |
| Flood  H | 7 weeks | 7 |
| Flood  L | 11 weeks | 11 |

For both the 3 week wet (top) and constant flood (bottom) runs pore water conditions reached supersaturation with respect to anglesite by the end of the first 3 week flood (week D) (table 3.5). For the constant flood run pore water conditions then change from supersaturated to saturated by weeks H and L. This was not the case for the 3 week wet run where conditions remained supersaturated over the entire treatment period.

### 3.3.9 Equilibration with Anglesite

In some cases the control of trace metal solutes by equilibrium with a mineral can be demonstrated (Appelo and Postma, 2010). The flood run, unlike the variable runs, was not periodically drained and the sediment, to a large extent, remained saturated and the water stagnant so it is possible that this system could have moved towards an equilibrium state.

To test that theory, a simple script was run using the WATEQ4F database to calculate the anglesite precipitation (mmoles) that would occur if the input data (table 3.8) for weeks D, H, L reached saturation with respect to anglesite. The program also calculated the concentration of Pb that would be expected in pore

water under these new saturated conditions (table 3.10). The script was run for both the flood run and the 3 week wet run for comparison.

**Table 3.10. Calculated precipitation of anglesite (mmoles) and Pb (mg/L) in pore water if conditions were to reach saturation with respect to anglesite.**

| Week | Sample | Location | Anglesite precipitation Mmoles | Predicted Lead mg/L |
|------|--------|----------|-------------------------------|---------------------|
| D | 3wwet | Top | 0.0685 | 13.12 |
| H | 3wwet | Top | 0.038 | 11.11 |
| L | 3wwet | Top | 0.045 | 8.84 |
| D | Flood | Bottom | 0.054 | 8.70 |
| H | Flood | Bottom | 0.003 | 6.9 |
| L | Flood | Bottom | 0.00 | 5.10 |

In theory, if pore water conditions reach supersaturation with respect to anglesite, as was found to occur for the 3 week wet and constant flood run (week D), according to Le Chaterier's principle the reaction below would move to the left and anglesite precipitation would occur and result in the decline in dissolved Pb and sulphate concentrations.

$$\text{Log\_k } 10^{-7.79} \quad = \quad [PbSO_4^{2-}]_{(s)} \quad \longleftrightarrow \quad [Pb]_{(aq)} \ [SO4^{2-}]_{(aq)}$$

For the flood run, by week L conditions were no longer supersaturated and Pb declined to 5mg/L. Predicted Pb concentrations at equilibrium for the flood run, weeks H and L (table 3.10) were similar to the measured pore water data for these weeks (table 3.8).

However, predicted Pb concentrations for the three week wet run at the top of the mesocosm (table 3.10) were lower than measured pore water data (table 3.8). For this run, conditions reached supersaturation at the end of a three week flood and anglesite precipitation was predicted to occur but the measured pore water data shows that this process did not result in a decline in dissolved Pb concentrations.

### 3.3.10 Ratio of Pb to sulphate

Galena was one of the primary minerals mined at the Ystwyth site (Hughes, 1981) and therefore there was a high possibility that galena was present in the sediment. Oxidation of sulphide minerals could account for the high concentrations of Pb released over flood periods (Younger, 1998). In order to infer whether oxidation processes may have resulted in the dissolution of galena and the release of Pb and sulphate, the ratio of this trace metal to sulphate was calculated. The ratio was derived from the assumed 1:1 molar relationship between Pb:S.

**Table 3.11 Ratios of Pb to sulphate for weeks D, H, and L, 3 week wet (top) and flood (bottom).**

| Sample Week | D | H | L |
|---|---|---|---|
| 3wwet_ratio Pb:SO$_4^{2-}$ | 0.26 | 0.15 | 0.11 |
| Flood_ratio Pb:SO$_4^{2-}$ | 0.11 | 0.03 | 0.02 |

For the 3 week wet run, the ratio of Pb to sulphate (table 3.11) for weeks H and L was higher than for the flood run. By week H, for the flood run, the ratio was close to zero.

Ratios were lower than the 1:1 expected for galena dissolution alone indicating that dissolution of other sulphur or sulphate bearing minerals were contributing to the higher sulphate concentrations.

**3.3.11 Comparison of diluted Pb and Zn concentrations to Environmental Quality Standards (EQS).**

Dissolved concentrations of Pb and Zn measured during mesocosm experiments, in confined conditions over periods of a week or greater, are unlikely to reflect surface water concentrations in the natural river bank environment where these trace metals may be subjected to dilution effects. In order to compare the release of dissolved Pb and Zn to EQS, dilution effects were calculated and compared to EQS.

Using maximum and minimum average dissolved Pb and Zn concentrations (mg/L) taken from table 3.3, an estimated dilution calculation was carried out, to determine the concentration of dissolved Pb and Zn, if 1 L of pore water were to exfiltrate from the river bank and become diluted with uncontaminated river water. The dimensions were based on the morphology of the river at the sample site (width 6 m x depth 0.5 m x length 0.25 m) = $0.75m^3$ * 1000 = 750 L water. The diluted concentrations of dissolved Pb and Zn were then compared to EQS.

It can be seen (table 3.12) that all average concentrations of dissolved Pb and Zn in pore water exceeded EQS even after dilution indicating the sediments pose a significant environmental risk.

**Table 3.12 Comparison of diluted Pb and Zn min and max average concentrations (mg/L) with EQS.**

|  | Pb (max) | Pb (min) | Zn (max) | Zn (min) |
|---|---|---|---|---|
| (mg/L) | 21.5 | 10.9 | 26.8 | 7.7 |
| After dilution (μg/L) | 28.6 | 14.5 | 35.7 | 10.3 |
| *EQS Pb & Zn (μg/L) | 7.2 | Dissolved concentration | 8 | 0 – 50 mg/L $CaCO_3$ (hardness) Total Concentration |

*EQS for Pb and Zn for the protection of surface water, annual average values (Environment Agency, 2011)

### 3.3.12 Summary for Pb

Dissolved Pb concentrations were found to exceed EQS indicating sediments may pose an environment risk.

The highest average concentration of Pb at the end of a flood was for the 3 week wet run at the top of the mesocosm. An increase in dissolved Pb concentration correlated negatively with pH and positively with sulphate and manganese.

The lowest average concentration of Pb was for the constant flooded run at the bottom of the mesocosm.

Geochemical analysis found that for the three week wet run and flood run pore water conditions became saturated with respect to anglesite. Further geochemical analysis brought calculated solutions for the three week wet run and constant flood run to equilibrium with respect to anglesite. Predicted Pb concentrations closely matched the measured pore water data for the constant flood run but not the 3 week wet run. Results indicated anglesite precipitation enforced a solubility control over dissolved Pb concentrations in pore water for the flood run and the three week wet run. However only the flood run at the bottom of the mesocosm resulted in a decline in dissolved Pb concentrations.

Ratio of Pb to sulphate, used to infer dissolution of galena was found to decline for the constant flood. This was contrary to the three week wet run at the top of the mesocosm where ratios were higher.

### 3.3.13 Summary for Zn

Dissolved Zn concentrations were found to exceed EQS indicating sediments may pose an environment risk.

Average concentrations of dissolved Zn at the end of a flood were found to be higher for all runs at the bottom of the mesocosm compared to the top. The highest average concentration of dissolved Zn was for the 3 week dry run at the bottom of the mesocosm.

The highest average concentration of dissolved Zn at the start of a flood, following a long dry antecedent period was for the 3 week dry run. This run, the 2 week dry and 1 week wet/dry run all displayed a significant linear upward trend in dissolved Zn over the treatment period at the bottom of the mesocosm.

For PCA part A Zn loaded highly onto factor 1 that could represent redox potential conditions factor scores for the longer wetter runs loaded highly onto this factor indicating that, for these runs, the release of Zn may be influenced by components associated with a fall in redox potential conditions.

For PCA part B Zn loaded highly onto factor 2 along with sulphate. The factor scores for the longer dryer runs also loaded highly onto this factor indicating, for these runs, the release of Zn may be influenced by components associated with release of sulphate.

## 3.4 Discussion

An experimental approach was used to determine the effect of wetting and drying sequences on the release of metal contaminants, Pb and Zn, from polluted sediments. Results indicated sulphate Pb, Zn, Fe, Mn, nitrate and Ca were dominant elements measured in the pore water samples. This fits with historical site data, regarding the presence of primary minerals galena, sphalerite (Hughes, 1981) and other historical (water/sediment) measurements made at the sample site (Fuge et al., 1991; Montserrat, 2010). Sulphate was present at higher concentrations than other anions (chloride, nitrate, phosphate) and processes relating to the oxidation of sulphide and dissolution of sulphate bearing minerals may have produced some acidity. Alkalinity was below detection as was inorganic carbon in the sediment and so pH values ranging between pH 4.8 and 5.8 may be a reflection of the poor buffering capacity of the water - in response to acid producing processes. These processes are discussed in detail throughout this section.

Concentrations of dissolved Pb and Zn were found to exceed environmental quality standards (EQS) by up to four orders of magnitude – prior to dilution calculations (table 3.12). This is higher than field results for this site (Montserrat, 2010) but not unexpected as weathering rates in laboratory experiments have been reported to far exceed those measured in the field (Evans and Banwart, 2006) due to differences between field and laboratory, such as temperature, pH and water rock ratios (Evans and Banwart, 2006). In the current study, the polluted nature of the sediment at the site (Montserrat, 2010) and the confined nature of the mesocosms is likely to have contributed to the build-up of these pollutants.

Similar concentrations of dissolved Zn however have been recorded for laboratory inundation studies of contaminated sediment (Du Laing et al., 2007; Wragg and Palumbo-Roe, 2011) with slightly lower values for Pb (0.4 mg/L maximum) (Wragg and Palumbo-Roe, 2011).

The observed results showed very different patterns of trace metal release for dissolved Pb and Zn. In order to clearly highlight trends for the different trace metals and make inferences as to the processes responsible for the mobility of Pb and Zn, they are discussed separately.

### 3.4.1 Key Mechanisms controlling the release of dissolved Pb

Dissolved Pb concentrations were found to increase significantly over flood periods at the top of the mesocosm whereas at the bottom (24 cm deep) no significant increase was observed for most runs (figure 3.3). The highest average increase in dissolved Pb over a flood period was for the 3 week wet run at the top of the mesocosm. At the bottom of the mesocosm dissolved Pb was found to decrease over the flood periods for most runs. The lowest average concentration of dissolved Pb was for the flood run at the bottom of the mesocosm (table 3.3). In order to try to understand the reason for the contrasting trends in the mobility of Pb, the runs with the highest and lowest average concentrations of Pb, the 3 week wet run (top) and the flood run (bottom), were selected for statistical analysis.

One possible explanation for the decline in Pb at the bottom of the mesocosm is the precipitation of this trace metal as a carbonate (Khodaverdiloo et al., 2012). Cerrusite ($PbCO_3$) has been found to form as a coating on galena during sulphide weathering (Wragg and Palumbo-Roe, 2011). However, this process generally

occurs at more alkaline pH and where bicarbonate concentrations reach saturation (VanLoon and Duffy, 2011). For this reason it is unlikely that cerrusite precipitation was a dominant process in this study because the pH conditions were slightly acidic and alkalinity was below detection. It is also unlikely that substitution of Pb for Ca in carbonate minerals such as calcite ($CaCO_3$), aragonite ($CaMg(CO_3)_2$, ankerite ($Ca(Fe,Mg)CO_3)_2$) occurred (Cravotta, 2008; Fairchild et al., 2010). If carbonate minerals were present in the sediment they were not present at detectable levels.

It is possible that poor penetration of oxygen to lower depths at the bottom of the mesocosm for the flood run resulted in a decline in redox potential. Under highly reducing conditions production of hydrogen sulphide and precipitation of Pb sulphide may have occurred. The precipitation of galena, a mineral highly insoluble under reducing conditions (Du Laing et al., 2007) could have acted as a sink for this trace metal contaminant (Andrews et al., 2008, Du Laing et al., 2007). Certainly nitrate concentrations become depleted and Mn and Fe are mobilised indicating a decline in redox potential conditions. High reactive carbon is necessary to create the anoxic conditions suitable for the reduction of sulphate (Morrison and Aplin, 2009) and reported redox potential conditions for formation of hydrogen sulphide are very low (<120 mV) (Ross, 1989; Gambrell et al., 1991; Bartlett, 1999). In the current study metals that may also have formed sulphides such as dissolved Mn, Fe and Zn were found to increase rather than decrease. However, Fe and Mn sulphides are orders of magnitude more soluble than galena (Nordstrom et al., 1999; Du Laing et al., 2007) and a previous study found Pb was preferentially sequestered in metal sulphide precipitates whilst Fe, Mn and Zn

remained mobile in solution (Weber et al., 2009). A fall in sulphate concentrations would be expected as a result of the reduction in sulphate (Weber et al., 2009; Morrison and Aplin 2009) but this was not observed in the current study and no sulphurous smell was apparent. Additionally, DOC concentrations were low to medium (Meybeck, 1982), and that could have been a rate limiting factor with respect to sulphate reduction (Morse et al., 2002; Ku et al., 2008). Although this mechanism of Pb attenuation will not be discounted, it is possible that other mechanisms were responsible for the control of dissolved Pb concentrations at the bottom of the mesocosm.

Anglesite has been reported to form as a weathering product from the oxidation of galena in mine drainage environments (Harris et al., 2003; Palumbo-Roe et al., 2013) and dissolved Pb concentrations can be controlled at low levels by anglesite solubility (Nordstrom and Alpers, 1999). In order to investigate further whether conditions had reached saturation with respect to anglesite, WATEQ4F was used to calculate SI. For the 3 week wet run, supersaturation, with respect to anglesite, was observed at the end of every 3 week flood period (table 3.9). However, for the constant flood run, by weeks H and L conditions had declined to a saturated state perhaps indicating conditions were at equilibrium. A further script was run to predict the concentration of dissolved Pb that would remain in pore water if the system reached saturation with respect to anglesite (table 3.10). For the constant flood run, predicted concentrations (table 3.10) were found to match observed dissolved Pb concentrations (table 3.8) in pore water by week L. This was not the case for the three week wet run, where observed concentrations of dissolved Pb in pore water were higher than concentrations predicted at saturation. That could

mean that the constant flood run had achieved equilibrium conditions with respect to anglesite precipitation by week L, but the three week wet run at the top of the mesocosm had not.

At the top of the mesocosm, dissolved Pb was found to correlate positively with dissolved Mn and sulphate and negatively with pH (section 3.3.4). Mn is more sensitive to low redox potential and pH conditions than Fe (Patrick and Henderson, 1981; Lee et al., 2002) and would be expected to reduce at a faster rate (Patrick and Delaune, 1972). It is therefore possible at the top of the mesocosm that the reductive dissolution of Mn hydroxides over flooded periods and co-precipitation of Mn hydroxides with Pb over dry oxidised periods was a controlling factor with respect to Pb mobility. This mechanism of trace metal control will be investigated further in chapter 4. Furthermore, the periodic draining and addition of fresh oxidised ARW may have kept conditions sufficiently oxidised at the top of the mesocosm to allow for the ongoing oxidation of reduced minerals in the sediment. Analysis of the molar ratio of Pb to sulphate for the 3 week wet run (table 3.11) indicates that the dissolution of galena could account for the higher pore water concentrations of Pb for this run and that this process was ongoing over each flood period throughout the treatment. On the other hand, for the flood run, by week L, the ratio of Pb to sulphate is almost an order of magnitude lower than the 3 week wet run. This could indicate that galena dissolution was no longer an important process with regards to the mobility of Pb and precipitation of anglesite may have had some control over dissolved Pb concentrations.

The oxidation of sulphides such as galena would not necessarily produce lots of acidity however any subsequent hydrolysis (Younger, 1998) or adsorption reactions (Dzombak and Morel, 1987) would result in proton release. Increases in acidity would be poorly buffered in this low alkalinity environment and this could explain the observed drop in pH over flood periods at the top of the mesocosm for the 3 week wet run and, in fact, may contribute to the drop in pH over flooded periods for all runs at the top of the mesocosms. This fall in pH is likely to have mobilised Pb further. Although the sorption edge for Pb is quite low (pH 3 - 5) (Smith, 1999; Lee et al., 2002), the rate of galena dissolution is reported to be enhanced at low pH (Domenech et al., 2002). At the bottom of the mesocosm, the pH tended to increase slightly over flood periods for all runs. The observed decline in nitrate and mobilisation of reduced Mn and Fe indicate that reduction processes that produce bicarbonate alkalinity (Younger, 1995, Whitehead et al., 2005) may have had some buffering effect over acid producing processes (Younger, 1998).

The results seem to indicate that, at river bank locations, where reduced minerals such as galena are present in the sediment, periodic flooding and drying could promote the oxidation of this reduced mineral. Under confined conditions (at depth 24 cm) the rate of oxidation may be slow and anglesite precipitation could provide a solubility control. However, at the surface, the oxidation of galena could result in the on-going release of dissolved Pb that may only be poorly controlled by the precipitation of anglesite.

### 3.4.2 Key Mechanisms controlling the release of dissolved Zn

Significantly high concentrations of dissolved Zn were released into pore water over a flood period for all variable runs at the top and bottom of the mesocosm,

indicating that the sediments can become a source of Zn contamination under fluctuating wet and dry conditions. However, patterns of release were different for Zn than for Pb, with the highest dissolved concentrations observed at the bottom of the mesocosms.

Zn is reported to be more mobile than Pb under oxic conditions (Merrington and Alloway, 1994; Carrol et al., 1998; Galan et al., 2003). The solubility of minerals such as bianchite and zincosite are orders of magnitude higher than anglesite (Minteq.dat) and so precipitation of these minerals was unlikely to occur at the concentrations of Zn observed in pore water. Zn has a higher sorption edge (pH 5 – 6.5) than Pb (Smith, 1999; Lee et al., 2002) so conditions would have favoured Zn mobilisation over Pb.  Additionally reports indicate that Pb can out-compete Zn for sorption sites (Desbarats and Dirom, 2007) and that can raise the Zn sorption edge further (Hamilton-Taylor et al., 1997).

The above mechanisms are likely to have served to mobilise Zn at the bottom of the mesocosm, although the patterns of Zn release were found to vary depending on the wet and dry treatment. Zn displayed a 'pulsed' release over flooded periods for the longer wetter runs and concentrations of dissolved Zn were significantly higher at the end of a flood compared to the start. However, for the longer dryer runs, dissolved Zn concentrations showed an upward trend over the whole treatment period and for the 3 week dry run the highest concentrations of dissolved Zn  were observed at the start of a flood (within 2 – 3 hours of flooding). The 3 week dry run resulted in the highest average concentration of dissolved zinc over the treatment period. The contrasting trends in the mobilisation of dissolved

Zn at the bottom of the mesocosm could have been as a result of conditions favouring different biogeochemical processes.

 PCA was used to explore the underlying factors that contributed to the release of dissolved Zn in pore water at the bottom of the mesocosms. PCA was split into two parts based on the formative statistical correlation analysis that indicated that the biogeochemical mechanisms that could control the mobility of Zn were different depending on the wet and dry sequence. PCA part A analysed the longer wetter runs and also the  field capacity run (an unsaturated, possibly oxidised sediment) for comparison and PCA part B analysed the longer dryer runs and also both control runs (for comparison).

PCA part A, identified two factors greater than Kaiser's criterion of '1' and 63.02% of the variance was explained by factor 1. Dissolved Mn and Fe loaded highly onto this factor and nitrate loaded negatively suggesting this factor could represent redox potential conditions with positive loading indicating reducing conditions. Dissolved Zn  loaded highly onto this factor and the factor scores for the longer or more frequent wet runs were closely (positively) linked to this factor (figure 3.6) indicating that the pulsed release of Zn  found for these runs could be related to negative redox potential conditions.

In the case of the longer wetter runs at the bottom of the mesocosms it may be that easily reducible Fe and Mn influenced the release of dissolved Zn. Historical field studies at the Cwmystwyth site (Evans, 1991) found that the most enriched labile phases in the sediment were easily reducible Fe and Mn hydroxides. This author suggested that co-precipitation with hydrous oxides of Fe and Mn was an important control over the mobility of dissolved Zn and Pb. Under slightly acidic pH

conditions (~pH 5) as measured in this study (table 3.3), Fe reduction has been reported to occur at a higher redox potential (300 mV) than at pH 7 (~100 mV) (Gotoh and Patrick, 1974). The increase in dissolved Fe and Mn over flooded periods for the longer wetter runs indicates that conditions seem to have become reducing enough for the reductive dissolution of Fe and Mn. Moreover where these reduced metals were exposed to atmospheric oxygen on draining of the mesocosms, subsequent co-precipitation of Mn and Fe hydroxides with dissolved Zn could have served to attenuate this contaminant trace metal. Reactive Fe forms such as ferrihydrite are highly adsorbent and very little freshly precipitated Fe and Mn may be required to scavenge high concentrations of Zn (Caetano et al., 2003; Burton et al., 2005). The composition of the pore water in this study, the high sulphate and Fe concentrations could have resulted in the formation of Fe hydroxysulphate minerals on precipitation. The surface composition of these minerals has been reported to influence the sorption properties of Zn by lowering the Zn sorption edge (Webster et al., 1998) and that could have enforced a solubility control over Zn. Therefore it is possible that the lower concentrations of dissolved Zn observed at the start of a flood for the longer wetter runs compared to the 3 week dry run (figure 3.5), was due to Zn co-precipitation with and sorption to Fe and Mn hydroxide minerals. On subsequent flooding the reductive dissolution of Fe and Mn hydroxides could account for the 'pulsed' pattern of release of Zn into pore water observed for the longer wetter runs.

PCA part B, was intended to uncover underlying factors associated with Zn mobility for the longer dry runs (2 and 3 weeks dry). Two factors were identified greater than Kaiser's criterion of '1' and explained 78.7 % of the variance.

Dissolved Mn and Fe loaded highly onto factor 1 and nitrate loaded negatively, suggesting this factor could have represented redox potential conditions, with positive loading indicating reducing conditions. Factor scores for the constant flood run were closely (positively) linked to this factor. Contrary to PCA part A however, dissolved Zn was found to load highly onto factor 2 along with sulphate and calcium and factor scores for the longer dryer runs (with the exception of the first week) were positively linked to this factor indicating that the upward trend in Zn observed for these runs may be related to the release of sulphate and calcium.

Inundation studies have found that, for some mining contaminated sediments, the on-going oxidation of sphalerite can strongly influence concentrations of dissolved Zn and sulphate in pore water (Wragg and Palumbo-Roe, 2011). However, it is also possible that the dissolution of other Zn bearing solid species could account for the high concentrations of Zn. Over long dry periods the evaporation of pore water could have promoted the formation of metal sulphate salts (Buckby et al., 2003, Harris et al., 2003; Nordstrom 2009). Effluorescent salts have been reported to form over long dry periods in mining impacted environments (Nordstrom, 2009) and Zn has been reported to substitute for ferric and ferrous iron in hydrated Fe sulphate salts (Alpers et al., 1993). Other authors report the precipitation of a soluble dietrichite-pickeringite-apjohnite type phase $(Zn, Mg, Mn)Al_2(SO_4)_4.22H_2O$ (Harris et al., 2003). Field studies have linked high fluxes of Pb during storm flows to long dry antecedent periods (Byrne et al 2013) this study indicated that metal sulphate salts accumulated on the surfaces of contaminated sediment over long dry periods and on flood wetting these salts dissolved flushing sulphate and trace metal contaminants back into the river system (Byrne et al 2009). Hudson-

Edwards et al (1999b) described the dissolution of metal sulphate salts (that had formed over long dry periods) and the subsequent flushing of trace metal contaminants such as Pb and Zn back into river systems during periods of high rainfall. This could explain the high concentrations of Zn  and sulphate released at the start of a flood (figure 3.5) and the lower pH observed for the longer dryer runs at the bottom of the mesocosm (table 3.3).

Ca too was highly loaded against factor 2 for PCA. Other mescocosm studies have reported a Ca release over flooded periods (Du Laing et al., 2007), possibly as a result of carbonate dissolution following a fall in pH. In the current study however, although the presence of carbonates in the sediment are not discounted, they were below detection and so the mobility of Ca is more likely related to the dissolution of gypsum ($CaSO_4.2H_2O$) often present in mining impacted catchments (Younger, 1998; Harris et al., 2003; Kuechler et al., 2004).

Low concentrations of dissolved Mn and Fe were observed for the longer dryer runs. Therefore the precipitation of these metals on oxidation may not have exerted a strong control on dissolved Zn concentrations. Without the co-precipitation of dissolved Zn with Fe and Mn hydroxides, the uncontrolled release of this trace metal over the whole treatment period seems to have resulted in a significant upward trend in Zn.

## 3.5 Conclusions

Calculations of saturation indices indicated that anglesite solubility was a controling factor with respect to dissolved Pb concentrations. At the bottom of the mesocosm for the constant flood run this mechanism appeared to maintain Pb concentrations at low levels over the flood period and geochemical calcuations indicated that conditions may have reached equilibrium.

At the top of the mesocosm, for all runs, anglesite precipitation only poorly controlled Pb concentrations, possibly due to processes favouring the release of dissolved Pb such as the ongoing oxidation of galena. The fall in pH observed over flooded periods in the surface water may have mobilised Pb further. The highest concentration of dissolved Pb was measured at the end of a flood period at the top of the mesocosm for the 3 week wet run.

The highest dissolved Zn concentrations were observed at the bottom of the mesocosms and different patterns of Zn release were apparent depending on the wet and dry treatment.

Zn displayed a pulsed pattern of release over the flood period for the longer or more frequent wet runs (1 week wet, 2 week wet and 3 week wet). Statistical analysis results indicated that this may be due to co-precipitation of Zn with Fe and Mn hydroxides over dry oxidised periods and subsequent reductive dissolution and release of Zn over flooded periods.

Zn displayed a significant upward trend in concentration over the treatment period for the 2 week dry and 3 week dry runs. The highest concentration of Zn released at the start and end of a flood period was for the 3 week dry run.  It is possible that

the high releases of dissolved Zn at the start of a flood were due to precipitation of highly soluble Zn sulphate salts over longer dry antecedent periods that dissolved quickly upon flooding releasing Zn back into pore water.

All concentrations of both Pb and Zn were found to exceed EQS even after dilution indicating the sediments posed a significant environmental risk.

# 4. INVESTIGATING THE ROLE OF FE AND MN HYDROXIDES AS A MINERAL SOURCE OF PB AND ZN IN RESPONSE TO DIFFERENT WET AND DRY SEQUENCES

## 4.1 Introduction

This chapter investigates the role of labile Fe and Mn hydroxides in the release of Pb and Zn into pore water over flooded periods during the mesocosm experiments detailed in chapter 3. Fe and Mn minerals have been reported as volumetrically the most important contaminant hosts in metal mining contaminated sediment in England and Wales (Hudson-Edwards, 2003). Many studies have observed the partitioning of Pb and Zn with Fe and Mn hydroxides in trace metal contaminated river sediments (Macklin and Dowsett, 1989; Evans, 1991; Hudson-Edwards, 2003; Burton et al., 2005; Byrne et al., 2010; Farnsworth and Hering, 2011). Dynamic changes in redox potential conditions and pH can bring about the dissolution and precipitation of Fe and Mn hydroxides (Lovley and Phillips, 1986, Lee et al., 2002) and result in the release of partitioned Pb and Zn contaminants into river water (Charlatchka and Cambier, 2000; Lesven et al., 2010).

During a storm event, high flow and an increase in river stage can result in infiltration of surface water laterally through the river bank. In direct response to flood wetting the microbial depletion of oxygen may occur within hours (Ponnamperuma et al., 1967) or days (van der Geest and Paumen, 2008) the rate depending on factors important to microbial processes such as availability of labile organic matter, sediment grain size (Gambrell et al., 1991) and temperature (Younger et al., 2002). On depletion of oxygen, microbes can couple the oxidation of organic matter with the reduction of other electron acceptors that follows a

traditionally reported order: nitrate, Mn hydroxides, Fe hydroxides and sulphate (reflecting highest to lowest energy efficiency) (Ponnamperuma et al., 1967; Lovley, 1991). In addition to reduction through oxidation of organic matter the reduced bi-products of microbial metabolism can further undergo oxidative reactions (Appelo and Postma, 2010):

$$5\ Fe^{2+} + NO_3^- + 7\ H_2O \longrightarrow 5FeOOH + {}^1\!/_2N_2 + 9H^+$$

$$2\ Fe^{2+} + MnO_2 + 2\ H_2O \longrightarrow Mn^{2+} + 2FeOOH + 2H^+$$

$$H_2S + 2FeOOH \longrightarrow 2\ Fe^{2+} + S^0 + 4\ OH^-$$
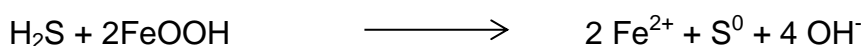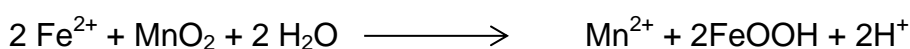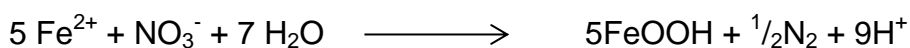
(Appelo and Postma, 2010; Thamdrup et al., 1994)

Reduction of Fe and Mn hydroxides is catalysed by the microbial transfer of electrons from an electron donor (organic matter or reduced metal) via surface functional groups to the oxidised Fe or Mn mineral centre. The electron transfer leads to a change in oxidation state of the metal to reduced Fe or Mn. The reduced metal has a more labile bond with oxygen than its oxidised form and is more easily detached (Stumm and Sulzberger, 1992). The reductive dissolution of Fe and Mn hydroxides can serve to remobilize partitioned contaminants such as Pb and Zn (Torres et al., 2013) and release them back into river water, potentially increasing the bioavailability of these contaminants.

When flooding subsides, exfiltration of water from the river bank and decline in river stage can expose previously reduced sediment surfaces to atmospheric 'oxidised' conditions. Reduced Fe and Mn oxidise and undergo hydrolysis (Lovley and Phillips, 1989; Grundl and Delwiche, 1993). The co-precipitation of Fe and Mn

hydroxides with Pb and Zn is a key process controlling the mobility of aqueous Pb and Zn contaminants under dynamic redox potential conditions. Studies have found the removal of dissolved contaminants through co-precipitation to be twice as high compared to adsorption (Appelo and Postma, 2010) and co-precipitation has been reported to occur at 1 – 2 pH units lower than for adsorption (Karthikeyan et al., 1997), it has been suggested that this is due to the enhanced surface area and sorption site availability for extremely fine grain hydroxide precipitates (Crawford et al., 1993). Moreover, freshly precipitated hydrous Fe and Mn oxides have a large (Schuman, 1977; Ford et al., 1997) and complex surface area (Stumm and Sulzberger, 1992; Cravotta and Bilger, 2001) that makes them better able to sorb trace metal contaminants such as Zn and Pb than older more crystalline forms (Younger, 1995; Nordstrom and Alpers, 1999). Trace metal sorption capacities have been reported as 10 times greater than for aged hydroxides (Burton et al., 2005, Shuman, 1977).

If left undisturbed, with aging, Fe and Mn hydroxide minerals may become more crystalline and less reactive (Ford et al., 1997). Ferrihydrite has been reported to convert to hematite if conditions remain at pH (pH 5 - 7). Outside of that range ferrihydrite has been found to dissolve and re-precipitate as goethite (Nordstrom and Alpers, 1999). However, hematite and goethite display slow growth kinetics (Nordstrom and Alpers, 1999) and the aging of ferrihydrite to crystalline, stable forms can be retarded by sorption of organic or inorganic species (Baltpurvins, 1996; Axe and Trivedi, 2002). Therefore labile Fe and Mn hydroxides may persist in the subsurface and under dynamic redox potential conditions could build-up within mining polluted sediments.

Microbes have been found to preferentially reduce younger poorly crystalline forms of Fe (Lovley and Phillips, 1987) and reduction rates have been reported to increase up to 50 fold for ferrihydrite compared to more crystalline goethite and hematite (Lovley and Phillips, 1986). So when flood conditions return, this form of Fe is likely to be the first to undergo reductive dissolution. Trace metal contaminants that have been freshly sorbed to Fe and Mn hydroxides over oxidised periods are likely to be easily released at low redox potential due to reductive dissolution. However, if the sediment is left undisturbed, relatively non-reversible partitioning of trace metals with less reactive Fe and Mn hydroxides may occur due to mechanisms such as incorporation of trace metal contaminants into the crystal structure during crystallisation (Ford et al., 1997), the migration of weakly sorbed trace metals deeper into the crystal lattice (Ford et al., 1997; Axe and Trivedi, 2002) or the formation of a solid solution, not so easily dissolved or desorbed (Linge, 2008; Appelo and Postma, 2010).

The extent to which reactive Fe and Mn hydroxides may accumulate in the sediments under dynamic redox potential conditions is unclear. However it is these more labile mineral forms that may control the mobility of Pb and Zn contaminants. Therefore identifying the different forms of Fe and Mn hydroxide that are partitioned with Pb and Zn is useful in determining the risk metal contaminated sediment may pose. One method to achieve this is through the application of sequential extractions. A large number of different sequential extraction procedures have been designed to measure different forms of Fe and Mn hydroxides and many are variants on those devised by Tessier et al. (1979) (Heron et al., 1994; Licheng and Guijiu, 1996; Fernandez Albores et al., 2000;

Larsen and Mann, 2005). Sequential extractions have been widely accepted as a useful technique for bulk analysis of sediment samples and results provide an indication of the environmental conditions under which trace metals contaminants may be released and become bioavailable. Chemical extractions are intended to be selective for one phase, however total selectivity is highly improbable and there are a number of known issues:

Different extraction schemes targeting the same phase may produce very different results for the same sediment type. Influencing factors are variations in chemical composition or strength of the extraction, extraction times, temperature and treatment of the sediment prior to extraction (Tack and Verloo, 1995; Linge, 2008).

Some minerals may be extracted over several, and sometimes all, operationally defined phases. For example Leinz et al. (2000) reported Pb recovery from anglesite and cerussite over five of the Tessier et al. (1979) extractions and that galena was soluble in HCl.

Control standards with a fixed chemical composition, structure and grain size may not mimic the reactivity of amorphous complex mixtures of similar mineral types in the sediment (Linge, 2008).

Mineralogical analysis such as X-ray diffraction (XRD) or scanning electron microscopy with energy dispersive spectroscopy (SEM/EDS) are sometimes used along-side sequential extractions (Leinz et al., 2000) and can help determine the association of trace metal contaminants with mineral phases. Even so, at mining impacted sites challenges can arise as many Pb and Zn bearing mineral phases are amorphous or poorly crystalline (Hudson-Edwards, 2003) or present at

concentrations too low to detect through relatively insensitive techniques such as SEM/EDS and XRD analysis.

Although direct comparisons are difficult, many sequential extraction techniques have identified high concentrations of Pb and Zn partitioned with labile Fe and Mn hydroxides in mining impacted river sediment. Wang et al., (2010) observed that the highest percentage of Pb was associated with the easily reducible Fe phase ($NH_2OH.HCl$, 20 ml, 16 hours, < 63 μm) in the surface sediments of the severely metal polluted Jinjiang River, China. A similar study of the sediments in the Kangjiaxi River Shuikonushan Pb-Zn mine area, China reported high concentrations of Zn (29 – 54 %) and Pb (43 – 61 %) partitioned with easily reducible Fe and Mn hydroxides (0.04M $NH_2OH.HCl$ in 25% (v/v) acetic acid) (Licheng and Guijiu, 1996). A study of the sediment at the Grogwynion metal mining polluted site, UK, found a high percentage of Pb (up to 69%) and Zn (up to 20%) partitioned with labile Fe and Mn hydroxides (0.04M $NH_2OH.HCl$ in 25% (v/v) acetic acid, 96°C, 4 h, < 63 μm) (Palumbo-Roe et al., 2009) and in the river bed sediments of the Afon Twymyn, central Wales, UK, reducible Fe and Mn hydroxides (< 63 μm) were reported to constitute the second largest sink for trace metal contaminants Pb and Zn (Byrne et al., 2010).

The results from chapter 3 showed that for some wet and dry runs dissolved Pb and Zn were found to correlate positively with dissolved Fe and Mn. This may have been due to the co-precipitation of Pb and Zn with Fe and Mn hydroxides over dry oxidised antecedent periods and the reductive dissolution of Fe and Mn hydroxides and the release of Pb and Zn into pore water over flooded periods. That could account for the 'pulsed' pattern of Pb and Zn release (concentrations of

Pb and Zn were significantly higher at the end of a flood compared to the start) observed for certain wet and dry runs at the top and bottom of the mesocosm. If this mechanism was an important control over the treatment period higher concentrations of easily reducible Fe and Mn and associated Pb and Zn would be present in the sediment of that run.

Sequential extractions were carried out on the sediment remaining at the end of the wet and dry treatments (chapter 3) in order to identify the runs where Fe and Mn hydroxides were a key mineral source of dissolved Pb and Zn contamination.

### 4.1.1 Aim, Objectives, Hypothesis

The overall aim of this chapter was to measure different Fe and Mn forms in the sediment along with partitioned Pb and Zn in order to understand whether there had been a build-up of reactive Fe and Mn hydroxide that may have acted as a source of Pb and Zn contamination for certain wet and dry sequences. Within the overall aim several objectives were identified:

Determine the mineral phases responsible for the release of Pb and Zn during extraction step 1 using a combination of literature and results from chapter 3, SEM/EDS analysis and geochemical calculations.

Identify wet and dry sequences that were significantly different from the initial sediment and control run with regards to the concentration of Fe, Mn, Pb and Zn recovered from the easily reducible Fe extraction (extraction step 2).

Determine dominant mechanisms of release of Pb and Zn into pore water using a combination of the extraction results, results from chapter 3, literature and SEM/EDS analysis.

Compare total Pb and Zn values to (i) PEL guideline values and (ii) to concentrations of Pb and Zn found in sediment local to the sediment sample site.

**Hypothesis**

A higher concentration of Pb and Zn would be recovered from the easily reducible Fe extraction for the wet and dry run(s) where dissolved Pb and Zn had been found to correlate positively with dissolved Fe and/or Mn and Pb and Zn had displayed a 'pulsed' pattern of release into pore water and surface water during the mesocosm experiments (chapter 3).

Runs where this was apparent were:

At the bottom of the mesocosm for the 3 week wet run and 1 week wet run (dissolved Fe, Mn and Zn)

At the top of the mesocosm for the longer wetter runs (dissolved Mn, Pb and Zn)

## 4.2 Methods

Different Fe phases may display a wide range of reactivity (adsorption capacity and susceptibility to reduction). It is generally agreed that the most reactive forms of Fe are freshly precipitated, younger forms (Shuman, 1977; Lovley and Phillips, 1987; Ford et al., 1997; Du Laing et al., 2009). In order to determine whether the mesocosm experiments run in chapter 3 had resulted in a build-up of more reactive forms of Fe in the sediment a sequential extraction procedure was carried out on sediment remaining at the end of a sub-set of the runs.

Samples were taken from the initial sediment and the following sub-set of runs:

A) One week wet and one week dry (top and bottom of the mesocosm)

B) One week wet and three weeks dry (top and bottom of the mesocosm)

C) Three weeks wet and one week dry (top and bottom of the mesocosm)

D) Flood run (top and bottom of the mesocosm)

E) Field capacity (bottom of the mesocosm)

The above sub-set of runs were chosen because, based on the results in chapter 3, contrasting patterns in trace metal mobility were observed between runs.

All samples were run in triplicate

## 4.2.1 Sediment Preparation

Approximately 1 gram of sediment was collected from the top (0-1 cm deep) and bottom (24 cm deep) of each mesocosm using a plastic spatula and added to a small polyethylene zip bag. All collected sediment was frozen at $20^{\circ}C$ immediately

after sampling and once frozen was then freeze dried (-70$^{\circ}$C) for storage in order to preserve redox state.

Prior to extraction, samples were divided into two size fractions < 63 μm (clay/silt) and <2000 - > 63 μm (fine – coarse sand) by dry sieving in order to investigate differences in metal concentration and geochemical partitioning between these two size fractions.

The sediment was weighed (as close as possible to 0.1g) and then added to a 15ml polyethylene centrifuge tube. A blank was run with each extraction.

## 4.2.2 Ferrihydrite synthesis

Ferrihydrite was synthesised based on Poulton and Cranfield (2005) methodology to be used as a reference standard during the extractions.

50mM solution of $Fe(NO_3)_3.9H_2O$ was titrated to pH 6.5 with 1 M KOH After hydrolysis the ferrihydrite was washed thoroughly to remove traces of nitrate and then freeze dried at - 70$^{\circ}$C.

## 4.2.3 X-ray Diffraction (XRD)

Shavings were taken from galena and sphalerite reference minerals (Northern Geological Supplies) to determine recoveries of Pb and Zn from galena and sphalerite phases for each extraction. Each mineral was identified through XRD analysis using a Rigaku Miniflex XRD with 30 kV/ 15 mA Cu X-ray (Liverpool John Moores University). The 2Ө angle data collected through XRD was imported as a txt file into data processing software package SIeve for PDF2. PDF2 though I.C.D.D.'s SIeve option (I.C.D.D. 2008) treated the data to remove background x-

rays, normalise intensities and identify peaks. These peaks were then matched by 2Ө angle to a database of minerals. Many minerals have characteristic peaks at high 'd' spacings (low Ө angles). Therefore intensity overlaps are common at low angles. For this reason intensity 'maxima' were obtained over a wide angle range (20 – 85 degrees). This technique was for qualitative identification purposes only. See general methods section 2.2.11 for full details.

XRD analysis was also carried out to identify unknown crystalline solids in the sediment samples. Freeze dried sediment remaining at the end of the treatment runs was ground into a fine powder (< 10 µm) and smoothed onto a mount. The 2Ө angle data was collected through XRD analysis and imported as a txt file into data processing software package SIeve for PDF2 for identification of crystalline minerals. See method section 2.2.11 for full details.

## 4.2.4 Scanning Electron Microscopy with Energy Dispersive Spectroscopy (SEM/EDS)

A combination of SEM/EDS was carried out on a Philips XL30 FEG ESEM fitted with an Oxford Instruments X-Sight EDS ATW X-Ray detector, University of Birmingham, (UOB) (figures 4.8 – 4.12) and a FEI Quanta 200 ESEM, Liverpool John Moores University, (LJMU) (figures 4.13 and 4.14). Freeze dried sediment was dusted lightly onto carbon stubs and coated in carbon or platinum to encourage conductivity.  Image and elemental data was collected from the surface of the sediment samples for areas at a micron scale (see general methods section 2.2.10 for full details).

### 4.2.5 Sequential Extraction

A modified four step sequential extraction procedure was run to identify 4 Fe phases along with any partitioned Pb, Zn, Mn (table 4.1). See general methods section 2.2.5 for full details.

**Table 4.1 Sequential extraction steps**

| Step # | Extractant | Purpose | References |
|---|---|---|---|
| 1 | 0.5M HCl | To measure reduced Fe(II) and Mn (II) loosely sorbed to the surfaces of minerals in sediment. This procedure may also be applicable to other di-valent metals (i.e. Pb and Zn). | Lovley and Phillips (1986) |
| 2 | 0.25M Hydroxylamine hydrochloride in 0.25M HCl | To reduce, labile, easily reducible forms of Fe – likely to be ferrihydrite and Lepidocrocite. | Lovley and Phillips (1987) Poulton and Canfield (2005) |
| 3 | 50g/L sodium dithionite with 0.2M in 0.35M acetic acid | To reduce, reducible forms of iron – ferrihydrite, lepidocrocite and also more crystalline forms of Fe goethite, hematite and akaganeite. | Poulton and Canfield (2005) |
| 4 | Aqua Regia | Considered effective for the extraction of most metals in sediment and soil. A measure of pseudo-total metals | Wilson and Pyatt (2007) Montserrat (2012) |

### 4.2.6 Analysis of extracted samples

All sequentially extracted samples were added to labelled tubes for analysis of metals (Fe, Mn, Pb and Zn), via FAAS (Perkin Elmer Analyst 300). Each batch included triplicates, and blanks. Standards were made up in matrix matched solutions and independent check (quality control) 'standards' were used to measure accuracy at the start, middle, and end of the run. The run was considered acceptable if the data were within 5% of the expected concentration e.g. 5 ppm (4.75 - 5.25 ppm). See general methods section 2.2.3 for full method details.

### 4.2.7 PHREEQC Analysis

Geochemical computer program PHREEQC was run to calculate the moles of ferrihydrite ($Fe(OH)_3$) dissolved when extraction step 1 – 0.5 M HCl was added.

The expected pH of the solution was calculated. HCl is a strong acid and dissociates fully. Therefore for each 0.5 mole of Cl, there is 0.5 mole $H^+$. Using equation:

$pH = - \log[H^+] = - \log[0.5] = 0.3$

Therefore a charge balanced solution, volume 5 ml, of 0.5 mole HCl (pH 0.3 and 0.5 mole Cl) was added to equilibrium_phase $Fe(OH)_3$ and brought to equilibrium. The program output provided the moles in the initial mineral assemblage, final moles in assemblage and final solution molarity (mol/L). The mole of mineral phase used for the input was based on the weight of synthesised ferrihydrite used

for the extractions (0.1g) and the Appelo and Postma (2010) conversion of 1 mole of ferrihydrite = 89 g.

**Script :**

```
SOLUTION 1
pH 0.3 charge              # 0.5 mole H+, charge balanced
Cl 500                     # 0.5 mole Cl-
water 0.005                # 5 ml extraction volume
end
USE solution 1             # use an earlier defined or saved solution
EQUILIBRIUM_PHASES 1     # equilibrate with ferrihydrite
Fe(OH)3(a)    0.0    1.12e-3  # Mineral_name, Saturation Index, initial moles
END
```

### 4.2.8 Statistical analysis

Analysis of difference was carried out in SPSS. The assumptions under which the F statistic is reliable for ANOVA (independent observations, measurements at least to interval scale, similar variances for each experimental condition (Levene statistic) and normality of distribution (skewness and Shapiro – Wilk test)) were met for Fe, Zn, Pb (Field, 2009). For Mn the field capacity run data displayed high errors and therefore were not included. Additionally no Mn was recovered from sediment at the bottom of the mesocosm of the flood run during extraction step 2

and only one sample contained Mn from the three week wet run, therefore this data was not included in ANOVA analysis.

The parametric one-way independent ANOVA was carried out to determine whether there was a significant difference between runs in the concentration of Fe, Zn, Pb and *Mn (*selected runs only) recovered during extraction step 2. F was deemed significant if $p < .05$. A further post hoc Tukey test was selected to highlight significant differences between runs. Differences were deemed significant if $p < .05$.

Further ANOVA analysis was then carried out to determine whether there was a significant difference in the concentration of Fe, Zn, Pb, *Mn (*selected runs only) recovered from the sediment of the variable runs at the top and bottom of the mesocosm during extraction step 2. F was deemed significant if $p < .05$. A post hoc Tukey test was run to highlight significant differences. Differences were deemed significant if $p < .05$.

## 4.3 Results

### 4.3.1 Summary

During the mesocosm experiments detailed in chapter 3, freshly precipitated, more labile forms of Fe and Mn may have built up in the sediment as a result of certain wet and dry cycles. Co-precipitation with, and sorption onto, Fe and Mn hydroxides could scavenge high concentrations of aqueous Pb and Zn in pore water and, on flooding, these contaminants could be released back into pore water as a result of dissolution of easily reducible Fe or Mn hydroxides. Sequential extractions were run to quantify the concentration of easily reducible Fe and Mn hydroxides and partitioned Pb and Zn in order to identify the key wet and dry runs this process may have been a controlling factor for.

Extraction step 1 was intended to remove any loosely sorbed reduced Fe from the sediment surface and extraction step 2 was expected to recover easily reducible Fe and Mn along with any partitioned Pb and Zn. The first two extractions therefore were expected to recover the most labile forms of Pb and Zn. The highest concentration of Pb and Zn was recovered from the fine grained fraction (< 63 $\mu$m) of the sediment during extraction steps 1 and 2 (figures 4.2 and 4.3). Therefore the extraction step 1 and 2 results for sediment samples (< 63 $\mu$m) are primary focus of the results and discussion.

Approximately 90 % Pb, 35 – 50 % Zn, 25 – 60 % Mn and 20 – 32% Fe were recovered from extraction steps 1 and 2. Pb concentrations were 5 – 10 times higher than for Fe and Zn. While Mn concentrations were 2 – 3 times lower than for Fe and Zn (see appendix 4.3.1 for detailed concentration (mg/kg) tables).

Less than 10% Pb was extracted during steps 3 and 4 indicating that almost all of the Pb was recovered in the first two extractions (figure 4.2). Higher concentrations of Zn were extracted during steps 3 and 4 (figure 4.3) however there was no pattern of release, such as that observed during step 2, that indicated Zn may be controlled by changes in Fe and/or Mn hydroxide form in response to certain wet and dry runs (discussed in section 4.4.2).

## 4.3.2 Extraction step 1

Reduced Fe can form a monolayer on sediment surfaces and may not be released into solution until all sorption sites are filled (Lovley and Phillips, 1986). Extraction step 1 was therefore intended to remove loosely sorbed ferrous Fe from the sediment. Lovley and Phillips (1986) used this extraction on 0.1 g sediment and reported that during this procedure ferric Fe was not reduced and ferrous Fe was not oxidized as determined by additions of $FeCl_2$ and amorphous Fe oxyhydroxide to sediments in control experiments.

The highest average concentration (mg/kg) of Pb was recovered during extraction step 1 in the fine grained fraction (< 63 µm) of sediment from the 3 week dry run, (54,391 $\pm$9071 mg/kg) and flood run (52,189 $\pm$4237 mg/kg) at the top of the mesocosms and the initial sediment (52, 914 $\pm$3864 mg/kg) (figure 4.2). This represented approximately 40 – 70 % of the total extracted Pb. Average concentrations were 4 – 5 times higher for these runs than for Fe (figure 4.1).

Approximately 30 % of Zn was recovered during extraction step 1 in the fine grained (< 63 µm) fraction of the sediment. The highest average concentration of Zn recovered during extraction step 1 was in sediment of the 3 week dry run (690.5 $\pm$38.67 mg/kg), 1 week wet run (639 $\pm$6.4 mg/kg) and 3 week wet run (607.4 $\pm$17.61 mg/kg) (figure 4.4) at the bottom of the mesocosms. These average concentrations were approximately two orders of magnitude lower than Pb.

The average concentrations (mg/kg) of Mn recovered were generally lower than for Fe, Pb and Zn. The highest average concentration recovered during extraction

step 1 was for the field capacity run (< 63 µm fraction) (201.3 $\pm$56.4 mg/kg) (figure 4.4).

Approximately 15 – 30 % of total Fe was recovered during extraction step 1 from the fine grained fraction of the sediment. The highest average concentration of Fe was recovered from the coarse grained fraction of the sediment (< 2 mm - > 63 µm) of the 3 week dry run at the top (29380.1 $\pm$2996.8) and bottom of the mesocosm (29204.08 $\pm$2803.6) (figure 4.1).

## 4.3.3 Stacked Bar Graphs
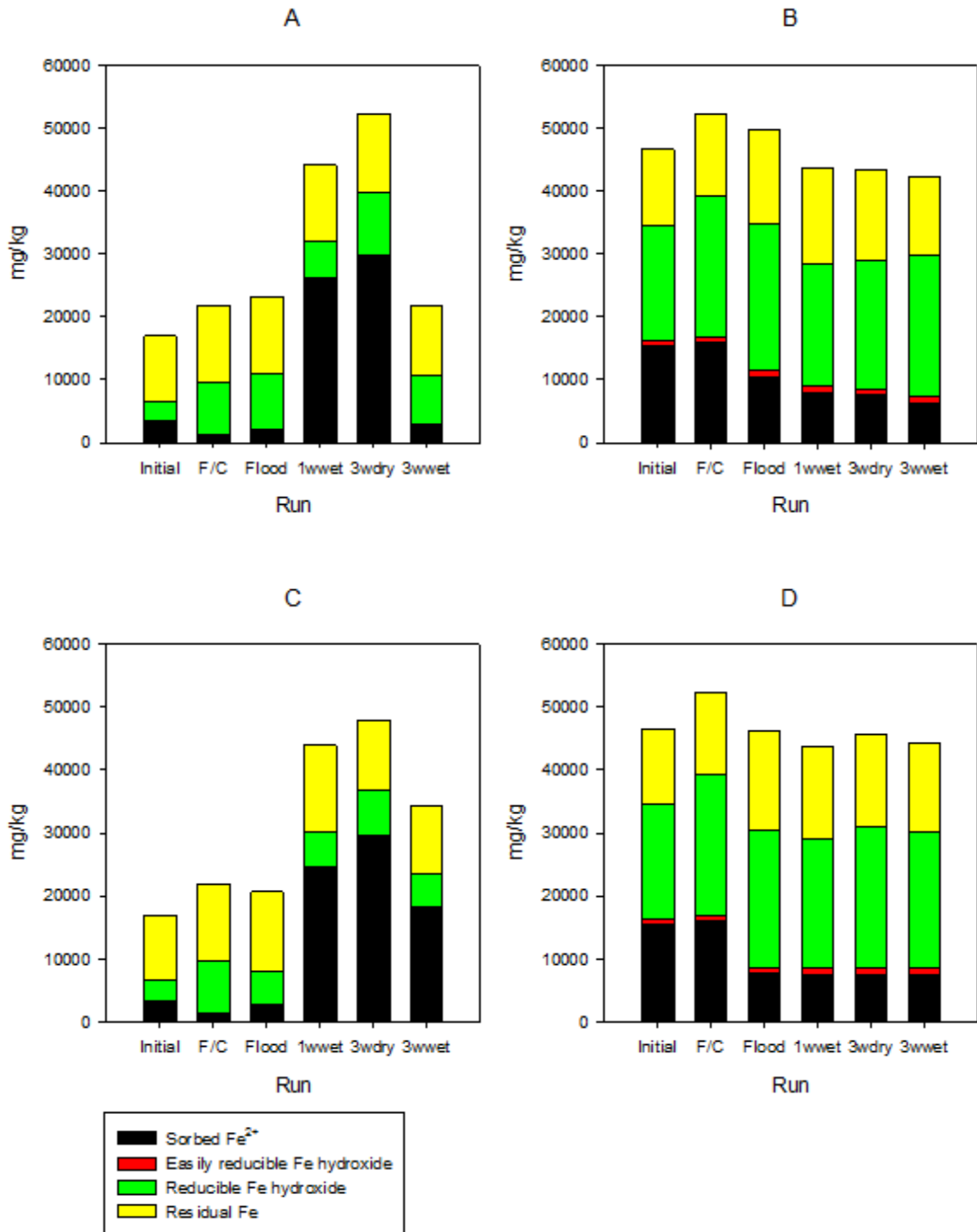


**Figure 4.1. Fe (mg/kg dry weight) for each extraction; A) <2000 μm >63 μm top; B) <63μm top; C) <2000 μm >63 μm bottom; D) <63μm bottom**
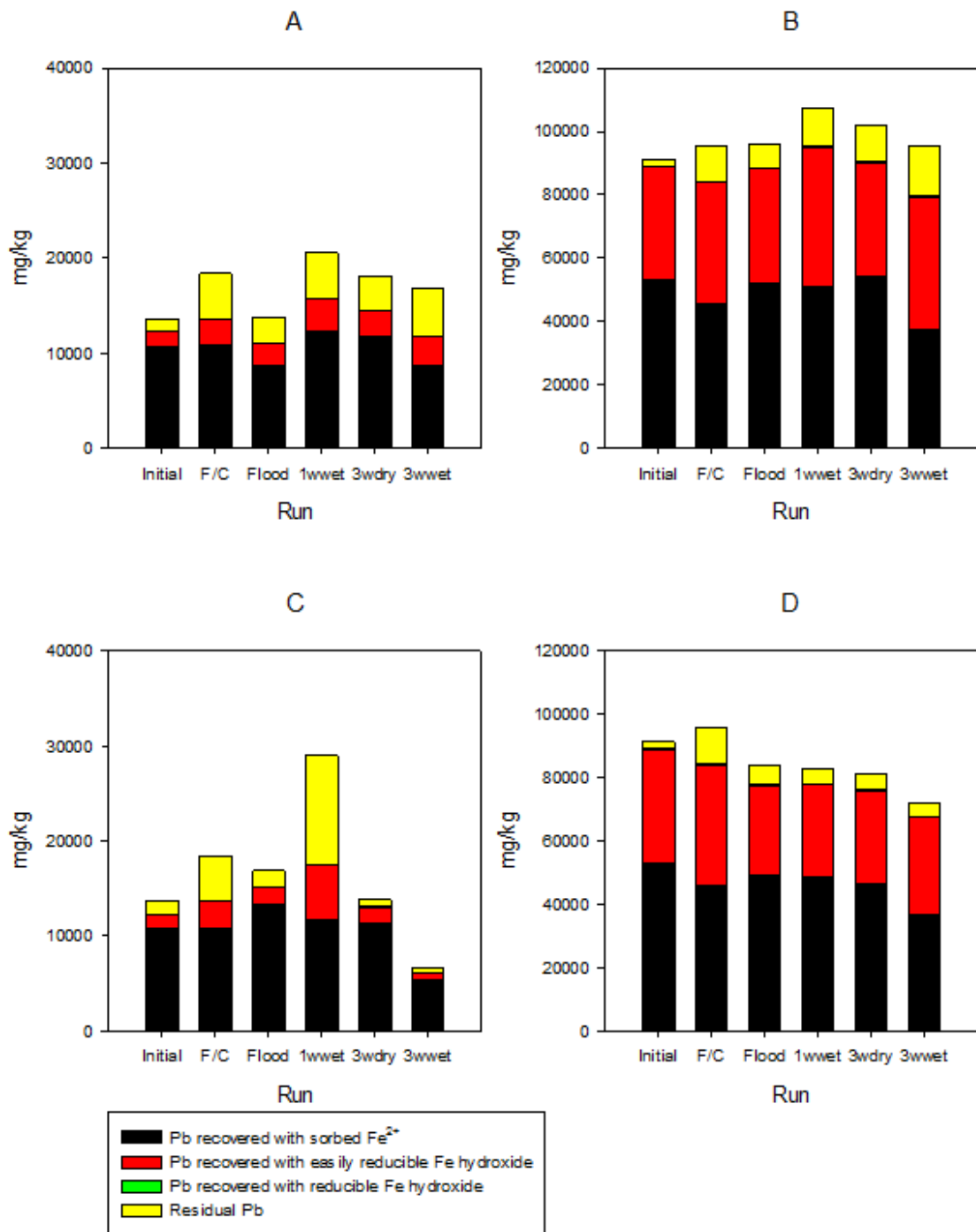
**Figure 4.2. Pb (mg/kg dry weight) for each extraction; A) <2000 μm >63 μm top; B) <63μm top; C) <2000 μm >63 μm bottom; D) <63μm bottom**
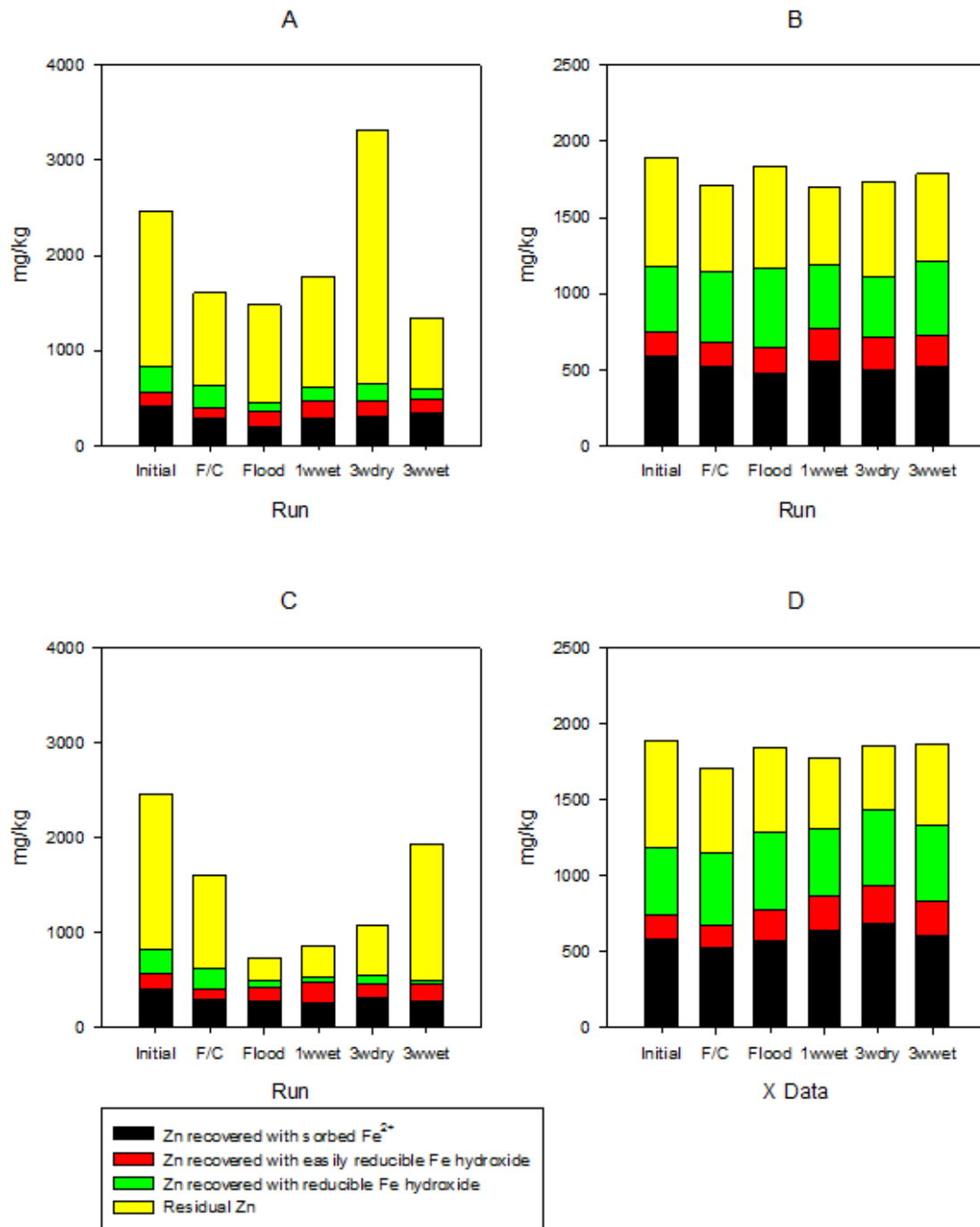
**Figure 4.3. Zn (mg/kg dry weight) for each extraction; A) <2000 µm >63 µm top; B) <63µm top; C) <2000 µm >63 µm bottom; D) <63µm bottom**
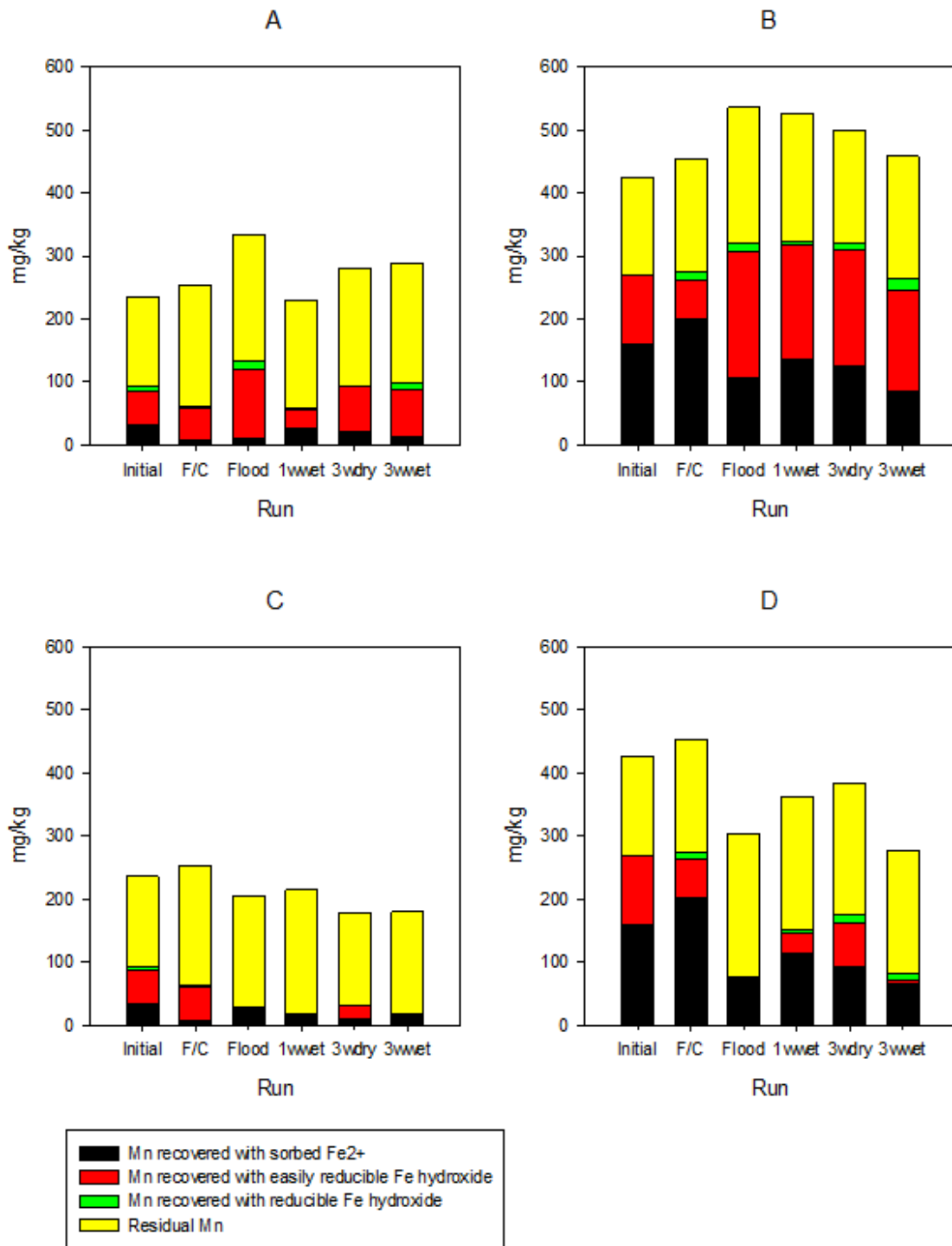
**Figure 4.4. Mn (mg/kg dry weight) for each extraction; A) <2000 μm >63 μm top; B) <63μm top; C) <2000 μm >63 μm bottom; D) <63μm bottom**
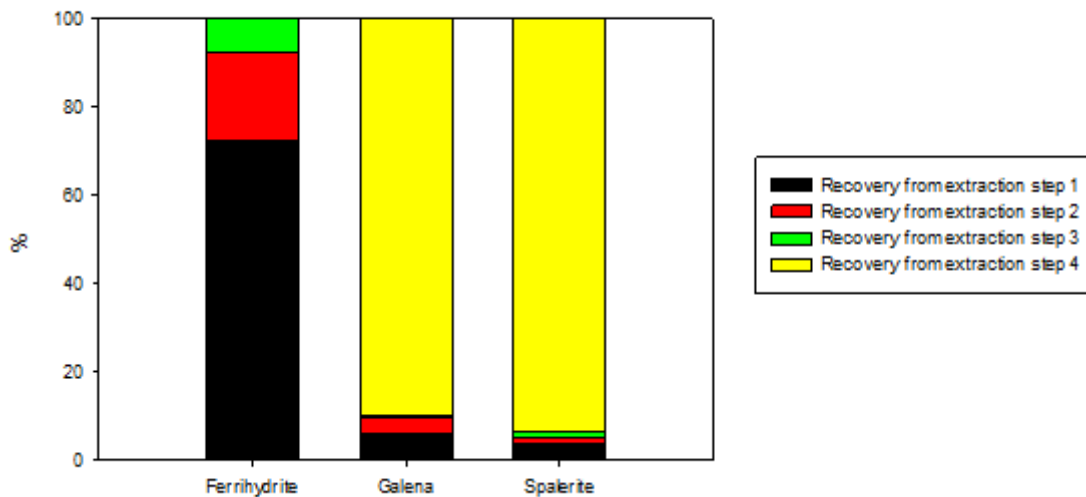
**Figure 4.5. Percentage Fe, Pb, Zn recovered from ferrihydrite, galena and sphalerite respectively for extraction steps 1 – 4**

Recovery of Pb and Zn  from control standards galena and sphalerite respectively was found to be < 10% during extraction steps 1 and 2 (figure 4.5).

Ferrihydrite synthesised using Poulton and Cranfield (2005) methodology showed a 77% Fe recovery during extraction step 1.

X-ray diffraction for identification of galena and sphalerite standards was carried out. The 2Ө angles, (table 4.2) were found to match the galena and sphalerite reference data sheets obtained from the SIeve for PDF2 software data processing package. See appendix 4.3.2 for X-ray diffraction patterns for control standards.

**Table 4.2 First three 2Ө 'maxima' and Ө angles for crystal standards of galena (PbS) and spalerite (ZnS) for incident wave length (λ) copper Kα (1.542 Å)**

| Mineral | 2Ө angle | Ө angle | d Å |
|---------|----------|---------|-----|
| Galena | 25.96 | 12.98 | 3.43 |
| Galena | 30.07 | 15.035 | 2.97 |
| Galena | 43.05 | 21.525 | 2.1 |
| Sphalerite | 28.56 | 14.28 | 3.12 |
| Sphalerite | 47.5 | 23.75 | 1.91 |
| Sphalerite | 56.27 | 28.13 | 1.63 |

Samples were analysed to identify crystalline minerals in sediment through XRD using the SIeve for PDF2 software. No difference between sediment samples was observed. XRD can only identify minerals that are crystalline however key mineral types likely to influence pore water Pb and Zn concentrations are reactive poorly crystalline or amorphous mineral types, less likely to be identified through XRD (Hudson-Edwards, 2003). Moreover XRD has been reported as relatively insensitive to contaminant minerals when they are present at low concentration in the sediment (Heron et al., 1994, Leinz et al., 2000). The results obtained by the diffractometer for the heterogeneous sediment samples contained a high number of closely spaced intensity maxima and propensity for peak overlap resulted in ambiguous and therefore inconclusive results. A few selected mineral types (table

4.3) indicate that impure mineral mixtures containing Fe, Mn, Zn, Pb and sulphate may exist in the sediment. However, the author acknowledges, owing to the reasons noted above, it is unlikely that the minerals identified are a true representation of those in the sediment.

**Table 4.3 XRD results from sediment samples. Minerals were identified through Sleve PDF2 software (see text notes above regarding the accuracy of results).**

| Mineral | D1 | D2 | D3 | D4 | D5 | D6 | D7 | D8 |
|---|---|---|---|---|---|---|---|---|
| Fe sulphate hydrate | 3.36 | 2.75 | | | | | 2.76 | 3.5 |
| Pb Bi Sulphide | 3.341 | 3.391 | 3.528 | 2.94 | | | | |
| Pb Se Sulphate | 3.34 | 3.23 | 3.020 | 2.086 | | | 4.32 | |
| Zn Mn Fe Sulphide | 3.35 | | 2.96 | 1.91 | | | | |
| Ca Mn Sulphate Hydroxide Hydrate | 3.34 | 4.26 | 2.129 | | 2.57 | | | |
| Mn Ca Zn Te oxide | 3.375 | 28.13 | | 2.033 | | 3.26 | | |

A geochemical programming script was run to calculate the expected recovery of Fe from a ferrihydrite phase, $Fe(OH)_3$, when brought to equilibrium with a 5 ml HCl extraction at pH 0.3 (the calculated pH for 0.5 mole HCl) (table 4.4). It can be seen that a 95 % recovery of Fe was predicted.

**Table 4.4 Calculations using PHREEQC.dat to estimate recovery of Fe from ferrihydrite, using 0.5 mole HCl (pH 0.3).**

| Mineral Phase | pH | Initial moles in assemblage 0.1 g | Final moles in assemblage | Final Molality (mol/L) Fe in solution | Recovery % |
|---|---|---|---|---|---|
| Fe(OH)3 | 0.3 | 1.12e-3 | 5.912e-5 | 1.061e-3 | 95 |

### 4.3.4 Extraction step 2

Extraction step 2 was intended to determine whether there had been a build-up of easily reducible Fe in the sediment and to quantify the concentration of Zn and Pb and Mn associated with that fraction of Fe. Both Tessier and BCR methods use hydroxylamine hydrochloride to recover Fe from the easily reducible Fe fraction, although each method uses a different extraction composition and temperature (Fernandez Albores et al., 2000).

Only a small percentage (20%) of Fe was recovered from synthesised ferrihydrite during extraction step 2 (figure 4.5) and results from geochemical programming show that 95% Fe would be recovered from ferrihydrite using a 0.5 M HCl extraction. It is therefore possible that labile Fe hydroxide was removed during extraction 1. However although the easily reducible Fe phase represented only 1 – 3 % of the total Fe recovered, the equivalent dry weight was approximately 700 mg/kg Fe, that concentration was approximately 4 – 5 times higher than Zn and similarities in the patterns of Fe and Zn recovery for this extraction were apparent in the fine grained (<63 $\mu$m) sediment of the variable wet and dry runs at the top and bottom of the mesocosm. Additionally, high percentages of Pb (30 – 40 %), Zn (10 %) and Mn (~30 % - top of mesocosm) were extracted from this phase.

Figures 4.6 and 4.7 show that there was a higher concentration of easily reducible Fe and Zn recovered at the top and bottom of the mesocosm from the sediment of the variable wet and dry runs compared to the initial sediment and field capacity run. At the bottom of the mesocosm lower concentrations of Pb were recovered from the sediment of the variable wet and dry runs compared to the initial sediment and field capacity run. Contrary to this at the top of the mesocosm, higher concentrations of Pb were recovered from the sediment of the variable wet and dry runs, particularly for the 1 week wet and 3 week wet runs.
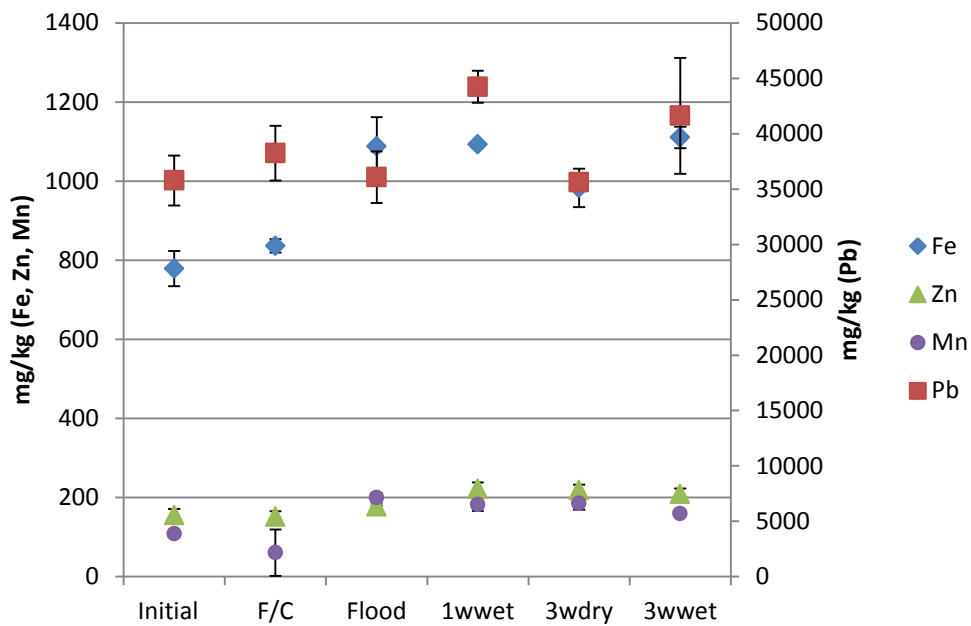


**Figure 4.6 Average concentration (mg/kg), with standard error, of Fe, Mn, Pb, Zn recovered during extraction step 2, by run, in the fine grained (<63 μm) sediment at the top of the mesocosms (Pb on the secondary axis).**
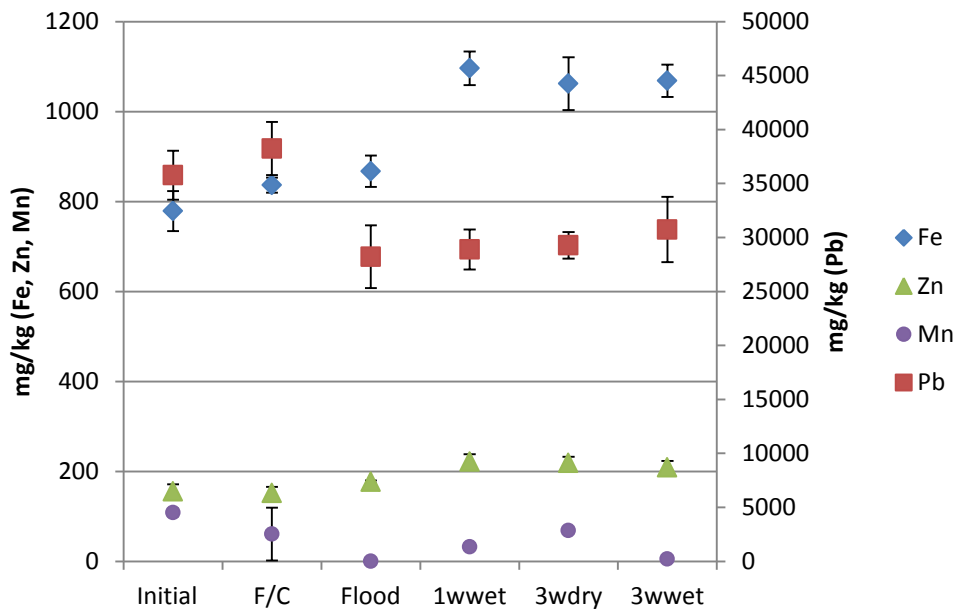
**Figure 4.7 Average concentration (mg/kg) of Fe, Mn, Pb, Zn recovered during extraction step 2 (with standard error), by run, in the fine grained (<63 μm) sediment at the bottom of the mesocosms (Pb on the secondary axis).**

Results from one-way independent ANOVA (table 4.5) found there was a significantly higher concentration of Fe and Zn recovered from the sediment of the variable wet and dry runs compared to the initial sediment and control runs during extraction step 2.

At the bottom of the mesocosm, results from post hoc Tukey tests (see appendix 4.3.4) found there was a significantly higher concentration of Zn (p = <.5) for the 3 week wet run compared to the initial sediment and field capacity run and that corresponded with a significantly higher concentration of Fe (p = <.00) for the 3 week wet run.

**Table 4.5 Results from ANOVA, Fe, Zn, Pb, Mn recovered during extraction step 2, initial sediment and control runs compared to variable runs at the top and bottom of the mesocosm (see appendix 4.3.4 for full Tukey results)**

| | Compared Runs | n | dfm | dfr | F statistic | Sig | Significant difference Y/N |
|---|---|---|---|---|---|---|---|
| Fe (bottom) | 1 - 6 | 18 | 5 | 12 | 12.11 | .00 | Y |
| Zn (bottom) | 1,2,6 | 9 | 2 | 6 | 10.631 | .01 | Y |
| Pb (bottom) | 1 - 6 | 18 | 5 | 12 | 3.06 | .05 | N |
| Fe (top) | 1 - 6 | 18 | 5 | 12 | 11.19 | .00 | Y |
| Zn (top) | 1 - 6 | 18 | 5 | 12 | 5.295 | .01 | Y |
| Pb (top) | 1 - 6 | 18 | 5 | 12 | 1.665 | .22 | N |
| Mn (top) | 1,4,5,6 | 12 | 3 | 8 | 8.497 | .01 | Y |

| Run # | Description |
|---|---|
| 1 | Initial Sediment |
| 2 | Field Capacity |
| 3 | Flood |
| 4 | 1 week wet |
| 5 | 3 weeks dry |
| 6 | 3 weeks wet |

At the top of the mesocosm, results from post hoc Tukey test found a significantly higher concentration of Zn (p = <.05), Fe (p = <.00) and Mn (p = <.01) recovered from the sediment of the 1 week wet run compared to the initial sediment.

Comparing concentrations (mg/kg) of Fe, Mn, Pb, Zn recovered from sediment of the variable runs at the top of the mesocosm with concentrations of these metals at the bottom, results from ANOVA found a significantly higher concentration of Pb was recovered from the sediment of the variable runs at the top compared to the bottom F (5, 12) = 5.955, p = <.05. Results from post hoc Tukey tests (see appendix 4.3.4) found that significantly more Pb was recovered from the sediment of the 1 week wet run at the top of the mesocosm (p = < .05) compared the

variable runs at the bottom. Significantly more Pb was also recovered from the sediment of the 3 week wet run at the top of the mesocosm ($P = < .05$) compared to the 1 week wet and 3 week dry runs at the bottom. There was also a significantly higher concentration of Mn recovered from the sediment of the 1 week wet run and 3 week dry run at the top of the mesocosm compared to the bottom $F_{(3, 8)} = 46.299$, $p = <.00$, as confirmed through Tukey analysis for the 1 week wet run ($p = < .00$) and the 3 week dry run ($p = < .00$). It can be seen (figure 4.7) that very little Mn was recovered from the sediment of the 3 week wet run at the bottom of the mesocosm, higher concentrations of Mn were recovered from the sediment at the top of the mesocosm for this run (figure 4.6), however this run was not included in the ANOVA analysis.

There was no significant difference in the concentration of Fe or Zn recovered during extraction step 2 from sediment of the variable runs at the top of the mesocosm compared to the bottom.
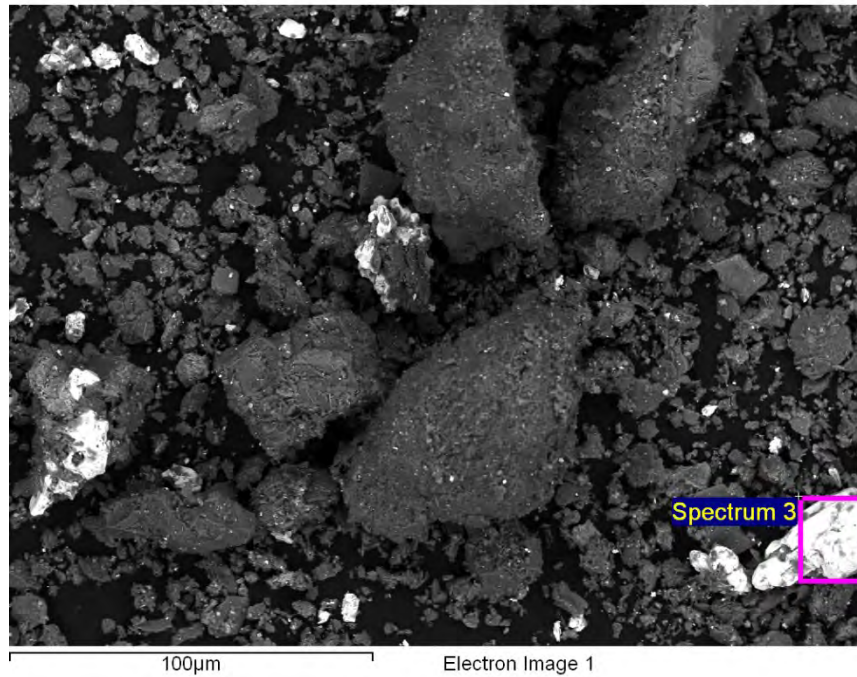
**Figure 4.8 Back scattered electron image of sediment for flood run (UOB)**

Figure 4.8 shows a back scattered electron image of the sediment remaining at the end of the flood run. Spectrum 3 was selected for further analysis through EDS and the resulting quant specification (table 4.6) shows an atomic % close to 1:1 ratio for Pb and S. Possibly indicating the presence of galena.

**Table 4.6 Quant specification for spectrum 3 (figure 4.8) (UOB)**

| Element | Weight% | Atomic% |
|---------|---------|---------|
| S K | 13.13 | 45.43 |
| Mn K | -0.07 | -0.14 |
| Fe K | 2.85 | 5.65 |
| Zn L | 3.46 | 5.87 |
| Pb M | 80.64 | 43.19 |
| Totals | 100.00 | |

The smart map pattern displayed (figure 4.10) shows that the grain in spectrum 3 is likely to be a Pb, S mineral. A similar pattern of Pb and S was found throughout the sediment for all runs indicating Pb S minerals were prevalent in the sediment. Fe and Zn do not show the same pattern but there may be some association between Fe and Zn (bright spot far right, middle). Zn and Mn were difficult to quantify through SEM/EDS, possibly due to lower total concentrations of these elements in the sediment.



20µm    Electron Image 1
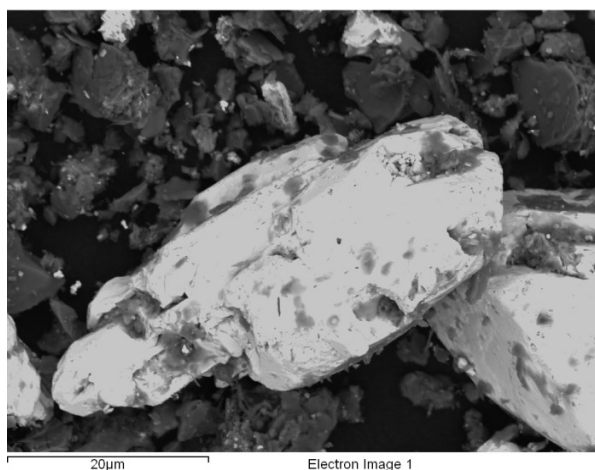
**Figure 4.9 Magnified BSE image of spectrum 3 (figure 4.8) (UOB)**
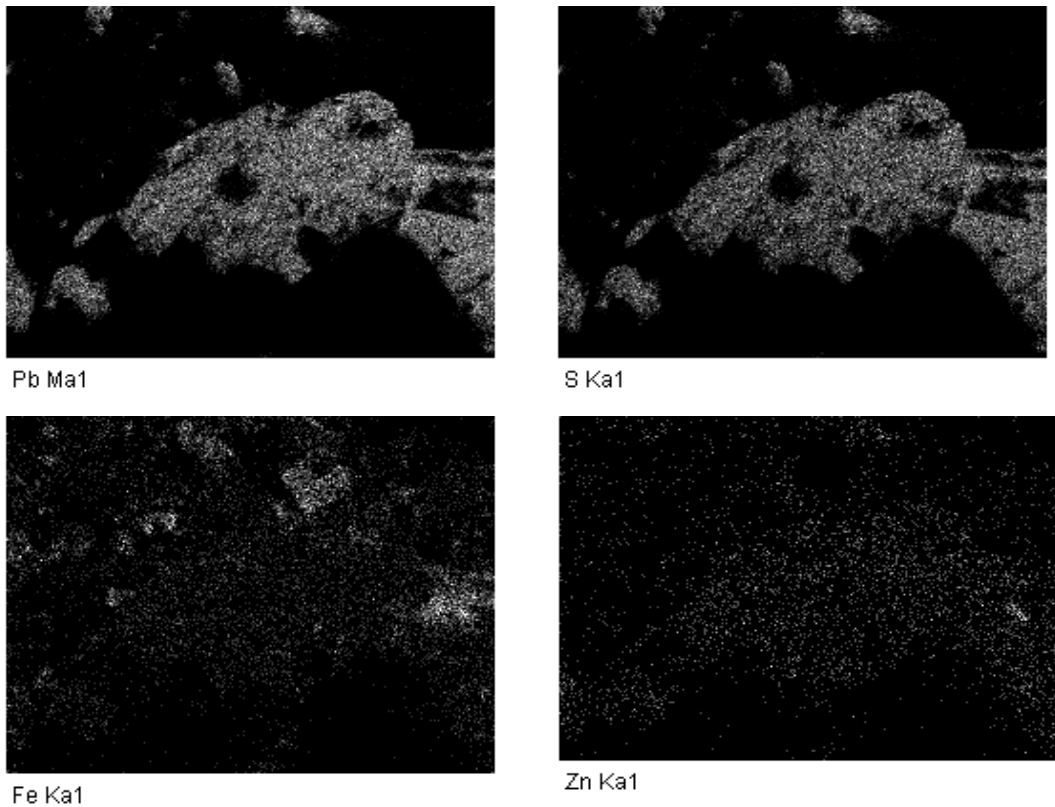
**Figure 4.10 Smart map of elements using acquired X-ray data for spectrum 3 (figure 4.8) (UOB)**

The smart map pattern (figure 4.12) displayed shows a grain with associated Zn, Pb and S, an indication of the heterogeneous mix of S minerals in the sediment.

Although not part of the current mesocosm study, SEM/EDS was carried out at Liverpool John Moores University (LJMU) on sediment remaining at the end of sub-set of mesocosm runs described in detail in chapter 5. The sediment was collected from the same stretch of river near the original sample site. Findings from SEM/EDS analysis show what seems to be grains with a mixed layer Mn, Fe, Pb, Zn and sulphate on the surface sediment at the top of the mesocosm of the 1 week wet run (figures 4.13 and 4.14).
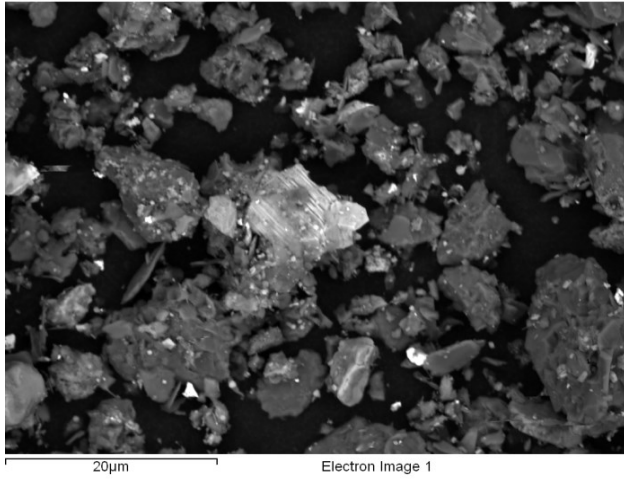
**Figure 4.11 Back scattered electron image for the sediment of the 3 week dry run (UOB)**
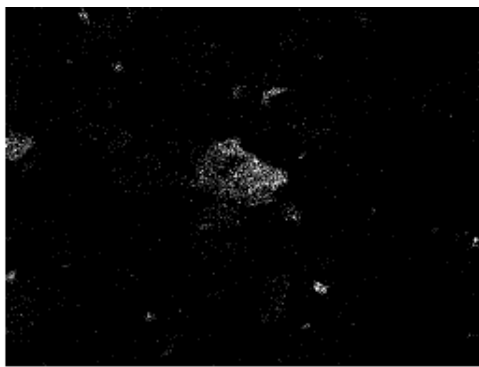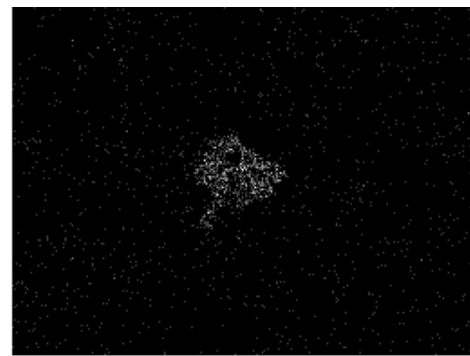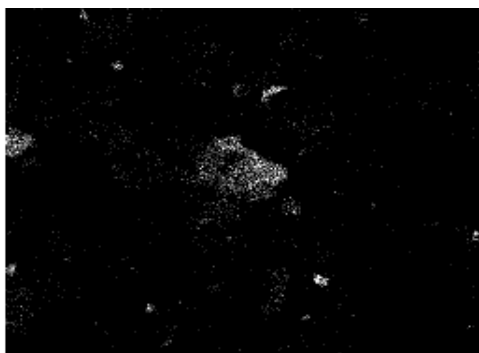


**Figure 4.12 Smart map of elements using acquired X-ray data for figure 4.11 (UOB)**
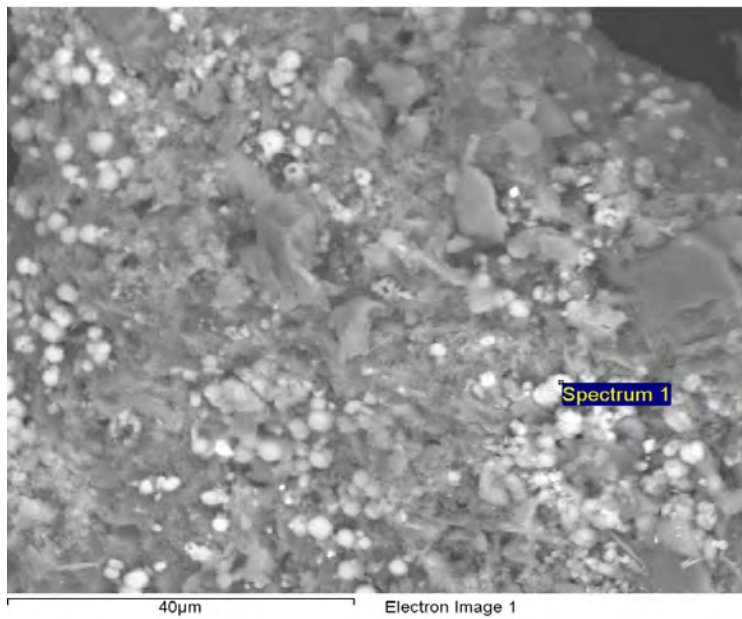
Figure 4.13 Back scattered electron image of the surface sediment (top), 1 week wet run, subsequent mesocosm study (LJMU).
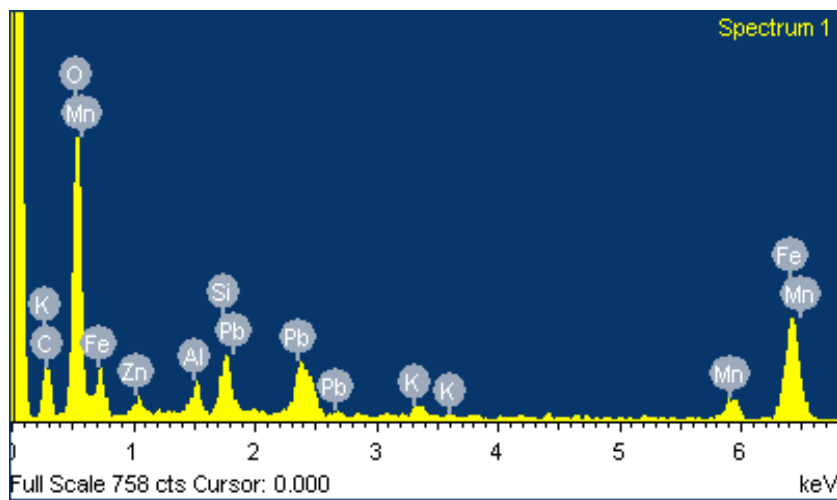


Figure 4.14 EDS spectrum (histogram) for spectrum 1, figure 4.13 (LJMU).

**4.4 Discussion**

The main aim of this experiment was to measure different forms of Fe and Mn hydroxide in the sediment along with partitioned Pb and Zn in order to understand whether there had been a build-up in more reactive forms of Fe and Mn for certain wet and dry runs. More reactive forms of Fe and Mn may have controlled the mobility of Pb and Zn and that could account for the pulsed pattern of release observed for these trace metal contaminants observed over flooded periods during the wet and dry treatments (chapter 3).

Fe, Mn, Pb Zn were recovered over 4 sequential extractions. The highest concentrations of the Pb and Zn were recovered from the fine grained fraction of the sediment (<63 µm). Trace metals are often reported as most highly associated with the fine grained fraction of the sediment (Stone and Droppo, 1996; Butler, 2009; Byrne et al., 2010) and that may be due to the larger surface area per unit mass in the clay and silt size fractions (Stone and Droppo, 1996; Byrne et al., 2010).

The first two extractions were expected to recover the most bioavailable forms of Pb and Zn. The Fe and Mn extracted during these steps (i) loosely sorbed reduced Fe/Mn (II) and (ii) easily reducible Fe/Mn hydroxides would be most sensitive to changes in redox potential brought about by the wet and dry treatments. Therefore quantifying the metals extracted during these steps could provide an indication of whether Fe/Mn hydroxides had controlled the attenuation and release of contaminant trace metals Pb and Zn in response to certain wet and dry treatments. As noted in methodology chapter section 2.2.5 steps 3 and 4 were expected to extract more residual forms of Fe and Mn hydroxide and associated

trace metals. A previous paper had hypothesised that more residual forms of Fe and Mn hydroxide would be less likely to change form in response to changes in redox potential brought about by wetting and drying of the sediment and so would have less influence on the mobilisation of Pb and Zn (Lynch et al., 2014). Furthermore patterns of Zn and Pb extracted in steps 3 and 4 (figures 4.2 and 4.3) indicated residual Fe and Mn mineral forms had little influence on the release of Pb and Zn in response to the alternating wet and dry sequences. Almost all of the Pb was extracted in the first 2 steps indicating that Pb was present in a highly labile form. For these reasons only the results of the first two extractions carried out on the fine grained fraction of the sediment (<63 µm) are discussed in detail below.

### 4.4.1 Extraction step 1 (discussion)

Extraction 1 was intended to remove loosely sorbed ferrous Fe (II) from the sediment along with any loosely sorbed Pb, Zn and Mn (II). A high percentage of Pb (40 – 70 %), Fe (20 - 50%), Zn (30 %) and Mn (20 – 40 %) of the total metals were recovered during this extraction and it is possible that several mineral phases in addition to any sorbed metals, contributed to the recovery of Pb and Zn.

Although chemical extractions are intended to be phase specific the literature reports that total specificity is highly unlikely (Leinz et al., 2000; Linge, 2008). In the case of the current experiment the 0.5 M HCl extraction used in step one has been found to extract a variety of sulphur minerals partitioned with trace metals. For example Baba et al. (2011) reported that a 0.5 mole HCl extraction (ratio 0.1g:10ml) resulted in 30% Pb extracted from an anglesite sample (<63 µm) within

1 hour. Furthermore, at higher concentrations (6 – 12 moles) HCl extractions have been reported to dissolve acid volatile sulphides (Linge, 2008). It is therefore possible that Pb and Zn partitioned with sulphur minerals in the sediment were extracted during step 1. Precipitation of anglesite was one of the proposed mechanisms controlling Pb concentrations in pore water over the mesocosm experiments (chapter 3) and therefore high concentrations of this mineral may have been present in the sediment. That could account for the high concentration of Pb in this extraction step.  Moreover, at the Cwmystwyth mine site the primary minerals mined were galena and sphalerite (Hughes, 1981) therefore high concentrations of primary sulphide minerals were likely to be present in the sediment. This was indicated through tentative XRD analysis (table 4.3) and through SEM/EDS analysis (table 4.6) that identified Pb S species in the sediment at an atomic 1:1 ratio expected for galena. An association of elements Pb and S was indicated through smart map patterns (figure 4.10) and a similar association between Pb and S was found throughout the sediment for all runs. Smart map patterns (figure 4.12) also identified mixtures of Zn, Pb and S in close association and it is highly likely that reactive secondary mineral precipitates were present in the sediment.

A 0.5 M HCl produces a low pH extraction (table 4.4). Both sphalerite and galena dissolution increases as pH declines. Cama et al. (2005) measured galena dissolution as a function of pH and reported an increase in aqueous Pb concentration with a decrease in pH from pH 3 to 1. Normalising to the geometric surface area they found the galena dissolution rates varied by one order of magnitude between pH 3 and 1 respectively. The dissolution rate of sphalerite has

also reported to increase in response to a fall in pH. Stanton et al. (2006) used the rate of production of aqueous Zn to estimate sphalerite dissolution and reported that the sphalerite solubilisation rate was three times faster at pH 2 than pH 4.

Only low concentrations (< 10 %) of Pb and Zn were recovered from the control standards during extraction step 1. However the control standards were crystalline (as identified through XRD analysis) and it is likely that the sediment contained high concentrations of amorphous minerals, as confirmed through previous analysis of metal mine waste (Leinz et al., 2000; Hudson-Edwards, 2003). It is also likely that the minerals in the sediment were not pure as indicated through SEM/EDS (figure 4.12) and XRD (table 4.3) analysis. Surface structure, grain size and mineral composition have all been found to influence sphalerite and galena mineral reactivity and dissolution rates. Stanton et al. (2006) noted that fine grained sphalerite leached at pH 4 produced concentrations of dissolved Zn that were 20 times higher than coarse grained sphalerite and they found Zn recovery was higher for sphalerite high in Fe than for sphalerite with low Fe content. It is therefore likely that the control minerals had different structural and chemical characteristics to similar minerals in the sediment and so may not have mimicked their behaviour.

A high percentage of Fe (77%) was recovered from the synthesised ferrihydrite during extraction step 1 and results from a simple geochemical program show a 95% recovery of Fe. It is unlikely that the synthesised ferrihydrite mimicked precisely the behaviour of natural Fe/Mn hydroxides in the sediment as natural sediments are a complex mix of metal oxides, clays and organics that form a heterogeneous coating on sediment surfaces. Even so it is probable that labile

'easily reducible' Fe and Mn hydroxide was recovered during extraction step 1 and this is likely to have influenced the results from extraction step 2. Quantifying how much is difficult because, as discussed, Pb and Zn may have been associated with a number of phases.

The original extraction carried out by Lovley and Phillips (1986) was on tidal river surface sediments with a lower sulphate concentration (0.2 Mm). Although sulphide concentrations were not reported in their paper, the authors indicated concentrations were low. The pore water sulphate concentrations observed during the mesocosm experiments (chapter 3) were in some cases an order of magnitude higher than those reported by Lovley and Phillips (1986). The difference in sediment composition between the two studies seems to have influenced the results. Considering sediment composition is therefore clearly important when deciding on whether to include an extraction step. This is a consideration that would be taken into account in future studies.

Alternative methodologies could be used, for example extractions by Stecko and Bendell-Young (2006) and Lopez-Gonzalez et al. (2006) carried out the hydroxylamine hydrochloride extraction to extract easily reducible Fe and Mn hydroxides as step 1 (step 2 in the current experiment). However, as material extracted during this step would include reduced Fe/Mn(II) sorbed to the surface of sediments the results would give falsely high observations for easily reducible Fe and Mn hydroxide. A less stringent first extraction would be considered in future. A first extraction step in the technique proposed by Tessier et al. (1979) is the use of 1M $MgCl_2$ at pH 7 to remove loosely bound exchangeable ions. However, one of the reasons Lovley and Phillips (1986) used the 0.5 Mole HCl extraction was

because they found it did not alter the redox state of Fe (II), so Fe and Mn

hydroxides did not precipitate out during extraction step 1. Therefore any

alternative 1$^{st}$ step aimed at extracting reduced Fe/Mn(II) would need to be carried

out under anoxic conditions. Heron et al. (1994) reported 100% recovery of sorbed

ferrous Fe (II) from aquifer sediment using an anaerobic extraction of 1 mole

$CaCl_2$ at pH 7 that left other minerals  FeS, $FeS_2$, $FeCO_3$ unattacked. Therefore,

where the facilities were available, this extraction could be considered as a first

extraction step in future studies.

### 4.4.2 Extraction step 2 (discussion)

Extraction step 2 was intended to determine whether there had been a build-up of

easily reducible Fe and Mn hydroxides in the sediment of the variable wet and dry

treatments  (chapter 3) and whether these minerals may have acted as a source

of Pb and Zn contamination to pore and surface water over flooded periods.

Results from extraction step 2 showed a significantly higher concentration of Zn

(mg/kg) was recovered from the sediment at the bottom of the mesocosm for the 3

week wet run compared to the initial sediment or field capacity control and that

corresponded with a significantly higher concentration of Fe recovered during

extraction 2 for that run. During the mesocosm experiments (chapter 3) dissolved

Zn (mg/L) concentrations were found to increase significantly over flood periods at

the bottom of the mesocosm for the 3 week wet run and there was a positive

correlation between dissolved Zn and dissolved Fe. Furthermore the results from

PCA (chapter 3, section 3.3.7) indicated that the underlying components for factor

1 were related to redox potential conditions that influenced the mobility of Zn and

the factor scores for the 3 week wet run were found to fall along this factor. It is

therefore possible that for the 3 week wet run at the bottom of the mesocosm easily reducible Fe hydroxides controlled the mobility of Zn and resulted in the pulsed pattern of Zn and Fe release observed over flooded periods for that run.

A higher percentage of Pb (30 – 40 %) compared to Zn (10%) was recovered in the easily reducible Fe extraction from the fine grained (< 63 µm) fraction of the sediment. Pb has often been reported to preferentially sorb to freshly precipitated Fe hydoxides over Zn (Licheng and Guijiu, 1996; Hamilton-Taylor et al., 1997; Desbarats and Dirom, 2007; Wang et al., 2010). Pb has a lower sorption edge (pH 3-5) than Zn (pH 5-6.5) (Smith, 1999; Lee et al., 2002; Appelo and Postma, 2010) and so at the pH of the pore water during the mesocosm experiments (pH 5 - 5.5) higher concentrations of Pb would likely sorb to Fe hydroxide surfaces than Zn. That could account for the high concentrations of Pb recovered during extraction step 2. However, at the bottom of the mesocosms, the concentration of Pb recovered from sediment of the variable runs during extraction step 2 was not significantly higher compared to the initial sediment or constant control runs (figure 4.7) as would be expected if co-precipitation and sorption of Pb with Fe hydroxide had occurred over the wet and dry treatments. That could be because during the mesocosm experiments there was less dissolved Pb released into pore water over a flood at the bottom of the mesocosm and less therefore to be scavenged through co-precipitation with Fe or Mn hydroxides over subsequent dry oxidised periods. Results from the mesocosm study (chapter 3, section 3.3.2) found significantly lower concentrations of Pb were released at the bottom of the mesocosm than at the top and (chapter 3, section 3.3.4) the release of dissolved Pb was negatively correlated with dissolved Fe. In chapter 3 the results of

geochemical calculations indicated anglesite solubility was the main mechanism controlling dissolved Pb concentrations in pore water (section 3.3.8). As previously discussed an extraction is unlikely to be totally specific for one phase (Linge, 2008). Leinz et al. (2000) carried out a series of Tessier et al. (1979) extractions and reported a 60,000 mg/kg recovery of Pb from anglesite using an extraction of 0.25 M hydroxylamine hydrochloride in 0.25 M HCl extraction for 30 minutes at 50°C. It is therefore possible that for extraction step 2 some of the Pb recovered was from anglesite.

At the top of the mesocosm the recovery of Zn, Fe and Mn during extraction step 2 was significantly higher for the 1 week wet run compared to the initial sediment. However, for this run dissolved Fe was not found to correlate with the release of dissolved Zn during the mesocosm experiments in chapter 3. This may have been because conditions remained oxic at the surface as has been reported for some inundation studies. For example a 10 week inundation study of metal polluted sediment reported that a steep redox gradient formed at the sediment / surface interface where conditions remained oxic at the surface whilst just below the sediment surface conditions became reducing within two days (van der Geest and Paumen, 2008).  Similarly over a 3 month inundation study of mining contaminated sediments conditions were reported to remain oxic at the surface (Wragg and Palumbo-Roe, 2011). It is therefore unlikely that reductive dissolution of easily reducible Fe hydroxide over flooded periods controlled the pulsed release of Zn into surface water.

The high concentration of easily reducible Fe recovered from the sediment at the top of the mesocosm may have been due to the upward diffusion of reduced Fe

and the formation of an oxidised layer at the sediment surface as reported by some authors (Patrick and Delaune, 1972; Wragg and Palumbo-Roe, 2011). Oxidation of Fe is an acid generating process:

$$Fe^{2+} + 1/4 O_2 + H^+ \longrightarrow Fe^{3+} + \frac{1}{2} H_2O \qquad (1)$$

$$Fe^{3+} + 3 H_2O \longrightarrow Fe(OH)_3 + 3H^+ \qquad (2)$$

(Appelo and Postma, 2010)

Subsequent sorption of Pb and Zn onto hydroxide surfaces is also an acid generating process:

$$\equiv FeOH + Pb^{2+} \longrightarrow \equiv FeOPb^+ + H^+ \qquad (3)$$
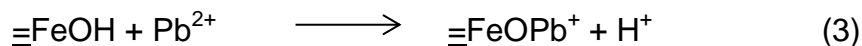
(Appelo and Postma, 2010)

That could account for the slight fall in pH that was observed over flooded periods at the top of the mesocosms.

A higher concentration of Mn was recovered during extraction step 2 at the top of the mesocosm compared to the bottom (figure 4.6 and 4.7). It is possible that the dissolution and precipitation of Mn hydroxides accounted for the pulsed release of Zn and possibly Pb at the top of the mesocosm over flooded periods. Dissolved Mn was found to correlate significantly with dissolved Zn (chapter 3, section 3.3.5) and Pb (section 3.3.4) in the pore water at the top of the mesocosms and although not part of this study, SEM/EDS analysis carried out on sediment remaining at the end of the 1 week wet run, detailed in chapter 5, shows a mix of Mn, Fe, Pb and Zn precipitates on the surface of sediment grains at the top of the mesocosm (figures 4.13 and 4.14).

Mn hydroxide solubility is more sensitive to a fall in redox potential conditions than Fe (Lee et al., 2002) and laboratory studies have shown Mn hydroxides reduce at a higher redox potential than Fe (Patrick and Henderson, 1981) and at a faster rate (Patrick and Delaune, 1972). The further reduction of Mn (hydr)oxides could also be coupled to the oxidation of Fe:

$$2Fe^{2+} + MnO_2 + 4H^+ \longrightarrow 2Fe^{3+} + Mn^{2+} + 2H_2O \qquad (4)$$
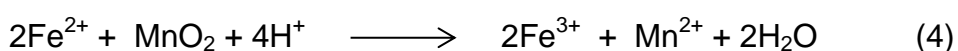
(Appelo and Postma, 2010)

This is an acid consuming process, although any subsequent hydrolysis of oxidised Fe (2) and sorption processes (3) would negate this effect.

The release of dissolved Pb into pore water at the top of the mesocosm may have been partly controlled by Mn hydroxides over flooded periods, however, Pb concentrations (mg/kg) recovered from the sediment were in most cases two orders of magnitude higher than Mn. Geochemical calculations (chapter 3, table 3.10) indicated that precipitation of anglesite may have occurred to a greater extent at the top of the mesocosm compared to the bottom and as discussed previously that could account for the higher recovery of Pb (figure 4.6).

In summary a combination of sequential extraction results and pore water analysis indicate that at the bottom of the mesocosm labile Fe hydoxides may have been a mineral source of Zn contamination into pore water over flooded periods for the 3 week wet run.

At the top of the mesocosm it is possible that Mn hydoxides partly controlled the release of Zn and possibly Pb into pore water. However, the high percentage of

Pb recovered during extraction step 2 was probably due to dissolution of anglesite during this extraction.

### 4.4.3 Comparison of total sediment concentrations with guideline value predicted effect level (PEL)

All sediment samples (figures 4.1 – 4.4) contained total Zn and Pb concentrations that exceeded predicted effect level (PEL) indicating that concentrations of these trace metals in the river bank sediment could pose a serious environmental risk and have an adverse biological effects (Environment agency, 2008b).

**Table 4.7 Total concentrations of Pb and Zn found in sediment samples compared to other findings from the literature (\*Montserrat, 2012; \*\*Palumbo-Roe et al., 2013, \*\*\*Palumbo-Roe et al., 2009, \*\*\*\*Cave et al., 2005) Note: Grain sizes are <2 mm unless specified otherwise.**

| Site | Pb (mg/kg) | Zn (mg/kg) |
|---|---|---|
| This study (range) | 72,186 – 107,149 | 1,891 – 1,702 |
| Cwmystwyth (mine site in stream) * | 7,800 ±5,700 | 2,600 ±1,900 |
| Cwmystwyth upstream (unmined)* | 50 ±60 | 640 ±640 |
| Wemyss (tailings)** | 131,000 (<250µm) | - |
| Ystwyth ** (mine 'waste') | 32,000 (<250µm) | - |
| Frongoch (mine tailings)*** | 10,000 - 130,000 | 11,000 - 110,000 |
| Grogwynion (mine tailings)*** | 10,000 - 52,000 | 1,100 – 2,900 |
| Unmined *** | 100 | |
| Pre-industrial – Humber Estuary sediments**** | 22 | 84 |
| Environment Agency draft sediment quality guidelines: Threshold Effect Level (TEL) | 35 | 123 |
| Environment Agency draft sediment quality guidelines: Predicted Effect Level (PEL) | 91.3 | 315 |

Previous studies of mining impacted sites in the local area found similarly high total concentrations of Zn (Montserrat, 2012). The total concentrations of Pb recovered from the sediment in this study however were more similar to those recovered from mine tailings (Palumbo-Roe et al., 2013) and that may be because this study included sediment collected from waste heaps forming the river bank at the Cwmystwyth site as opposed to in-stream samples measured in previous studies (Montserrat, 2012). Concentrations of Pb and Zn were found to be far higher than background levels reported for unmined, upstream and pre-industrial sediments (table 4.7).

TEL and PEL values are for total metals (including residual forms) and so provide no indication of the potential bioavailability of trace metals in response to environmental perturbations. The current study found that up to 90% Pb and 50% Zn were present in the most labile fractions of the sediment and as a result high concentrations of these trace metals may easily be released into pore and surface water in response to environmental perturbations, particularly changes in redox potential. That could have serious adverse effects on water quality, aquatic flora and fauna and the surrounding agricultural and grazing land (Walling et al., 2003, Foulds et al., 2014).

## 4.5 Conclusions

Pb and Zn may have been recovered from a number of different mineral phases during extraction step 1 (in addition to loosely sorbed Fe and associated Mn, Pb and Zn).  The high concentration of Pb and Zn sulphur species in the sediment is likely to have influenced the results.

Significantly higher concentrations of Fe and Zn were recovered from the sediment of the 3 week wet run at the bottom of the mesocosm compared to the initial sediment and constant control indicating that there may have been a build-up of easily reducible Fe. It is possible that reductive dissolution of Fe hydroxides may have acted as a mineral source of Zn contamination into pore water over flooded periods for the 3 week wet run.

At the top of the mesocosm Mn hydroxides may have partly controlled the release of Zn and possibly Pb into surface water. However, the high percentage recovery of Pb at the top of the mesocosm for extraction step 2 could, in part, be due to dissolution of anglesite.

Total concentrations of Pb and Zn in the sediment exceeded PEL guideline values indicating that concentrations of these trace metals in the river bank sediment could pose a serious environmental risk and have adverse biological effects.

# 5. USE OF DET TO DETERMINE THE KEY MECHANISMS OF PB AND ZN RELEASE INTO PORE WATER IN RESPONSE TO DIFFERENT WET AND DRY SEQUENCES

## 5.1 Introduction

This chapter utilised the technique diffusional equilibration in a thin film (DET) in combination with pore water analysis to investigate the key biogeochemical mechanisms responsible for the release of dissolved Pb and Zn in response to different wet and dry treatments.

DET measures solutes in pore water at equilibrium (Davison et al., 2000). Developed by Davison et al., (1991), and originally used to determine vertical concentration profiles of reduced Fe in freshwater sediment cores taken from lake Esthwaite, UK, DET can measure multiple analytes in a pore water sample (Docekalova et al., 2002). Therefore it is a useful technique to understand the mechanistic interactions of solutes in response to changes in environmental conditions (Bennett et al., 2012). DET studies have investigated the mobilisation of contaminants in response to changes in redox potential with depth; Gao et al. (2006) carried out an inter-laboratory study to measure Fe, Mn and Co gradients in freshwater sediment (13 cm deep) from the Upper Scheldt River, Belgium and found a strong correlation between DET profiles of Fe and Co in the upper 8-10 cm in response to changes in redox gradients with depth. Tankere-Muller et al. (2007) measured the co-incident profiles of Co and Mn at fine scale (mm) in contaminated marine sediment during a flume study. These authors found a maxima of Co at 5 – 8 mm that coincided with the mobilisation of Mn. Currently

DET studies have focussed on aqueous systems where the concentrations of trace metal contaminants Pb and Zn were low. Measuring Pb and Zn at low concentrations has been problematic, particularly where measurements were made at high spatial resolution (mm scale), due to the relatively high blank DET values (Gao et al., 2006; Pradit et al., 2013). Docekalova et al. (2002) however were able to measure the vertical profile (13 cm) of Pb and Zn at low concentrations in a sediment core from the Seine estuary, France and in tidal sediment of the river Authie, France by utilising a sensitive ICP-MS technique. Additionally Leermakers et al. (2005) reported the successful determination of Pb and Zn profiles at mm scale in cores taken from the tidal Rupel River, Belgium. These authors reported that the DET profiles of the sediment cores indicated that the mobility of Pb and Zn was linked to the reductive dissolution of Fe and Mn oxides.

Although the above studies show that DET has been used to measure the co-distribution of redox sensitive solutes and trace metal contaminants under varying redox potential with depth, currently only one study is known of that utilises DET to measure the mechanistic interactions of redox sensitive solutes under changing redox potential conditions. This study compared the DET vertical profile of Fe and As (i) under anoxic conditions and (ii) on oxidation of anoxic sediments (Bennett et al., 2012) and was useful in understanding the role Fe played in sequestration of As(III) on oxidation of anoxic sediment. This approach could therefore be used to determine the control Fe and Mn hydroxides have on the mobility of Pb and Zn in response to various wet and dry treatments.

The studies discussed so far were carried out on 'soft' fine grained sediment and DET was originally designed for use in this type of sediment (Ullah et al., 2012) where probes could be easily deployed by pushing them into the sediment. Insertion of DET probes in coarse grained river bed sediment presents a challenge, as direct deployment of the probe could snag the delicate filter membrane (Ullah et al., 2012). Recently however successful DET measurement of pore water solutes at high spatial resolution (cm scale) in armoured, coarse grained, river bed sediments has been made: Ullah et al. (2012) created and utilised a stainless steel dummy for deployment of a modified DET gel probe that was 30 cm long into a gravel dominated river bed in order to measure the vertical profile of nitrate, ammonia and reduced Mn at 1 cm resolution. The same authors utilised this technique to measure the influence of emergent vegetation on nitrate cycling in sediments of the River Leith, Cumbria (Ullah et al., 2013). Byrne et al. (2014) made use of this protective stainless steel cover to measure the vertical profile of nitrate, sulphate and dissolved Fe and Mn to investigate the effects of hyporheic exchange on the attenuation of nitrate rich groundwater in the upper 15 cm of river sediment of the River Leith, Cumbria.

Pore water analysis methods, such as that carried out in chapter 3, and conventional box core anoxic slicing followed by centrifugation techniques involve removing relatively large volumes (ml) of pore water sample. As a result redox sensitive solutes such as Fe and Mn may be exposed to atmospheric conditions during sampling. The resulting precipitation and sorption reactions could influence pore water results (Leermakers et al., 2005; Gao et al., 2006) moreover key biogeochemical processes occurring at fine spatial scale in the sediment may be

missed (Mortimer et al., 1998). In-situ methods of sampling such as DET are of benefit when measuring redox sensitive species in sediment pore water as samples are not exposed to atmospheric conditions (Bennett et al., 2012) furthermore a smaller volume (µl) of pore water is sampled allowing solute concentrations at a higher spatial resolution (mm – cm) to be measured than can be achieved through conventional box core anoxic slicing methods (Harper et al., 1997, Mortimer et al., 1998).

Previous chapters established that certain wet and dry sequences promoted the release of Pb and Zn into pore water and patterns in mobility of these contaminants varied spatially and temporally depending on the run. Re running a subset of mesocosms and utilising DET to measure the release of these contaminants and co-distributions of Fe and Mn on a varied temporal scale (at the start and end of a flood period) and at higher spatial resolution (cm scale), with depth, in the sediment was of benefit to (i) confirm the patterns of release and therefore the mechanisms of release were the same as observed in chapter 3 (ii) uncover further spatial detail regarding the release of contaminants to corroborate findings (iii) highlight important biogeochemical processes occurring at a smaller spatial scale that may have been missed through the bulk pore water sampling. Used in combination with SEM/EDS, statistical and geochemical analysis the key biogeochemical mechanisms that promoted the release of Pb and Zn were identified.

### 5.1.1 Aim, Objectives and Hypothesis

The aim of this experiment was to use a combination of DET and pore water analysis to identify the trends in Pb and Zn mobility in response to different wet and dry treatments in order to determine what key biogeochemical mechanisms were responsible for Pb and Zn release. Within the overall aim several objectives were identified:

- Identify key differences between data from the current chapter and pore water and sediment data from chapters 3 and 4.

- Determine if the patterns of mobility for dissolved Pb, Zn, Mn and Fe measured through averaged pore water data were similar to patterns observed for average DET data.

- Determine the key biogeochemical mechanisms responsible for the release of Pb and Zn

- Determine the potential for the mining contaminated sediments to become a source of Pb and Zn contamination under certain wet and dry sequences and evaluate the environmental implications.

**Hypothesis**

The mobility of Pb and Zn in response to wet and dry treatments will show similar trends to those observed in chapter 3 indicating the key biogeochemical mechanisms responsible for the release of Pb and Zn are the same and the methodology repeatable.

The patterns of mobility for dissolved Pb, Zn, Fe and Mn measured through average DET results will be comparable to pore water results.

Depth concentration profiles for Pb, Zn, Fe and Mn measured through DET in response to wet and dry runs will allow measurement of co-distribution of species occurring at higher spatial resolution that will further corroborate pore water findings.

The results will enable an assessment to be made regarding the potential for the sediment to become a source of Pb and Zn contamination to river systems in response to certain wet and dry sequences and allow an evaluation to be made of the environmental implications.

## 5.2 Methods

### 5.2.1 Sediment collection

The Cwmystwyth mine site (SN799743), described in methods section (2.1.2 - 5), was re-visited in order to collect sediment from the north bank of the river Ystwyth (plates 5.1 and 5.2). In contrast to the sediment collected on the first sampling trip that was (in some cases) located away from river channel, the sediment collected during the 2nd sampling trip was closer to the river channel and at a similar height to the river channel. It was believed that the location of the second sediment sampling was more likely to experience wetting and drying episodes due to changes in river stage and mesocosm results would therefore more accurately indicate the potential environmental risk of the sediment.

Visual inspection indicated that sediment was made up of predominantly sandy gravel interspersed with some finer silt particles. This site was reported as generally without ground water except at shallow depths (NERC, 2015). A shallow subsurface lateral flow path was observed where the sediment sample was taken (plate 5.2). A stainless steel shovel was used to collect samples from the river bank within the top 10 cm of sediment.

The pH, temperature and conductivity of river water was measured on the day of sediment sampling (11th December 2013) using a calibrated Aquaread multiparameter probe aquameter. The surface water physicochemical characteristics were: pH 5.6, temperature 6°C, ORP +537 mV, DO 119.6%. Sediment sub-surface physicochemical characteristics were: pH 5.7, temperature 6°C, ORP +383 mV, DO <50%, EC 119 μS/cm.

**Plate 5.1 Sediment collection site (see blue arrow)**



**Plate 5.2 Sediment collection site on shallow lateral flow path (white arrow)**

## 5.2.2 Laboratory Analysis

Sediment collected from the sample site was transported to the laboratory at Liverpool John Moores University (LJMU).  In order to encourage similar conditions in each mesocosm the sediment was first homogenised by hand using a plastic trowel. Larger pebbles were removed and similar particle sized sediment was picked out by hand and added to each mesocosm. Larger pebbles were not removed in chapter 3 because they were found to help with drainage, necessary for sampling. Drainage was sufficient in the current study and therefore larger pebbles were removed to increase homogeneity. Each mesocosm was packed to the same height (20 cm deep) using a plastic trowel. Additionally, as noted in section 2.2.1, each column was then held at field capacity for 20 days prior to the start of wet and dry treatment. That was intended to allowed time for mesocosms to settle into a steady pattern and help to encourage similar conditions.

Grain size analysis was carried out using a vibration platform (Fritsch) and a series of Endecotts sieves. Size-separated fractions were then divided into the following Wentworth size classes: granuals and pebbles (> 2000 μm), very coarse to very fine sand 63 μm – 2000 μm, silt/clay <63 μm.

Moisture content of the sediment was determined. An empty aluminium boat was weighed and weight noted. A wet sediment core was placed on the aluminium 'boat' and weighed. The core was placed in an oven and dried overnight at 105°C. After drying the sediment was re-weighed:

Moisture content (wt of water) (g) = weight of wet sediment (g) – weight of dry sediment (g)

% moisture content by weight = (wt of water / wt of dry sediment) x 100

## 5.2.3 Mesocosm Experiments

A sub-set of wet and dry treatments were run, similar to those run in chapter 3.
The uPVC (unplasticized polyvinyl chloride) drain-pipes were re-used without taps.
Rubber bungs were used to block the sample holes (figure 5.1).



**Figure 5.1 Mesocosm Runs**

The wet and dry runs chosen for re-run were selected because they had

(A) resulted in the highest release of Zn and Pb into pore and surface water and

(B) had shown different patterns of release between runs that could be linked to

different biogeochemical mechanisms of release.

Runs selected were:

- 1 week wet run (week A – week J)

- 3 week wet run (week A – week L)

- 3 week dry run (week A – week J)

- The flood run was included as a constant control (week A – week J)

The treatment period ran over 10 – 12 weeks.

A similar experimental method as noted in general methods section 2.2.1 was used for the wet and dry treatments, with slight variations where additional pore water analysis was carried out:

At the start of a flood, ARW was added to the columns up to 5 cm above the sediment level to simulate flood conditions (Du Laing et al., 2007). Water was left for 2 - 3 hours to allow for contact time between sediment and pore water. Water samples were then taken first from the top using a plastic syringe and from the bottom, in that order to avoid mixing between levels.

Using a Hanna Combo pH/EC and temperature hand held stick meter model No 98129, the pH, conductivity and temperature were recorded for each sample.

Using an Aquaread aquameter multiparameter water quality probe, DO and redox potential (ORP) measurements were taken. The ORP reference electrode was type: 3MPK1 AgCl and ORP readings $E_{(measured)}$ were then converted to the hydrogen scale (Eh) as instructed by Aquaread  (Aquaread, 2014). Eh = $E_{(measured)}$ + $E_{(ref.)}$

Water samples were filtered through a 0.45 μm PTFE syringe filter into three metal-free 30 ml centrifuge tubes for analysis as follows:

A) A Spectroquant sulphide test (1.14779.0001) was carried out on 5 ml filtered water sample to test for dissolved hydrogen sulphide: In waters between pH 5 – 6, water-soluble dissolved $H_2S$ gas may occur alongside dissolved $HS^-$. If dissolved hydrogen sulphide were present this would react with dimethyl-p-phenylenediamine and Fe(III) ions to form methylene blue. The measurement was determined using a spectrophotometer (LJMU). The measuring range was 0.1 – 1.55 mg/L (Spectroquant, 2010). Measurement results were tested for accuracy though the creation of standard solutions for sulphide using a titration technique as specified by Merck (Merck, 2013) (See appendix 5.2.3 for full titration method).

B) A filtered water sample was acidified with nitric acid ($HNO_3$) to below pH 2 for metal analysis through (i) Inductively Coupled Plasma with Optical Emission Spectroscopy (ICP/OES) (iCAP 6500 Duo) (LJMU) to analyse for Fe, Mn, Zn, Pb, see section 5.2.5 and (ii) Flame photometer analysis (BWT Techonologies) (LJMU) to analyse for Na, K, Ca see method 5.2.6.

C) A filtered water sample was frozen (-20 °C) for subsequent anion analysis through (i) IC2000 Anion Dionex, (University of Manchester) see general methods section 2.2.4 for full details and (ii) TC/NPOC analysis (Shimadzu) at LJMU see general methods section 2.2.6.

After sampling, mesocosms were then left *'in flood'*, with the bungs in for the allotted timeframe.

At the end of a wet period the above sample methodology was repeated and any pore water remaining in the mesocosm after sampling was drained out via the bottom tap into a bucket and discarded. Mesocosms were then left '*dry*' for the allotted timeframe. For the constant flood, samples were taken weekly at the same time as the variable runs.

At the end of the treatment period sediment was collected using a plastic spatula from the surface and the bottom of the mesocosm and added to a small polyethylene zip bag. Sediment was frozen at -20$^{\circ}$C immediately after sampling and once frozen was then freeze dried (-70$^{\circ}$C) for storage in order to preserve redox state. Freeze-dried sediment was used for:

**(i) Scanning Electron Microscopy with Energy Dispersive Spectroscopy (SEM/EDS)**

A combination of SEM/EDS was carried out on a FEI Quanta 200 ESEM to create images, and identify associations of elements, at micron scale on the surface of the sediment samples. Freeze dried sediment was dusted lightly onto carbon stubs and either coated with carbon or platinum to encourage conductivity (see general methods section 2.2.10 for full method)

**(ii) Sequential extraction analysis (SEQ)**

Sequential extraction was carried out in triplicate on sediment samples from (i) 2012 and (ii) from the current study, in order to determine differences in partitioning of Pb, Zn, Fe and Mn in the labile fraction of the sediment (see general methods section 2.2.5).

### 5.2.4 Solid TOC and IC % measurements

For determination of total carbon (TC) a sub sample of sieved (2 mm) sediment was weighed (no greater than 50 mg), and oven dried at $140^{\circ}C$ for 24 hours. The prepared sediment sample was combusted at $900^{\circ}C$ in a stream of oxygen to ensure complete conversion to $CO_2$. For inorganic carbon (IC) analysis phosphoric acid was added to the sample producing $CO_2$ that is purged at $200^{\circ}C$ (Shimadzu, 2014). The results provided information regarding % TC and % TIC that allowed % TOC to be calculated (see general methods section 2.2.7).

### 5.2.5 Inductively Coupled Plasma - Optical Emission Spectroscopy (ICP-OES)

An ICP OES (iCAP 6500 Duo) instrument was used to measure dissolved Fe, Mn, Pb and Zn in pore water and in sequential extraction (SEQ) solutions. For ICP/OES a liquid sample, as an aerosol, is introduced into plasma at $8000^{\circ}C$. At this temperature elements are excited and emit light at a characteristic wavelength. The light passes through a diffraction grating. The diffracted light is collected by wavelength and amplified to provide an intensity measurement that, when compared to known standards, can be converted to concentration. This method has the advantage in that it is more sensitive than FAAS, can determine many elements simultaneously and can work over a concentration range of several orders of magnitude (Evans Analytical Group, 2007).

Quality check standards were used every 10 samples to check for drift along with blanks, either de-ionised water, or matrix matched solutions for SEQ. The run was considered acceptable if the data were within 5% of the expected concentration

e.g. 1 ppm (0.95-1.05 ppm). ICP detection limits and selected wavelengths are shown below (table 5.1).

**Table 5.1 ICP detection limits**

| Metal | Detection Limit (ppb) (Evans Analytical Group, 2007) | Selected Wavelengths |
|-------|------------------------------------------------------|----------------------|
| Fe    | 5                                                    | 2382                 |
| Mn    | 1                                                    | 2593                 |
| Pb    | 50                                                   | 2614                 |
| Zn    | 5                                                    | 2138                 |

## 5.2.6 Flame photometer detection of Na, K, Ca

Detection of Na, K, Ca in filtered water samples was carried out manually using a flame photometer BWB technologies (LJMU). The flame photometer thermally excited the aspirated water sample. The wavelength measured was characteristic of the element. The intensity of the signal was directly proportional to the concentration of the element and has been found to increase linearly at low concentrations < 50 mg/L (BWB Technologies, 2012). All samples were found to be < 50 mg/L. Quality standards and blanks were measured every 10 samples. Samples were considered accurate if $\leq$ 5%.

## 5.2.7 DET analysis

In addition to pore water and sediment analysis DET analysis was carried out. The aim of using DET was to measure the interaction of solutes at a higher spatial resolution (cm scale) than could be achieved through bulk pore water analysis. It was hoped this would (i) further corroborate the results obtained so far through pore water analysis, (ii) minimise oxidation, precipitation and sorption of redox sensitive solutes that could occur due to exposure to atmospheric conditions, (iii) provide information regarding the co-distribution of solutes at a higher spatial scale to identify the mechanisms of dissolved Pb and Zn release that may have been missed through bulk pore water analysis.

The DET probe consisted of a high porosity polyacrylamide gel made of 95% water. The gel was under and overlain with a 0.45 µm filter membrane and secured in a plastic casing with a window opening of 15 cm length and 1.8 cm width (figure 5.2). The window allowed direct contact with pore water once deployed (Ullah et al., 2012). See section 2.2.15 for full DET method details).
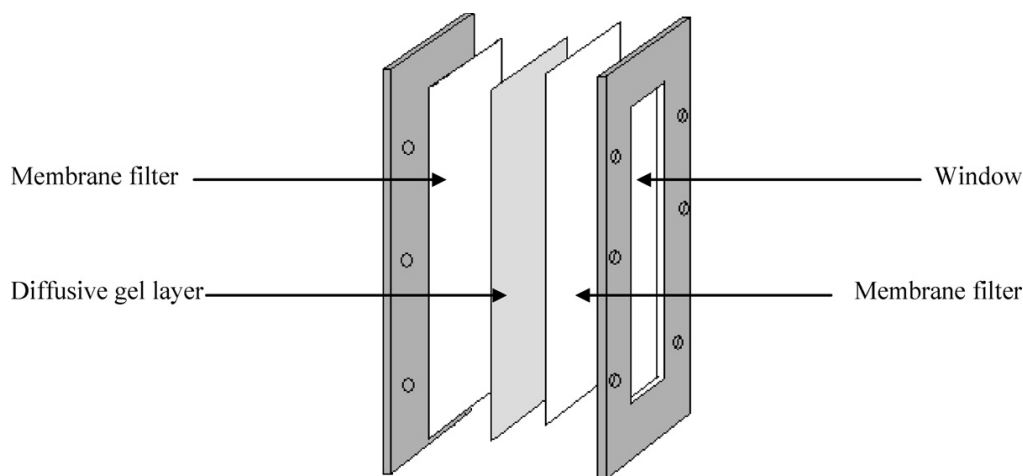


**Figure 5.2 DET gel assembly (Ullah et al., 2012)**

### 5.2.8 Statistical analysis non-parametric tests

Tests for normality indicated that the data was not normally distributed therefore the non-parametric Wilcoxon rank sum test (see section 2.2.12) was carried out to identify significant differences in pore water data using SPSS 20.0.

Wilcoxon rank sum test was used to identify differences in a) dissolved Pb and Zn concentrations at the start and end of a flood b) the release of dissolved Pb over a flood between the top and bottom of the mesocosm and c) average concentrations of dissolved Zn at the end of a flood between the top and bottom of the mesocosm d) concentration of dissolved Zn and Pb at the end of a flood between first mesocosm run (chapter 3) and second mesocosm run (chapter 5).

Spearman's rho, a non – parametric version of Pearson correlation (see general methods section 2.2.12), was used to test for relationships between Pb and pore water variables and Zn and pore water variables. As the nature of the relationship between Zn/Pb and other variables was unknown the 2-tailed (non-directional) test was selected.

### 5.2.9 Principal Component Analysis (PCA)

PCA was carried out to determine key factors linked to the mobility of dissolved Zn and Pb in pore water for selected variable runs at the top and bottom of the mesocosms (see general methods section 2.2.13 for full details).

### 5.2.10 Geochemical Calculation of Mineral Saturation Index

WATEQ4F.dat database (the PHREEQC.dat database extended) was used to calculate saturation indices of various minerals, using input data derived from pore

water measurements for all runs (weeks A, J and L) at the top and bottom of the mesocosm (averaged data was used for week A) (See general methods section 2.2.14).

Data was considered acceptable if charge balance ($\leq$ 5%). Data was charge balanced by altering Na ($\pm$6 mg/L) for selected runs. Altering Na slightly did not alter the SI for minerals displayed.

Saturation state $\Omega$ can be expressed as the ratio between ion activity product (IAP) and the solubility product K and is generally expressed on a logarithmic scale to allow for comparison against a SI.

SI = log (IAP / K)

SI = < 0 subsaturation, SI = 0 ($\pm$ 0.2) saturated, SI > 0 Supersaturation

For subsaturation dissolution would be expected and supersaturation suggests precipitation (Appelo and Postma, 2010).

## 5.2.11 Piper Diagram

A piper diagram was created in GW_chart (free software downloaded from the USGS web site) to graphically display the bulk chemical composition of the pore water at the end of each run compared to the chemical composition at the start at the top and bottom of the mesocosm. Only charge balanced data was used.

For a Piper diagram, the relative proportion of cations and anions are plotted in two triangles. From the plots two lines are drawn until they intersect in the diamond above to provide information regarding classification of water (figure 5.3).
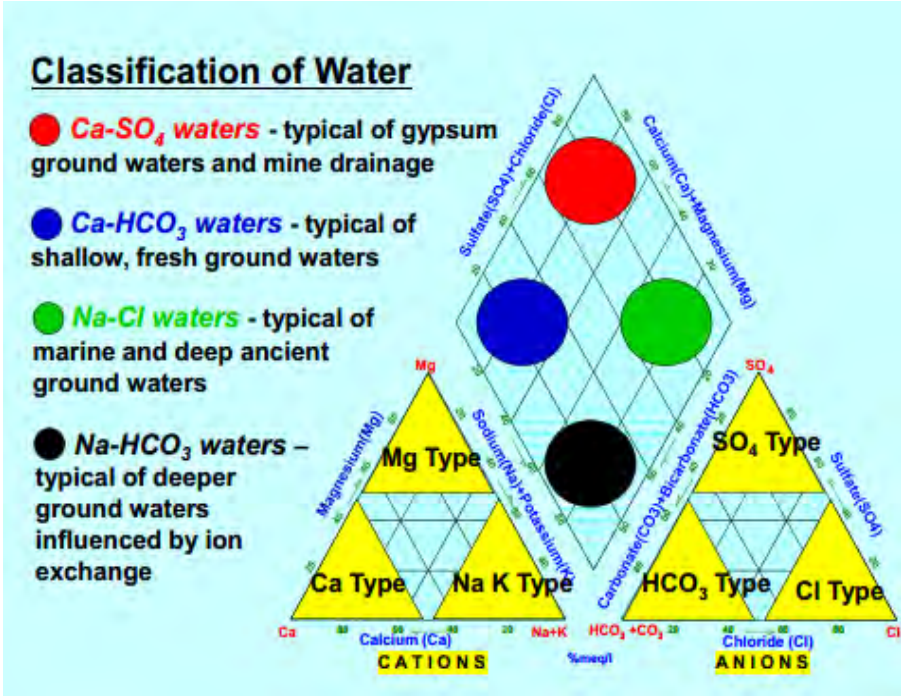
**Figure 5.3 Interpretation of a Piper diagram (USGS, 2008)**

## 5.3 Results

### 5.3.1 Pore water summary

Throughout the experiment duration, for all runs, pore water pH remained slightly acidic (pH 5.7, range 5.1 – 5.8). An average of pH 0.4 units higher than for previous mesocosm experiments run in chapter 3. Total inorganic carbon (TIC) concentrations (Shimadzu) were low (1.9 mg/L, range 0.2 – 4.3 mg/L) an indication that alkalinity was low. Average NPOC analysis was (3.02 mg/L, range 1.9 – 4.3 mg/L). Based on other literature values (Meybeck, 1982), this range was low – medium. Solid analysis of the sediment (Shimadzu), found inorganic carbon (IC) below detection both prior to treatment and at the end of the run.

Analysis of a sediment core found sediment moisture by weight (14.5 %).

The sediment was predominantly sandy, interdispersed with larger granules and pebbles. Grain sizes showed similar percentages for each grain size compared to sediment sampled in 2012 (figure 5.4) although in 2012 larger pebbles (>8 mm) were included.
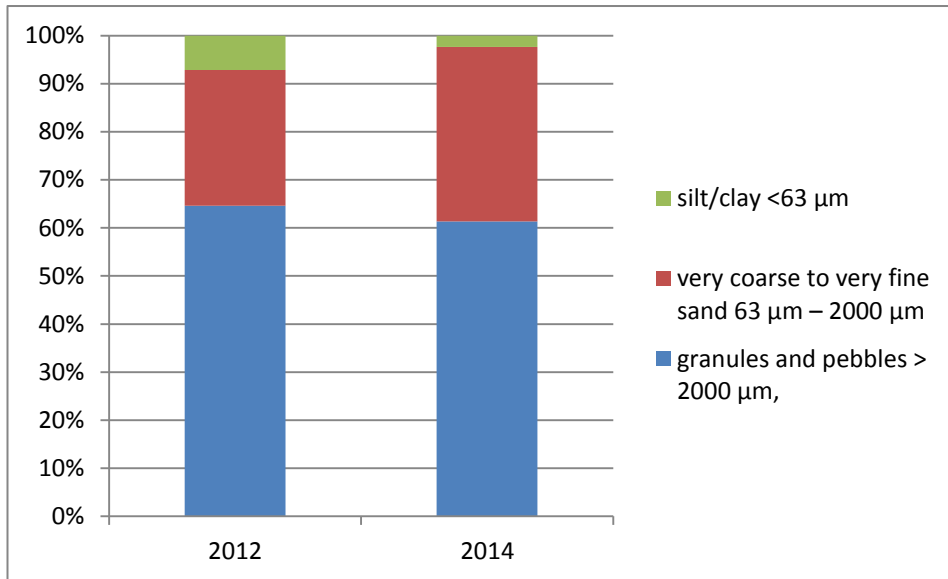
**Figure 5.4 Grain Size % by weight 2012 and 2014**

For a given Eh the distribution of all redox equilibria are fixed (Appelo and Postma, 2010) and therefore theoretically the concentration of solutes at the fixed Eh, pH and temperature could be calculated using the Nernst equation (Appelo and Postma, 2010). However typical sediment pore water samples contain many species interacting as a variety of different redox couples and therefore non-equilibrium redox potential conditions are common in natural heterogeneous systems (Nordstrom and Alpers, 1999; vanLoon and Duffy, 2011; Appelo and Postma, 2010). Furthermore when sampling waters of low redox potential issues such as poisoning of the ORP electrode due to precipitation of Fe or Mn hydroxides where reduced Fe or Mn come into contact with oxygen adsorbed to the electrode surface can occur (Appelo and Postma, 2010). Disturbingly large variations in computed and measured field Eh values have been reported (Appelo and Postma, 2010) that indicate it is not possible to take precise ORP readings within heterogeneous systems (vanLoon and Duffy, 2011) and so a single Eh

cannot be assigned to a water sample (Nordstrom and Alpers, 1999). It is however possible to gain an approximate measurement of Eh and categorise redox potential conditions of pore water as generally oxidising or reducing (vanLoon and Duffy, 2011). Berner (1981) (cited in Nordstrom and Alpers 1999, p.142) created a classification to describe redox chemistry where the presence of oxygen classified the water as 'oxic' and the absence of oxygen and presence of reduced Fe as 'post oxic'. However, Nordstrom and Alpers (1999) note that even Berner's general classification may not work so well for surface waters that are usually of mixed redox chemistry.

In the current study oxygen was not found to decline to zero although a marked decline in dissolved oxygen % at the end of a flood at the bottom of the mesocosm (25.3%, range 52 – 7.8%) compared to the top of the mesocosm (99.5%, range 78 – 109%) was observed. Redox potential conditions (Eh) at the end of a flood remained oxic in the surface water at the top of the mesocosm (Eh 494 mV, range 446 – 603 mV) and showed a decline at the bottom (Eh 456 mV, range 381 – 530 mV). The lowest redox potential measurements were taken for the 3 week wet and flood run at the bottom of the mesocosm (table 5.2). For these runs a marked increase in dissolved Mn at the end of a flood was observed and dissolved Fe was measured in some cases.

Aqueous sulphide was below detection for all samples

## 5.3.2 Piper diagrams
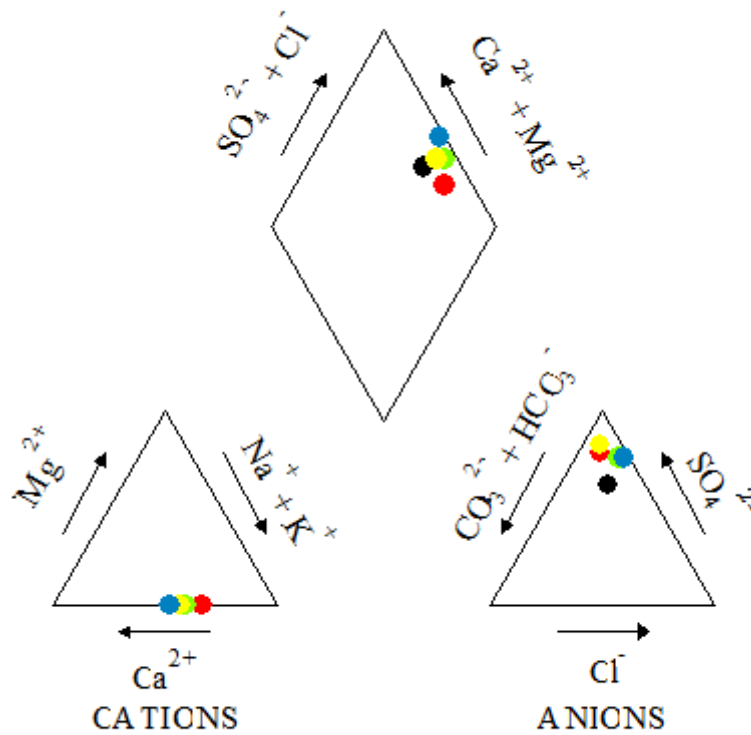


**Figure 5.5 Piper diagram showing chemical composition of surface water at the start of the run(s) (avg) (black) and at the end of the run for 1wwet (red), 3wwet (green), 3wdry (yellow) and flood (blue)**
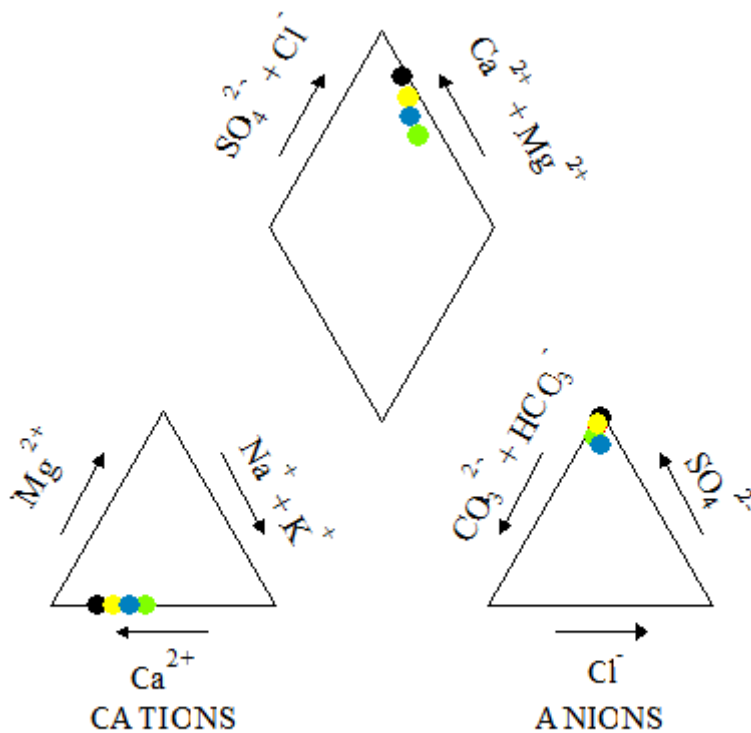
**Figure 5.6 Piper diagram showing chemical composition of pore water at the bottom of the mesocosm at the start of the run(s) (avg) (black) and at the end of the run for 1wwet (red*), 3wwet (green), 3wdry (yellow) and flood (blue). *Red circle hidden behind yelow circle.**

Results from piper analysis indicated that the water samples were typical of mine drainage (Ca - sulphate) water type. There was little change in chemical composition between the start and end of the run (figures 5.5 and 5.6).

### 5.3.3 Summary for dissolved Pb and Zn

Patterns in the release of Pb and Zn into pore and surface water were found to be similar to patterns observed for the mesocosm runs in chapter 3 (table 3.3).

For dissolved Pb, average concentrations were higher in the pore water at the top (T) of the mesocosms compared to the bottom (B) for all runs. The highest average concentration was measured for the three week wet run at the top of the mesocosm (10 ±2.1 mg/L), followed by the flood run (top) (8.6 ±1 mg/L) and 1 week wet run (top) (8.3 ±0.2 mg/L). The lowest average concentration was for the flood run at the bottom of the mesocosm (3.8 ±0.3 mg/L) (table 5.2).

For dissolved Zn, average concentrations were higher in the pore water at the bottom of the mesocosms for all runs. The highest average concentrations was measured for the three week dry run at the bottom (61.1 ±6.8 mg/L) followed by the three week wet run (58.9 ±5.6). All average concentrations of dissolved Zn at the bottom of the mesocosm were > 50 mg/L (table 5.2).

**Table 5.2 Mean and range (in parenthesis) of dissolved (<0.45μm) metals (mg/L), pH, Conductivity (μS/cm), Temperature (°C), DOC (%), TIC (mg/L) at the end of a flood, by run, Top (T) and Bottom (B) of the mesocosm, key average values (bold and underlined), n = #[1]**

| | 1wwet (T) | 1wwet (B) | 3wdry (T) | 3wdry (B) | 3wwet (T) | 3wwet (B) | flood (T) | Flood (B) |
|---|---|---|---|---|---|---|---|---|
| | n=5 | n=5 | n = 3 | n = 3 | n = 3 | n = 3 | n = 10 | n = 10 |
| pH | 5.5 | 5.7 | 5.6 | 5.7 | 5.6 | 5.8 | 5.7 | 5.8 |
| (range) | (5.1 - 5.7) | (5.6 - 5.8) | (5.5 - 5.7) | (5.6 - 5.7) | (5.4 - 5.7) | (5.7 - 5.8) | (5.4 - 5.8) | (5.6 - 5.8) |
| Temp | 17.5 | 17.8 | 17.7 | 17.7 | 18.4 | 18.9 | 17.9 | 18.2 |
| (range) | (16 - 20) | (16.4 - 20.1) | (16.2 - 20.3) | (16.3 - 20.3) | (17 - 19.6) | (17.5 - 20) | (16 - 20.3) | (16.5 - 20.3) |
| Cond | 225.2 | 392 | 175.3333 | 382 | 230.6667 | 405 | 264.9 | 408.4 |
| (range) | (148 - 373) | (336 - 435) | (170 - 186) | (338 - 415) | (206 - 276) | (359 - 436) | (162 - 416) | (342 - 452) |
| D.O. % | 100 | 34 | 102 | 37 | 94 | 18 | 102 | 12 |
| (range) | (78 - 109) | (10.4 - 43.2) | (99 - 105) | (13.1 - 52.7) | (80.5 - 101) | (8.3 - 28.1) | (98 - 111) | (7.8 - 23) |
| Redox Eh | 509 | 482 | 499 | 491 | 483 | 428 | 485 | 423 |
| (range) | (459 - 603) | (456.9 - 530) | (479 - 525) | (478.9 - 509) | (468 - 504) | (412.7 - 436) | (446 - 555) | (381 - 485) |
| Fe | 0.0 | 0.1 | 0.0 | 0.1 | 0.7 | 0.1 | 0.0 | 0.3 |
| (range) | 0.0 | (0 - 0.1) | (0 - 0.1) | (0 - 0.2) | (0 - 2) | (0.1 - 0.2) | (0 - 0.2) | (0.1 - 0.6) |
| Mn | 0.1 | 0.1 | 0.0 | 0.1 | 0.1 | 3.5 | 0.2 | 5.8 |
| (range) | (0 - 0.1) | (0.1 - 0.2) | 0.0 | (0 - 0.2) | (0 - 0.1) | (2.2 - 5.3) | (0 - 0.7) | (1 - 10.1) |
| Pb | **8.3** | 4.9 | 6.1 | 5.8 | **10.0** | 4.9 | **8.6** | **3.8** |
| (range) | (8 - 9.2) | (3.8 - 5.6) | (5 - 6.7) | (4.3 - 7) | (7.5 - 14.2) | (2.3 - 6.9) | (5 - 15) | (1.7 - 4.8) |
| Zn | 15.6 | 53.9 | 14.8 | **61.1** | 22.8 | **58.9** | 24.6 | 52.0 |
| (range) | (10.1 - 29.2) | (55.4 - 50) | (13.1 - 16.3) | (47.5 - 68.2) | (17.7 - 27) | (49.3 - 68.5 ) | (9.6 - 47.2) | (45.5 - 62.7) |
| Ca | 2.4 | 11.8 | 2.0 | 13.7 | 4.7 | 15.7 | 5.7 | 13.6 |
| (range) | (0 - 8) | (8 - 14) | (0 - 4) | (16 - 12) | (3 - 7) | (14 - 17) | (0 - 18) | (4 - 19) |
| Nitrate | 1.6 | 1.4 | 0.6 | 1.9 | 1.1 | 0.1 | 0.7 | 0.0 |
| (range) | (0.2 - 2.8) | (0.6 - 2.3) | (0 - 1.2) | (1 - 2.5) | (0.4 - 1.7) | (0 - 0.2) | (0 – 2.1) | (0 - 0.5) |
| Chloride | 8.5 | 3.3 | 1.7 | 2.6 | 4.0 | 3.5 | 7.8 | 6.0 |
| (range) | (2.4 - 23.5) | (2.6 - 4.8) | (1.27 - 2.48) | (1.4 - 3.4) | (1.6 - 6.4) | (1.1 - 5.5) | (1.5 - 27.6) | (0.7 - 17.5) |
| Sulphate | 25.3 | 95.2 | 17.7 | 120.3 | 36.0 | 110.3 | 35.5 | 94.6 |
| (range) | (8.5 - 64) | (121.9 - 47.7) | (8.8 - 35.2) | (90 - 145) | (19.3 - 52.9) | (66.6 - 147.7) | (7 - 115) | (46 - 138) |
| Na | 2.2 | 4.8 | 3.0 | 4.7 | 5.3 | 14.3 | 7.3 | 8.8 |
| (range) | (0 - 4) | (3 - 7) | (1 - 6) | (3 - 7) | (4 - 7) | (9 - 19) | (1 - 22) | (2 - 18) |
| K | 1.2 | 1.0 | 0.0 | 0.7 | 0.3 | 1.0 | 2.8 | 0.7 |
| (range) | (0 - 4) | 1.0 | 0.0 | (0 - 1) | (0 - 1) | 1.0 | (0 - 25) | (0 - 1) |
| DOC | 2.5 | 3.1 | 1.9 | 3.1 | 2.6 | 4.3 | 2.6 | 3.6 |
| (range) | (2.1 - 3.2) | (2.4 - 3.5) | (1.9 - 2) | (2.6 - 3.8) | (1.9 - 3) | (3.7 - 4.9) | (1.9 - 4.9) | (2.5 - 4.8) |
| TIC | 0.8 | 1.2 | 0.6 | 1.1 | 0.8 | 2.8 | 0.7 | 2.5 |
| (range) | (0.4 - 1.1) | (0.6 - 1.8) | (0.3 - 0.9) | (0.7 - 1.6) | (0.7 - 1.1) | (2.3 - 3.4) | (0.2 - 1.4) | (1.1 - 4.3) |

---

[1] Note: 'n' relates to number of samples taken at the end of a flood period. The 'n' varied between runs because certain runs had more flood periods than others over the treatment period.

### 5.3.4 Release of dissolved Pb over flooded periods

The concentration of Pb (mg/L) at the start of a flood was compared to the concentration at the end to determine whether individual wet and dry treatments resulted in a significant increase in dissolved Pb over a flood.

All variable  wet and dry runs at the top of the mesocosm were found to release significantly higher concentrations of Pb at the end of a flood compared to the start of a flood ($z = < -1.96$, $p = < .05$). That 'pulsed' release over a flood period was not apparent at the bottom of the mesocosm for the 3 week dry and 3 week wet runs ($z = > -1.96$, $p = > .05$) and nor for the constant flood at the top ($z = -0.73$, $p = .465$) and bottom ($z = -0.63$, $p = .53$) (See Wilcoxon rank sum test summary table appendix 5.3.4 for full details).

The average concentration of dissolved Pb released over a flood period was significantly higher at the top of the mesocosm compared to the bottom ($z = -2.525$, $p = < .05$, $n = 16$) for all variable wet and dry runs (figure 5.7).

The average concentration of Pb at the end of a flood (figure 5.8) was $> 4$ mg/L for all variable runs at the top and bottom of the mesocosm. At the bottom of the mesocosm almost all of the dissolved Pb was released into pore water at the start of a flood (within 2 – 3 hours of flooding) and concentrations then remained relatively constant over a flood period. However at the top of the mesocosm Pb continued to be released into surface water over the duration of the flood.
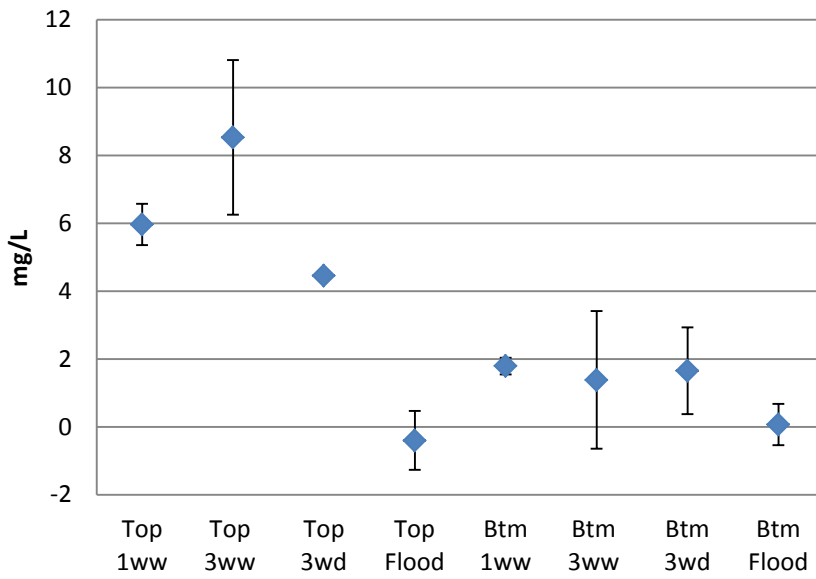
**Figure 5.7 Average concentration of dissolved Pb released over a flood period (mg/L) (concentration at the end of a flood minus concentration at the start) for all runs, top and bottom of the mesocosm. Bars indicate standard error (n = 3 for 3 week wet and 3 week dry, n = 5 for 1 week wet and flood)**
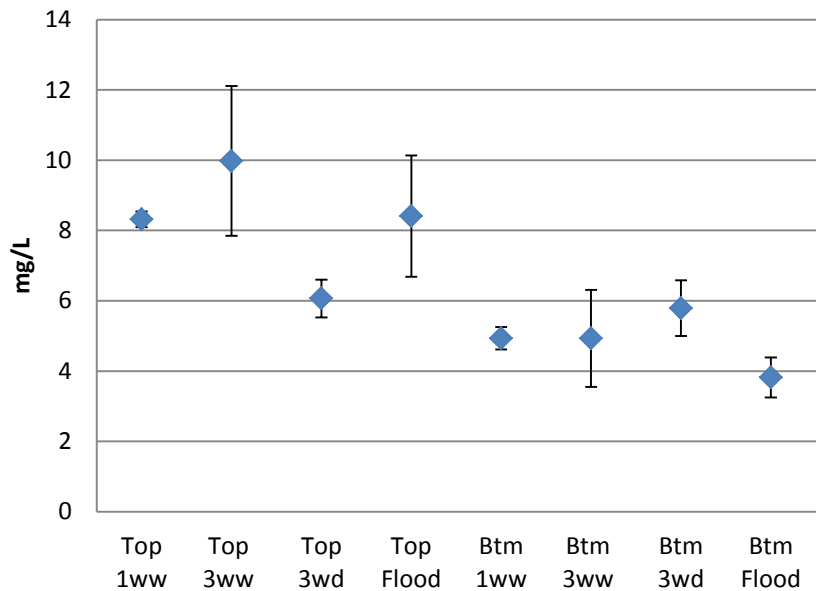


**Figure 5.8 Average concentration of Pb released at the end of a flood period (mg/L). Bars indicate standard error (n = 3 for 3 week wet and 3 week dry, n = 5 for 1 week wet and flood)**

### 5.3.5 Release of dissolved Zn over flooded periods

All variable  wet and dry runs at the top and bottom of the mesocosm were found to release significantly higher concentrations of Zn at the end of a flood compared to the start of a flood (z = < -1.96, p = < .05). That 'pulsed' release was not apparent for the constant flood at the top (z = -0.52, p =  .602) and bottom (z = -0.1, p =  .917) (See Wilcoxon rank sum test summary table appendix 5.3.4 for full details).

Average concentrations of dissolved Zn  (mg/L) at the end of a flood were found to be significantly higher for all runs at the bottom of the mesocosm (z = -4.824, p = .00, n = 16) compared to the top (figure 5.9).
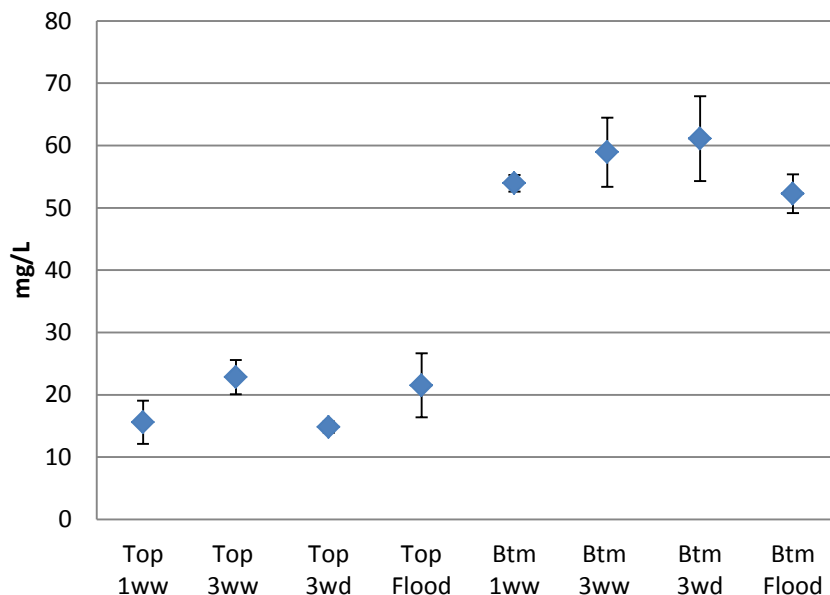


**Figure 5.9 Average dissolved Zn concentrations (mg/L) at the end of a flood period, for all runs, top and bottom of the mesocosm. Bars indicate standard error (n = 3 for 3 week wet and 3 week dry, n = 5 for 1 week wet and flood)**

Dissolved Zn concentrations at the start of a flood were higher for all runs at the bottom of the mesocosm (figure 5.10) and show that $\geq$ 40 mg/L dissolved Zn was released within 2 – 3 hours of flooding.
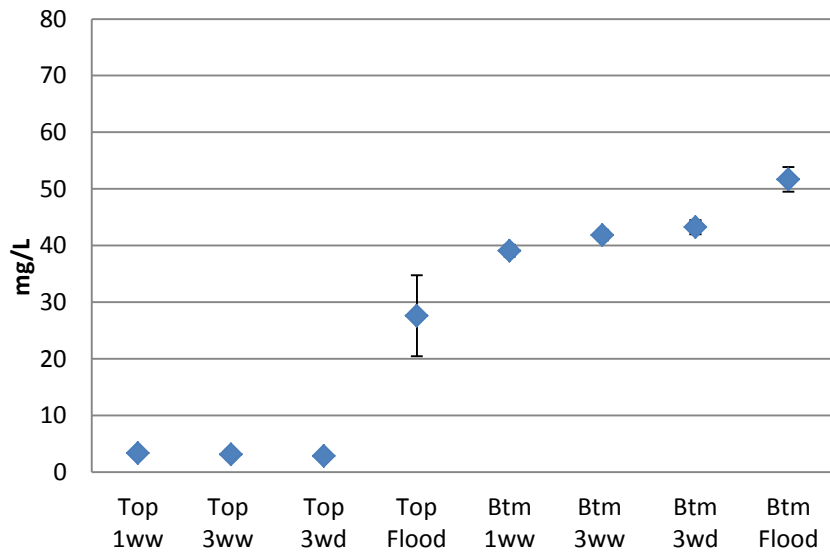


**Figure 5.10 Average Zn concentrations (mg/L) at the start of a flood period, for all runs, top and bottom of the mesocosm. Bars indicate standard error (n = 3 for 3 week wet and 3 week dry, n = 5 for 1 week wet and flood)**

**5.3.6 Differences in the average concentration of dissolved Pb and Zn released at the end of a flood between the 2012 and the current (2014) mesocosm run.**

Similarities in the patterns of Pb and Zn release were apparent between the 2012 and 2014 mesocosm runs (section 5.3.3). However the total concentrations of dissolved Pb and Zn released into pore water were observed to be different in 2014 compared to 2012 (figures 5.11 and 5.12).

For the 2014 mesocosm run there was a significantly lower average concentration of dissolved Pb at the end of a flood period for all runs at the top and bottom of the mesocosm ($z = < -1.96$, $p = < 0.05$). (See Wilcoxon rank sum test summary table appendix 5.3.6 for full details ). Average concentrations were approximately 2 – 3 times lower (figure 5.11).

For Zn in 2014 there was a significantly higher concentration at the end of a flood for all runs at the bottom of the mesocosm ($z = < -1.96$, $p = < 0.05$) (See Wilcoxon rank sum test summary table appendix 5.3.6 for full details). Average concentrations were approximately 2 - 3 times higher (figure 5.12).
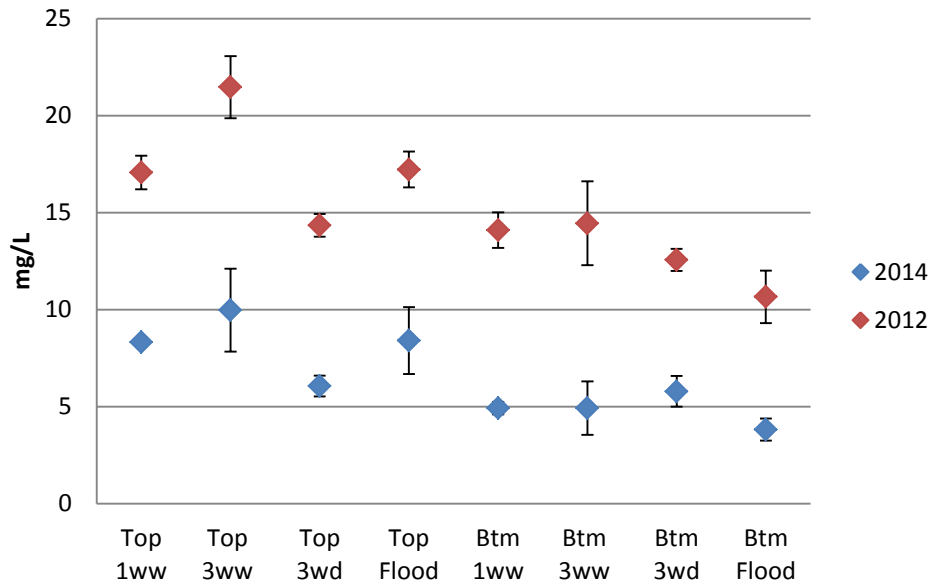
**Figure 5.11 Average concentration (mg/L) of Pb released at the end of a flood for mesocosm runs in 2012 and 2014 by run at the top and bottom.**
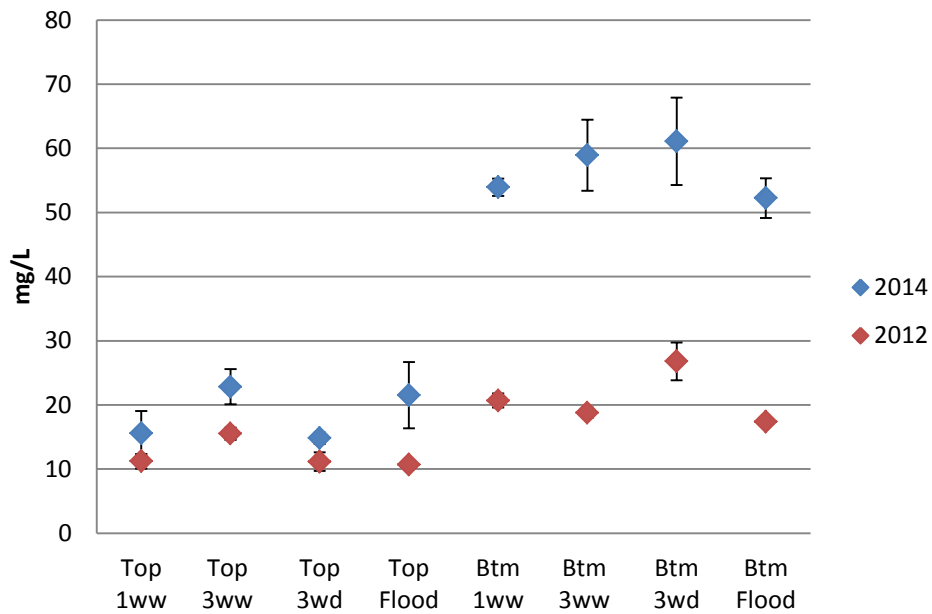


**Figure 5.12 Average concentration (mg/L) of Zn released at the end of a flood for mesocosm runs in 2012 and 2014 by run at the top and bottom.**

## 5.3.7 Sequential extraction to measure Pb, Zn, Fe and Mn in sediment samples from 2012 and 2014

The sequential extraction carried out (chapter 4) was re-run and concentrations of Pb, Zn, Fe and Mn (mg/kg) recovered from the sediment in 2012 were compared to that recovered in 2014 (< 63 $\mu$m grain size). The results show that in 2014, higher concentrations of Zn and Mn were recovered from the first and second extraction believed to be the most bioavailable forms and a lower concentration of Pb was recovered from the second extraction (see appendix 5.3.7 for mg/kg dry weight values with standard error).

Approximately 3 times more Zn (~ 1931 mg/kg more) and Mn (~ 215 mg/kg more) were recovered from the loosely sorbed fraction and approximately 2 times more Zn (~132 mg/kg more) and Mn (~ 46 mg/kg more) was recovered from the easily reducible Fe extraction in 2014 compared to 2012.

Approximately 1.5 times less Pb was recovered from the easily reducible Fe extraction (~ 9030 mg/kg less). As discussed in chapter 4 some of the Pb recovered during extraction step 2 may have been due to recovery of Pb from anglesite.

It can be seen that a small increase of Zn (2063 mg/kg) in the labile fraction of the sediment (extraction steps 1 and 2) resulted in a large increase of Zn released into pore water (bottom) in 2014 compared to 2012 (section 5.3.6).  However a large reduction of Pb recovered from extraction step 2 (9030 mg/kg) in 2014 compared to 2012 resulted in only a moderate decrease of Pb released into pore water in 2014 compared to 2012 (section 5.3.6). Pb concentrations were very high in the

sediment in both 2014 and 2012 compared to Zn (figure 5.13). It is notable that even though Zn is almost three orders of magnitude lower in concentration (mg/kg) than Pb in the sediment, the pore water dissolved Zn concentrations (mg/L) are almost four times higher.
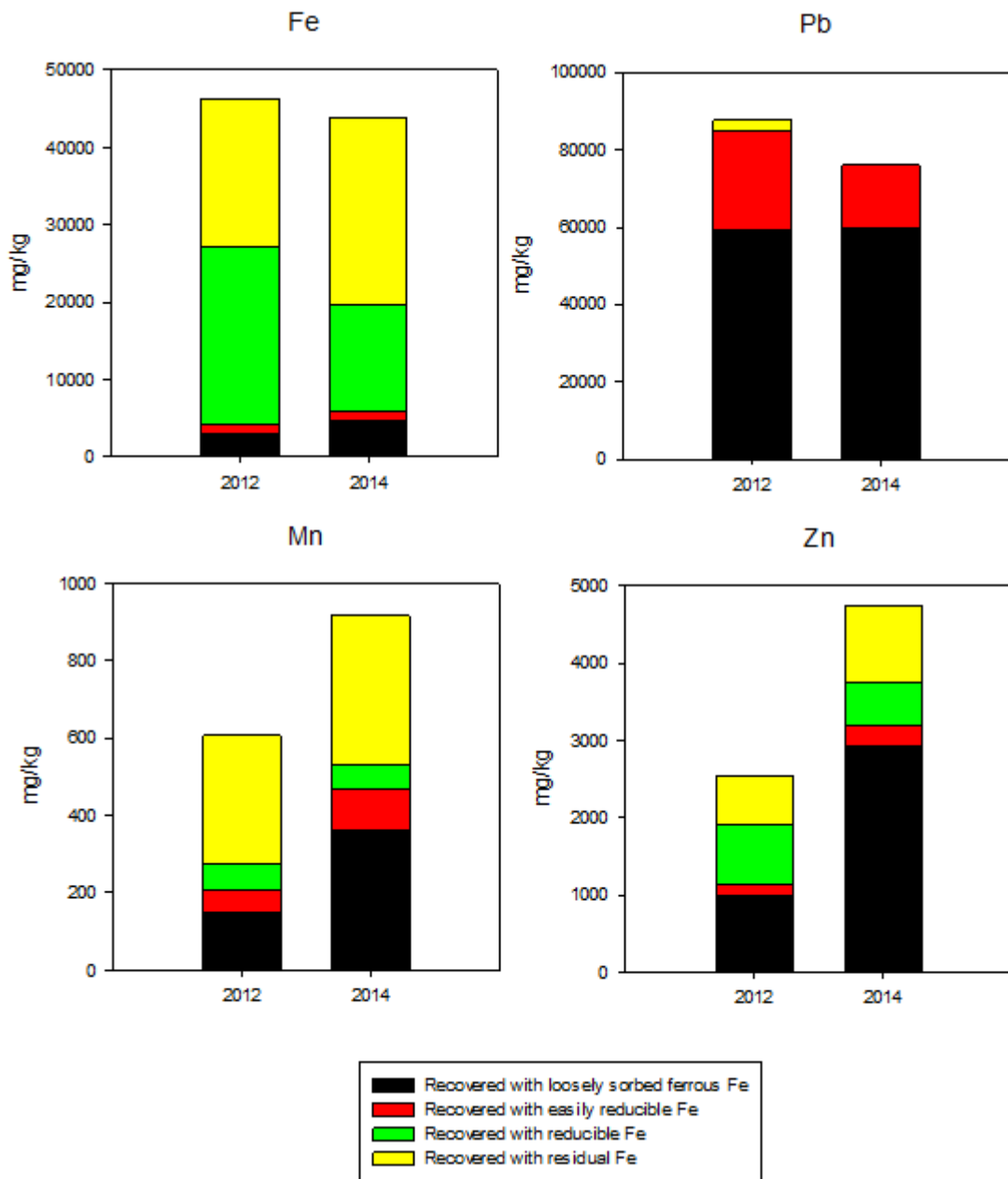


**Figure 5.13 Fe, Mn, Pb and Zn (mg/kg dry weight) recovered from the sediment in 2012 and 2014 (< 63 μm grain size) (note the different scales on the graphs).**

### 5.3.8 Spearman Rho, bivariate correlation between dissolved Pb and Zn and other variables

At the top of the mesocosm for the one week wet run there was a significant relationship between dissolved Pb and sulphate (r = .661, p = <.05) and dissolved Pb and Mn (r = .750, p = <.05). For all other runs at the top of the mesocosm there was a significant relationship between dissolved Pb and Mn (p = < .5). There was a significant relationship between dissolved Zn and sulphate (p = <.05) and dissolved Zn and Mn(p = < .05) for all runs at the top of the mesocosm (except the 3 week dry run) (see appendix 5.3.8 for correlation matrices).

At the bottom of the mesocosm for the 3 week wet run there was a significant negative relationship between dissolved Zn and pH (r = -.899, p = <.05) and a significant positive relationship between dissolved Zn and Mn (r = .928, p = <.01). For the 3 week dry run there was a significant negative relationship between dissolved Zn and pH (r = -.899, p  = <.05) and a significant positive relationship between dissolved Zn and sulphate (r = .886, p = <.05) (see appendix 5.3.8 for correlation matrices).

## 5.3.9 Saturation indices

The saturation indices for selected minerals were calcuated for all runs, weeks A (average values), J and L at the top and bottom of the mesocosms.

**Table 5.3. PHREEQC input pore water data (mg/L) for mineral phases all runs top and bottom of the mesocosm**

| Week | A | J | J | L | J | A | J | J | L | J |
|---|---|---|---|---|---|---|---|---|---|---|
| Sample | Avg | 1wwet | 3wdry | 3wwet | Fld | Avg | 1wwet | 3wdry | 3wwet | Fld |
| Loc | Top | Top | Top | Top | Top | Btm | Btm | Btm | Btm | Btm |
| pH | 5.7 | 5.1 | 5.5 | 5.4 | 5.6 | 5.8 | 5.6 | 5.6 | 5.7 | 5.7 |
| Pe | 8.7 | 10 | 8.86 | 8.5 | 8.3 | 8.7 | 9 | 8.6 | 7.4 | 7 |
| Temp $^0$C | 18.2 | 20.1 | 20.3 | 19.6 | 20.3 | 18.9 | 20.1 | 20.3 | 20 | 20 |
| Fe (2) | .03 | 0 | 0 | 0 | 0 | 0 | 0 | 0.0 | 0.05 | 0.2 |
| Mn (2) | .01 | 0 | 0 | 0 | 0.7 | 0.6 | 0.1 | 0.0 | 3 | 10 |
| Pb | 2.3 | 8 | 5 | 8.2 | 9.5 | 4.7 | 5.2 | 6.1 | 5.6 | 3.7 |
| Zn | 4.7 | 10 | 16.3 | 17.7 | 47.2 | 41.4 | 55.4 | 68.2 | 68.5 | 55.4 |
| Ca | 2 | 2 | 4 | 3 | 18 | 8 | 14 | 16 | 17 | 17 |
| N(5) | 1.95 | 0.1 | 0.6 | 0.4 | 1 | 3.3 | 0.6 | 2.5 | 0 | 0 |
| Cl$^-$ | 3 | 2.3 | 2.5 | 6.4 | 25 | 2.1 | 2.7 | 2.9 | 5.5 | 9.9 |
| S(6) | 11.19 | 25.3 | 35.2 | 36 | 115 | 94 | 121.9 | 145 | 148 | 123.5 |
| Na | 2.25 | 3 | 4 | 5 | 22 | 7 | 6 | 7 | 10 | 4 |
| K | 0.5 | 1 | 0 | 0 | 1 | 0.5 | 1 | 1 | 1 | 1 |
| C(4) | 0.7 | 1 | 0.9 | 0.7 | 1 | 0.4 | 1.7 | 1.6 | 3.4 | 3.2 |

**Table 5.4 Mineral Phases, SI and charge balance (%)**

| Week | A | J | J | L | J | A | J | J | L | J |
|---|---|---|---|---|---|---|---|---|---|---|
| Sample | Avg | 1wwet | 3wdry | 3wwet | Fld | Avg | 1wwet | 3wdry | 3wwet | Fld |
| Location | Top | top | Top | Top | Top | Btm | Btm | Btm | Btm | Btm |
| Charge bal % | 4 | 4 | 4.48 | 1.73 | 4.5 | -5 | 1.6 | -0.1 | 5.43 | 5.46 |
| **\*Anglesite** | -1.2 | -0.4 | -0.5 | -0.3 | **0.1** | -0.2 | **-0.1** | **-0.0** | **-0.1** | -0.3 |
| \*Gypsum | -3.8 | -3.5 | -3.1 | -3.2 | -2.1 | -2.4 | -2.1 | -2 | -2 | -2.1 |
| \*Bianchite | -6.4 | -5.8 | -5.5 | -5.5 | -4.7 | -4.8 | -4.6 | -4.4 | -4.4 | -4.6 |
| \*Larnakite | -2.5 | -2.31 | -1.84 | -1.6 | -0.9 | -1.1 | -1.4 | -1.1 | -1.1 | -1.5 |
| Pb(OH)2 | -2.0 | -2.64 | -2.1 | -2.1 | -1.7 | -1.6 | -2 | -1.78 | -1.8 | -1.9 |
| Zincite ZnO | -11.5 | -5.1 | -4.1 | -4.3 | -3.5 | -3.2 | -3.5 | -3.2 | -3.2 | -3.3 |
| ZnO(a) | -4.11 | -5.01 | -4 | -4.2 | -3.4 | -3.1 | -3.4 | -3.1 | -3.1 | -3.2 |
| ZnSO4:H2O | -7.81 | -7.12 | -6.8 | -6.8 | -6 | -6.1 | -5.9 | -5.8 | -5.8 | -5.9 |

**\*** Anglesite $PbSO_4$, Gypsum $CaSO_4.2H_2O$, Bianchite ZnSO4:6H2O, LarnakitePbO:PbSO4

It can be seen that pore water conditions were saturated with respect to anglesite for the flood run (top) and all variable wet and dry runs at the bottom of the mesocosms. At the top of the mesocosm Pb concentrations were close to saturation with respect to anglesite.

The saturation state of the water indicates the direction processes proceed in. Where a mineral is super-saturated according to Le Chaterier's principle the reaction below would move to the left and anglesite precipitation would occur. This would serve to lower dissolved Pb concentrations in pore water. Under sub-saturation conditions the reaction would proceed to the right and dissolution would be expected.

$$\text{Log\_k } 10^{-7.79} \quad = \quad [PbSO_4^{2-}]_{(s)} \quad \rightleftharpoons \quad [Pb]_{(aq)} \, [SO4^{2-}]_{(aq)}$$

As discussed in chapter 3 the saturation of anglesite may suggest that this mineral is providing a solubility control for concentrations of dissolved Pb in pore water (Nordstrom and Alpers, 1999).

All Zn minerals remained below saturation (table 5.4) even though pore water measurements showed that dissolved Zn concentrations are close to 70 mg/L for the 3 week wet and 3 week dry runs at the bottom of the mesocosm (table 5.3). Precipitation of Zn minerals would not therefore have controlled dissolved Zn concentrations in pore water over flooded periods.

### 5.3.10 Average dissolved (mg/L) Fe, Mn, Pb and Zn measured through DET

The purpose of using DET was to measure dissolved Fe, Mn, Pb and Zn at high spatial resolution (cm scale). It was envisaged that this in situ method would corroborate pore water results and provide further information regarding the key biogeochemical mechanisms responsible for the release of Pb and Zn into pore water in response to certain wet and dry treatments.

General trends for average dissolved Pb and Zn concentrations measured through DET were found to be similar to the pore water values at the bottom of the mesocosm. Indicating the averaged results obtained using the two methods were comparable. The highest concentration of dissolved Zn released at the start of a flood (in the first 72 hours) was for the 3 week dry run (26.1 $\pm$1.45 mg/L). Dissolved Zn was found to increase over a flood period for all runs, the highest average concentration of dissolved Zn at the end of a flood was for the 3 week dry run (32.5 $\pm$1.17 mg/L) and the flood run (51.8 $\pm$0.9 mg/L). For dissolved Pb the highest concentrations were released at the start of a flood and over the flood

period concentrations remained constant or declined slightly (table 5.5). The DET results for Mn were found to be similar to pore water results. Mn concentrations were found to increase over a flood period, the highest concentrations were measured for the runs with longer flooded periods (3 week wet and flood run) (table 5.5).

Dissolved Fe concentrations were much higher than for the pore water results. Fe concentrations for some runs (3 week wet and 3 week dry) were higher at the start of a flood compared to the end (table 5.5).

**Table 5.5 Summary table for DET results. Average concentration (mg/L) and range () for Fe, Mn, Pb, Zn at the start and end of a flood (n = 15). The week is noted in brackets. Significant values are in bold and underlined.**

|  | Fe strt | Fe end | Mn strt | Mn end | Pb strt | Pb end | Zn strt | Zn end |
|---|---|---|---|---|---|---|---|---|
| **1wwet (weeks I & J)** | 2.7 | 4.5 | 0.1 | 0.5 | 8.4 | 8.3 | 17.5 | 22.6 |
| **1wwet (weeks I & J)** | (0.7 - 9) | (1 - 22.3) | (0 - 0.1) | (0.3 - 0.9) | (5.9 - 14.2) | (6 - 16.5) | (13.4 - 20) | (19 - 29.4) |
| **3wwet (weeks I & L)** | 8.0 | 0.4 | 0.9 | 2.4 | 7.4 | 6.8 | 18.8 | 29.8 |
| **3wwet (weeks I & L)** | (0.7 - 41.6) | (0 - 3.4) | (0.3 - 2.1) | (1.1 - 5.6) | (5.8 - 9.6) | (4.8 - 10.7) | (15.6 - 24.5) | (24 - 41.4) |
| **3wdry (Weeks I & J)** | 4.9 | 2.8 | 0.1 | 0.2 | 6.8 | 6.6 | **26.1** | **32.5** |
| **3wdry (Weeks I & J)** | (0.7 - 43.3) | (1 - 7.5) | (0 - 0.8) | (0.1 - 0.2) | (5.2 - 14.1) | (4.6 - 9.5) | (17.4 - 34.2) | (21.7- 44.2) |
| **Flood (weeks B & J)** | 2.5 | 2.8 | 0.4 | 5.2 | 10.5 | 8.0 | 25.9 | **52** |
| **Flood (weeks B & J)** | (0.4 – 8.9) | (0.8 - 17.6) | (0.2 - 1) | (4.3 - 7.1) | (4.9 – 34.9) | (5.5 - 15.3) | (22.2 – 30.4) | (45.4 - 58) |

Sulphate could not be detected through IC analysis of DET samples. The back equilibration of solutes into 1 mol nitric acid resulted in nitrate concentrations that were too high. The author was aware issues could arise from measuring anions and cations using one DET probe, however, after research, plus discussion with and advice from a number of sources, including DGT Ltd, the author made the decision to go ahead with the current method. An alternative method previously used to measure both anions and cations using one DET probe was to elute the gels in DIW prior to acidifying them in HCl (Byrne et al., 2014). Back equilibration in DIW would allow for the elution of sulphate but not Fe and Mn because the latter would precipitate out in the gel on exposure to atmospheric conditions and prevent them being lost. However the current study included analysis of Zn. Zn is known to be more soluble than Fe under oxic conditions (Jarvis and Mayes, 2012) and there was a chance that some Zn would have been lost. As Zn was one of the two key trace metal contaminants analysed the author didn't want to take the risk. The patterns of mobility of Zn and Pb measured through pore water analysis were found to be similar to those measured for DET and these patterns indicated that the key mechanisms of attenuation and release of dissolved Pb and Zn were similar. Therefore it was believed that Pb and sulphate and Zn and sulphate pore water analysis could be used to to support the findings relating to DET analysis.

**5.3.11 DET depth concentration (mg/L) profiles of Fe, Mn, Zn and Pb**

Figures 5.14 – 5.15 show the DET depth profiles for dissolved Fe, Mn, Pb and Zn at the start of a flood (week I) (1 week wet, 3 week dry and 3 week wet) and end of a flood period (week J) (1 week wet, 3 week dry) and (week L) (3 week wet). For the constant flood, because there were no dry periods the weeks B – J are shown for comparison between conditions at the start of a flood (week B) (allowing a week for pore water conditions to settle) and after a period of prolonged flooding (week J).

Each of the runs were found to show different patterns of dissolved Zn, Mn, Pb and Fe release. For the 3 week dry run, at the start of a flood (within 72 hours), the highest Zn concentrations were measured at the bottom > 10cm depth of the mesocosm (figure 5.14). Over the course of the flood for this run Zn concentrations increased closer to the top < 10cm depth. Mn was not released over the 3 week dry run. There were a few intermittent 'peaks' of Fe. Pb vertical depth profile remained fairly constant and there was little visible change between weeks I and J (figure 5.14).

For the 3 week wet run, dissolved Zn can be seen to increase throughout the whole depth profile between week I and L and at the end of the flood dissolved Zn seemed to be slightly higher at the bottom of the mesocosm. Dissolved Mn seemed to follow a similar pattern of release over the flood period. That could indicate the release of dissolved Zn was related to the dissolution of Mn at the bottom of the mesocosm for this run. Once again peaks of dissolved Fe were observed (figure 5.15).

For the constant flood run there was a large increase in dissolved Zn and an increase in dissolved Mn between week B and J over the entire depth profile (figure 5.15).

Peaks of dissolved Fe were observed even where Mn was not reduced and where bulk pore water redox potential and DO measurements indicated that conditions were oxic (figures 5.14-5.15). In some cases dissolved Pb showed a similar pattern of release particularly week B for the flood run (figure 5.15).
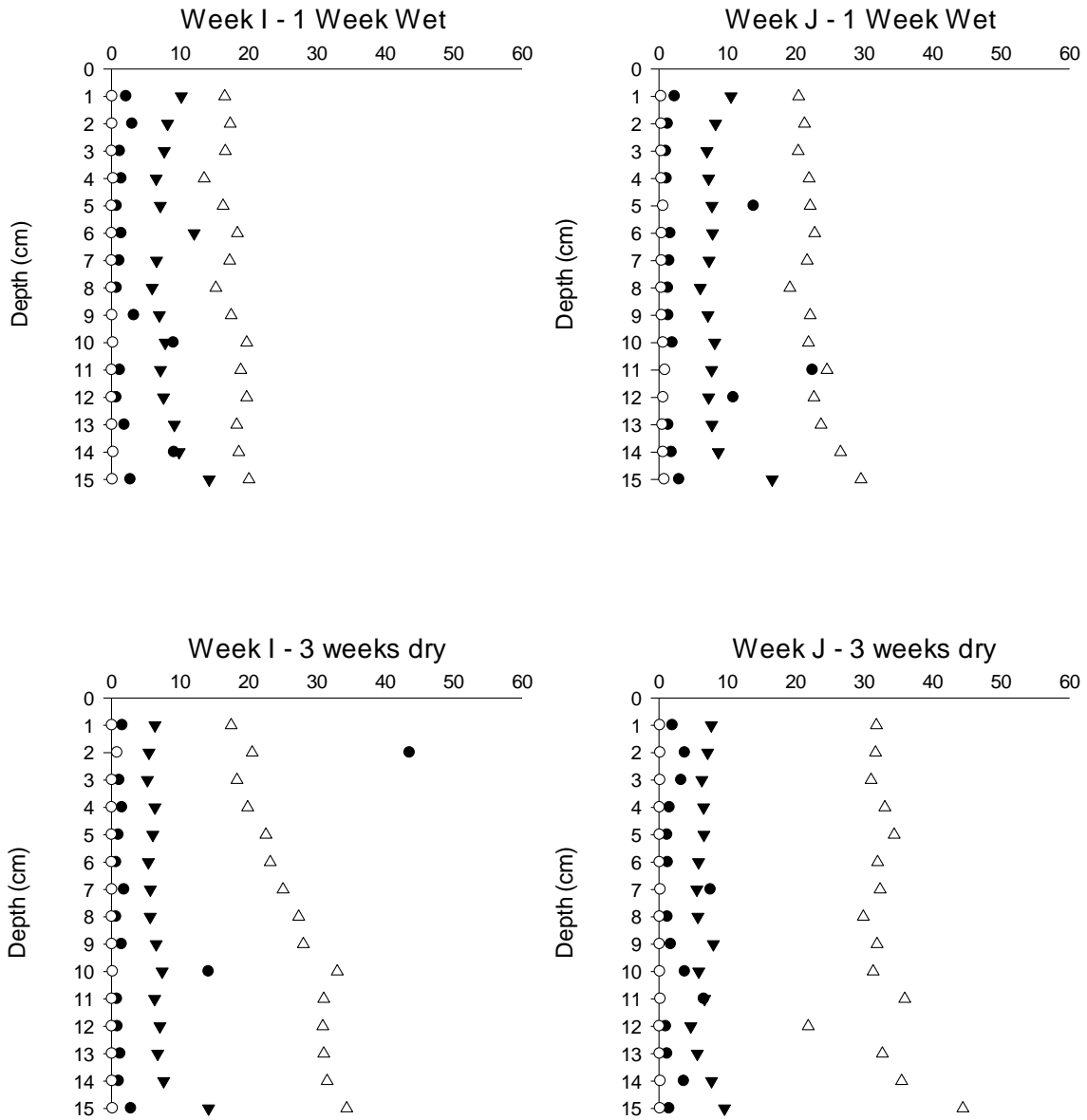
**Figure 5.14 Depth profile for dissolved Fe, Mn, Pb, Zn (mg/L) in pore water measured through DET for runs 1 week wet and 3 week dry at the start (week I) and end (week J) of a flood period.**

**Key:**

| | |
|---|---|
| ● | Fe |
| ○ | Mn |
| ▼ | Pb |
| △ | Zn |
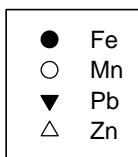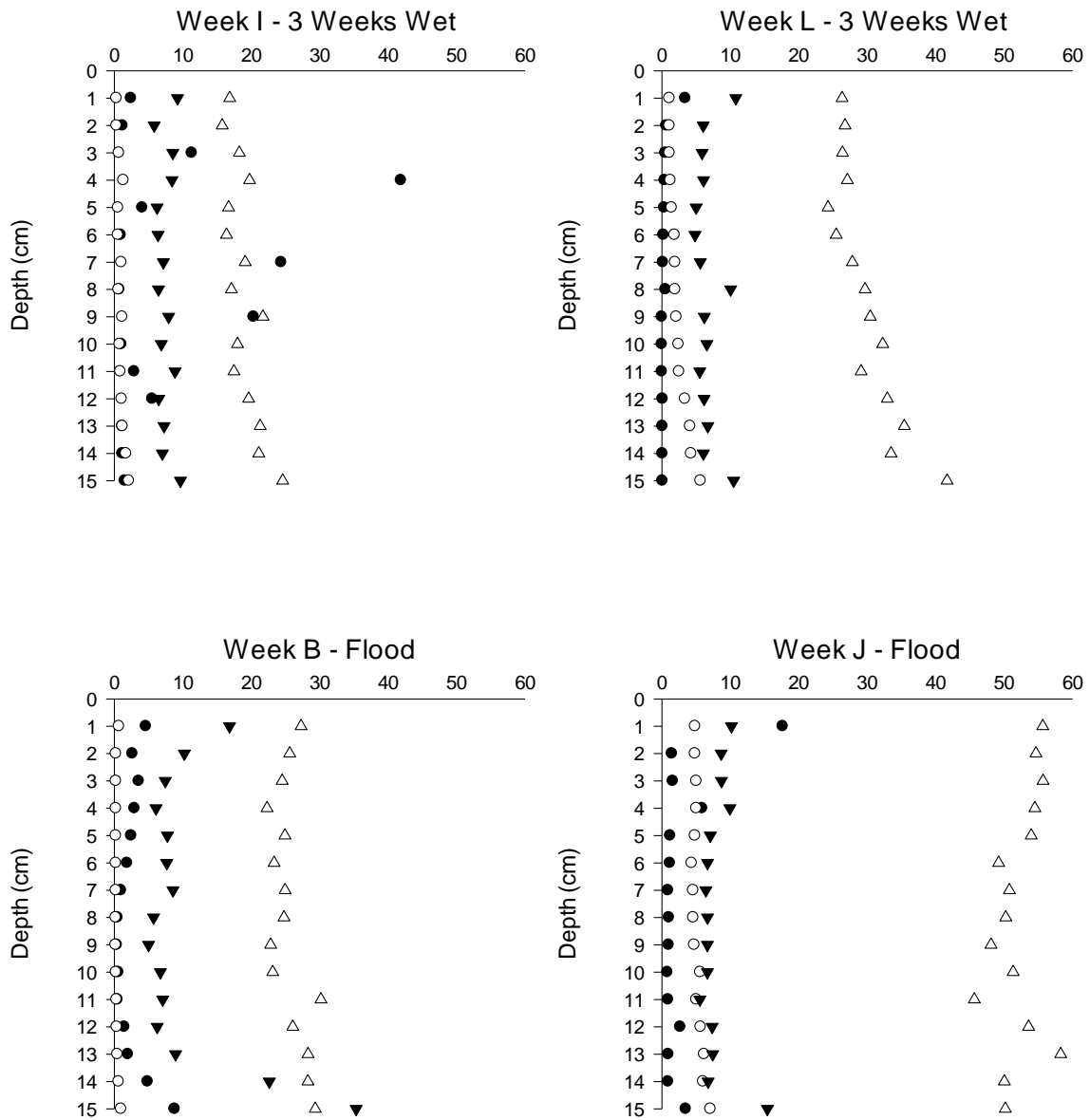
**Figure 5.15 Depth profile for dissolved Fe, Mn, Pb, Zn (mg/L) in pore water measured through DET for 3 week wet at the start (week I) and end (week L) and for flood run at the start (week B) and end (week J) of a flood period.**

**Key:**

| | |
|---|---|
| ● | Fe |
| ○ | Mn |
| ▼ | Pb |
| △ | Zn |
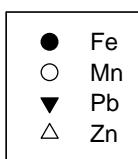
### 5.3.12 Analysis of difference for Zn, Mn, Fe, Pb measured through DET

Results from Wilcoxon rank sum tests found that for all runs there was a significant increase in the concentration of dissolved Zn and Mn released between the start and end of a flood period (p = .001) for samples measured through DET. There was no significant increase between the start and end of a wet period in dissolved Pb or Fe for any of the runs (table 5.6).

**Table 5.6 Wilcoxon rank sum test to analyse for significant difference in the concentration of dissolved Zn, Pb, Mn and Fe measured through DET between the start and end of a flood for all runs**

| | Run & week compared | Test statistic Calc W | Calc W2 | Calc Z | P | If Z <- 1.96 Reject Null H. | n |
|---|---|---|---|---|---|---|---|
| Zn | 1wwet (wks I&J) | 123 | 342 | -4.5 | .001 | Y | 15 |
| Zn | 3wdry (wks I&J) | 158 | 307 | -3.09 | .001 | Y | 15 |
| Zn | 3wwet (wks I&L) | 121 | 344 | -4.6 | .001 | Y | 15 |
| Zn | Flood (wks B&J) | 120 | 345 | -4.66 | .001 | Y | 15 |
| Pb | 1wwet (wks I&J) | 107 | 227 | -.228 | .838 | N | 15 |
| Pb | 3wdry (wks I&J) | 220 | 245 | -.518 | .604 | N | 15 |
| Pb | 3wwet (wks I&L) | 181 | 284 | -2.1 | .05 | Y | 15 |
| Pb | Flood (wks B&J) | 231 | 233 | -.041 | .967 | N | 15 |
| Mn | 1wwet (wks I&J) | 120 | 345 | -4.67 | .001 | Y | 15 |
| Mn | 3wdry (wks I&J) | 153 | 311 | -3.28 | .001 | Y | 15 |
| Mn | 3wwet (wks I&L) | 144 | 321 | -3.67 | .001 | Y | 15 |
| Mn | Flood (wks B&J) | 120 | 345 | -4.67 | .001 | Y | 15 |
| Fe | 1wwet (wks I&J) | 216 | 249 | -.687 | .494 | N | 15 |
| Fe | 3wdry (wks I&J) | 191 | 274 | -1.72 | .085 | N | 15 |
| Fe | 3wwet (wks I&L) | 129 | 336 | -4.295 | .001 | Y | 15 |
| Fe | Flood (wks B&J) | 221 | 243 | -.456 | .648 | N | 15 |

### 5.3.13 Spearmans rho correlation analysis for DET

Spearman's rho correlation analysis found that for the one week wet run week J ($r = .807$, $p = .01$), the 3 week wet run week I ($r = .932$, $p = .01$) and week L ($r = .886$, $p = .01$), there was a significant relationship between dissolved Zn and Mn that was not apparent for the 3 week dry run (figures 5.16 - 5.18). For the flood run, week B there was a correlation between Pb and Fe ($r = .764$, $p = .01$) (figure 5.19) and for the flood run week J there was a correlation between Pb and Fe ($r = .870$, $p = 0.1$).
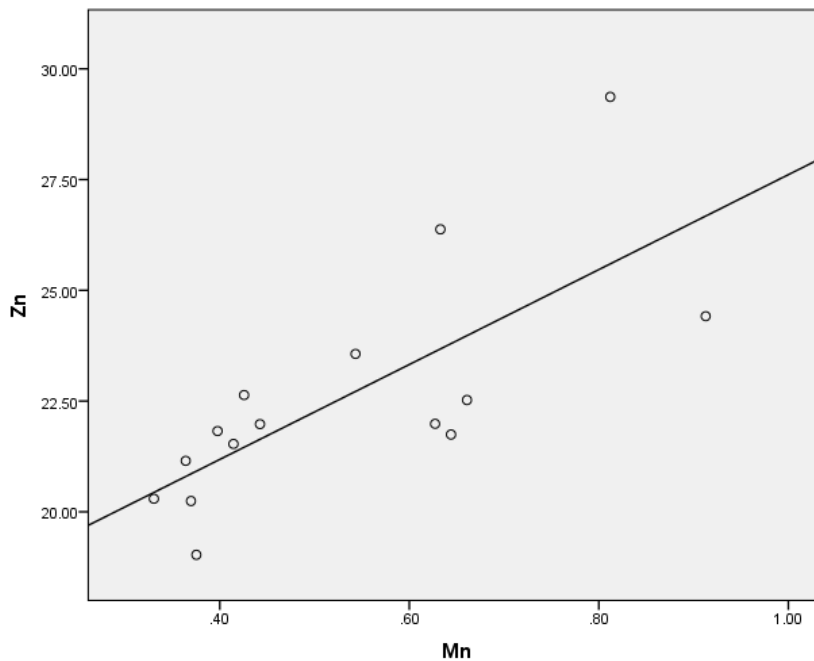


**Figure 5.16 Correlation between dissolved Zn and Mn (mg/L), 1 week wet run week J (end of a flood)**
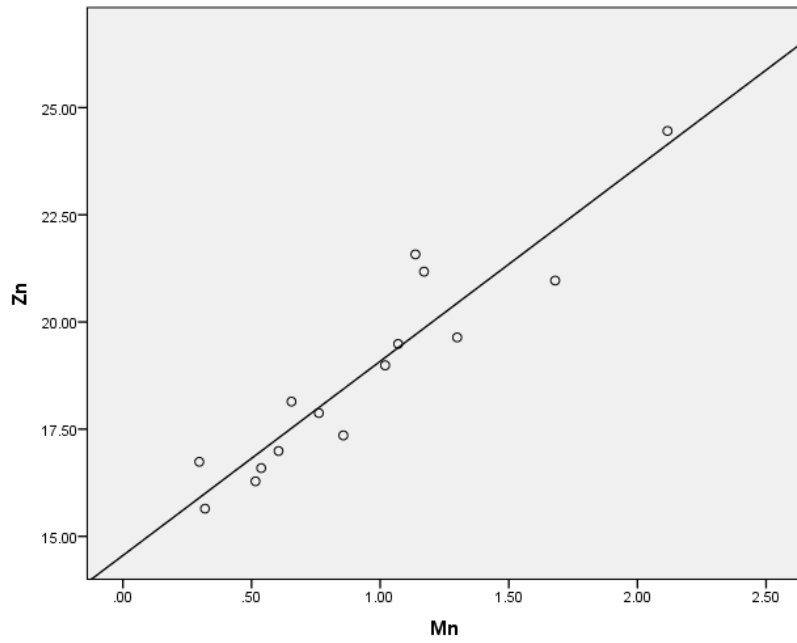
**Figure 5.17 Correlation between dissolved Zn and Mn (mg/L), 3 week wet run week I (start of flood)**
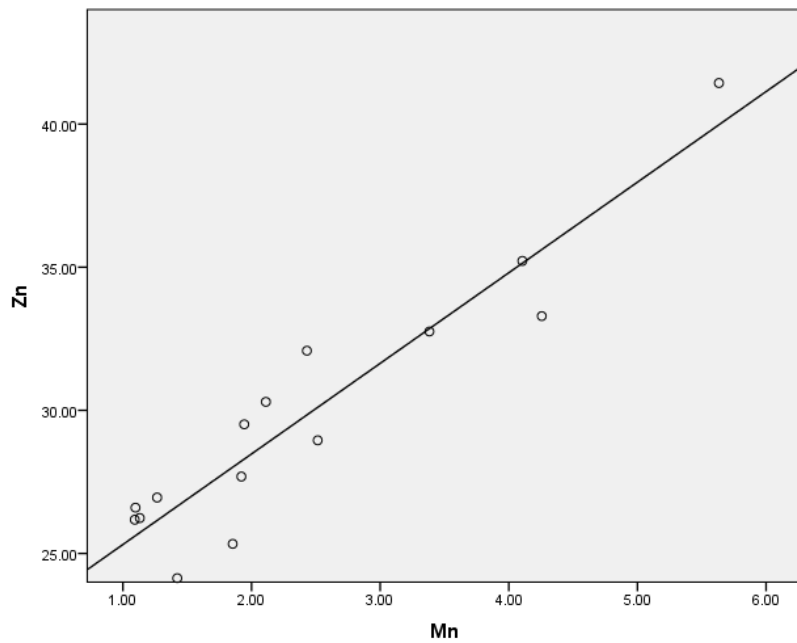


**Figure 5.18 Correlation between graph for dissolved Zn and Mn (mg/L), 3 week wet run week L (end of flood) (note the change in scale from week I)**
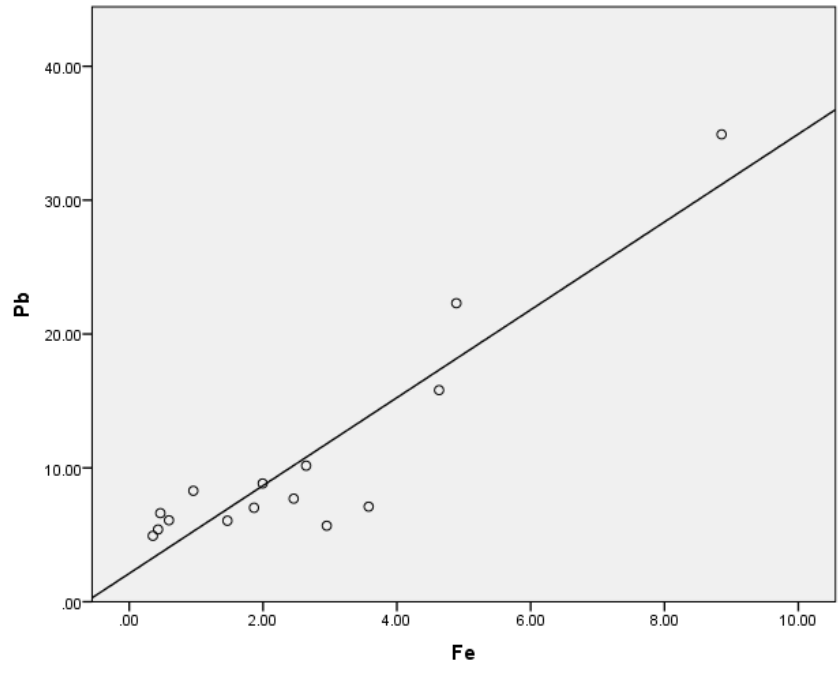
**Figure 5.19 Correlation between dissolved Pb and Fe (mg/L),
Flood run week B**

## 5.3.14 Principal components analysis (PCA) of pore water samples

Analysis of DET samples identified a significant correlation between dissolved Zn and Mn for the 1 week wet and 3 week wet run (section 5.3.13). Furthermore dissolved Zn and Mn measured through DET were found to increase significantly between the start and end of a wet period for these runs (section 5.3.12). This was in line with pore water data analysis where there was a significant correlation between Zn and Mn at the bottom of the mesocosm for the 3 week wet run (section 5.3.8). Additionally, for DET a significant correlation between dissolved Fe and Pb was observed for the flood run (week B) (section 5.3.13).

To further explore the underlying factors relating to the release of Pb and Zn for the 1 week wet, 3 week wet and flood runs principal component analysis (PCA) was carried out on weekly pore water data. DET measurements were not included as they were not taken on a weekly basis. However, using the pore water data to analyse trends for DET measurements was considered acceptable because similar trends in the release of dissolved Pb and Zn for DET and pore water data were observed (section 5.3.10).

PCA was conducted on 10 items with orthogonal rotation (varimax). The Kaiser-Meyer-Olkin measure verified the sampling adequacy for the analysis, KMO = 0.74 (good, according to Field, 2009) and well above the acceptable limit of 0.5 (Field, 2009). Bartlett's test of sphericity ($\alpha$ = <0.001) indicated that correlations between variables was sufficiently large for PCA. An analysis was run to obtain eigenvalues for each factor in the data. Eigenvalues over 1.5 were chosen based on the point of inflexion on the scree plot (Field, 2009). Factor 1 explained 50.6%

of the variance and factor 2 explained 13.4%. Table 5.7 shows factor loadings after rotation.

**Table 5.7 Rotated Factor Loadings, (loadings > 0.4 appear in bold)**

| Variables | Factor1 | Factor2 |
|-----------|---------|---------|
| DO | **-.875** | -.034 |
| Ca | **.874** | .066 |
| Zn | **.845** | .159 |
| Sulphate | **.797** | -.019 |
| Mn | **.782** | .023 |
| Redox | **-.756** | -.107 |
| TIC | **.718** | -.218 |
| pH | **.630** | -.103 |
| Pb | -.211 | **.855** |
| Fe | .203 | **.708** |

Dissolved Zn, Mn, sulphate, pH, Ca, TIC (positive) and redox potential, DO (negative) all loaded highly onto factor 1. This cluster of variables suggests that factor 1 could represent redox potential. Factor 2 only Pb and Fe loaded highly onto this factor.

It can be seen from the factor scores for each porewater sample (figure 5.20) that samples for the longer wetter runs at the bottom of the mesocosm 'B' eg. the 3 week wet run and flood run (blue circles and orange circles) scored highly against factor 1, whereas samples for the runs at the top of the mesocosm (squares) tended to score negatively against factor 1. PCA analysis indicates that a fall in redox potential conditions influenced the release of dissolved Zn, Mn and sulphate for the 3 week wet run and flood run.
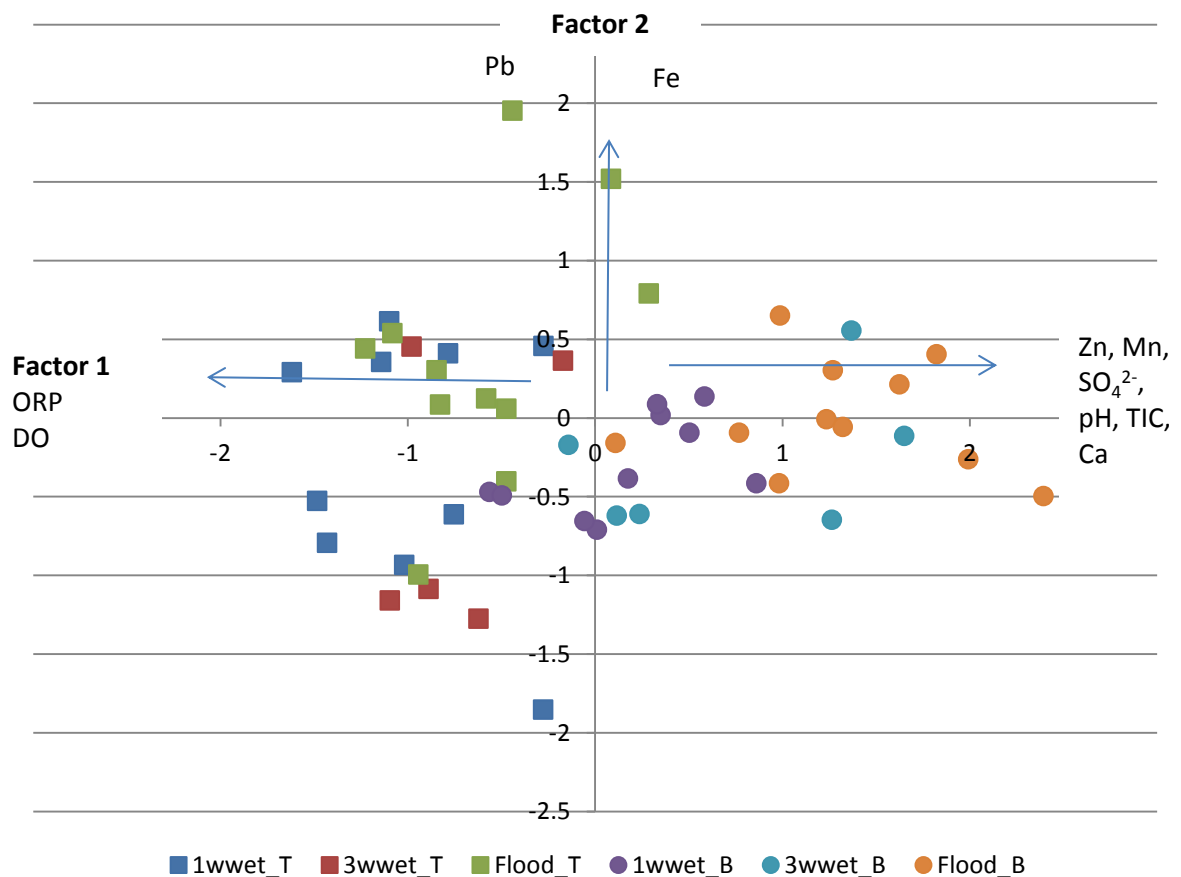


**Figure 5.20 Factor scores for individual pore water samples, grouped by run, top (T) squares, bottom (B) circles**

Some samples for the flood run scored highly against factor 2, where Pb and Fe were loaded highly.

### 5.3.15 SEM/EDS analysis of sediment samples

SEM/EDS analysis indicated the sediment sampled in 2012 and in the current study (2014) had similar mineralogy.

Figure 5.21 shows a back scattered electron (BSE) image of a sediment grain with a bright grain (red circle). The smart map X-ray images of this grain (figure 5.22) show an Fe, O rich area overlain by a Pb, S rich grain. Although SEM/EDS provides no indication of redox species at the location of the Pb, S rich grain there is a darkening of the Fe, O areas on the maps indicating these elements are not present, or present at low concentration (see red circles). This seems to indicate as for previous XRD analysis (table 4.3) and SEM EDS analysis (chapter 4) that minerals of mixed redox potential were present in the sediment.
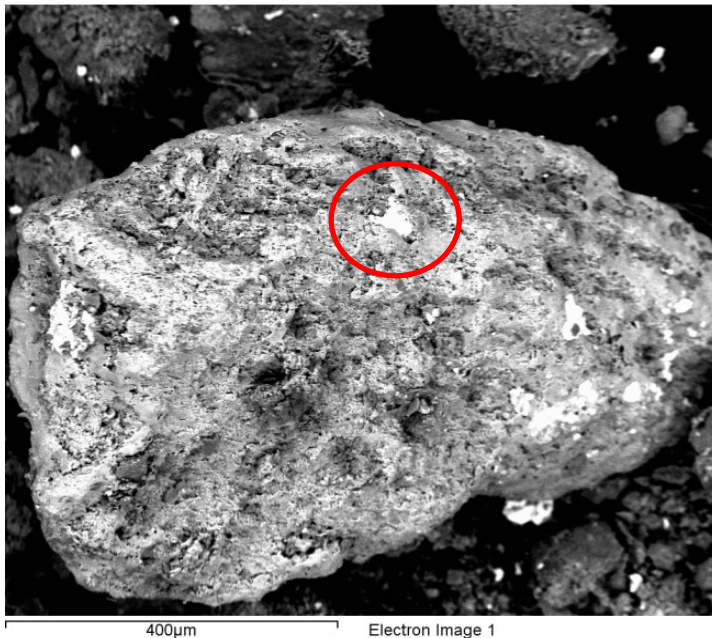


**Figure 5.21 BSE image of grain in the sediment. Note bright grain (red circle).**
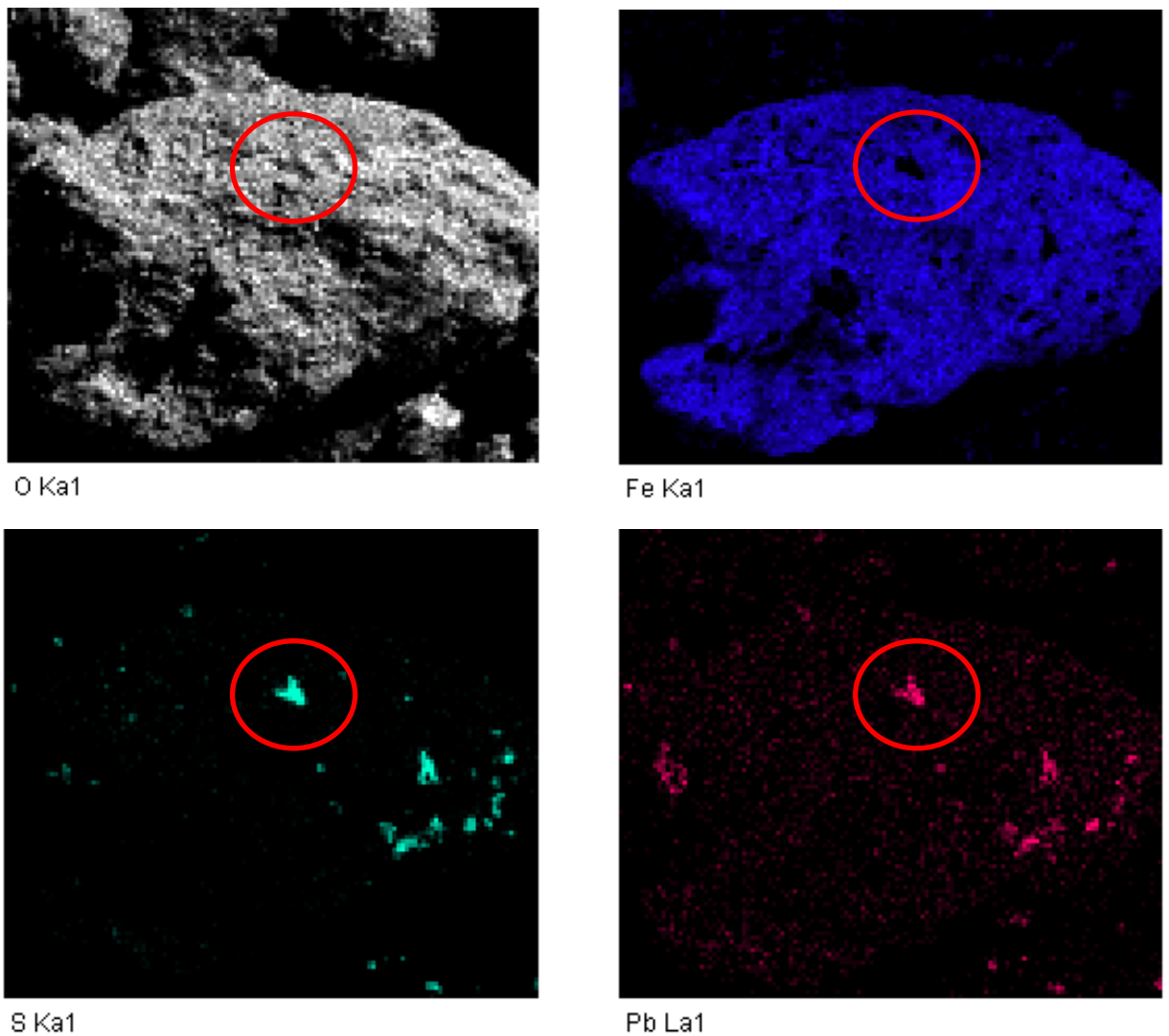
**Figure 5.22 Smartmap x-ray image for O (oxygen), Fe, S (sulphur) and Pb.**

The EDS and quant specification for spectrum 2 (figures 5.23 – 5.24) show a sediment grain high in Zn, sulphur and Fe. The oxidation state of sulphur was unknown. The mineral could be a mixed sulphide or sulphate. The high Si content and presence of Al are likely attributed to the clay fraction of the sediment particularly as SEM/EDS favoured analysis of the finer fraction of the sediment. Pd was used to coat the sample (table 5.8).
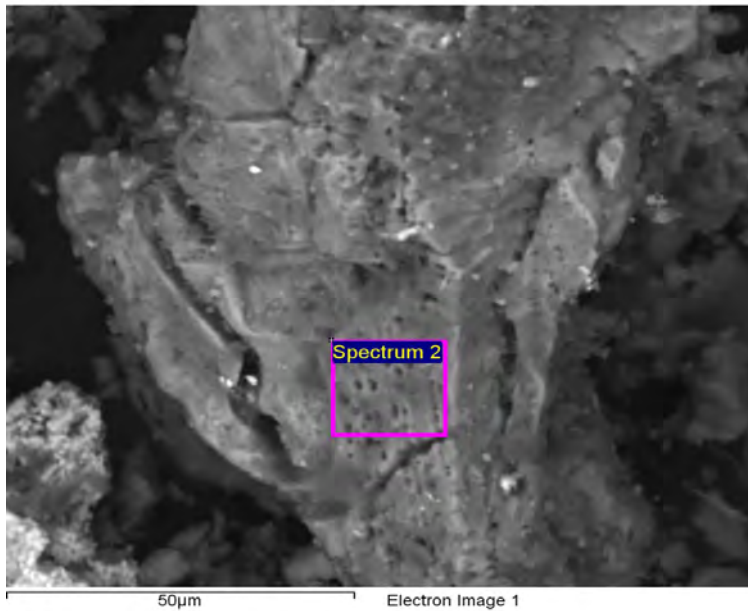
**Figure 5.23 BSE of a sediment grain.**
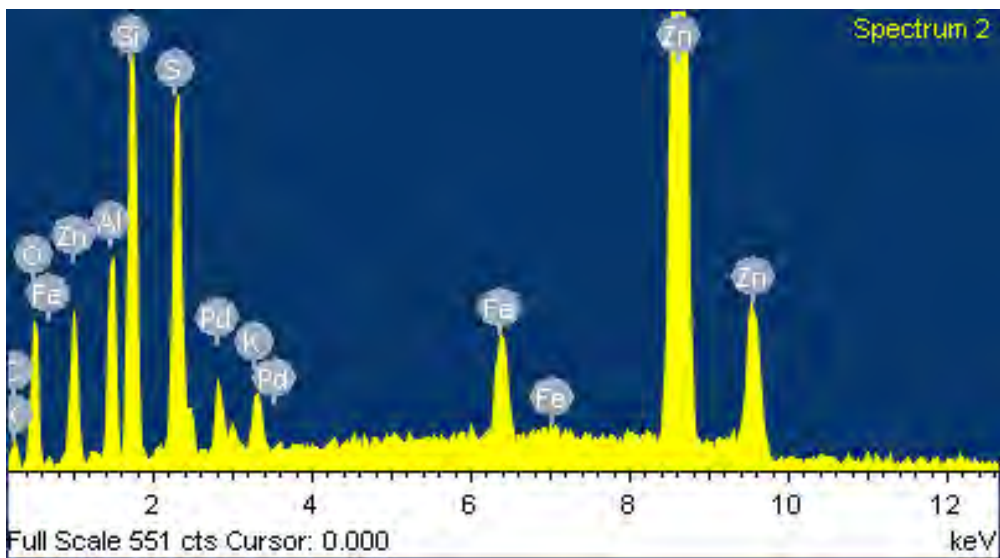


**Figure 5.24 EDS (histogram) for spectrum 2, figure 5.23.**

**Table 5.8 Quant specification,**

**Element weight% and atomic% for 'spectrum 2', figure 5.23**

| Element | Weight% | Atomic% |
|---------|---------|---------|
| C K | 0.00 | 0.00 |
| O K | 4.06 | 12.83 |
| Al K | 3.17 | 5.94 |
| Si K | 5.78 | 10.42 |
| **S K** | **4.11** | **6.49** |
| K K | 0.77 | 1.00 |
| **Fe K** | **2.76** | **2.50** |
| **Zn K** | **77.34** | **59.86** |
| Pd L | 2.00 | 0.95 |
| Totals | 100.00 | |

**5.3.16 Comparison of diluted Pb and Zn concentrations to Environmental Quality Standards**

Dissolved concentrations of Pb and Zn measured during mesocosm experiments, in confined conditions over periods of a week or greater, are unlikely to reflect surface water concentrations in the natural river bank environment where these trace metals may be subjected to dilution effects due to mixing with river water. In order to compare dissolved concentrations of Pb and Zn measured in pore water to EQS, dilution effects were calculated and compared to EQS.

Using maximum and minimum average dissolved Pb and Zn concentrations (mg/L) taken from table 5.2, an estimated dilution calculation was carried out, to determine the concentration of dissolved Pb and Zn, if 1 L of pore water were to exfiltrate from the river bank and become diluted with uncontaminated river water. The dimensions were based on the morphology of the river at the sample site (width 6 m x depth 0.5 m x length 0.25 m) = $0.75m^3$ * 1000 = 750 L water. The diluted concentrations of dissolved Pb and Zn were then compared to EQS (table 5.9).

**Table 5.9 Min and max average dissolved concentration of Pb and Zn (mg/L) measured in pore water, dissolved concentration after dilution in river water and EQS**

|  | Pb (max) | Pb (min) | Zn (max) | Zn (min) |
|---|---|---|---|---|
| Pore water (mg/L) | 10 | 3.8 | 61.1 | 14.8 |
| After dilution (μg/L) | 13.3 | 5.06 | 81.5 | 19.7 |
| *EQS Pb & Zn (μg/L) | 7.2 | Dissolved concentration | 8 | Total Concentration 0 – 50 mg/L CaCO3 (hardness) |

*EQS for Pb and Zn for the protection of surface water, annual average values (Environment Agency, 2011)

It can be seen that after dilution the minimum average concentration of dissolved Pb at the bottom of the mesocosm did not exceed EQS. However the maximum average concentration for the 3 week wet run at the top of the mesocosm did exceed EQS and the calculations indicate that at any concentration > 6 mg/L dissolved Pb would exceed EQS after dilution. That is a concern because all average values for dissolved Pb at the top of the mesocosm exceeded 6 mg/L. Average concentrations of Pb measured through DET were found to exceed EQS. All concentrations of Zn were found to exceed EQS for water with a low hardness (low hardness was indicated in pore water samples through TIC measurements).

## 5.4 Discussion

The main objectives of this chapter were to (i) compare DET, pore water and sediment data with the results from chapter 3 and 4 to determine whether the mechanisms of trace metal mobility in response to the wet and dry treatments were similar and confirm reproducibility of the methodology (ii) analyse DET results alongside pore water results in combination with statistical, geochemical, solid analysis (SEM/EDS) and literature data to determine the key biogeochemical mechanisms responsible for the release of Pb and Zn in response to the wet and dry treatments and (iii) determine the potential for the mining contaminated sediments to become a source of Pb and Zn contamination under certain wet and dry treatments and discuss the environmental implications.

Sediment was collected from the same site but at a slightly different location to the sediment collected for the mesocosm experiments discussed in chapter 3. The sediment was of a similar grain size predominantly sandy with larger granules and pebbles, with a similar low inorganic carbon and low to medium organic carbon content. The mineralogy of the sediment was also similar as confirmed through SEM and XRD analysis. However the concentration of Pb and Zn were slightly different. Sequential extraction analysis showed Zn was present at a higher concentration in the more labile loosely sorbed and easily reducible fraction and Pb was present at lower concentration, primarily in the easily reducible Fe fraction that, as noted in chapter 4, may also have included anglesite. The differences in Pb and Zn concentration could be due to differences in the composition of primary minerals at different locations at the site (Evans, 1991) or may be as a result of leaching from the waste piles that surrounded the sample site (Fuge et al., 1991).

The samples were taken from a location at a lower river bank height than samples collected in 2012 and were on a shallow sub surface lateral flow path. Runoff from tailing heaps and waste piles can contain high concentrations of Pb and Zn (Hofman and Schuwirth, 2008; Lu and Wang, 2012) and studies investigating the release of trace metals from waste piles report the greater mobility of Zn compared to Pb (Merrington and Alloway, 1994). Sequential extraction analysis found that Mn was also present at higher concentration in the more labile fraction of the sediment and that could indicate leaching of Zn from waste piles and attenuation of this trace metal through sorption and co-precipitation with redox sensitive Mn oxides (Hudson-Edwards, 2003; Byrne et al., 2010).

For DET average dissolved Pb concentrations were slightly higher and dissolved Zn concentrations slightly lower than pore water results. It is possible that there was an enrichment of Pb and displacement of Zn in the polyacrylamide gel, as reported by one DET performance study (Garmo et al., 2008). However this effect was most problematic where trace metals were present at low concentrations (2 – 20 µg/L). At higher concentration (> 0.2 mg/L) DET performance tests of mixed metal solutions indicated dissolved Zn and Pb achieved the same concentration in a polyacrylamide gel as in sediment pore waters, providing the gel was pre-soaked in an electrolyte solution matching that of the sample pore water (Zhang and Davison, 1999; Garmo et al., 2008).

Average concentrations of dissolved Fe and Mn measured through DET were also higher compared to pore water results. Errors can occur through the insufficient de-oxygenation of probes prior to deployment resulting in high Fe and Mn values for DET (Davison et al. 2000), that was not believed to be the case in the current

study. It is possible that exposure of pore water to atmospheric conditions during sampling, subsequent oxidation of reduced Mn and/or Fe and sorption of Mn and Fe hydroxides could have resulted in lower average concentrations of Mn and Fe. Other studies have reported similar observations (Leermakers et al., 2005; Gao et al., 2006).

As observed in chapter 3 Pb and Zn displayed different patterns of release in response to wet and dry treatments therefore they are discussed separately.

### 5.4.1 The mobility of Pb in response to wet and dry sequences

The lower concentration of dissolved Pb measured in pore water compared to the mesocosm runs in chapter 3, was possibly reflective of the lower concentration of Pb in the labile fraction of the sediment. However the patterns of mobility in response to wet and dry treatments were similar indicating (i) the methodology used in chapter 3 was repeatable and (ii) the biogeochemical mechanisms controlling Pb mobility in response to the wet and dry treatments were similar. DET and pore water results displayed similar patterns for dissolved Pb providing evidence that the results from the two methods were comparable.

The average concentration of dissolved Pb released over flooded periods was significantly higher at the top of the mesocosms compared to the bottom. The highest concentration was for the 3 week wet run. High (> 4 mg/L) concentrations of Pb were released at the start of a flood at the top and bottom of the mesocosm. At the bottom of the mesocosm over a flood period dissolved Pb concentrations remained the same or declined slightly. Geochemical saturation indices indicated that conditions reached saturation with respect to anglesite and therefore

anglesite was likely to provide a key solubility control over dissolved Pb concentrations at the bottom of the mesocosm. At the top of the mesocosm there was an on-going release of Pb into surface water. Redox potential and DO measurements indicated conditions were more oxic in the surface water compared to the bottom of the mesocosm, and as discussed in chapter 3 that could encourage the oxidation of reduced sulphide minerals. Moreover conditions were slightly below saturation with respect to anglesite at the top of the mesocosm indicating (i) anglesite solubility was not controlling dissolved Pb concentrations (ii) a tendency for anglesite to dissolve.

For DET dissolved Pb displayed a uniform depth concentration profile apart from occasional peaks of dissolved Pb. In some cases peaks of Pb were found to coincide with peaks of Fe and the concentration profiles for dissolved Pb and Fe were found to correlate significantly for the constant flood run (week B). Dissolved Fe was not expected as redox potential measurements indicated that reductive dissolution of Fe would be unlikely to occur (Gotoh and Patrick, 1974: Patrick and Henderson, 1981). There could be several reasons for these peaks. Sphalerite compositions can vary between different mineral deposits and substitution of elements such as Fe, Mn and Pb are reported to occur (Stanton et al., 2006). A mixed Zn Mn Fe sulphide mineral was identified in chapter 4 through XRD (table 4.3) and a mixed Zn, Fe, S mineral grain identified through SEM/EDS analysis in the current chapter (figures 5.23 – 5.24). Findings from a laboratory study investigating the oxidation of mixtures of sphalerite and galena (pH 6) suggested ferrous Fe released during oxidation of impure sphalerite could oxidise to ferric Fe and serve to oxidise galena in the following process (Heidel et al., 2013):

$$PbS + 8Fe^{3+} + 4H_2O \longrightarrow Pb^{2+} + SO_4^{2-} + 8Fe^{2+} + 8H^+$$

An alternative mechanism was reported where minor amounts of ferrous Fe in galena were observed to influence the oxidation mechanism of galena (pH 6) in a similar fashion to that described above (Heidel and Tichomirowa, 2011). These authors suggested that, on oxidation of galena, ferrous Fe sorbed to the mineral surface was oxidised to ferric Fe. The ferric Fe served as an electron acceptor from galena sulphur sites and thus ferric Fe was reduced to ferrous Fe (Heidel and Tichomirowa, 2011). Peaks of Fe could also result from the dissolution of Fe sulphate mineral grains. Fe sulphate minerals such as melanterite ($Fe^{II}SO_4.7H_2O$) are highly soluble (Nordstrom and Alpers, 1999). Fe sulphate minerals were identified in the sediment in chapter 4 (table 4.3) and have been reported at mining impacted sites (Alastuey et al., 1999; Buckby et al., 2003; Nordstrom 2009).

Pore water concentrations of Pb were not found to exceed EQS (i) at the start of a flood or (ii) at the bottom of the mesocosm, although slightly higher average concentrations were measured for DET indicating pore water results could be an under estimation. At the top of the mesocosm however dissolved Pb concentrations were found to exceed EQS for all runs by the end of the flood.

The results indicate the sediment could become a significant source of Pb contamination over flooded periods due to the on-going release of Pb into surface water in some cases the solubility of anglesite may not be sufficient to maintain concentrations of dissolved Pb at a sufficiently low level and therefore dissolved Pb could build-up to high concentrations. On flood subsidence and exfiltration

from the river bank the 'pulse' of dissolved Pb released to the river water could exceed EQS.

Infringement of EQS for dissolved Pb could represent a serious barrier to achieving 'good' ecological status as defined in the EU Water Framework Directive, although, as suggested above, pulses of dissolved Pb released to the river in response to prolonged flood events may occur intermittently. Previous sampling of the site found dissolved Pb concentrations in the river water below detection (Montsserat, 2010). Studies have however detected dissolved Pb at 'enhanced' concentrations (58 – 92 $\mu$g/L) up to 7.5 km below the Ystwyth mine area (Fuge, 1991). In other mining impacted catchments sharp increases in dissolved Pb were observed in response to flood events resulting in severe exceedance of EQS (Byrne et al., 2013). In the absence of continuous sampling methodologies, Pb pollution events that occur in response to flooding could go unnoticed. This is a concern as Pb has no biological role and is toxic at very low doses. Uncontrolled pulses of Pb contamination released into the river could have a serious deleterious effect on aquatic and riparian river habitats (Palumbo-Roe et al., 2012).

### 5.4.2 The mobility of Zn in response to wet and dry sequences

Higher concentrations of dissolved Zn were measured in pore water compared to the mesocosm runs in chapter 3, possibly reflective of the higher concentration of Zn in the labile fraction of the sediment. The patterns of mobility in response to wet and dry treatments for pore water were similar to that observed through DET analysis and the results from chapter 3.

Average concentrations of Zn at the end of a flood were found to be significantly higher at the bottom of the mesocosm compared to the top. As a result the focus of the discussion relates to patterns of Zn release into pore water at the bottom of the mesocosm. These patterns were found to vary depending on the wet and dry sequence. Moreover DET analysis revealed clear differences in dissolved Zn depth concentration profiles between treatments particularly for the 3 week wet run and 3 week dry run that provided further information regarding mechanisms of Zn release. Runs are discussed separately below and the environmental implications of the findings are discussed.

**Release of Zn in response to prolonged flood periods, 3 week wet run**

PCA analysis carried out in chapter 3 (section 3.3.7) indicated that for the longer wetter runs the mobility of Zn was linked to a fall in redox potential conditions. Furthermore sequential extraction analysis of the sediment in chapter 4 (section 4.3.4) indicated that reactive Fe hydroxides may have acted as a mineral source of dissolved Zn to pore water over flooded periods during the 3 week wet run. In the current study results from pore water analysis for the 3 week wet run found dissolved Zn concentrations correlated positively with dissolved Mn and negatively with pH. PCA analysis of pore water data revealed that dissolved Zn and Mn were related positively to a fall in redox potential conditions and a decline in dissolved oxygen particularly for the longer flooded runs at the bottom of the mesocosms.

Zn was found to be partitioned with high concentrations of easily reducible Fe and Mn hydroxides in the sediment. Redox potential conditions were not low enough for the reductive dissolution of Fe (Gotoh and Patrick, 1974; Emerson and

Cranston, 1979). However, Mn solubility is more sensitive to a fall in redox potential conditions (Lee et al., 2002; Patrick and Henderson 1981; Patrick and Delaune 1972) and visual inspection of simplified Pourbaix diagrams for Mn (Najafpour et al., 2014, Fruh, 2006) (e.g. figure 5.25) indicated reductive dissolution of Mn hydroxides would be likely to occur over the 3 week flood period at the Eh and pH measured in pore water and could potentially release high concentrations of Zn into pore water.
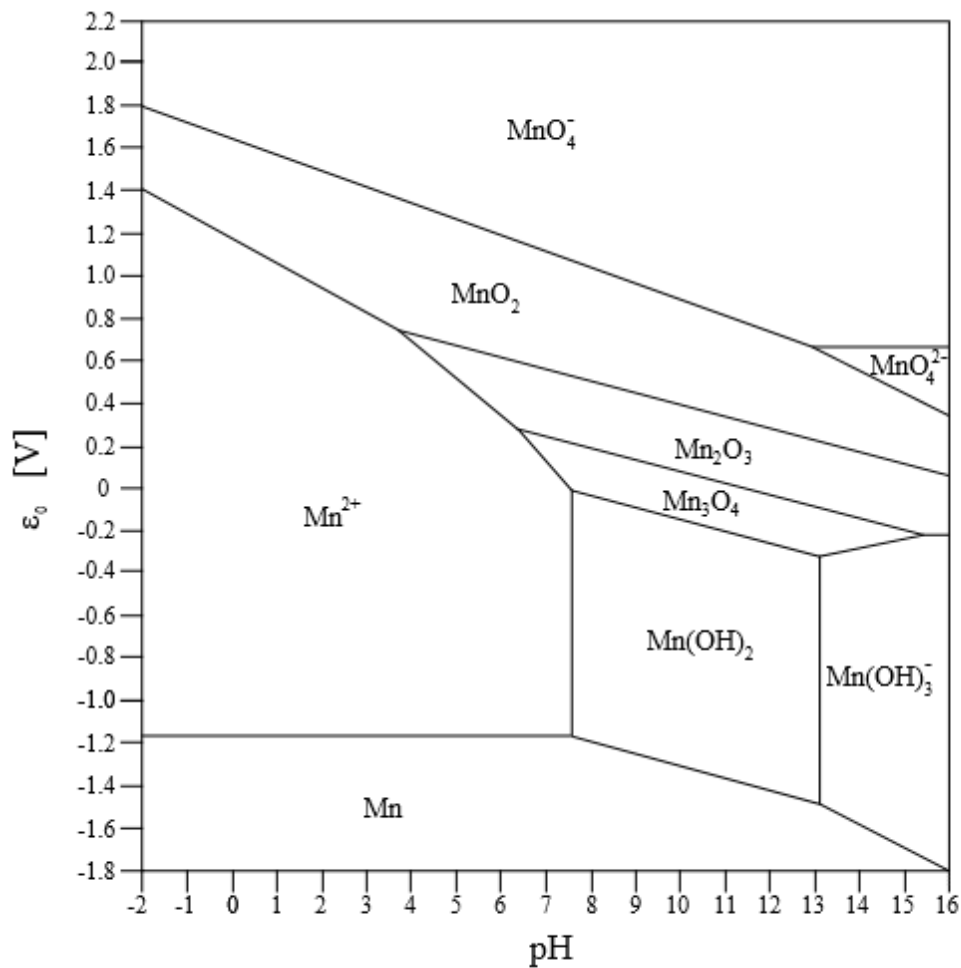


**Figure 5.25 Simplified Pourbaix diagram for Mn at 25°C, c(Mn) = 1 mol/L (Fruh, 2006).**

Over subsequent dry periods, on exposure to atmospheric conditions, Mn hydroxides could partially oxidise and sorb high concentrations of Zn. Mn hydroxide minerals such as manganite MnO(OH) have a low (< pH 4) point of zero charge (Clark et al., 2012) and the resulting negative surface charge on the surface of Mn hydroxides at the pH of the pore water would encourage sorption of cations such as Zn (Appelo and Postma, 2010).

For DET the vertical concentration profile of dissolved Mn showed an increase at the end of a flood period (week L) at depth 5 – 15 cm. This was found to correspond with a similar increase in dissolved Zn. Furthermore a significant correlation was observed between the concentration profiles of dissolved Mn and Zn for both weeks I and L. DET studies of coarse grained sediment of the River Leith recorded the occurrence of dissolved Mn at similar depths > 10 cm (Ullah et al., 2012; Byrne et al., 2014). The medium to low DOC observed in the current study seemed sufficient to promote reduction of Mn over the 3 week flood period. In the field the introduction of DOC through carbon rich downwelling surface water and lateral subsurface flows was reported as a key driver of microbial reduction in the shallow sandy sediments (Byrne et al., 2013; Byrne et al., 2014). At mining impacted sites additional sources of DOC introduced in this fashion could promote the microbial oxidation of labile organic carbon and accelerate the reduction of Mn hydroxides resulting in the release of any partitioned Zn into pore water over shorter flood periods (Patrick and Delaune, 1972). Mn hydroxides could partially control the release of Zn at the start of a flood and while conditions remain oxic, however these minerals may quickly become a source of Zn contamination during prolonged flooding.

**Release of Zn during flooding following long dry antecedent periods, 3 week dry run**

The highest concentrations of dissolved Zn were observed for the 3 week dry run compared to the other variable runs. PCA analysis in chapter 3 (section 3.3.7) revealed for the 3 week dry run the release of dissolved Zn was closely related to the release of sulphate and Ca. Moreover dissolved Zn concentrations were found to increase significantly over the treatment period for the 3 week dry run (section 3.3.6). In the current chapter dissolved Zn was found to correlate significantly with sulphate (positive) and pH (negative) for this run. The depth concentration profile measured through DET showed that at the start of the flood (week I) dissolved Zn increased with depth (> 5 cm). At the end of the flood Zn concentrations had increased towards the surface (< 10 cm). With the greatest increase in dissolved Zn concentration closest to the sediment / water interface. The fall in pH over the flood period (0.1 pH units between weeks I and J) may have served to mobilise Zn further. The mobilisation of Zn in response to small changes in pH has been encountered in other mesocosm studies. For example Shope et al. (2006) on investigating the influence of hydrous Mn-Zn oxides in an alkaline stream in Montana found a slight fall in pH (0.2 pH units) brought about through diel variation in biofilm activity strongly influenced the mobility of Zn.

On draining sediment moisture by weight was found to be 14.5% and wet oxidising conditions may have promoted the ongoing oxidation of reduced sulphide minerals in the sediment (Hudson-Edwards, 2003). The evaporation of pore water and chemical saturation of solutes during the prolonged dry period could have promoted the formation of soluble metal sulphates (Alastuey et al.,

1999; Harris et al., 2003; Buckby et al., 2003; Nordstrom, 2009). The dissolution of these salts on flooding could account for the high concentrations of dissolved Zn released into pore water at the start of a flood. Over flooded periods redox potential conditions and dissolved oxygen were found to remain high at the bottom of the mesocosm for this run. The observed increase in dissolved Zn concentrations could therefore be due to the oxidation of Zn sulphide minerals under more oxic conditions particularly towards the sediment / water interface.

Mn concentrations were very low for this run and contrary to the 3 week wet run it is unlikely the oxidation of previously reduced Mn minerals would have provided a solubility control over the release of dissolved Zn concentrations, particularly at the start of a flood. Therefore the sediment could, within hours, become a significant source of Zn contamination following prolonged dry periods due to formation of soluble sulphates (Buckby et al., 2003; Nordstrom, 2009) and the dissolution of these salts on flooding. This process has been reported to introduce high concentrations of contaminant metals and acidity into river systems (Byrne et al., 2013, Harris et al., 2003) and was discussed in chapter 3. Any fall in pH would be poorly buffered in the low alkalinity waters and could serve to promote dissolved Zn release further.

**Release of Zn during the constant flood run**

DET analysis revealed high concentrations of Zn were released between week B and J for the constant flood run, although pore water analysis found concentrations were slightly lower. High concentrations of Zn were observed throughout the vertical concentration profile by week J. High concentrations of

dissolved Mn were also observed and, as sequential extraction results showed Zn was released with labile forms of Mn hydroxide in the sediment. During the constant flood run Mn hydroxides may have provided a source of Zn contamination in addition to the oxidation of reduced sulphide minerals and dissolution of sulphate salts, as previously discussed. Long water residence times have been reported as typical of field hydrological conditions at mining impacted sites (Evans et al., 2006). Bank storage following a rise in river stage could take weeks to return to the stream and where overbank flooding occurs the return could take much longer (USGS, 2013). The results of the current study showed that although pore water concentrations of dissolved Zn rose to > 60 mg/L all Zn sulphate minerals were under saturated indicating the solubility of these minerals would have no control over dissolved Zn concentrations therefore under prolonged flood conditions increases in dissolved Zn could continue unchecked.

The 1 week wet run, by comparison resulted in lower concentrations of dissolved Zn. This was particularly evident for the DET results that showed lower average concentrations of Zn at the start and end of a flood period compared to the other variable runs. This is likely due to (i) shorter antecedent dry period that would restrict the build-up of soluble sulphate salts and (ii) shorter flooded period minimising a fall in redox potential conditions that would promote the mobilisation of Mn hydroxides and any partitioned Zn.

**Summary and environmental implications with regards to Zn contamination**

Clear differences in the patterns of Zn release were observed depending on the wet and dry treatment. However, all concentrations of dissolved Zn were found to

exceed EQS, even at the start of a flood, within 2 – 3 hours, indicating the sediments pose a significant environmental risk. The changes in dissolved Zn concentrations in response to wet and dry treatments may therefore be most critical, with regards to meeting EU WFD requirements, where Zn is present at lower concentration in the sediment. Similar patterns of release were observed for chapter 3, where Zn was present at lower concentrations and provided an indication that the mechanisms of release in response to wet and dry treatments did not alter at lower Zn concentrations.

The results show that the sediment could be a significant source of Zn contamination to the river at the Cwmystwyth site. This evident from previous field studies where high concentrations of dissolved Zn were measured in the river water (410$\pm$318 µg/L) compared to upstream sites (6.25$\pm$9.46 µg/L) (Montserrat, 2010). Furthermore, high concentrations of dissolved Zn (307 µg/L) have been recorded half a km below the Cwmystwyth mine area, with concentrations remaining high (168 µg/L) up to 7.5 km downstream (Fuge et al., 1991). Although Zn is a biologically essential trace metal, it is toxic at high doses. The results from the current study show that high concentrations of Zn could be released from the sediment to the river in response to flooding and that would pose a significant environmental risk. The harmful ecological effects of Zn at high concentration are similar to those for Pb at lower concentration. They include detrimentally effecting macroinvertebrate structure and function (Environment Agency, 2008a; Montserrat, 2010), fish mortalities (Fuge et al., 1991), phytotoxic effects that could result in river bank instability (Environment Agency, 2008b) and contamination of agricultural farmland (Dennis et al., 2003; Dennis et al., 2009; Foulds et al., 2014).

**5.5 Conclusion**

This study confirmed that DET could be used successfully in coarse grained mining impacted sediments high in Pb and Zn. Patterns of release for DET and pore water compared favourably with the results from chapter 3 indicating that the mechanisms of release in response to wet and dry treatments were the same and the method was reproducible. Anglesite solubility was identified as a key control mechanism over dissolved Pb concentrations and the additional peaks of Pb identified through DET could indicate biogeochemical processes occurring on a smaller scale were contributing to dissolved Pb concentrations. Patterns of Zn release were found to vary depending on the wet and dry treatment and the DET depth concentration profiles allowed a more detailed analysis of the key mechanisms controlling Zn mobility than could be gained through pore water analysis alone.

In a recent Environment Agency report the importance of identifying the exact sources of pollution in non-coal mine 'impacted' water bodies was listed as a key requirement for an effective management and remediation program (Environment Agency 2012a). The current study has shown the sediments at the Cwmystwyth site become a significant source of dissolved Pb and Zn contamination in response to certain wet and dry sequences. At the concentrations present in the sediment Zn contamination may be prolific particularly at the start of a flood following a long dry antecedent period or over prolonged flooded periods. For Pb transient pulses of contamination may be released into the river, potentially following longer flooded periods, and in the absence of continuous sampling methods pollution episodes could be missed and the extent of pollution unknown.

## 6. DISCUSSION

The results of a series of laboratory studies have been presented and discussed with the aim of establishing the environmental risk metal mining contaminated river bank sediments pose in response to wet and dry sequences of different duration and frequency. This chapter will discuss the key findings from the project in relation to some of the wider issues and challenges surrounding metal mine contamination and management.

### 6.1 Significance of main findings in the context of current management efforts

In a national strategy to identify, prioritise and manage pollution from abandoned non-coal mine sites in England and Wales, the Afon Ystwth was identified as a top 30 priority mining 'impacted' water body in the western Wales river basin district (Environment Agency, 2012b). The impact scores were based on (i) the severity and number of Environmental Quality Standards (EQS) failures, (ii) suspected impacts on ecology and (iii) downstream higher impacts that relate to recreational activities and commercial fisheries or ground and surface water abstractions (Environment Agency, 2012b). 'Impacted' as opposed to 'probably impacted' indicates that a direct link between abandoned non-coal mine and river water pollution has been established. However the exact location of sources of contamination is often unknown. There are 469 waterbodies categorised as 'impacted' and 'probably impacted' by non-coal mine water pollution in England and Wales. Identifying the exact sources of contamination and understanding pollution dynamics in a catchment are listed as key priorities for effective management and remediation efforts (Environment Agency, 2012a).

237

This research has determined that the river bank sediments at the Cwmystwyth mine site become a significant source of pollution in response to wet and dry sequences. EQS exceedances were observed in most cases for all scenarios. This shows that the river would likely fail EU Water Framework Directive requirements of achieving 'good' chemical and ecological status due to river bank sediments sources alone - without taking into account any other pollutant sources e.g. point sources.

**6.2 Importance of understanding the properties of the sediment**

Sediment analysis carried out in chapters 4 and 5 indicated that up to 50% Zn and 90% Pb were partitioned with labile mineral forms in the sediment, primarily Fe, Mn hydroxide and sulphur minerals sensitive to redox potential changes and drying. The geochemical partitioning of Pb and Zn was found to influence the temporal and spatial patterns of contaminant trace metal release depending on the wet and dry sequence. Indications were that more reactive mineral forms built up in the sediment in response to certain wet and dry sequences. Moreover other properties of the sediment e.g. grain size, organic content and carbonate content all influenced the mechanisms of trace metal mobility. There are no mandatory standards for sediment and, although there are guideline values for total metals, the partitioning of trace metal contaminants with different fractions of the sediment is not considered in management plans (Environment Agency, 2008b). This study has shown there is a clear link between the properties of the sediment, Pb and Zn mineral forms and trace metal bioavailability. Characterisation of the sediment is therefore essential at contaminated sites to understand trace metal contaminant dynamics in response to wet and dry sequences.

Considering the findings from the current study, in order to understand the environmental risk of trace metal contaminants, it would be highly beneficial to use a tool for sediments similar to the contaminated land exposure assessment (CLEA) model. The Environment Agency uses this model to develop soil guideline values (SGV) (Environment Agency, 2009). Used in combination with human health criteria values the CLEA model aims to assess the "tolerable or minimal risk to health from chronic exposure" to contaminants (Environment Agency, 2009). As with TEL and PEL, SGV's are guideline values that trigger further investigation. However the CLEA model takes into account the chemical properties of the contaminant and the soil type to enable a more accurate prediction of the potential bioavailability of contaminants (Environment Agency, 2009). Site specific data can replace generic data in the model including estimated exposure time frames and the sensitivity of the receptor (Environment Agency, 2009). In this way a site specific risk assessment can be made.

## 6.3 The link between geochemical processes, mineral form and trace metal bioavailability

This project identified key geochemical processes that control trace metal mobility in response to wet and dry sequences of different duration and frequency. Geochemical processes were found to be different depending on the trace metal and sediment properties including mineral form. The results from chapters 3, 4 and 5 were used to create a modified version of the hazard-pathway-receptor framework. The aim was to summarise the key geochemical processes and the environmental conditions that could promote bioavailability in response to wet and dry sequences of different duration and frequency. The pathway was sub-divided

to include the key flood stage, the key geochemical 'change', the subsequent metal speciation and conditions that would promote bioavailability of the trace metal (table 6.1).

The benefit of this table is that it includes spatial and temporal information regarding the risk the sediments pose in response to changes in wet and dry sequences. Used in combination with the sediment properties it identifies the key mechanisms controlling pollutant sources in response to wetting and drying. This provides a first step towards a more targeted and less labour intensive approach to management and remediation of pollutant loads. These findings are likely to be relevant on a much wider scale as Fe, Mn hydroxide and sulphur minerals are prolific at mining polluted sites. Moreover much of mid and north Wales rises on similar base poor geology to the study area (Natural Resources Wales, 2004). Therefore it is likely that these processes are occurring in river bank sediments at many mining impacted sites.

**Table 6.1 Modified Hazard Pollutant Pathway to show potential for Pb and Zn release into rivers and streams in response to wet and dry runs**

| Hazard | Pathway | | | Receptor | |
|---|---|---|---|---|---|
| Trace metal 'dissolved' | Key flood stage | Key geochemical process and metal speciation | Env. conditions promoting bioavailability | Location | Receptor |
| Pb | Over flood Period | Galena oxidation | mildly oxic | Surface water | rivers / streams |
| Pb | >3 days | Galena oxidation >> anglesite (SI > 0 precipitation / SI < 0 dissolution) | mildly oxic / Anglesite SI < 0 | Surface water | rivers / streams |
| Zn | 7 - 21 days dry | Sphalerite oxidation >> Zn Sulphate salt saturation and precipitation | Hydrologically unsaturated / oxic / moist >> dry | 0 - 20 cm | |
| Zn | 2 -3 hours flooding | Zn sulphate salt dissolution | Flood wetting following a long dry (7-21 days) antecedent period | 0 - 20 cm | Pore waters/rivers / streams |
| Zn | Flooding 3 - 7 days | Sphalerite oxidation | Flood following a long dry (7-21 days) antecedent period | > 10 cm | Pore waters/rivers / streams |
| Zn | Dry period | Sorption of Zn to Mn hydroxides | On draining - follows long (2-3 week) flood | < 10 cm | |
| Zn | End of flood > 14 - 21 days | Mn hydroxide dissolution and release of sorbed Zn | Over long (2–3 weeks) flood period, low oxygen, moderately low redox potential, moderate DOC | < 10 cm | Pore waters/rivers / streams |

**Oxidation of galena and precipitation of anglesite as a key control mechanism for Pb releases into surface water**

Results indicated there was an on-going release of Pb into surface water over long flooded periods. Redox potential measurements indicated conditions were more oxic in surface water at the top of the mesocosms compared to the bottom and Pb concentrations released into surface water was consistently higher than at the bottom. An inundation study on Rookhope Burn sediment samples by Wragg and Palumbo-Roe (2011) resulted in a similar pattern of Pb release into surface water. These authors suggested the releases were due to the high concentration of primary mineral galena in the sediment. Results from SEM/EDS in the current study provided evidence of this primary mineral in the sediment. In the case of the Rookhope Burn inundation study the mineral cerussite was found to be saturated in surface water and the authors believed that Pb concentrations were controlled by the solubility of this mineral (Wragg and Palumbo-Roe, 2011). However, in the current study alkalinity was low in pore and surface water and carbonate minerals were below detection in the sediment. Anglesite is a commonly reported secondary mineral product formed from the oxidation of galena (Heidel and Tichomirowa, 2011; Hayes et al., 2012; Luo et al., 2014). Column leach kinetic tests over a 30 week period found that, following the oxidation of galena, porous anglesite formed rapidly (Parbhakar-Fox et al., 2013). Furthermore macroscopic batch-type experiments investigating the interaction of gypsum with Pb in aqueous solutions observed the rapid dissolution of gypsum and simultaneous formation of anglesite on the gypsum surface and in solution (Astillerox et al., 2010). In the current study geochemical calculations indicated that anglesite was close to

saturation. Results from piper diagrams (chapter 5) indicated the water was Ca-sulphate type, typical of mine drainage. Sulphate concentrations were high and geochemical calculations indicated gypsum was undersaturated (indicating a tendency for mineral dissolution). It is likely therefore that the high concentration of sulphate and possibly the presence of the mineral gypsum encouraged the rapid precipitation of anglesite. Where saturation was reached with respect to anglesite it would have provided a control on Pb concentrations, however where conditions became undersaturated the dissolution of anglesite in addition to the oxidation of galena could provide a source of Pb to surface water; for example Parbhakar-Fox et al. (2013) observed weathering and dissolution of anglesite in later weeks. Results from the current study indicate that where the sediment is contaminated with primary mineral galena, under low alkalinity conditions, the prolonged inundation of sediment is likely to result in releases of Pb into surface water to levels above current EQS limits. Where anglesite is undersaturated the dissolution of this mineral could further contribute to Pb concentrations.

This is a concern with regards to climate predictions where the amount and intensity of rainfall is expected to increase, particularly in winter. UK climate projections indicate peak river flows in Wales will increase by 13% by 2020, 20.8% by 2050, and 27.6% by 2080– for medium (P50) scenarios. River flooding would therefore be expected to increase in frequency (DEFRA 2012b) and duration. That could result in prolonged flooding, particularly during the winter months, and subsequently the release of high concentrations of dissolved Pb into surface water. The current study found the highest concentrations of dissolved Pb in surface water by the end of the 3 week wet run (chapters 3 and 5). However,

dissolved Pb exceeded EQS in surface water by the end of a flood for all wet and dry scenarios. The results indicated that future scenarios could include larger or more frequent transient pulses of dissolved Pb released to impacted river systems. These short lived pollution episodes are likely to be difficult to quantify, manage and remediate. Even so the potential implications of future climate change need to be taken into account during management and remediation efforts.

**Precipitation and reductive dissolution of Mn hydroxides as a key control mechanism for Zn releases into surface water**

Results from the current study indicated a key mechanism controlling patterns of Zn release into pore water was (i) the reductive dissolution of Mn hydroxides and the release of partitioned Zn during long wet periods, and (i) the precipitation of Mn hydroxides and sorption of Zn on draining (and atmospheric exposure of sediment). Field studies have reported the presence of hydrous Mn Zn oxide crusts along mining impacted streams that formed following the oxidation of reduced Mn(II) (Shope et al., 2006). Laboratory experiments with streambed sediments have shown that in the hyporheic zone (a dynamic redox environment) ongoing Mn oxide formation enhanced dissolved Zn uptake and this uptake increased with Mn oxide concentration (Fuller and Harvey, 2000). Furthermore extended X-ray absorption fine structure investigation of sediments in the hyporheic zone, Pinal Creek, Arizona showed that contaminant Zn co-varied with Mn in sediment grain coatings, supporting the mechanism of Zn attenuation controlled by sorption to Mn oxides (Fuller and Bargar 2014). Studies on mining contaminated soil, Ronneburg, Germany found, at low pH (pH 4.7 – 5.1),  the

formation of Mn oxide layers efficiently immobilised contaminant trace metals including Zn (Mayanna et al., 2015). As noted in chapter 5, Mn oxides have a low point of zero charge (Clark et al., 2012) and the negative surface charge at the surface of Mn hydroxides at the pH of the pore water in the current study would likely encourage sorption of positive cations such as Zn (Appelo and Postma, 2010). It is clear therefore that Mn (hydr)oxides have the capacity to sorb (and attenuate) high concentrations of dissolved Zn. However, as discussed, Mn hydroxides are highly sensitive to a fall in redox potential conditions and therefore where previously exposed sediment is inundated the fall in redox potential conditions could encourage the reductive dissolution of Mn hydroxides releasing any partitioned Zn. Studies have reported release of contaminant trace metals as a result of the reductive dissolution of Fe and Mn hydroxides in response to a fall in redox potential conditions (Lesven et al., 2010; Charlatchka and Cambier, 2000; Davis and Kent, 1990). In chapter 5, DET analysis, showed patterns of Mn release were coupled to the release of Zn during prolonged flooding. Similarly, DET field studies on coarse grained sediments of the river Leith have reported Mn mobilisation at a similar depth (~ 10 cm) to that observed in chapter 5. This was believed to have been due to a fall in redox potential conditions brought about by carbon rich downwelling surface water (Byrne et al., 2013; Byrne et al., 2014).

For the longer wetter runs, the above mechanism of dissolved Zn attenuation and release was believed to be a key control. However, for runs with longer dry periods, Mn was only poorly mobilised. Therefore it was unlikely reductive dissolution of Mn hydroxides controlled the release of dissolved Zn for these runs.

**Precipitation of Zn sulphate salts and dissolution and release of Zn and sulphate on wetting**

The highest releases of Zn were observed for the 3 week dry run. Results from chapters 3 and 5 found that high concentrations of dissolved Zn were released into pore water within 2 – 3 hours of flooding, with the highest concentrations of Zn released at the start of a flood following a long dry antecedent period. The build-up of soluble metal sulphate salts on the surface of mining contaminated soils and sediments over long dry periods is well documented (Nordstrom, 2009; Hudson-Edwards et al., 2005; Buckby et al., 2003; Hudson-Edwards et al., 1999b; Alastuey et al., 1999; Alpers et al., 1993) and has been discussed in previous chapters. Studies have described a 'spike' in trace metal concentrations on the rising limb of river discharge during storm events due to the dissolution and 'flushing' of these salts back into river channels following long dry antecedent periods (Nordstrom, 2011). Byrne et al. (2013) report a similar high flux of trace metals during storm events linked to extended dry antecedent periods. These authors noted the 'immediacy' of initial contaminant trace metal peaks (and lack of peaks thereafter), indicated the dissolution of soluble metal sulphate salts on the surface of mine spoil was the principle source of contamination. It is likely, particularly considering the speed dissolved Zn was released into pore water,  that soluble metal sulphate salts built up in the mesocosm over long dry periods and were quickly dissolved on wetting, releasing a 'spike' of Zn into pore water.

This raises serious concerns in light of UK climate projections (UKCP09) that indicate there will be a shift towards aridity by 2020. Summer river flows are expected to decline and Q95 (flow that is exceeded 95% of the time) may reduce

by 26% by 2050 and 35% by 2080 in western Wales - using the medium emissions (P50) scenarios (DEFRA 2012a). These changes would be expected to increase the length of antecedent dry period along river banks and, as a result, acute releases of dissolved Zn to impacted river systems could increase in magnitude or/and become more frequent.

## 6.4 Future management – scoping studies

As part of the recommended approach to management of environmental impacts of abandoned non-coal mines, within the investigative stage are catchment wide scoping studies (Environment Agency 2012c). The main objective is to understand the catchment scale trace metal fluxes. A three stage approach is recommended and includes:

- Stage 1. Reconnaissance surveys to identify possible diffuse sources and agreeing monitoring locations.

- Stage 2. Preliminary sampling under base flow conditions, calculating and revising metal flux estimates and identifying main sources of contamination.

- Stage 3. A full monitoring investigation at finalised monitoring stations under a range of hydrological conditions. Revising the allocation of monitoring stations where sudden increases in metal loads occur.

(Environment Agency, 2012c).

The findings from the current study indicate that sediment associated trace metal contamination may be transient, responding to changes in wet and dry sequences and therefore sudden increases in metal loads are to be expected. In order to assess pollutant sources and designate monitoring stations at appropriate

locations as accurately as possible first time, identifying locations along the river bank where sediments will become a pollutant source in response to wet and dry events at an early stage would be ideal. Characterising the sediment to understand where high risk areas may be located and the use of DET to identify changes in trace metal mobility could be appropriate tools to use along river reaches during the early scoping stages e.g. reconnaissance surveys.

## 6.5 Use of DET in the field studies

DET was successfully used in the current study (chapter 5) to understand the temporal and spatial changes in contaminant trace metal mobility in response to wet and dry sequences of different duration and frequency. Patterns in the release of trace metals at the start and end of a flood period and the co-distribution of dissolved metals, used in combination with geochemical, statistical and sediment analysis enabled an assessment to be made regarding the mechanisms of release of trace metal contaminants in response to flood events. This information allowed an assessment of the environmental risk the sediment posed in response to different wet and dry sequences.

DET has been used during field studies to measure the mobility of Mn and Fe in coarse grained river sediments (Ullah et al., 2012; Ullah et al., 2013; Byrne et al., 2014). However there are no known DET field studies that have investigated the release of trace metal contaminants Pb and Zn in mining polluted river reaches under varying hydrological conditions. In light of the current study this methodology would prove useful during early reconnaissance surveys to understand how the mechanisms of trace metal release may change in response

to different wet and dry sequences and allow for a prediction to be made regarding temporal and spatial changes in the sources of pollution.

## 6.6 Remediation issues and challenges

The attenuation and removal of Zn (a common pollutant at metal mine sites) can be problematic due to its high solubility under oxic conditions (Environment Agency, 2012c). The wetland approach used to successfully treat coal mine pollution high in Fe would require far larger areas of land for sufficient Zn removal so this is unlikely to be a feasible option (Environment Agency, 2012c). Pilot scale passive compost bioreactor treatment systems have been set up in the UK and have successfully remediated Zn in water emanating from point sources at Nenthead, Cumbria and Cwm Rheidol, Wales (Environment Agency, 2014). However, in line with previous research work (Gozzard et al., 2011; Byrne et al., 2013; Mayes et al., 2013,), the current project has indicated treating point sources alone is unlikely to reduce the concentration of trace metal pollutants in river water to within EQS standards and diffuse sources of pollution must be taken into account.

This study has shown treating diffuse sources of pollution arising from contaminated sediments will be challenging because

(i)     the exact sources of contamination are likely to change depending on hydrological conditions

(ii)    metal load quantification (necessary knowledge for treatment) would be difficult because the magnitude of releases may alter in response to changing hydrological conditions

(iii)      the mechanisms of trace metal mobility are likely to depend on the properties of the sediment however characterisation of the sediment is not currently included in management studies.

Sediment analysis carried out in chapter 5 indicated that runoff from waste piles and tailings heaps had contributed to the secondary pollution of river bank sediments at the Cwmystwyth mine site. Dealing with pollution arising from the waste could therefore prove beneficial. One possibility would be removal of the waste, capping and re-vegetation. This was successfully carried out at Durham as part of the Turning the Tide partnership. From 1997 – 2002 12 km of coastline was restored by capping colliery waste at a cost of £10 million. The land has now been designated an SSSI (Durham County Council, 2013). However, the high treatment costs and technical challenges likely to be encountered at a remote mountainous location such as Cwmystwyth could prove prohibitive (Environment Agency, 2012c). Furthermore the Cwmystwyth mining site has been designated an SSSI in part because of the mineralization exposed in rock outcrops and spoil tips (Natural Resources Wales, 2000). Waste removal, capping and any form of modification would therefore go against stakeholder interests. Similar issues are likely to be encountered at other metal mining sites throughout the UK as many are designated SSSI and located in remote mountainous areas.

The use of permeable reactive barriers (PRBs) could be another option for dealing with the transient nature of diffuse sources of pollution. However it would only prove effective if the contaminated water passed through the barrier and the reactive media used in the barrier was effective in removing the contamination (Environment Agency, 2012c). This would not be possible where there was little

understanding of how the sources and magnitude of pollution altered in response to changes in wet and dry sequences. The challenge therefore is to understand the key mechanisms of release of trace metal contaminants under different hydrological conditions. Characterisation of the sediment including determination of trace metal partitioning and utilisation of DET to gain an understanding of the co-incidental releases of Pb and Zn with Mn and Fe and potentially other solutes under different hydrological conditions is therefore recommended. This would provide information on the sources and magnitude of pollution to allow informed decisions to be made regarding remediation.

## 6.7 Overall Conclusions

The current project has gone some way to identifying the mechanisms controlling trace metal mobility in metal contaminated sediment under variable wet and dry sequences. It has established that mechanisms are different depending on the trace metal, mineral form and sediment composition. The magnitude of contaminant release and temporal and spatial factors are influenced by these mechanisms.

The next step is to locate the precise sources of pollution in the field. In light of climate change predictions it is likely that trace metal pollution events will increase in magnitude and frequency and sources of metal contamination are likely to change. Understanding how future climate change may influence pollution events is necessary for effective remediation. This can only be achieved if the mechanisms of release in response to changes in wet and dry sequence are understood. This study has shown that sediment characterisation and use of DET can provide this information. Moreover this information could be used to develop a site specific tool, similar to CLEA, to assess the environmental risk of metal contaminated sediment.

## 7. APPENDIX

**Appendix 2.2.11 Miller Indices**

Miller indices (h, k, l) are used to label the crystal planes. Each letter represents an axis of intersect (figure 2.11). The number of each letter represents the spacing between crystal planes, for example where the crystal planes intersects axis 'x' with a planar spacing of 1 the Miller indices would be (1, 0, 0). Where the planes run diagonally and intersect two axes such as x and y the Miller indices would be (1, 1, 0). Where crystal planes also intersect axes z this would be written as (1, 1, 1).

Once the spacing between crystal planes 'd' is known the following equation (based on Pythagoras theorem) can be used with the Miller Indices to calculate the lattice constant for a mineral :

$$d_{(h,k,l)} = a \, / \, Sqrt \, (h^2 + k^2 + l^2) \quad \text{or} \quad a = d_{(h,k,l)} \; x \; Sqrt \, (h^2 + k^2 + l^2)$$

Where : a = lattice constant
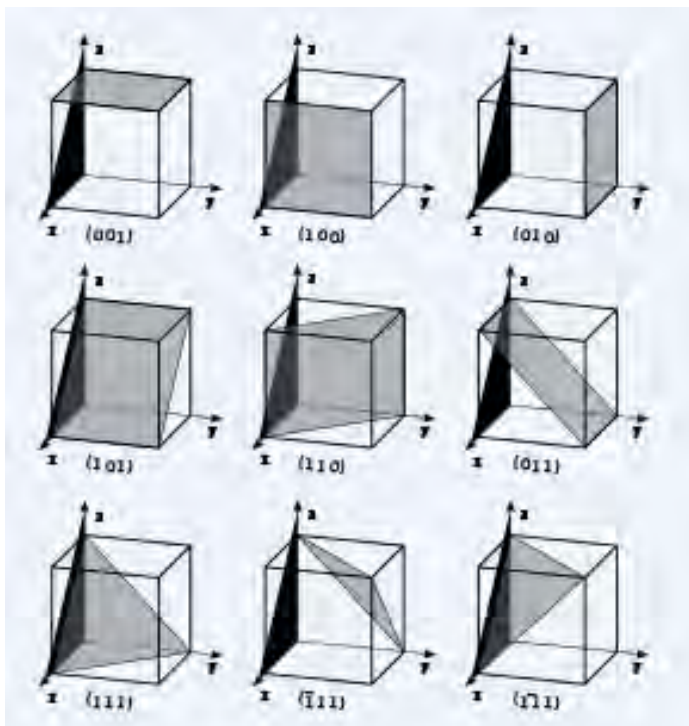


**Crystallographic planes (in grey) intersecting axis x, y, and z and Miller indices (h, k, l) for a cubic structure (Miller Indices Cubes.svg 2010)**

## Appendix 3.3a Summary of results from Wilcoxon Rank Sum test to determine whether there was a significant increase in lead and zinc flux from sediment to pore water over flooded periods

| Element | Run | Loc | Median strt | Std Dev | Median end | Std Dev | Test statistic Calc W | Calc W2 | Calc Z | α | n = | If Z < -1.96 Reject Null H. Y/N |
|---|---|---|---|---|---|---|---|---|---|---|---|---|
| Pb | 1wwet | B | 10.92 | 2.34 | 13.13 | 3.86 | 266 | 400 | -2.120 | 0.034 | 18 | Y |
| Pb | 1wwet | T | 5.48 | 2.42 | 17.61 | 3.70 | 172.00 | 499.00 | -5.094 | 0.000 | 18 | Y |
| Zn | 1wwet | B | 13.68 | 3.11 | 22.9 | 4.58 | 215.5 | 450.5 | -3.718 | 0.000 | 18 | Y |
| Zn | 1wwet | T | 1.17 | 1.37 | 9.60 | 4.91 | 173.00 | 493.00 | -5.063 | 0.000 | 18 | Y |
| Pb | 2wdry | B | 13.99 | 4.33 | 13.85 | 0.77 | 150 | 150 | 0.000 | 1 | 12 | N |
| Pb | 2wdry | T | 8.78 | 3.80 | 15.70 | 1.38 | 88.00 | 212.00 | -3.580 | 0.000 | 12 | Y |
| Zn | 2wdry | B | 15.1 | 3.68 | 22.69 | 6.4 | 107 | 193 | -2.483 | 0.013 | 12 | Y |
| Zn | 2wdry | T | 1.68 | 1.47 | 8.52 | 2.76 | 78.00 | 222.00 | -4.161 | 0.000 | 12 | Y |
| Pb | 2wwet | B | 11.62 | 4.74 | 11.49 | 3.86 | 149 | 151 | -0.058 | 0.954 | 12 | N |
| Pb | 2wwet | T | 9.23 | 3.05 | 18.01 | 2.72 | 79.00 | 221.00 | -4.099 | 0.000 | 12 | Y |
| Zn | 2wwet | B | 15.66 | 2.2 | 22.13 | 3.02 | 86 | 214 | -3.695 | 0.000 | 12 | Y |
| Zn | 2wwet | T | 2.37 | 1.69 | 14.53 | 4.81 | 78.00 | 222.00 | -4.158 | 0.000 | 12 | Y |
| Pb | 3wdry | B | 10.78 | 3.71 | 12.21 | 1.72 | 75 | 96 | -0.927 | 0.354 | 9 | N |
| Pb | 3wdry | T | 8.55 | 2.93 | 14.33 | 1.76 | 50.00 | 121.00 | -3.135 | 0.002 | 9 | Y |
| Zn | 3wdry | B | 17.8 | 7.08 | 27.82 | 8.82 | 71 | 100 | -1.280 | 0.2 | 9 | N |
| Zn | 3wdry | T | 3.53 | 2.60 | 10.39 | 4.32 | 49.00 | 122.00 | -3.223 | 0.001 | 9 | Y |
| Pb | 3wwet | B | 9.71 | 1.21 | 10.48 | 6.48 | 61.1 | 110 | -2.163 | 0.031 | 9 | Y |
| Pb | 3wwet | T | 8.66 | 2.29 | 20.14 | 4.80 | 45.00 | 126.00 | -3.579 | 0.000 | 9 | Y |
| Zn | 3wwet | B | 12.07 | 2.85 | 19.03 | 2.4 | 45 | 126 | -3.576 | 0.000 | 9 | Y |
| Zn | 3wwet | T | 2.30 | 0.88 | 17.03 | 2.81 | 45.00 | 126.00 | -3.576 | 0.000 | 9 | Y |
| Pb | F/C | B | 7.87 | 6.15 | 9.86 | 4.43 | 306.5 | 359.5 | -0.838 | 0.402 | 18 | N |
| Zn | F/C | B | 6.85 | 2.08 | 8.2 | 2.54 | 280 | 386 | -1.677 | 0.094 | 18 | N |
| Pb | Flood | B | 9.33 | 6.82 | 8.33 | 5.75 | 323 | | -0.316 | 0.752 | 18 | N |
| Pb | Flood | T | 14.98 | 6.04 | 15.40 | 3.91 | 288.00 | 378.00 | -1.424 | 0.155 | 18 | N |
| Zn | Flood | B | 17.24 | 2.01 | 16.79 | 2.15 | 321.5 | 344 | -0.364 | 0.716 | 18 | N |
| Zn | Flood | T | 8.84 | 4.17 | 11.35 | 2.68 | 311.00 | 355.00 | -0.696 | 0.486 | 18 | N |

## Appendix 3.3b. Spearman correlation coefficients and significance values for physic-chemical values and dissolved metals (mg/L)

One Week Wet (Top)

| Spearman's rho | | ph | cond | Fe | Mn | Pb | Zn | Ca | nitrate | Cl | Sulphate |
|---|---|---|---|---|---|---|---|---|---|---|---|
| pH | Correlation Coeffic. | 1.000 | -.562** | . | -.401* | -.610** | -.656** | -.472** | -.022 | -.043 | -.601** |
| | Sig. (2-tailed) | . | .000 | . | .015 | .000 | .000 | .004 | .897 | .803 | .000 |
| Cond | Correlation Coeffic. | -.562** | 1.000 | . | .899** | .778** | .929** | .922** | .650** | .377* | .904** |
| | Sig. (2-tailed) | .000 | . | . | .000 | .000 | .000 | .000 | .000 | .023 | .000 |
| Fe | Correlation Coeffic. | . | . | . | . | . | . | . | . | . | . |
| | Sig. (2-tailed) | . | . | . | . | . | . | . | . | . | . |
| Mn | Correlation Coeffic. | -.401* | .899** | . | 1.000 | .734** | .838** | .891** | .651** | .544** | .747** |
| | Sig. (2-tailed) | .015 | .000 | . | . | .000 | .000 | .000 | .000 | .001 | .000 |
| Pb | Correlation Coeffic. | -.610** | .778** | . | .734** | 1.000 | .767** | .792** | .495** | .356* | .725** |
| | Sig. (2-tailed) | .000 | .000 | . | .000 | . | .000 | .000 | .002 | .033 | .000 |
| Zn | Correlation Coeffic. | -.656** | .929** | . | .838** | .767** | 1.000 | .823** | .476** | .371* | .886** |
| | Sig. (2-tailed) | .000 | .000 | . | .000 | .000 | . | .000 | .003 | .026 | .000 |
| Ca | Correlation Coeffic. | -.472** | .922** | . | .891** | .792** | .823** | 1.000 | .695** | .344* | .795** |
| | Sig. (2-tailed) | .004 | .000 | . | .000 | .000 | .000 | . | .000 | .040 | .000 |
| nitrate | Correlation Coeffic. | -.022 | .650** | . | .651** | .495** | .476** | .695** | 1.000 | .407* | .425** |
| | Sig. (2-tailed) | .897 | .000 | . | .000 | .002 | .003 | .000 | . | .014 | .010 |
| Cl | Correlation Coeffic. | -.043 | .377* | . | .544** | .356* | .371* | .344* | .407* | 1.000 | .247 |
| | Sig. (2-tailed) | .803 | .023 | . | .001 | .033 | .026 | .040 | .014 | . | .146 |
| Sulphate | Correlation Coeffic. | -.601** | .904** | . | .747** | .725** | .886** | .795** | .425** | .247 | 1.000 |
| | Sig. (2-tailed) | .000 | .000 | . | .000 | .000 | .000 | .000 | .010 | .146 | . |

N = 36

** Correlation is significant at the 0.01 (2-tailed).

*Correlation is significant at the 0.05 level (2-tailed).

## Appendix 3.3b continued: Two Weeks Dry (Top)

| Spearman's rho | | ph | cond | Fe | Mn | Pb | Zn | Ca | nitrate | Cl | Sulphate |
|---|---|---|---|---|---|---|---|---|---|---|---|
| pH | Correlation Coeffic. | 1.000 | -.064 | . | -.011 | -.145 | -.247 | .069 | .098 | -.144 | -.332 |
| | Sig. (2-tailed) | . | .765 | . | .960 | .499 | .245 | .749 | .650 | .502 | .113 |
| Cond | Correlation Coeffic. | -.064 | 1.000 | . | .858** | .624** | .908** | .856** | .782** | .296 | .924** |
| | Sig. (2-tailed) | .765 | . | . | .000 | .001 | .000 | .000 | .000 | .160 | .000 |
| Fe | Correlation Coeffic. | . | . | . | . | . | . | . | . | . | . |
| | Sig. (2-tailed) | . | . | . | . | . | . | . | . | . | . |
| Mn | Correlation Coeffic. | -.011 | .858** | . | 1.000 | .575** | .763** | .692** | .718** | .437* | .784** |
| | Sig. (2-tailed) | .960 | .000 | . | . | .003 | .000 | .000 | .000 | .033 | .000 |
| Pb | Correlation Coeffic. | -.145 | .624** | . | .575** | 1.000 | .674** | .503* | .339 | -.010 | .630** |
| | Sig. (2-tailed) | .499 | .001 | . | .003 | . | .000 | .012 | .105 | .965 | .001 |
| Zn | Correlation Coeffic. | -.247 | .908** | . | .763** | .674** | 1.000 | .715** | .644** | .276 | .939** |
| | Sig. (2-tailed) | .245 | .000 | . | .000 | .000 | . | .000 | .001 | .192 | .000 |
| Ca | Correlation Coeffic. | .069 | .856** | . | .692** | .503* | .715** | 1.000 | .755** | .057 | .775** |
| | Sig. (2-tailed) | .749 | .000 | . | .000 | .012 | .000 | . | .000 | .790 | .000 |
| nitrate | Correlation Coeffic. | .098 | .782** | . | .718** | .339 | .644** | .755** | 1.000 | .243 | .617** |
| | Sig. (2-tailed) | .650 | .000 | . | .000 | .105 | .001 | .000 | . | .253 | .001 |
| Cl | Correlation Coeffic. | -.144 | .296 | . | .437* | -.010 | .276 | .057 | .243 | 1.000 | .348 |
| | Sig. (2-tailed) | .502 | .160 | . | .033 | .965 | .192 | .790 | .253 | . | .096 |
| Sulphate | Correlation Coeffic. | -.332 | .924** | . | .784** | .630** | .939** | .775** | .617** | .348 | 1.000 |
| | Sig. (2-tailed) | .113 | .000 | . | .000 | .001 | .000 | .000 | .001 | .096 | . |

N = 24

** Correlation is significant at the 0.01 (2-tailed).

*Correlation is significant at the 0.05 level (2-tailed).

## Appendix 3.3b continued: 3 Weeks Dry (Top)

| Spearman's rho | | pH | cond | Fe | Mn | Pb | Zn | Ca | Nitrate | Cl | sulphate |
|---|---|---|---|---|---|---|---|---|---|---|---|
| pH | Correlation Coeffic. | 1.000 | -.373 | . | -.159 | .089 | -.589* | .067 | .027 | -.093 | -.503* |
| | Sig. (2-tailed) | . | .128 | . | .529 | .726 | .010 | .791 | .916 | .714 | .033 |
| Cond | Correlation Coeffic. | -.373 | 1.000 | . | .942** | .630** | .921** | .607** | .601** | .870** | .913** |
| | Sig. (2-tailed) | .128 | . | . | .000 | .005 | .000 | .008 | .008 | .000 | .000 |
| Fe | Correlation Coeffic. | . | . | . | . | . | . | . | . | . | . |
| | Sig. (2-tailed) | . | . | . | . | . | . | . | . | . | . |
| Mn | Correlation Coeffic. | -.159 | .942** | . | 1.000 | .625** | .814** | .631** | .662** | .885** | .823** |
| | Sig. (2-tailed) | .529 | .000 | . | . | .006 | .000 | .005 | .003 | .000 | .000 |
| Pb | Correlation Coeffic. | .089 | .630** | . | .625** | 1.000 | .474* | .866** | .560* | .738** | .639** |
| | Sig. (2-tailed) | .726 | .005 | . | .006 | . | .047 | .000 | .016 | .000 | .004 |
| Zn | Correlation Coeffic. | -.589* | .921** | . | .814** | .474* | 1.000 | .399 | .480* | .695** | .901** |
| | Sig. (2-tailed) | .010 | .000 | . | .000 | .047 | . | .101 | .044 | .001 | .000 |
| Ca | Correlation Coeffic. | .067 | .607** | . | .631** | .866** | .399 | 1.000 | .492* | .792** | .610** |
| | Sig. (2-tailed) | .791 | .008 | . | .005 | .000 | .101 | . | .038 | .000 | .007 |
| Nitrate | Correlation Coeffic. | .027 | .601** | . | .662** | .560* | .480* | .492* | 1.000 | .748** | .373 |
| | Sig. (2-tailed) | .916 | .008 | . | .003 | .016 | .044 | .038 | . | .000 | .128 |
| Cl | Correlation Coeffic. | -.093 | .870** | . | .885** | .738** | .695** | .792** | .748** | 1.000 | .730** |
| | Sig. (2-tailed) | .714 | .000 | . | .000 | .000 | .001 | .000 | .000 | . | .001 |
| Sulphate | Correlation Coeffic. | -.503* | .913** | . | .823** | .639** | .901** | .610** | .373 | .730** | 1.000 |
| | Sig. (2-tailed) | .033 | .000 | . | .000 | .004 | .000 | .007 | .128 | .001 | . |

N = 18

** Correlation is significant at the 0.01 (2-tailed).

*Correlation is significant at the 0.05 level (2-tailed).

## Appendix 3.3b continued: 2 Weeks Wet (Top)

| Spearman's rho | | ph | cond | Fe | Mn | Pb | Zn | Ca | nitrate | Cl | Sulphate |
|---|---|---|---|---|---|---|---|---|---|---|---|
| pH | Correlation Coeffic. | 1.000 | -.661** | . | -.537** | -.535** | -.719** | -.472* | -.077 | -.385 | -.786** |
| | Sig. (2-tailed) | . | .000 | . | .007 | .007 | .000 | .020 | .721 | .063 | .000 |
| Cond | Correlation Coeffic. | -.661** | 1 | . | .497* | .792** | .966** | .849** | .644** | .532** | .925** |
| | Sig. (2-tailed) | .000 | . | . | 0.013 | 0.000 | 0.000 | 0.000 | 0.001 | 0.008 | 0.000 |
| Fe | Correlation Coeffic. | . | . | . | . | . | . | . | . | . | . |
| | Sig. (2-tailed) | . | . | . | . | . | . | . | . | . | . |
| Mn | Correlation Coeffic. | -.537** | .497* | . | 1 | .448* | .602** | 0.333 | 0.376 | .841** | .529** |
| | Sig. (2-tailed) | .007 | 0.013 | . | . | 0.028 | 0.002 | 0.112 | 0.070 | 0.000 | 0.008 |
| Pb | Correlation Coeffic. | -.535** | .792** | . | .448* | 1 | .691** | .765** | .486* | 0.341 | .692** |
| | Sig. (2-tailed) | .007 | 0.000 | . | 0.028 | . | 0.000 | 0.000 | 0.016 | 0.103 | 0.000 |
| Zn | Correlation Coeffic. | -.719** | .966** | . | .602** | .691** | 1 | .813** | .581** | .630** | .961** |
| | Sig. (2-tailed) | .000 | 0.000 | . | 0.002 | 0.000 | . | 0.000 | 0.003 | 0.001 | 0.000 |
| Ca | Correlation Coeffic. | -.472* | .849** | . | 0.333 | .765** | .813** | 1 | .696** | 0.292 | .814** |
| | Sig. (2-tailed) | .020 | 0.000 | . | 0.112 | 0.000 | 0.000 | . | 0.000 | 0.165 | 0.000 |
| nitrate | Correlation Coeffic. | -.077 | .644** | . | 0.376 | .486* | .581** | .696** | 1 | .430* | .453* |
| | Sig. (2-tailed) | 0.721 | 0.001 | . | 0.070 | 0.016 | 0.003 | 0.000 | . | 0.036 | 0.026 |
| Cl | Correlation Coeffic. | -.385 | .532** | . | .841** | 0.341 | .630** | 0.292 | .430* | 1 | .528** |
| | Sig. (2-tailed) | 0.063 | 0.008 | . | 0.000 | 0.103 | 0.001 | 0.165 | 0.036 | . | 0.008 |
| Sulphate | Correlation Coeffic. | -.786** | .925** | . | .529** | .692** | .961** | .814** | .453* | .528** | 1 |
| | Sig. (2-tailed) | 0.000 | 0.000 | . | 0.008 | 0.000 | 0.000 | 0.000 | 0.026 | 0.008 | . |

N = 24

** Correlation is significant at the 0.01 (2-tailed).

*Correlation is significant at the 0.05 level (2-tailed).

# Appendix 3.3b continued: Three Weeks Wet (Top)

| Spearman's rho | | pH | cond | Fe | Mn | Pb | Zn | Ca | Nitrate | Cl | Sulphate |
|---|---|---|---|---|---|---|---|---|---|---|---|
| pH | Correlation Coeffic. | 1.000 | -.357 | . | -.614** | -.519* | -.571* | -.302 | .263 | .119 | -.330 |
| | Sig. (2-tailed) | . | .146 | . | .007 | .027 | .013 | .224 | .292 | .637 | .181 |
| Cond | Correlation Coeffic. | -.357 | 1.000 | . | .835** | .731** | .913** | .808** | .311 | .547* | .857** |
| | Sig. (2-tailed) | .146 | . | . | .000 | .001 | .000 | .000 | .209 | .019 | .000 |
| Fe | Correlation Coeffic. | . | . | . | . | . | . | . | . | . | . |
| | Sig. (2-tailed) | . | . | . | . | . | . | . | . | . | . |
| Mn | Correlation Coeffic. | -.614** | .835** | . | 1.000 | .751** | .935** | .643** | -.127 | .292 | .787** |
| | Sig. (2-tailed) | .007 | .000 | . | . | .000 | .000 | .004 | .615 | .240 | .000 |
| Pb | Correlation Coeffic. | -.519* | .731** | . | .751** | 1.000 | .728** | .828** | -.016 | .449 | .605** |
| | Sig. (2-tailed) | .027 | .001 | . | .000 | . | .001 | .000 | .950 | .062 | .008 |
| Zn | Correlation Coeffic. | -.571* | .913** | . | .935** | .728** | 1.000 | .736** | .050 | .291 | .789** |
| | Sig. (2-tailed) | .013 | .000 | . | .000 | .001 | . | .000 | .845 | .241 | .000 |
| Ca | Correlation Coeffic. | -.302 | .808** | . | .643** | .828** | .736** | 1.000 | .186 | .605** | .748** |
| | Sig. (2-tailed) | .224 | .000 | . | .004 | .000 | .000 | . | .459 | .008 | .000 |
| Nitrate | Correlation Coeffic. | .263 | .311 | . | -.127 | -.016 | .050 | .186 | 1.000 | .625** | .226 |
| | Sig. (2-tailed) | .292 | .209 | . | .615 | .950 | .845 | .459 | . | .006 | .368 |
| Cl | Correlation Coeffic. | .119 | .547* | . | .292 | .449 | .291 | .605** | .625** | 1.000 | .540* |
| | Sig. (2-tailed) | .637 | .019 | . | .240 | .062 | .241 | .008 | .006 | . | .021 |
| Sulphate | Correlation Coeffic. | -.330 | .857** | . | .787** | .605** | .789** | .748** | .226 | .540* | 1.000 |
| | Sig. (2-tailed) | .181 | .000 | . | .000 | .008 | .000 | .000 | .368 | .021 | . |

N = 18

** Correlation is significant at the 0.01 (2-tailed).

*Correlation is significant at the 0.05 level (2-tailed).

Appendix 3.3b continued: Flood (Top)

| Spearman's rho | | pH | cond | Fe | Mn | Pb | Zn | Ca | nitrate | Cl | Sulphate |
|---|---|---|---|---|---|---|---|---|---|---|---|
| pH | Correlation Coeffic. | 1.000 | -.401* | .173 | -.653** | -.172 | -.539** | -.048 | .019 | -.326 | -.527** |
| | Sig. (2-tailed) | . | .015 | .312 | .000 | .317 | .001 | .779 | .911 | .056 | .001 |
| Cond | Correlation Coeffic. | -.401* | 1.000 | -.158 | .275 | .199 | .851** | .291 | .127 | .209 | .567** |
| | Sig. (2-tailed) | .015 | . | .358 | .104 | .244 | .000 | .085 | .460 | .229 | .000 |
| Fe | Correlation Coeffic. | .173 | -.158 | 1.000 | -.123 | -.286 | -.327 | -.229 | -.368* | -.226 | -.198 |
| | Sig. (2-tailed) | .312 | .358 | . | .474 | .090 | .052 | .179 | .027 | .192 | .246 |
| Mn | Correlation Coeffic. | -.653** | .275 | -.123 | 1.000 | .096 | .399* | -.402* | -.013 | .518** | .771** |
| | Sig. (2-tailed) | .000 | .104 | .474 | . | .579 | .016 | .015 | .942 | .001 | .000 |
| Pb | Correlation Coeffic. | -.172 | .199 | -.286 | .096 | 1.000 | .063 | .202 | -.142 | .118 | .139 |
| | Sig. (2-tailed) | .317 | .244 | .090 | .579 | . | .716 | .237 | .408 | .499 | .418 |
| Zn | Correlation Coeffic. | -.539** | .851** | -.327 | .399* | .063 | 1.000 | .159 | .103 | .235 | .641** |
| | Sig. (2-tailed) | .001 | .000 | .052 | .016 | .716 | . | .355 | .551 | .173 | .000 |
| Ca | Correlation Coeffic. | -.048 | .291 | -.229 | -.402* | .202 | .159 | 1.000 | .242 | -.315 | -.210 |
| | Sig. (2-tailed) | .779 | .085 | .179 | .015 | .237 | .355 | . | .155 | .065 | .218 |
| nitrate | Correlation Coeffic. | .019 | .127 | -.368* | -.013 | -.142 | .103 | .242 | 1.000 | .216 | .053 |
| | Sig. (2-tailed) | .911 | .460 | .027 | .942 | .408 | .551 | .155 | . | .212 | .761 |
| Cl | Correlation Coeffic. | -.326 | .209 | -.226 | .518** | .118 | .235 | -.315 | .216 | 1.000 | .419* |
| | Sig. (2-tailed) | .056 | .229 | .192 | .001 | .499 | .173 | .065 | .212 | . | .012 |
| Sulphate | Correlation Coeffic. | -.527** | .567** | -.198 | .771** | .139 | .641** | -.210 | .053 | .419* | 1.000 |
| | Sig. (2-tailed) | .001 | .000 | .246 | .000 | .418 | .000 | .218 | .761 | .012 | . |

N = 36

** Correlation is significant at the 0.01 (2-tailed).

*Correlation is significant at the 0.05 level (2-tailed).

## Appendix 3.3b continued: One Week Wet (Bottom)

N = 36

| Spearman's rho | | ph | cond | Fe | Mn | Pb | Zn | Ca | nitrate | Cl | Sulphate |
|---|---|---|---|---|---|---|---|---|---|---|---|
| pH | Correlation Coeffic. | 1 | .519** | .348* | 0.288 | -.508** | .633** | .452** | -0.307 | -.567** | .684** |
| | Sig. (2-tailed) | . | 0.001 | 0.037 | 0.088 | 0.002 | 0.000 | 0.006 | 0.068 | 0.000 | 0.000 |
| Cond | Correlation Coeffic. | .519** | 1 | .771** | .840** | 0.19 | .869** | .714** | -.687** | -0.096 | .772** |
| | Sig. (2-tailed) | 0.001 | . | 0.000 | 0.000 | 0.267 | 0.000 | 0.000 | 0.000 | 0.578 | 0.000 |
| Fe | Correlation Coeffic. | .348* | .771** | 1 | .747** | .368* | .699** | .599** | -.519** | -0.075 | .631** |
| | Sig. (2-tailed) | 0.037 | 0.000 | . | 0.000 | 0.027 | 0.000 | 0.000 | 0.001 | 0.665 | 0.000 |
| Mn | Correlation Coeffic. | 0.288 | .840** | .747** | 1 | 0.277 | .663** | .522** | -.800** | 0.111 | .561** |
| | Sig. (2-tailed) | 0.088 | 0.000 | 0.000 | . | 0.103 | 0.000 | 0.001 | 0.000 | 0.521 | 0.000 |
| Pb | Correlation Coeffic. | -.508** | 0.19 | .368* | 0.277 | 1 | 0.122 | .383* | -0.073 | 0.201 | -0.121 |
| | Sig. (2-tailed) | 0.002 | 0.267 | 0.027 | 0.103 | . | 0.477 | 0.021 | 0.673 | 0.239 | 0.481 |
| Zn | Correlation Coeffic. | .633** | .869** | .699** | .663** | 0.122 | 1 | .727** | -.448** | -0.182 | .769** |
| | Sig. (2-tailed) | 0.000 | 0.000 | 0.000 | 0.000 | 0.477 | . | 0.000 | 0.006 | 0.289 | 0.000 |
| Ca | Correlation Coeffic. | .452** | .714** | .599** | .522** | .383* | .727** | 1 | -.366* | -.401* | .538** |
| | Sig. (2-tailed) | 0.006 | 0.000 | 0.000 | 0.001 | 0.021 | 0.000 | . | 0.028 | 0.015 | 0.001 |
| nitrate | Correlation Coeffic. | -0.307 | -.687** | -.519** | -.800** | -0.073 | -.448** | -.366* | 1 | 0.036 | -.485** |
| | Sig. (2-tailed) | 0.068 | 0.000 | 0.001 | 0.000 | 0.673 | 0.006 | 0.028 | . | 0.833 | 0.003 |
| Cl | Correlation Coeffic. | -.567** | -0.096 | -0.08 | 0.111 | 0.201 | -0.182 | -.401* | 0.036 | 1 | -0.244 |
| | Sig. (2-tailed) | 0.000 | 0.578 | 0.665 | 0.521 | 0.239 | 0.289 | 0.015 | 0.833 | . | 0.152 |
| Sulphate | Correlation Coeffic. | .684** | .772** | .631** | .561** | -0.121 | .769** | .538** | -.485** | -0.244 | 1 |
| | Sig. (2-tailed) | 0.000 | 0.000 | 0.000 | 0.000 | 0.481 | 0.000 | 0.001 | 0.003 | 0.152 | . |

** Correlation is significant at the 0.01 (2-tailed).

*Correlation is significant at the 0.05 level (2-tailed).

## Appendix 3.3b continued: Two Weeks Dry (Bottom)

| Spearman's rho | | ph | cond | Fe | Mn | Pb | Zn | Ca | nitrate | Cl | Sulphate |
|---|---|---|---|---|---|---|---|---|---|---|---|
| pH | Correlation Coeffic. | 1 | .455* | .538** | 0.228 | -.619** | .594** | .692** | -0.336 | 0.068 | .559** |
| | Sig. (2-tailed) | . | 0.026 | 0.007 | 0.284 | 0.001 | 0.002 | 0 | 0.109 | 0.752 | 0.005 |
| Cond | Correlation Coeffic. | .455* | 1 | .781** | .733** | -0.377 | .820** | .470* | -.560** | 0.185 | .872** |
| | Sig. (2-tailed) | 0.026 | . | 0 | 0.000 | 0.069 | 0.000 | 0.021 | 0.004 | 0.387 | 0.000 |
| Fe | Correlation Coeffic. | .538** | .781** | 1 | .559** | -0.178 | .667** | .701** | -0.383 | 0.052 | .746** |
| | Sig. (2-tailed) | 0.007 | 0 | . | 0.004 | 0.404 | 0 | 0 | 0.065 | 0.811 | 0 |
| Mn | Correlation Coeffic. | 0.228 | .733** | .559** | 1 | -0.017 | 0.321 | 0.113 | -.706** | 0.134 | .537** |
| | Sig. (2-tailed) | 0.284 | 0 | 0.004 | . | 0.936 | 0.126 | 0.599 | 0.000 | 0.531 | 0.007 |
| Pb | Correlation Coeffic. | -.619** | -0.377 | -0.18 | -0.017 | 1 | -.699** | -0.221 | 0.167 | -.429* | -.410* |
| | Sig. (2-tailed) | 0.001 | 0.069 | 0.404 | 0.936 | . | 0.000 | 0.300 | 0.436 | 0.036 | 0.047 |
| Zn | Correlation Coeffic. | .594** | .820** | .667** | 0.321 | -.699** | 1 | .583** | -0.272 | 0.286 | .833** |
| | Sig. (2-tailed) | 0.002 | 0.000 | 0.000 | 0.126 | 0.000 | . | 0.003 | 0.198 | 0.176 | 0.000 |
| Ca | Correlation Coeffic. | .692** | .470* | .701** | 0.113 | -0.221 | .583** | 1 | -0.15 | -0.311 | .522** |
| | Sig. (2-tailed) | 0.000 | 0.021 | 0.000 | 0.599 | 0.300 | 0.003 | . | 0.484 | 0.139 | 0.009 |
| nitrate | Correlation Coeffic. | -0.336 | -.560** | -0.38 | -.706** | 0.167 | -0.272 | -0.15 | 1 | 0.014 | -.407* |
| | Sig. (2-tailed) | 0.109 | 0.004 | 0.065 | 0.000 | 0.436 | 0.198 | 0.484 | . | 0.950 | 0.049 |
| Cl | Correlation Coeffic. | 0.068 | 0.185 | 0.052 | 0.134 | -.429* | 0.286 | -0.311 | 0.014 | 1 | 0.313 |
| | Sig. (2-tailed) | 0.752 | 0.387 | 0.811 | 0.531 | 0.036 | 0.176 | 0.139 | 0.950 | . | 0.137 |
| Sulphate | Correlation Coeffic. | .559** | .872** | .746** | .537** | -.410* | .833** | .522** | -.407* | 0.313 | 1 |
| | Sig. (2-tailed) | 0.005 | 0.000 | 0.000 | 0.007 | 0.047 | 0.000 | 0.009 | 0.049 | 0.137 | . |

N = 24

** Correlation is significant at the 0.01 (2-tailed).

*Correlation is significant at the 0.05 level (2-tailed).

## Appendix 3.3b continued: Three Weeks Dry (Bottom)

| Spearman's rho | | ph | cond | Fe | Pb | Zn | Nitrate | Sulphate | Mn | Ca | Cl |
|---|---|---|---|---|---|---|---|---|---|---|---|
| pH | Correlation Coeffic. | 1 | .680** | 0.253 | -.513* | .621** | -0.048 | .742** | 0.143 | .528* | -0.29 |
| | Sig. (2-tailed) | . | 0.002 | 0.311 | 0.029 | 0.006 | 0.849 | 0 | 0.571 | 0.024 | 0.243 |
| Cond | Correlation Coeffic. | .680** | 1 | 0.116 | -0.364 | .851** | -0.372 | .966** | .532* | 0.43 | 0.046 |
| | Sig. (2-tailed) | 0.002 | . | 0.647 | 0.138 | 0.000 | 0.129 | 0.000 | 0.023 | 0.075 | 0.857 |
| Fe | Correlation Coeffic. | 0.253 | 0.116 | 1 | 0.043 | -0.176 | -.530* | 0.199 | 0.467 | -0.258 | 0.054 |
| | Sig. (2-tailed) | 0.311 | 0.647 | . | 0.866 | 0.484 | 0.024 | 0.43 | 0.051 | 0.302 | 0.831 |
| Pb | Correlation Coeffic. | -.513* | -0.364 | 0.043 | 1 | -0.33 | -0.239 | -0.335 | -0.118 | -0.235 | 0.315 |
| | Sig. (2-tailed) | 0.029 | 0.138 | 0.866 | . | 0.182 | 0.339 | 0.175 | 0.642 | 0.348 | 0.203 |
| Zn | Correlation Coeffic. | .621** | .851** | -0.18 | -0.33 | 1 | -0.046 | .849** | 0.148 | .746** | -0.046 |
| | Sig. (2-tailed) | 0.006 | 0.000 | 0.484 | 0.182 | . | 0.858 | 0.000 | 0.558 | 0.000 | 0.857 |
| Nitrate | Correlation Coeffic. | -0.048 | -0.372 | -.530* | -0.239 | -0.046 | 1 | -0.359 | -.747** | 0.359 | -0.312 |
| | Sig. (2-tailed) | 0.849 | 0.129 | 0.024 | 0.339 | 0.858 | . | 0.143 | 0.000 | 0.144 | 0.207 |
| Sulphate | Correlation Coeffic. | .742** | .966** | 0.199 | -0.335 | .849** | -0.359 | 1 | .508* | .469* | 0.116 |
| | Sig. (2-tailed) | 0.000 | 0.000 | 0.430 | 0.175 | 0.000 | 0.143 | . | 0.031 | 0.049 | 0.647 |
| Mn | Correlation Coeffic. | 0.143 | .532* | 0.467 | -0.118 | 0.148 | -.747** | .508* | 1 | -0.411 | 0.244 |
| | Sig. (2-tailed) | 0.571 | 0.023 | 0.051 | 0.642 | 0.558 | 0.000 | 0.031 | . | 0.090 | 0.329 |
| Ca | Correlation Coeffic. | .528* | 0.43 | -0.26 | -0.235 | .746** | 0.359 | .469* | -0.411 | 1 | -0.233 |
| | Sig. (2-tailed) | 0.024 | 0.075 | 0.302 | 0.348 | 0.000 | 0.144 | 0.049 | 0.090 | . | 0.352 |
| Cl | Correlation Coeffic. | -0.29 | 0.046 | 0.054 | 0.315 | -0.046 | -0.312 | 0.116 | 0.244 | -0.233 | 1 |
| | Sig. (2-tailed) | 0.243 | 0.857 | 0.831 | 0.203 | 0.857 | 0.207 | 0.647 | 0.329 | 0.352 | . |

N = 18

** Correlation is significant at the 0.01 (2-tailed).

*Correlation is significant at the 0.05 level (2-tailed).

## Appendix 3.3b continued: Two Weeks Wet (Bottom)

| Spearman's rho | | ph | cond | Fe | Mn | Pb | Zn | Ca | nitrate | Cl | Sulphate |
|---|---|---|---|---|---|---|---|---|---|---|---|
| pH | Correlation Coeffic. | 1 | .646** | .528** | .487* | -.704** | .779** | .411* | -.682** | -0.275 | .857** |
| | Sig. (2-tailed) | . | 0.001 | 0.008 | 0.016 | 0 | 0 | 0.046 | 0 | 0.194 | 0 |
| Cond | Correlation Coeffic. | .646** | 1 | .850** | .880** | -0.176 | .818** | .440* | -.822** | 0.031 | .803** |
| | Sig. (2-tailed) | 0.001 | . | 0 | 0.000 | 0.412 | 0.000 | 0.032 | 0.000 | 0.885 | 0.000 |
| Fe | Correlation Coeffic. | .528** | .850** | 1 | .850** | -0.036 | .754** | 0.325 | -.858** | 0.119 | .755** |
| | Sig. (2-tailed) | 0.008 | 0 | . | 0 | 0.867 | 0 | 0.121 | 0 | 0.579 | 0 |
| Mn | Correlation Coeffic. | .487* | .880** | .850** | 1 | -0.134 | .611** | 0.205 | -.769** | 0.26 | .750** |
| | Sig. (2-tailed) | 0.016 | 0 | 0 | . | 0.534 | 0.002 | 0.336 | 0.000 | 0.220 | 0.000 |
| Pb | Correlation Coeffic. | -.704** | -0.176 | -0.04 | -0.134 | 1 | -0.367 | -0.066 | 0.23 | -0.053 | -.575** |
| | Sig. (2-tailed) | 0.000 | 0.412 | 0.867 | 0.534 | . | 0.078 | 0.758 | 0.280 | 0.807 | 0.003 |
| Zn | Correlation Coeffic. | .779** | .818** | .754** | .611** | -0.367 | 1 | .566** | -.747** | -0.01 | .838** |
| | Sig. (2-tailed) | 0.000 | 0.000 | 0.000 | 0.002 | 0.078 | . | 0.004 | 0.000 | 0.963 | 0.000 |
| Ca | Correlation Coeffic. | .411* | .440* | 0.325 | 0.205 | -0.066 | .566** | 1 | -0.129 | -.497* | 0.399 |
| | Sig. (2-tailed) | 0.046 | 0.032 | 0.121 | 0.336 | 0.758 | 0.004 | . | 0.549 | 0.014 | 0.053 |
| nitrate | Correlation Coeffic. | -.682** | -.822** | -.858** | -.769** | 0.23 | -.747** | -0.129 | 1 | -0.063 | -.820** |
| | Sig. (2-tailed) | 0.000 | 0.000 | 0.000 | 0.000 | 0.280 | 0.000 | 0.549 | . | 0.771 | 0.000 |
| Cl | Correlation Coeffic. | -0.275 | 0.031 | 0.119 | 0.26 | -0.053 | -0.01 | -.497* | -0.063 | 1 | 0.025 |
| | Sig. (2-tailed) | 0.194 | 0.885 | 0.579 | 0.220 | 0.807 | 0.963 | 0.014 | 0.771 | . | 0.908 |
| Sulphate | Correlation Coeffic. | .857** | .803** | .755** | .750** | -.575** | .838** | 0.399 | -.820** | 0.025 | 1 |
| | Sig. (2-tailed) | 0.000 | 0.000 | 0.000 | 0.000 | 0.003 | 0.000 | 0.053 | 0.000 | 0.908 | . |

N = 24

** Correlation is significant at the 0.01 (2-tailed).

*Correlation is significant at the 0.05 level (2-tailed).

## Appendix 3.3b continued: Three Weeks Wet (Bottom)

| Spearman's rho | | ph | cond | Fe | Pb | Zn | nitrate | Sulphate | Mn | Ca | Cl |
|---|---|---|---|---|---|---|---|---|---|---|---|
| pH | Correlation Coeffic. | 1 | 0.365 | 0.283 | -0.318 | .509* | -0.435 | .651** | .594** | 0.274 | -.720** |
| | Sig. (2-tailed) | . | 0.137 | 0.255 | 0.199 | 0.031 | 0.071 | 0.003 | 0.009 | 0.271 | 0.001 |
| Cond | Correlation Coeffic. | 0.365 | 1 | .926** | 0.266 | .780** | -.896** | .853** | .919** | 0.444 | -0.093 |
| | Sig. (2-tailed) | 0.137 | . | 0 | 0.286 | 0.000 | 0.000 | 0.000 | 0.000 | 0.065 | 0.713 |
| Fe | Correlation Coeffic. | 0.283 | .926** | 1 | 0.442 | .754** | -.873** | .846** | .897** | .535* | -0.045 |
| | Sig. (2-tailed) | 0.255 | 0 | . | 0.066 | 0 | 0 | 0 | 0 | 0.022 | 0.861 |
| Pb | Correlation Coeffic. | -0.318 | 0.266 | 0.442 | 1 | 0.365 | -0.291 | 0.21 | 0.159 | .564* | .554* |
| | Sig. (2-tailed) | 0.199 | 0.286 | 0.066 | . | 0.136 | 0.241 | 0.403 | 0.529 | 0.015 | 0.017 |
| Zn | Correlation Coeffic. | .509* | .780** | .754** | 0.365 | 1 | -.724** | .822** | .808** | .727** | -0.126 |
| | Sig. (2-tailed) | 0.031 | 0.000 | 0.000 | 0.136 | . | 0.001 | 0.000 | 0.000 | 0.001 | 0.619 |
| nitrate | Correlation Coeffic. | -0.435 | -.896** | -.873** | -0.291 | -.724** | 1 | -.846** | -.894** | -0.442 | 0.294 |
| | Sig. (2-tailed) | 0.071 | 0.000 | 0.000 | 0.241 | 0.001 | . | 0.000 | 0.000 | 0.066 | 0.236 |
| Sulphate | Correlation Coeffic. | .651** | .853** | .846** | 0.21 | .822** | -.846** | 1 | .929** | .564* | -0.367 |
| | Sig. (2-tailed) | 0.003 | 0.000 | 0.000 | 0.403 | 0.000 | 0.000 | . | 0.000 | 0.015 | 0.134 |
| Mn | Correlation Coeffic. | .594** | .919** | .897** | 0.159 | .808** | -.894** | .929** | 1 | 0.421 | -0.358 |
| | Sig. (2-tailed) | 0.009 | 0.000 | 0.000 | 0.529 | 0.000 | 0.000 | 0.000 | . | 0.082 | 0.145 |
| Ca | Correlation Coeffic. | 0.274 | 0.444 | .535* | .564* | .727** | -0.442 | .564* | 0.421 | 1 | 0.118 |
| | Sig. (2-tailed) | 0.271 | 0.065 | 0.022 | 0.015 | 0.001 | 0.066 | 0.015 | 0.082 | . | 0.641 |
| Cl | Correlation Coeffic. | -.720** | -0.093 | -0.05 | .554* | -0.126 | 0.294 | -0.367 | -0.358 | 0.118 | 1 |
| | Sig. (2-tailed) | 0.001 | 0.713 | 0.861 | 0.017 | 0.619 | 0.236 | 0.134 | 0.145 | 0.641 | . |

N = 18

** Correlation is significant at the 0.01 (2-tailed).

*Correlation is significant at the 0.05 level (2-tailed).

## Appendix 3.3b continued: Flood (Bottom)

| Spearman's rho | | pH | cond | Fe | Pb | Zn | nitrate | Sulphate | Mn | Ca | Cl |
|---|---|---|---|---|---|---|---|---|---|---|---|
| pH | Correlation Coeffic. | 1 | .932** | .949** | -.915** | 0.205 | -.419* | .939** | .935** | .594** | .339* |
| | Sig. (2-tailed) | . | 0 | 0 | 0 | 0.23 | 0.011 | 0 | 0 | 0 | 0.043 |
| Cond | Correlation Coeffic. | .932** | 1 | .974** | -.858** | 0.321 | -.479** | .917** | .981** | .503** | .459** |
| | Sig. (2-tailed) | 0 | . | 0 | 0.000 | 0.056 | 0.003 | 0.000 | 0.000 | 0.002 | 0.005 |
| Fe | Correlation Coeffic. | .949** | .974** | 1 | -.885** | 0.241 | -.478** | .931** | .956** | .477** | .453** |
| | Sig. (2-tailed) | 0 | 0 | . | 0 | 0.157 | 0.003 | 0 | 0 | 0.003 | 0.005 |
| Pb | Correlation Coeffic. | -.915** | -.858** | -.885** | 1 | -0.131 | 0.216 | -.889** | -.863** | -.605** | -.483** |
| | Sig. (2-tailed) | 0 | 0 | 0 | . | 0.446 | 0.205 | 0.000 | 0.000 | 0.000 | 0.003 |
| Zn | Correlation Coeffic. | 0.205 | 0.321 | 0.241 | -0.131 | 1 | 0.016 | 0.16 | .367* | .393* | 0.28 |
| | Sig. (2-tailed) | 0.230 | 0.056 | 0.157 | 0.446 | . | 0.926 | 0.351 | 0.028 | 0.018 | 0.098 |
| Nitrate | Correlation Coeffic. | -.419* | -.479** | -.478** | 0.216 | 0.016 | 1 | -.479** | -.479** | 0.204 | -0.032 |
| | Sig. (2-tailed) | 0.011 | 0.003 | 0.003 | 0.205 | 0.926 | . | 0.003 | 0.003 | 0.233 | 0.852 |
| Sulphate | Correlation Coeffic. | .939** | .917** | .931** | -.889** | 0.16 | -.479** | 1 | .891** | .467** | .504** |
| | Sig. (2-tailed) | 0.000 | 0.000 | 0.000 | 0.000 | 0.351 | 0.003 | . | 0.000 | 0.004 | 0.002 |
| Mn | Correlation Coeffic. | .935** | .981** | .956** | -.863** | .367* | -.479** | .891** | 1 | .544** | .400* |
| | Sig. (2-tailed) | 0.000 | 0.000 | 0.000 | 0.000 | 0.028 | 0.003 | 0.000 | . | 0.001 | 0.016 |
| Ca | Correlation Coeffic. | .594** | .503** | .477** | -.605** | .393* | 0.204 | .467** | .544** | 1 | 0.228 |
| | Sig. (2-tailed) | 0.000 | 0.002 | 0.003 | 0.000 | 0.018 | 0.233 | 0.004 | 0.001 | . | 0.182 |
| Cl | Correlation Coeffic. | .339* | .459** | .453** | -.483** | 0.28 | -0.032 | .504** | .400* | 0.228 | 1 |
| | Sig. (2-tailed) | 0.043 | 0.005 | 0.005 | 0.003 | 0.098 | 0.852 | 0.002 | 0.016 | 0.182 | . |

N = 36

** Correlation is significant at the 0.01 (2-tailed).

*Correlation is significant at the 0.05 level (2-tailed).

Appendix 3.3b continued: Field Capacity

| Spearman's rho | | ph | cond | Fe | Mn | Pb | Zn | Ca | nitrate | Cl | Sulphate |
|---|---|---|---|---|---|---|---|---|---|---|---|
| pH | Correlation Coeffic. | 1 | -0.181 | 0.254 | 0.036 | -.340* | 0.083 | 0.026 | -.596** | -.520** | .483** |
| | Sig. (2-tailed) | . | 0.291 | 0.134 | 0.833 | 0.042 | 0.629 | 0.879 | 0 | 0.001 | 0.003 |
| Cond | Correlation Coeffic. | -0.181 | 1 | 0.313 | .602** | 0.23 | .656** | .705** | .397* | 0.131 | .461** |
| | Sig. (2-tailed) | 0.291 | . | 0.063 | 0.000 | 0.177 | 0.000 | 0.000 | 0.016 | 0.446 | 0.005 |
| Fe | Correlation Coeffic. | 0.254 | 0.313 | 1 | 0.314 | -0.052 | 0.077 | 0.214 | 0.049 | -0.056 | .347* |
| | Sig. (2-tailed) | 0.134 | 0.063 | . | 0.062 | 0.762 | 0.657 | 0.209 | 0.776 | 0.746 | 0.038 |
| Mn | Correlation Coeffic. | 0.036 | .602** | 0.314 | 1 | -0.004 | .599** | .388* | 0.033 | 0.181 | .433** |
| | Sig. (2-tailed) | 0.833 | 0 | 0.062 | . | 0.980 | 0.000 | 0.019 | 0.848 | 0.290 | 0.008 |
| Pb | Correlation Coeffic. | -.340* | 0.23 | -0.05 | -0.004 | 1 | 0.078 | 0.165 | .613** | -0.161 | -0.291 |
| | Sig. (2-tailed) | 0.042 | 0.177 | 0.762 | 0.980 | . | 0.650 | 0.337 | 0.000 | 0.349 | 0.085 |
| Zn | Correlation Coeffic. | 0.083 | .656** | 0.077 | .599** | 0.078 | 1 | .488** | -0.089 | 0.021 | .565** |
| | Sig. (2-tailed) | 0.629 | 0.000 | 0.657 | 0.000 | 0.650 | . | 0.003 | 0.606 | 0.902 | 0.000 |
| Ca | Correlation Coeffic. | 0.026 | .705** | 0.214 | .388* | 0.165 | .488** | 1 | .352* | 0.161 | .332* |
| | Sig. (2-tailed) | 0.879 | 0.000 | 0.209 | 0.019 | 0.337 | 0.003 | . | 0.035 | 0.348 | 0.048 |
| nitrate | Correlation Coeffic. | -.596** | .397* | 0.049 | 0.033 | .613** | -0.089 | .352* | 1 | .368* | -0.309 |
| | Sig. (2-tailed) | 0.000 | 0.016 | 0.776 | 0.848 | 0.000 | 0.606 | 0.035 | . | 0.027 | 0.067 |
| Cl | Correlation Coeffic. | -.520** | 0.131 | -0.06 | 0.181 | -0.161 | 0.021 | 0.161 | .368* | 1 | -0.098 |
| | Sig. (2-tailed) | 0.001 | 0.446 | 0.746 | 0.290 | 0.349 | 0.902 | 0.348 | 0.027 | . | 0.569 |
| Sulphate | Correlation Coeffic. | .483** | .461** | .347* | .433** | -0.291 | .565** | .332* | -0.309 | -0.098 | 1 |
| | Sig. (2-tailed) | 0.003 | 0.005 | 0.038 | 0.008 | 0.085 | 0.000 | 0.048 | 0.067 | 0.569 | . |

N = 36

** Correlation is significant at the 0.01 (2-tailed).

*Correlation is significant at the 0.05 level (2-tailed).

## Key to graphs for appendix 3.3c and 3.3d

| | |
|---|---|
| ▬ | 1wwet |
| ▬ | 2wdry |
| ▬ | 3wdry |
| ▬ | 2wwet |
| ▬ | 3wwet |
| ▬ | Flood |
| ▬ | F/C |

# Appendix 3.3c. Pore water graphs, top of the mesocosm

### a) Lead
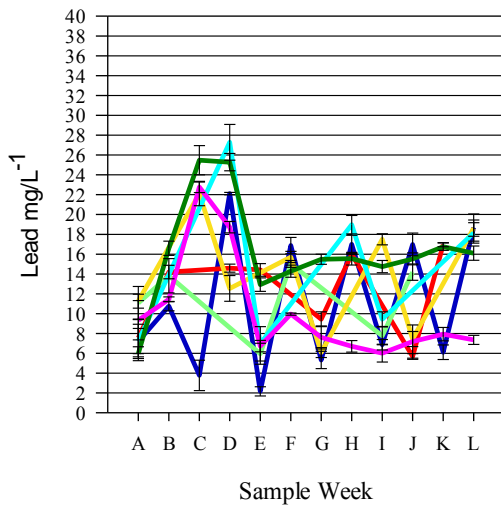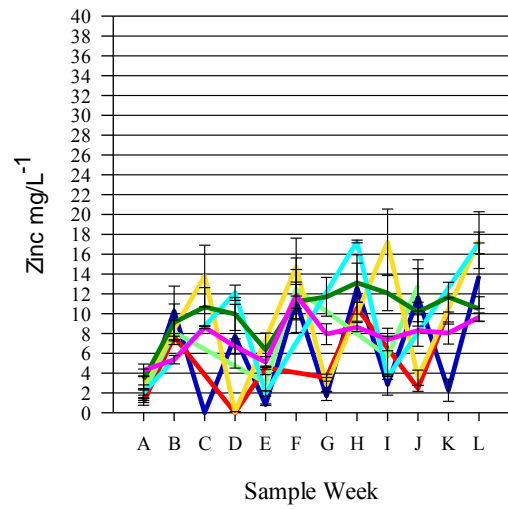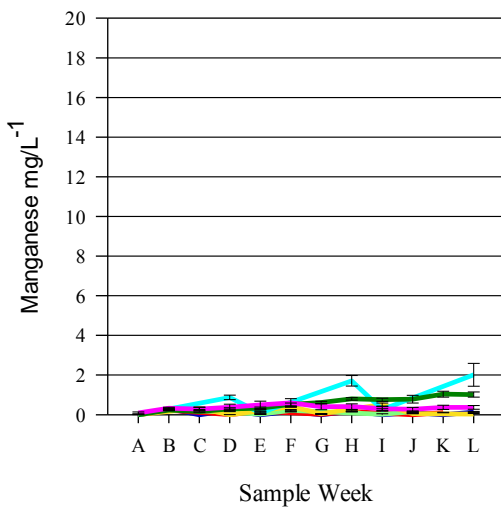


### b) Zinc
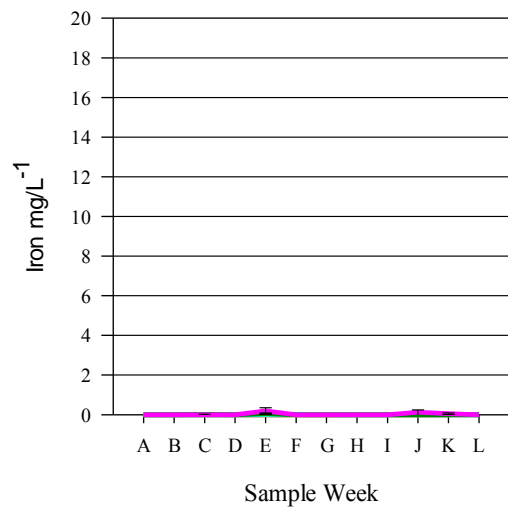


### c) Manganese
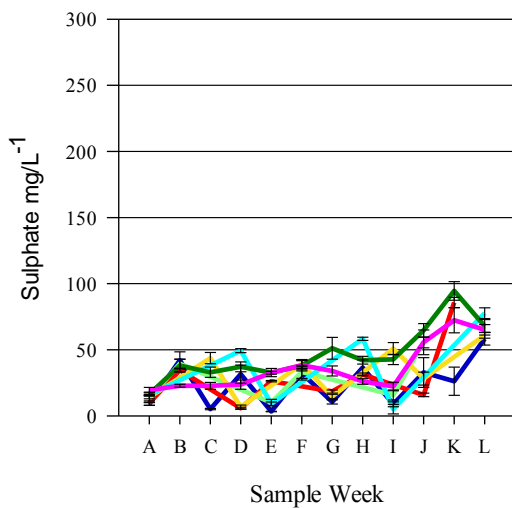


### d) Iron



### e) Sulphate



### f) Conductivity

g) Nitrate



h) Calcium



i) Chloride



j) pH



k) Temperature



269
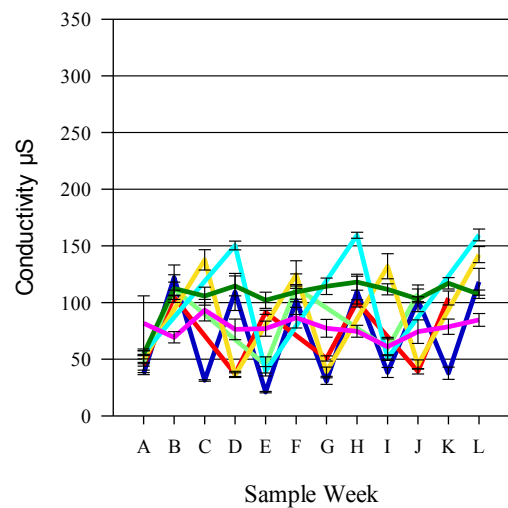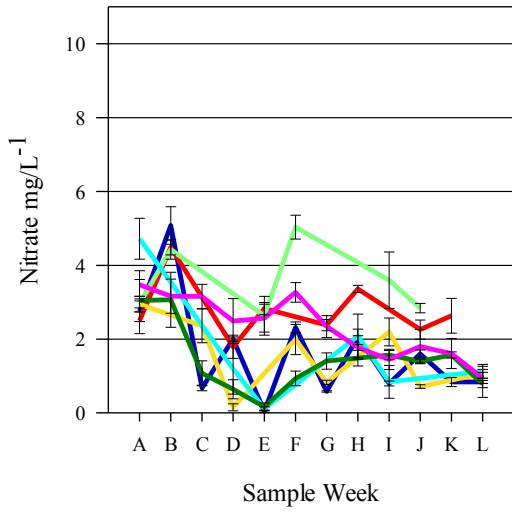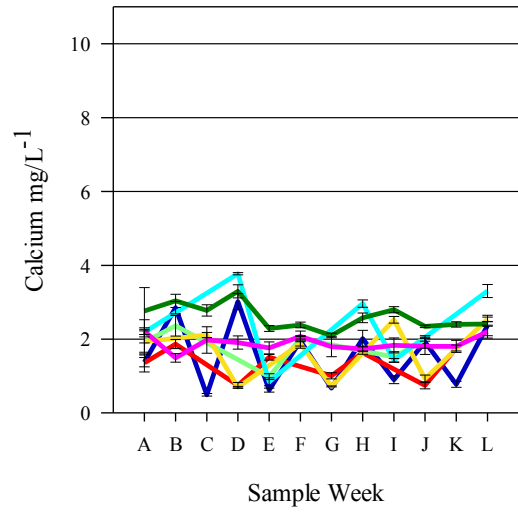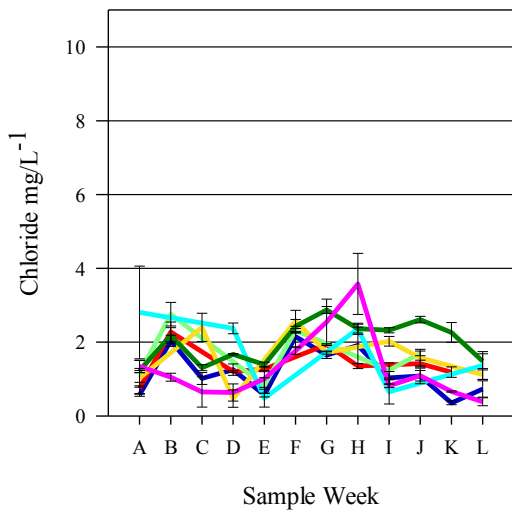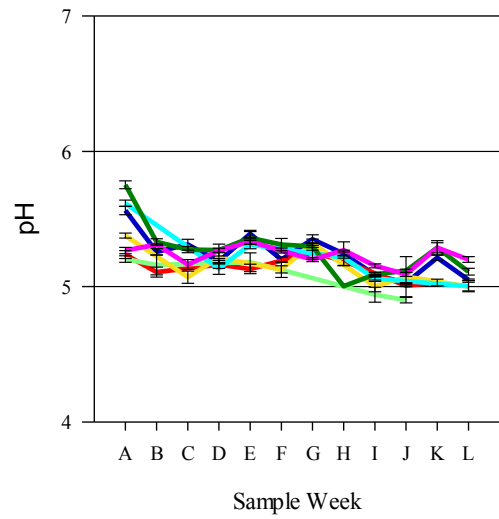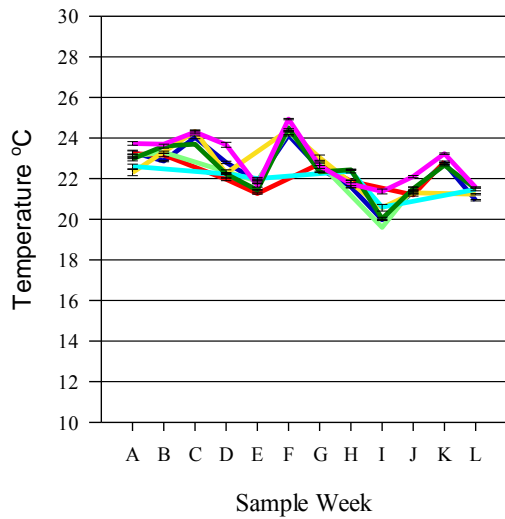
# Appendix 3.3d. Pore water graphs, bottom of the mesocosm

## a) Lead



## b) Zinc



## c) Manganese



## d) Iron



## e) Sulphate



## f) Conductivity



270
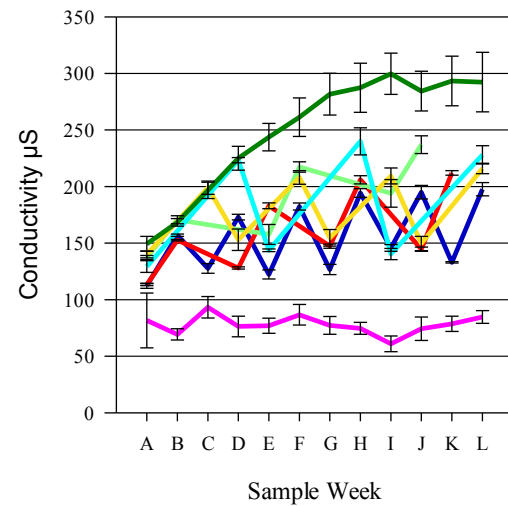
g) Nitrate
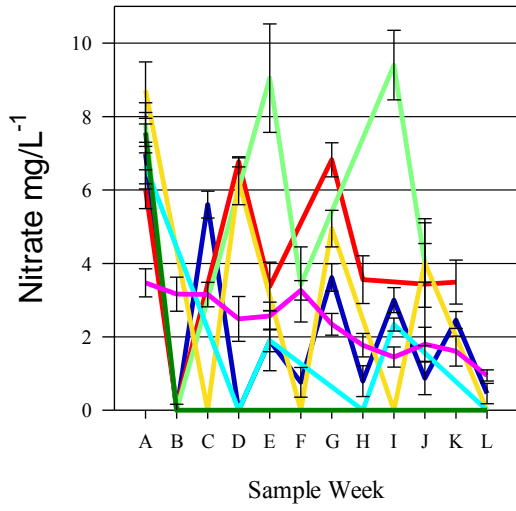
h) Calcium
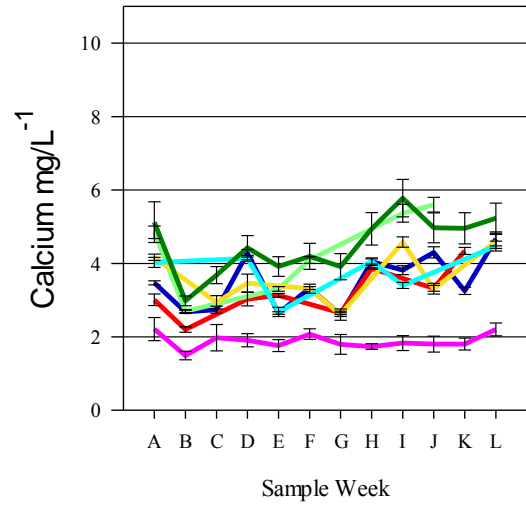
i) Chloride
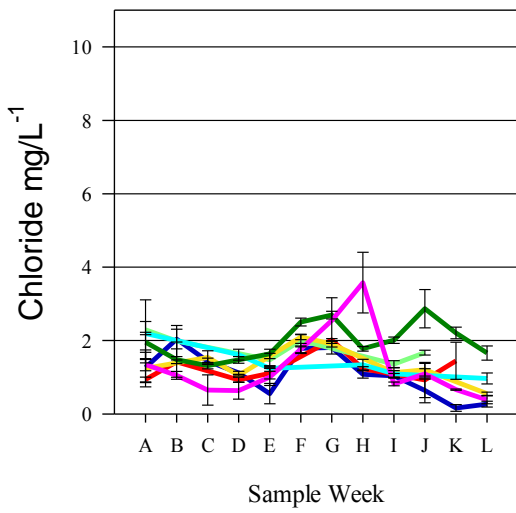
j) pH
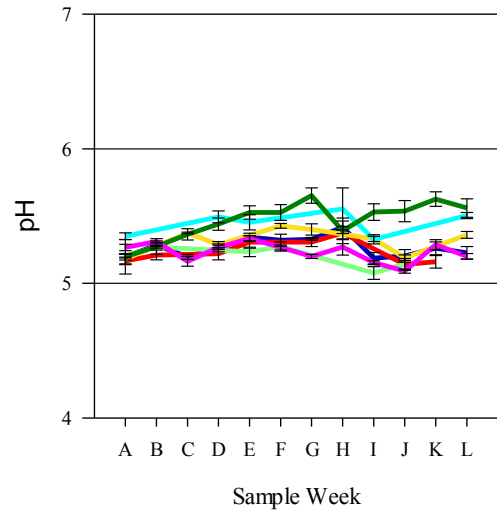
k) Temperature 0C
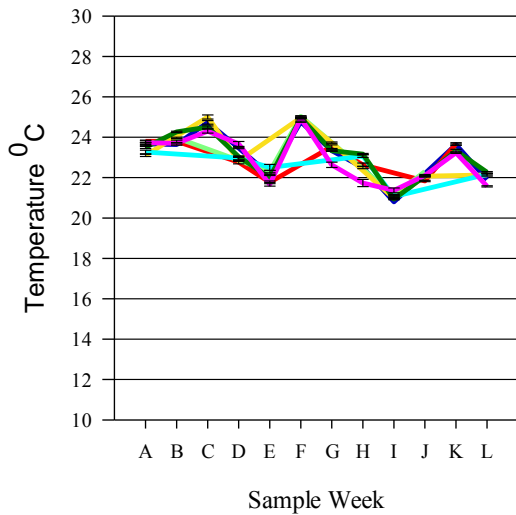
## Appendix 3.3e. PCA analysis. Pore water analysis

## Part A – Exploration of factors relating to the mobility of zinc, longer wetter runs

| | Total Variance Explained | | | | | | | | |
|---|---|---|---|---|---|---|---|---|---|
| | Initial Eigenvalues | | | Extraction Sums of Squared Loadings | | | Rotation Sums of Squared Loadings | | |
| Component | Total | % of Variance | Cumulative % | Total | % of Variance | Cumulative % | Total | % of Variance | Cumulative % |
| 1 | 5.042 | 63.019 | 63.019 | 5.042 | 63.019 | 63.019 | 5.040 | 62.995 | 62.995 |
| 2 | 1.297 | 16.213 | 79.232 | 1.297 | 16.213 | 79.232 | 1.299 | 16.237 | 79.232 |
| 3 | .796 | 9.945 | 89.177 | | | | | | |
| 4 | .331 | 4.133 | 93.309 | | | | | | |
| 5 | .301 | 3.768 | 97.078 | | | | | | |
| 6 | .128 | 1.595 | 98.673 | | | | | | |
| 7 | .068 | .848 | 99.521 | | | | | | |
| 8 | .038 | .479 | 100.000 | | | | | | |

Extraction Method: Principal Component Analysis.

## Part B – Exploration of the factors relating to the mobility of zinc, longer dryer runs

| | Total Variance Explained | | | | | | | | |
|---|---|---|---|---|---|---|---|---|---|
| | Initial Eigenvalues | | | Extraction Sums of Squared Loadings | | | Rotation Sums of Squared Loadings | | |
| Component | Total | % of Variance | Cumulative % | Total | % of Variance | Cumulative % | Total | % of Variance | Cumulative % |
| 1 | 4.702 | 58.773 | 58.773 | 4.702 | 58.773 | 58.773 | 3.410 | 42.622 | 42.622 |
| 2 | 1.595 | 19.936 | 78.709 | 1.595 | 19.936 | 78.709 | 2.887 | 36.087 | 78.709 |
| 3 | .898 | 11.222 | 89.931 | | | | | | |
| 4 | .346 | 4.321 | 94.252 | | | | | | |
| 5 | .229 | 2.863 | 97.116 | | | | | | |
| 6 | .148 | 1.847 | 98.963 | | | | | | |
| 7 | .056 | .698 | 99.661 | | | | | | |
| 8 | .027 | .339 | 100.000 | | | | | | |

Extraction Method: Principal Component Analysis.

**Appendix 3.3f. Pore water data, by week and run, at the top and bottom of the mesocosms (mean and standard error).**

| Week | Sample | Cycle No | Loc | pH | Temp | Cond | Fe | Mn | Pb | Zn | Ca | Ni | NO$_3^-$ | Cl$^-$ | SO$_4^{2-}$ |
|------|--------|----------|-----|-----|------|------|------|------|------|------|------|------|------|------|------|
|      |        |          |     |     | $^0$C | µS/s | mg/L | mg/L | mg/L | mg/L | mg/L | mg/L | mg/L | mg/L | mg/L |
| A | Mean | 1wwet | T | 5.6 | 23.30 | 37.3 | 0.00 | 0.00 | 7.20 | 1.28 | 1.38 | 0.17 | 2.76 | 0.57 | 9.01 |
| A | Std Error | 1wwet | T | 0.0 | 0.10 | 0.9 | 0.00 | 0.00 | 1.72 | 0.25 | 0.13 | 0.04 | 0.28 | 0.04 | 0.98 |
| B | Mean | 1wwet | T | 5.3 | 22.87 | 122.0 | 0.00 | 0.30 | 10.76 | 10.25 | 2.85 | 0.03 | 5.08 | 2.04 | 42.15 |
| B | Std Error | 1wwet | T | 0.0 | 0.03 | 11.1 | 0.00 | 0.05 | 0.48 | 2.52 | 0.17 | 0.02 | 0.51 | 0.15 | 6.26 |
| C | Mean | 1wwet | T | 5.3 | 24.03 | 31.3 | 0.00 | 0.00 | 3.78 | 0.00 | 0.49 | 0.00 | 0.68 | 1.02 | 5.13 |
| C | Std Error | 1wwet | T | 0.0 | 0.07 | 0.7 | 0.00 | 0.00 | 1.53 | 0.00 | 0.04 | 0.00 | 0.07 | 0.16 | 0.54 |
| D | Mean | 1wwet | T | 5.2 | 22.80 | 109.3 | 0.00 | 0.22 | 22.11 | 7.73 | 3.02 | 0.00 | 2.00 | 1.26 | 31.62 |
| D | Std Error | 1wwet | T | 0.0 | 0.06 | 16.4 | 0.00 | 0.07 | 0.12 | 3.22 | 0.22 | 0.00 | 0.06 | 0.15 | 6.86 |
| E | Mean | 1wwet | T | 5.4 | 21.87 | 21.0 | 0.00 | 0.00 | 2.17 | 0.83 | 0.62 | 0.01 | 0.04 | 0.57 | 3.32 |
| E | Std Error | 1wwet | T | 0.0 | 0.12 | 0.6 | 0.00 | 0.00 | 0.47 | 0.08 | 0.05 | 0.01 | 0.03 | 0.05 | 0.16 |
| F | Mean | 1wwet | T | 5.2 | 24.13 | 102.0 | 0.00 | 0.17 | 16.87 | 11.28 | 1.95 | 0.00 | 2.32 | 2.15 | 32.17 |
| F | Std Error | 1wwet | T | 0.0 | 0.03 | 12.6 | 0.00 | 0.03 | 0.82 | 3.18 | 0.14 | 0.00 | 0.15 | 0.28 | 5.07 |
| G | Mean | 1wwet | T | 5.4 | 22.50 | 30.7 | 0.00 | 0.00 | 5.33 | 1.71 | 0.67 | 0.00 | 0.58 | 1.65 | 10.59 |
| G | Std Error | 1wwet | T | 0.0 | 0.00 | 2.8 | 0.00 | 0.00 | 0.88 | 0.47 | 0.00 | 0.00 | 0.02 | 0.09 | 1.60 |
| H | Mean | 1wwet | T | 5.2 | 21.60 | 109.7 | 0.00 | 0.19 | 17.00 | 12.59 | 2.02 | 0.00 | 2.06 | 1.91 | 36.58 |
| H | Std Error | 1wwet | T | 0.0 | 0.06 | 13.5 | 0.00 | 0.04 | 0.91 | 3.35 | 0.22 | 0.00 | 0.21 | 0.49 | 5.81 |
| I | Mean | 1wwet | T | 5.1 | 19.97 | 38.3 | 0.00 | 0.00 | 6.87 | 2.86 | 0.90 | 0.00 | 0.80 | 1.03 | 8.77 |
| I | Std Error | 1wwet | T | 0.0 | 0.03 | 4.5 | 0.00 | 0.00 | 0.53 | 1.07 | 0.11 | 0.00 | 0.06 | 0.17 | 1.80 |
| J | Mean | 1wwet | T | 5.0 | 21.37 | 102.0 | 0.00 | 0.11 | 16.98 | 11.64 | 1.92 | 0.00 | 1.60 | 1.08 | 32.78 |
| J | Std Error | 1wwet | T | 0.0 | 0.07 | 10.0 | 0.00 | 0.02 | 1.14 | 2.89 | 0.17 | 0.00 | 0.11 | 0.21 | 11.20 |
| K | Mean | 1wwet | T | 5.2 | 22.77 | 37.7 | 0.00 | 0.00 | 6.11 | 2.28 | 0.78 | 0.00 | 0.84 | 0.35 | 26.23 |
| K | Std Error | 1wwet | T | 0.0 | 0.03 | 5.4 | 0.00 | 0.00 | 0.74 | 1.11 | 0.08 | 0.00 | 0.12 | 0.05 | 10.67 |
| L | Mean | 1wwet | T | 5.1 | 20.93 | 118.3 | 0.00 | 0.13 | 18.69 | 13.82 | 2.37 | 0.00 | 0.84 | 0.73 | 58.37 |
| L | Std Error | 1wwet | T | 0.0 | 0.03 | 11.8 | 0.00 | 0.03 | 1.36 | 3.32 | 0.28 | 0.00 | 0.42 | 0.22 | 4.86 |

| Week | Sample | Cycle No | Loc | pH | Temp $^0C$ | Cond µS/s | Fe mg/L | Mn mg/L | Pb mg/L | Zn mg/L | Ca mg/L | Ni mg/L | $NO_3^-$ mg/L | $Cl^-$ mg/L | $SO_4^{2-}$ mg/L |
|------|--------|----------|-----|-----|------|------|------|------|------|------|------|------|------|------|------|
| A | Mean | 2wdry | T | 5.2 | 23.23 | 45.0 | 0.00 | 0.00 | 7.55 | 1.11 | 1.36 | 0.24 | 2.50 | 0.75 | 9.69 |
| A | Std Error | 2wdry | | 0.0 | 0.13 | 1.0 | 0.00 | 0.00 | 1.91 | 0.33 | 0.24 | 0.03 | 0.35 | 0.16 | 1.74 |
| B | Mean | 2wdry | T | 5.1 | 23.17 | 104.7 | 0.00 | 0.22 | 14.20 | 7.69 | 1.87 | 0.05 | 4.49 | 2.28 | 34.57 |
| B | Std Error | 2wdry | T | 0.0 | 0.09 | 1.9 | 0.00 | 0.01 | 0.68 | 0.31 | 0.12 | 0.02 | 0.20 | 0.27 | 0.98 |
| D | Mean | 2wdry | T | 5.2 | 21.97 | 37.0 | 0.00 | 0.00 | 14.58 | 0.00 | 0.75 | 0.03 | 1.79 | 1.20 | 5.75 |
| D | Std Error | 2wdry | T | 0.0 | 0.07 | 2.3 | 0.00 | 0.00 | 0.41 | 0.00 | 0.08 | 0.02 | 0.31 | 0.02 | 0.78 |
| E | Mean | 2wdry | T | 5.1 | 21.27 | 91.3 | 0.00 | 0.17 | 14.41 | 4.56 | 1.51 | 0.00 | 2.83 | 1.27 | 26.24 |
| E | Std Error | 2wdry | T | 0.0 | 0.03 | 1.8 | 0.00 | 0.02 | 0.63 | 0.16 | 0.08 | 0.00 | 0.17 | 0.07 | 0.56 |
| G | Mean | 2wdry | T | 5.3 | 22.73 | 50.7 | 0.00 | 0.02 | 9.44 | 3.55 | 1.01 | 0.00 | 2.38 | 1.93 | 18.47 |
| G | Std Error | 2wdry | T | 0.1 | 0.09 | 2.3 | 0.00 | 0.01 | 0.75 | 0.36 | 0.08 | 0.00 | 0.15 | 0.03 | 1.20 |
| H | Mean | 2wdry | T | 5.2 | 21.87 | 100.7 | 0.00 | 0.16 | 15.99 | 10.56 | 1.63 | 0.00 | 3.36 | 1.35 | 31.37 |
| H | Std Error | 2wdry | T | 0.0 | 0.07 | 1.9 | 0.00 | 0.01 | 0.04 | 0.60 | 0.04 | 0.00 | 0.10 | 0.07 | 1.06 |
| J | Mean | 2wdry | T | 5.0 | 21.20 | 39.3 | 0.00 | 0.00 | 5.68 | 2.48 | 0.75 | 0.00 | 2.26 | 1.42 | 15.83 |
| J | Std Error | 2wdry | T | 0.0 | 0.06 | 2.4 | 0.00 | 0.00 | 0.28 | 0.30 | 0.09 | 0.00 | 0.26 | 0.09 | 1.33 |
| K | Mean | 2wdry | T | 5.0 | 22.83 | 104.0 | 0.00 | 0.11 | 16.96 | 10.27 | 1.76 | 0.00 | 2.63 | 1.19 | 85.75 |
| K | Std Error | 2wdry | T | 0.0 | 0.03 | 6.1 | 0.00 | 0.02 | 0.20 | 1.33 | 0.08 | 0.00 | 0.47 | 0.14 | 3.85 |
| A | Mean | 3wdry | T | 5.2 | 23.10 | 47.3 | 0.00 | 0.01 | 11.07 | 2.03 | 1.92 | 0.22 | 2.95 | 1.14 | 13.17 |
| A | Std Error | 3wdry | T | 0.0 | 0.12 | 7.0 | 0.00 | 0.01 | 1.67 | 0.79 | 0.35 | 0.09 | 0.21 | 0.36 | 2.81 |
| B | Mean | 3wdry | T | 5.2 | 23.30 | 112.0 | 0.00 | 0.28 | 13.83 | 8.12 | 2.36 | 0.08 | 4.43 | 2.76 | 39.39 |
| B | Std Error | 3wdry | T | 0.1 | 0.06 | 6.0 | 0.00 | 0.03 | 1.73 | 1.23 | 0.28 | 0.05 | 0.26 | 0.32 | 3.39 |
| E | Mean | 3wdry | T | 5.2 | 21.87 | 45.0 | 0.00 | 0.03 | 5.96 | 3.05 | 0.99 | 0.00 | 2.63 | 0.83 | 10.05 |
| E | Std Error | 3wdry | T | 0.1 | 0.03 | 7.1 | 0.00 | 0.02 | 1.06 | 0.80 | 0.08 | 0.00 | 0.53 | 0.21 | 2.45 |
| F | Mean | 3wdry | T | 5.1 | 24.33 | 113.0 | 0.00 | 0.22 | 15.02 | 12.50 | 2.02 | 0.00 | 5.03 | 2.32 | 33.27 |
| F | Std Error | 3wdry | T | 0.1 | 0.03 | 12.3 | 0.00 | 0.04 | 0.35 | 3.12 | 0.06 | 0.00 | 0.33 | 0.05 | 4.93 |
| I | Mean | 3wdry | T | 4.9 | 19.60 | 59.7 | 0.00 | 0.03 | 7.76 | 5.70 | 1.52 | 0.00 | 3.60 | 1.23 | 15.84 |
| I | Std Error | 3wdry | T | 0.1 | 0.00 | 9.7 | 0.00 | 0.03 | 0.90 | 2.04 | 0.14 | 0.00 | 0.77 | 0.20 | 3.80 |
| J | Mean | 3wdry | T | 4.9 | 21.50 | 107.7 | 0.00 | 0.15 | 14.19 | 12.85 | 2.00 | 0.00 | 2.84 | 1.70 | 55.48 |
| J | Std Error | 3wdry | T | 0.0 | 0.10 | 7.8 | 0.00 | 0.02 | 0.82 | 2.59 | 0.05 | 0.00 | 0.13 | 0.06 | 4.02 |

| Week | Sample | Cycle No | Loc | pH | Temp | Cond | Fe | Mn | Pb | Zn | Ca | Ni | NO$_3^-$ | Cl$^-$ | SO$_4^{2-}$ |
|---|---|---|---|---|---|---|---|---|---|---|---|---|---|---|---|
| | | | | | $^0$C | µS/s | mg/L | mg/L | mg/L | mg/L | mg/L | mg/L | mg/L | mg/L | mg/L |
| A | Mean | 2wwet | T | 5.4 | 22.30 | 50.3 | 0.00 | 0.00 | 11.26 | 3.09 | 1.93 | 0.06 | 2.95 | 1.02 | 14.13 |
| A | Std Error | 2wwet | T | 0.0 | 0.15 | 3.2 | 0.00 | 0.00 | 0.70 | 0.64 | 0.29 | 0.02 | 0.21 | 0.21 | 1.24 |
| C | Mean | 2wwet | T | 5.1 | 24.33 | 137.7 | 0.00 | 0.33 | 22.08 | 13.80 | 2.11 | 0.01 | 2.36 | 2.40 | 43.66 |
| C | Std Error | 2wwet | T | 0.0 | 0.03 | 9.0 | 0.00 | 0.06 | 1.20 | 3.11 | 0.07 | 0.01 | 0.46 | 0.38 | 4.23 |
| D | Mean | 2wwet | T | 5.2 | 22.27 | 36.0 | 0.00 | 0.00 | 12.54 | 0.06 | 0.70 | 0.03 | 0.15 | 0.47 | 6.75 |
| D | Std Error | 2wwet | T | 0.0 | 0.03 | 2.1 | 0.00 | 0.00 | 1.29 | 0.06 | 0.02 | 0.03 | 0.10 | 0.24 | 1.51 |
| F | Mean | 2wwet | T | 5.1 | 24.40 | 124.7 | 0.00 | 0.40 | 15.71 | 14.70 | 1.88 | 0.00 | 1.99 | 2.57 | 39.23 |
| F | Std Error | 2wwet | T | 0.0 | 0.06 | 12.2 | 0.00 | 0.01 | 0.56 | 2.92 | 0.12 | 0.00 | 0.41 | 0.29 | 3.35 |
| G | Mean | 2wwet | T | 5.3 | 23.03 | 39.0 | 0.00 | 0.06 | 6.08 | 2.84 | 0.72 | 0.00 | 0.83 | 1.72 | 14.65 |
| G | Std Error | 2wwet | T | 0.0 | 0.13 | 4.0 | 0.00 | 0.00 | 0.50 | 0.73 | 0.01 | 0.00 | 0.06 | 0.04 | 1.72 |
| I | Mean | 2wwet | T | 5.0 | 20.57 | 132.0 | 0.00 | 0.51 | 17.50 | 17.22 | 2.53 | 0.00 | 2.20 | 2.02 | 50.84 |
| I | Std Error | 2wwet | T | 0.0 | 0.17 | 11.0 | 0.00 | 0.08 | 0.56 | 3.33 | 0.09 | 0.00 | 0.38 | 0.13 | 4.57 |
| J | Mean | 2wwet | T | 5.1 | 21.30 | 45.3 | 0.00 | 0.06 | 7.44 | 3.54 | 0.93 | 0.00 | 0.72 | 1.58 | 28.21 |
| J | Std Error | 2wwet | T | 0.1 | 0.06 | 4.1 | 0.00 | 0.01 | 0.76 | 0.77 | 0.10 | 0.00 | 0.05 | 0.22 | 4.93 |
| L | Mean | 2wwet | T | 5.0 | 21.23 | 142.3 | 0.00 | 0.03 | 18.63 | 17.42 | 2.54 | 0.00 | 1.06 | 1.12 | 60.86 |
| L | Std Error | 2wwet | T | 0.0 | 0.03 | 7.1 | 0.00 | 0.03 | 0.83 | 2.87 | 0.06 | 0.00 | 0.12 | 0.13 | 2.14 |
| A | Mean | 3wwet | T | 5.6 | 22.60 | 55.3 | 0.00 | 0.00 | 7.24 | 2.03 | 2.19 | 0.16 | 4.72 | 2.80 | 15.75 |
| A | Std Error | 3wwet | T | 0.0 | 0.12 | 2.2 | 0.00 | 0.00 | 1.27 | 0.26 | 0.12 | 0.04 | 0.56 | 1.26 | 0.39 |
| D | Mean | 3wwet | T | 5.1 | 22.23 | 150.3 | 0.00 | 0.87 | 27.28 | 12.11 | 3.77 | 0.02 | 1.20 | 2.37 | 49.29 |
| D | Std Error | 3wwet | T | 0.0 | 0.20 | 3.8 | 0.00 | 0.11 | 1.80 | 0.77 | 0.03 | 0.02 | 0.69 | 0.14 | 1.53 |
| E | Mean | 3wwet | T | 5.3 | 22.00 | 39.3 | 0.01 | 0.09 | 6.96 | 1.95 | 0.84 | 0.00 | 0.11 | 0.48 | 9.20 |
| E | Std Error | 3wwet | T | 0.0 | 0.06 | 4.2 | 0.01 | 0.04 | 1.73 | 0.26 | 0.11 | 0.00 | 0.06 | 0.24 | 1.34 |
| H | Mean | 3wwet | T | 5.2 | 22.37 | 159.3 | 0.00 | 1.71 | 18.97 | 17.29 | 2.96 | 0.00 | 2.09 | 2.36 | 58.30 |
| H | Std Error | 3wwet | T | 0.1 | 0.09 | 2.7 | 0.00 | 0.27 | 0.93 | 0.13 | 0.10 | 0.00 | 0.59 | 0.15 | 1.26 |
| I | Mean | 3wwet | T | 5.1 | 20.60 | 51.0 | 0.00 | 0.26 | 9.45 | 3.60 | 1.43 | 0.00 | 0.84 | 0.65 | 5.11 |
| I | Std Error | 3wwet | T | 0.0 | 0.00 | 2.1 | 0.00 | 0.05 | 0.74 | 0.22 | 0.05 | 0.00 | 0.44 | 0.33 | 3.64 |
| L | Mean | 3wwet | T | 5.0 | 21.47 | 159.7 | 0.00 | 2.01 | 18.15 | 17.15 | 3.30 | 0.00 | 1.13 | 1.37 | 77.67 |
| L | Std Error | 3wwet | T | 0.0 | 0.07 | 5.2 | 0.00 | 0.58 | 1.03 | 1.08 | 0.18 | 0.00 | 0.19 | 0.38 | 4.06 |

| Week | Sample | Cycle No | Loc | pH | Temp $^0$C | Cond µS/s | Fe mg/L | Mn mg/L | Pb mg/L | Zn mg/L | Ca mg/L | Ni mg/L | $NO_3^-$ mg/L | $Cl^-$ mg/L | $SO_4^{2-}$ mg/L |
|---|---|---|---|---|---|---|---|---|---|---|---|---|---|---|---|
| A | Mean | Flood | T | 5.8 | 22.97 | 54.7 | 0.00 | 0.00 | 5.96 | 3.40 | 2.76 | 0.12 | 3.05 | 1.23 | 16.40 |
| A | Std Error | Flood | T | 0.0 | 0.09 | 4.3 | 0.00 | 0.00 | 0.71 | 1.00 | 0.63 | 0.01 | 0.57 | 0.06 | 1.52 |
| B | Mean | Flood | T | 5.3 | 23.60 | 112.3 | 0.00 | 0.24 | 16.60 | 9.12 | 3.04 | 0.18 | 3.07 | 2.18 | 38.04 |
| B | Std Error | Flood | T | 0.0 | 0.10 | 12.2 | 0.00 | 0.04 | 0.72 | 1.86 | 0.18 | 0.02 | 0.75 | 0.21 | 4.90 |
| C | Mean | Flood | T | 5.3 | 23.70 | 105.7 | 0.01 | 0.16 | 25.47 | 10.68 | 2.78 | 0.09 | 1.08 | 1.31 | 32.97 |
| C | Std Error | Flood | T | 0.0 | 0.00 | 7.9 | 0.01 | 0.04 | 1.47 | 1.95 | 0.15 | 0.03 | 0.34 | 0.08 | 3.88 |
| D | Mean | Flood | T | 5.3 | 22.23 | 114.7 | 0.00 | 0.29 | 25.28 | 9.97 | 3.30 | 0.03 | 0.64 | 1.67 | 37.10 |
| D | Std Error | Flood | T | 0.0 | 0.03 | 8.8 | 0.00 | 0.06 | 0.87 | 1.67 | 0.18 | 0.01 | 0.26 | 0.02 | 3.79 |
| E | Mean | Flood | T | 5.4 | 21.43 | 102.0 | 0.06 | 0.33 | 12.92 | 6.34 | 2.29 | 0.00 | 0.17 | 1.39 | 32.73 |
| E | Std Error | Flood | T | 0.0 | 0.03 | 7.1 | 0.03 | 0.06 | 0.68 | 1.71 | 0.08 | 0.00 | 0.10 | 0.06 | 3.13 |
| F | Mean | Flood | T | 5.3 | 24.50 | 109.3 | 0.00 | 0.52 | 14.28 | 11.23 | 2.38 | 0.00 | 0.93 | 2.43 | 38.10 |
| F | Std Error | Flood | T | 0.0 | 0.00 | 6.5 | 0.00 | 0.07 | 0.62 | 1.71 | 0.08 | 0.00 | 0.20 | 0.19 | 4.08 |
| G | Mean | Flood | T | 5.3 | 22.33 | 114.3 | 0.00 | 0.62 | 15.49 | 11.70 | 2.10 | 0.00 | 1.41 | 2.87 | 51.11 |
| G | Std Error | Flood | T | 0.0 | 0.03 | 7.2 | 0.00 | 0.06 | 0.51 | 1.96 | 0.06 | 0.00 | 0.22 | 0.09 | 8.26 |
| H | Mean | Flood | T | 5.0 | 22.43 | 118.0 | 0.00 | 0.80 | 15.55 | 13.12 | 2.58 | 0.00 | 1.49 | 2.37 | 42.08 |
| H | Std Error | Flood | T | 0.0 | 0.03 | 7.0 | 0.00 | 0.06 | 0.64 | 1.99 | 0.13 | 0.00 | 0.21 | 0.12 | 2.94 |
| I | Mean | Flood | T | 5.1 | 20.03 | 111.7 | 0.00 | 0.75 | 14.75 | 12.08 | 2.80 | 0.00 | 1.57 | 2.32 | 42.70 |
| I | Std Error | Flood | T | 0.0 | 0.07 | 4.9 | 0.00 | 0.08 | 0.62 | 1.77 | 0.08 | 0.00 | 0.12 | 0.07 | 3.91 |
| J | Mean | Flood | T | 5.1 | 21.50 | 103.0 | 0.00 | 0.78 | 15.52 | 10.17 | 2.34 | 0.00 | 1.41 | 2.61 | 64.70 |
| J | Std Error | Flood | T | 0.0 | 0.06 | 2.1 | 0.00 | 0.19 | 0.60 | 0.98 | 0.03 | 0.00 | 0.05 | 0.09 | 5.07 |
| K | Mean | Flood | T | 5.3 | 22.67 | 117.0 | 0.00 | 1.03 | 16.75 | 11.67 | 2.40 | 0.00 | 1.57 | 2.26 | 94.51 |
| K | Std Error | Flood | T | 0.1 | 0.03 | 5.0 | 0.00 | 0.15 | 0.38 | 1.50 | 0.07 | 0.00 | 0.09 | 0.27 | 7.01 |
| L | Mean | Flood | T | 5.1 | 21.50 | 107.3 | 0.00 | 1.01 | 16.10 | 10.48 | 2.41 | 0.00 | 0.78 | 1.48 | 67.93 |
| L | Std Error | Flood | T | 0.0 | 0.00 | 3.7 | 0.00 | 0.13 | 0.72 | 1.23 | 0.06 | 0.00 | 0.10 | 0.20 | 4.93 |

| Week | Sample | Cycle No | Loc | pH | Temp | Cond | Fe | Mn | Pb | Zn | Ca | Ni | $NO_3^-$ | $Cl^-$ | $SO_4^{2-}$ |
|---|---|---|---|---|---|---|---|---|---|---|---|---|---|---|---|
| | | | | | $^0$C | µS/s | mg/L | mg/L | mg/L | mg/L | mg/L | mg/L | mg/L | mg/L | mg/L |
| A | Mean | 1wwet | B | 5.2 | 23.67 | 112.3 | 0.00 | 0.25 | 15.45 | 12.67 | 3.47 | 0.21 | 6.99 | 1.27 | 35.37 |
| A | Std Error | 1wwet | B | 0.0 | 0.07 | 2.3 | 0.00 | 0.02 | 0.27 | 0.28 | 0.06 | 0.04 | 0.82 | 0.41 | 1.83 |
| B | Mean | 1wwet | B | 5.3 | 23.63 | 157.0 | 0.00 | 1.40 | 10.15 | 13.83 | 2.68 | 0.07 | 0.00 | 2.04 | 61.14 |
| B | Std Error | 1wwet | B | 0.0 | 0.03 | 1.0 | 0.00 | 0.11 | 0.76 | 0.01 | 0.05 | 0.03 | 0.00 | 0.27 | 0.73 |
| C | Mean | 1wwet | B | 5.2 | 24.73 | 127.7 | 0.00 | 0.57 | 14.18 | 11.09 | 2.74 | 0.00 | 5.60 | 1.44 | 37.72 |
| C | Std Error | 1wwet | B | 0.0 | 0.09 | 4.3 | 0.00 | 0.10 | 1.57 | 1.39 | 0.09 | 0.00 | 0.36 | 0.09 | 2.13 |
| D | Mean | 1wwet | B | 5.3 | 23.47 | 173.0 | 0.14 | 1.72 | 21.51 | 15.45 | 4.28 | 0.08 | 0.00 | 1.12 | 62.24 |
| D | Std Error | 1wwet | B | 0.0 | 0.03 | 2.5 | 0.08 | 0.09 | 1.91 | 0.15 | 0.10 | 0.03 | 0.00 | 0.04 | 0.75 |
| E | Mean | 1wwet | B | 5.3 | 22.13 | 122.3 | 0.00 | 0.88 | 10.78 | 9.46 | 2.65 | 0.00 | 1.89 | 0.55 | 30.47 |
| E | Std Error | 1wwet | B | 0.0 | 0.03 | 4.1 | 0.00 | 0.09 | 0.20 | 0.64 | 0.03 | 0.00 | 0.82 | 0.28 | 9.44 |
| F | Mean | 1wwet | B | 5.3 | 24.77 | 182.3 | 0.48 | 1.64 | 14.23 | 21.47 | 3.33 | 0.00 | 0.76 | 1.78 | 70.68 |
| F | Std Error | 1wwet | B | 0.0 | 0.03 | 3.2 | 0.28 | 0.07 | 0.31 | 0.16 | 0.04 | 0.00 | 0.41 | 0.14 | 4.08 |
| G | Mean | 1wwet | B | 5.3 | 23.33 | 126.7 | 0.00 | 0.91 | 11.02 | 14.92 | 2.61 | 0.00 | 3.62 | 1.81 | 52.07 |
| G | Std Error | 1wwet | B | 0.0 | 0.03 | 4.5 | 0.00 | 0.10 | 0.09 | 0.73 | 0.05 | 0.00 | 0.37 | 0.18 | 5.46 |
| H | Mean | 1wwet | B | 5.4 | 22.50 | 194.3 | 0.70 | 1.69 | 13.53 | 24.43 | 4.05 | 0.00 | 0.79 | 1.08 | 74.45 |
| H | Std Error | 1wwet | B | 0.0 | 0.06 | 3.8 | 0.48 | 0.03 | 0.34 | 0.23 | 0.10 | 0.00 | 0.42 | 0.10 | 0.98 |
| I | Mean | 1wwet | B | 5.2 | 20.80 | 145.7 | 0.00 | 1.09 | 10.43 | 17.90 | 3.82 | 0.00 | 3.00 | 1.04 | 53.80 |
| I | Std Error | 1wwet | B | 0.0 | 0.00 | 3.0 | 0.00 | 0.04 | 0.07 | 0.20 | 0.12 | 0.00 | 0.34 | 0.06 | 0.63 |
| J | Mean | 1wwet | B | 5.2 | 22.20 | 195.0 | 0.68 | 1.56 | 12.61 | 24.21 | 4.30 | 0.00 | 0.87 | 0.64 | 83.91 |
| J | Std Error | 1wwet | B | 0.0 | 0.00 | 6.0 | 0.27 | 0.06 | 0.05 | 0.12 | 0.15 | 0.00 | 0.44 | 0.34 | 8.46 |
| K | Mean | 1wwet | B | 5.3 | 23.63 | 133.0 | 0.00 | 0.77 | 9.91 | 15.56 | 3.25 | 0.00 | 2.46 | 0.16 | 84.51 |
| K | Std Error | 1wwet | B | 0.1 | 0.03 | 0.6 | 0.00 | 0.02 | 0.05 | 0.39 | 0.10 | 0.00 | 0.23 | 0.09 | 3.70 |
| L | Mean | 1wwet | B | 5.2 | 21.90 | 197.7 | 0.34 | 1.34 | 12.58 | 24.78 | 4.67 | 0.00 | 0.46 | 0.27 | 74.72 |
| L | Std Error | 1wwet | B | 0.7 | 0.00 | 5.8 | 0.22 | 0.05 | 0.42 | 0.37 | 0.19 | 0.00 | 0.28 | 0.08 | 2.16 |

277

| Week | Sample | Cycle No | Loc | pH | Temp | Cond | Fe | Mn | Pb | Zn | Ca | Ni | $NO_3^-$ | $Cl^-$ | $SO_4^{2-}$ |
|------|--------|----------|-----|-----|------|------|-----|-----|-----|-----|-----|-----|-----|-----|-----|
|  |  |  |  |  | $^0$C | μS/s | mg/L | mg/L | mg/L | mg/L | mg/L | mg/L | mg/L | mg/L | mg/L |
| A | Mean | 2wdry | B | 5.2 | 23.80 | 113.3 | 0.00 | 0.40 | 16.80 | 12.71 | 3.01 | 0.24 | 6.02 | 0.94 | 34.96 |
| A | Std Error | 2wdry | B | 0.0 | 0.06 | 0.9 | 0.00 | 0.07 | 0.44 | 0.24 | 0.16 | 0.02 | 0.53 | 0.07 | 1.50 |
| B | Mean | 2wdry | B | 5.2 | 23.80 | 152.7 | 0.00 | 1.73 | 14.51 | 14.17 | 2.20 | 0.04 | 0.08 | 1.42 | 58.95 |
| B | Std Error | 2wdry | B | 0.0 | 0.06 | 0.7 | 0.00 | 0.28 | 0.37 | 0.60 | 0.07 | 0.02 | 0.08 | 0.05 | 0.85 |
| D | Mean | 2wdry | B | 5.2 | 22.77 | 128.0 | 0.00 | 0.96 | 20.37 | 10.33 | 3.03 | 0.05 | 6.77 | 0.93 | 36.10 |
| D | Std Error | 2wdry | B | 0.0 | 0.09 | 1.0 | 0.00 | 0.11 | 0.77 | 0.66 | 0.19 | 0.00 | 0.14 | 0.07 | 0.61 |
| E | Mean | 2wdry | B | 5.3 | 21.77 | 183.0 | 0.19 | 1.68 | 14.42 | 17.59 | 3.13 | 0.00 | 3.38 | 1.11 | 65.48 |
| E | Std Error | 2wdry | B | 0.0 | 0.07 | 2.6 | 0.08 | 0.13 | 0.18 | 0.85 | 0.05 | 0.00 | 0.66 | 0.15 | 0.58 |
| G | Mean | 2wdry | B | 5.3 | 23.53 | 147.3 | 0.00 | 1.00 | 11.89 | 17.98 | 2.65 | 0.00 | 6.82 | 2.02 | 54.38 |
| G | Std Error | 2wdry | B | 0.0 | 0.09 | 1.9 | 0.00 | 0.13 | 0.08 | 0.53 | 0.05 | 0.00 | 0.46 | 0.03 | 0.18 |
| H | Mean | 2wdry | B | 5.4 | 22.63 | 206.0 | 1.04 | 1.55 | 13.71 | 27.78 | 3.86 | 0.00 | 3.56 | 1.23 | 79.16 |
| H | Std Error | 2wdry | B | 0.0 | 0.09 | 3.6 | 0.23 | 0.15 | 0.02 | 1.06 | 0.02 | 0.00 | 0.65 | 0.06 | 0.53 |
| J | Mean | 2wdry | B | 5.1 | 21.83 | 144.7 | 0.00 | 0.81 | 9.94 | 18.49 | 3.32 | 0.00 | 3.43 | 0.92 | 59.10 |
| J | Std Error | 2wdry | B | 0.0 | 0.03 | 1.9 | 0.00 | 0.11 | 0.12 | 0.22 | 0.08 | 0.00 | 1.67 | 0.48 | 14.33 |
| K | Mean | 2wdry | B | 5.2 | 23.67 | 212.0 | 1.05 | 1.46 | 12.93 | 27.50 | 4.34 | 0.00 | 3.49 | 1.45 | 132.79 |
| K | Std Error | 2wdry | B | 0.0 | 0.07 | 2.0 | 0.45 | 0.26 | 0.32 | 0.94 | 0.10 | 0.00 | 0.60 | 0.51 | 6.38 |
| A | Mean | 3wdry | B | 5.2 | 23.63 | 137.3 | 0.00 | 0.34 | 17.50 | 16.89 | 4.85 | 0.21 | 7.78 | 2.29 | 46.98 |
| A | Std Error | 3wdry | B | 0.0 | 0.09 | 1.8 | 0.00 | 0.05 | 0.75 | 0.48 | 0.17 | 0.08 | 0.59 | 0.81 | 0.28 |
| B | Mean | 3wdry | B | 5.3 | 23.97 | 170.7 | 0.30 | 1.95 | 12.96 | 16.22 | 2.70 | 0.11 | 0.00 | 1.99 | 66.56 |
| B | Std Error | 3wdry | B | 0.0 | 0.03 | 3.5 | 0.25 | 0.48 | 1.62 | 0.54 | 0.04 | 0.02 | 0.00 | 0.42 | 3.16 |
| E | Mean | 3wdry | B | 5.2 | 22.30 | 157.7 | 0.00 | 0.80 | 10.89 | 16.37 | 3.31 | 0.00 | 9.04 | 1.48 | 49.48 |
| E | Std Error | 3wdry | B | 0.0 | 0.06 | 8.9 | 0.00 | 0.20 | 0.14 | 1.28 | 0.06 | 0.00 | 1.48 | 0.18 | 2.60 |
| F | Mean | 3wdry | B | 5.3 | 25.03 | 217.3 | 0.00 | 1.31 | 13.23 | 28.40 | 4.10 | 0.00 | 3.43 | 2.00 | 78.34 |
| F | Std Error | 3wdry | B | 0.0 | 0.03 | 4.6 | 0.00 | 0.21 | 0.44 | 0.69 | 0.09 | 0.00 | 1.02 | 0.17 | 4.75 |
| I | Mean | 3wdry | B | 5.1 | 21.13 | 194.0 | 0.00 | 0.63 | 9.68 | 29.94 | 5.37 | 0.00 | 9.40 | 1.36 | 72.50 |
| I | Std Error | 3wdry | B | 0.0 | 0.03 | 12.2 | 0.00 | 0.14 | 0.16 | 2.40 | 0.24 | 0.00 | 0.95 | 0.09 | 5.07 |
| J | Mean | 3wdry | B | 5.1 | 22.30 | 237.0 | 0.16 | 0.95 | 11.49 | 35.75 | 5.60 | 0.00 | 4.01 | 1.67 | 118.87 |
| J | Std Error | 3wdry | B | 0.0 | 0.00 | 7.8 | 0.16 | 0.17 | 0.48 | 2.38 | 0.20 | 0.00 | 1.21 | 0.06 | 5.92 |

| Week | Sample | Cycle No | Loc | pH | Temp | Cond | Fe | Mn | Pb | Zn | Ca | Ni | NO$_3^-$ | Cl$^-$ | SO$_4^{2-}$ |
|---|---|---|---|---|---|---|---|---|---|---|---|---|---|---|---|
| | | | | | $^o$C | µS/s | mg/L | mg/L | mg/L | mg/L | mg/L | mg/L | mg/L | mg/L | mg/L |
| A | Mean | 2wwet | B | 5.2 | 23.10 | 140.0 | 0.00 | 0.36 | 17.81 | 15.85 | 4.17 | 0.09 | 8.72 | 1.24 | 43.25 |
| A | Std Error | 2wwet | B | 0.0 | 0.06 | 3.0 | 0.00 | 0.04 | 2.81 | 0.20 | 0.09 | 0.02 | 0.77 | 0.50 | 3.45 |
| C | Mean | 2wwet | B | 5.4 | 25.00 | 199.0 | 2.97 | 5.32 | 19.53 | 17.42 | 2.94 | 0.04 | 0.00 | 1.54 | 71.82 |
| C | Std Error | 2wwet | B | 0.0 | 0.10 | 5.9 | 0.52 | 0.39 | 0.49 | 1.25 | 0.18 | 0.02 | 0.00 | 0.18 | 3.28 |
| D | Mean | 2wwet | B | 5.3 | 22.83 | 153.0 | 0.00 | 4.03 | 17.72 | 11.64 | 3.46 | 0.05 | 6.24 | 1.05 | 46.30 |
| D | Std Error | 2wwet | B | 0.0 | 0.03 | 9.5 | 0.00 | 0.46 | 1.87 | 0.92 | 0.24 | 0.03 | 0.64 | 0.02 | 3.31 |
| F | Mean | 2wwet | B | 5.4 | 24.97 | 208.0 | 3.14 | 5.72 | 11.50 | 20.55 | 3.31 | 0.00 | 0.00 | 2.09 | 83.33 |
| F | Std Error | 2wwet | B | 0.0 | 0.03 | 6.0 | 0.28 | 0.49 | 0.36 | 0.38 | 0.12 | 0.00 | 0.00 | 0.07 | 3.14 |
| G | Mean | 2wwet | B | 5.4 | 23.73 | 154.7 | 0.00 | 3.85 | 10.69 | 15.88 | 2.60 | 0.00 | 4.95 | 1.91 | 58.38 |
| G | Std Error | 2wwet | B | 0.0 | 0.03 | 7.3 | 0.00 | 0.38 | 0.15 | 0.60 | 0.15 | 0.00 | 0.50 | 0.08 | 2.85 |
| I | Mean | 2wwet | B | 5.3 | 20.97 | 209.3 | 3.26 | 5.75 | 10.81 | 23.87 | 4.58 | 0.00 | 0.00 | 1.12 | 91.14 |
| I | Std Error | 2wwet | B | 0.0 | 0.03 | 7.1 | 0.30 | 0.56 | 0.52 | 0.54 | 0.14 | 0.00 | 0.00 | 0.13 | 1.93 |
| J | Mean | 2wwet | B | 5.2 | 22.07 | 149.7 | 0.00 | 3.58 | 9.49 | 16.25 | 3.31 | 0.00 | 4.02 | 1.20 | 76.38 |
| J | Std Error | 2wwet | B | 0.0 | 0.03 | 6.4 | 0.00 | 0.45 | 0.13 | 0.65 | 0.15 | 0.00 | 0.53 | 0.17 | 6.10 |
| L | Mean | 2wwet | B | 5.4 | 22.13 | 216.0 | 2.71 | 4.47 | 10.95 | 23.95 | 4.60 | 0.00 | 0.00 | 0.55 | 85.17 |
| L | Std Error | 2wwet | B | 0.0 | 0.07 | 4.6 | 0.18 | 0.47 | 0.43 | 0.36 | 0.19 | 0.00 | 0.00 | 0.04 | 7.54 |
| A | Mean | 3wwet | B | 5.4 | 23.27 | 129.3 | 0.00 | 0.42 | 11.18 | 12.84 | 4.03 | 0.16 | 6.66 | 2.19 | 43.88 |
| A | Std Error | 3wwet | B | 0.0 | 0.09 | 5.2 | 0.00 | 0.06 | 0.52 | 1.18 | 0.14 | 0.01 | 0.63 | 0.03 | 1.91 |
| D | Mean | 3wwet | B | 5.5 | 22.97 | 223.3 | 5.55 | 7.03 | 22.99 | 16.35 | 4.14 | 0.09 | 0.00 | 1.61 | 82.18 |
| D | Std Error | 3wwet | B | 0.0 | 0.09 | 2.3 | 0.99 | 0.17 | 1.10 | 0.78 | 0.08 | 0.01 | 0.00 | 0.15 | 1.55 |
| E | Mean | 3wwet | B | 5.5 | 22.50 | 143.7 | 0.15 | 4.62 | 8.99 | 8.05 | 2.68 | 0.00 | 1.90 | 1.24 | 47.82 |
| E | Std Error | 3wwet | B | 0.1 | 0.15 | 1.2 | 0.15 | 0.11 | 0.48 | 0.70 | 0.12 | 0.00 | 0.31 | 0.08 | 1.69 |
| H | Mean | 3wwet | B | 5.6 | 23.07 | 240.0 | 7.20 | 8.34 | 10.28 | 20.76 | 4.05 | 0.00 | 0.00 | 1.34 | 91.71 |
| H | Std Error | 3wwet | B | 0.0 | 0.07 | 12.0 | 1.47 | 0.63 | 0.36 | 0.96 | 0.07 | 0.00 | 0.00 | 0.15 | 4.91 |
| I | Mean | 3wwet | B | 5.3 | 21.07 | 140.3 | 0.00 | 4.94 | 9.41 | 13.27 | 3.40 | 0.00 | 2.34 | 1.09 | 51.72 |
| I | Std Error | 3wwet | B | 0.0 | 0.03 | 4.9 | 0.00 | 0.26 | 0.28 | 0.77 | 0.08 | 0.00 | 0.18 | 0.09 | 0.95 |
| L | Mean | 3wwet | B | 5.5 | 22.17 | 228.0 | 5.27 | 7.79 | 10.08 | 19.27 | 4.47 | 0.00 | 0.00 | 0.97 | 111.08 |
| L | Std Error | 3wwet | B | 0.0 | 0.03 | 8.1 | 1.17 | 0.32 | 0.22 | 1.07 | 0.13 | 0.00 | 0.00 | 0.15 | 6.42 |

| Week | Sample | Cycle No | Loc | pH | Temp | Cond | Fe | Mn | Pb | Zn | Ca | Ni | NO$_3^-$ | Cl$^-$ | SO$_4^{2-}$ |
|---|---|---|---|---|---|---|---|---|---|---|---|---|---|---|---|
| | | | | | $^0$C | µS/s | mg/L | mg/L | mg/L | mg/L | mg/L | mg/L | mg/L | mg/L | mg/L |
| A | Mean | Flood | B | 5.2 | 23.50 | 149.3 | 0.00 | 0.62 | 12.27 | 17.53 | 5.13 | 0.14 | 7.56 | 1.96 | 53.23 |
| A | Std Error | Flood | B | 0.1 | 0.06 | 6.6 | 0.00 | 0.22 | 1.21 | 1.16 | 0.55 | 0.01 | 0.55 | 0.56 | 3.81 |
| B | Mean | Flood | B | 5.3 | 24.27 | 168.3 | 0.24 | 2.01 | 16.47 | 14.96 | 2.98 | 0.18 | 0.00 | 1.48 | 62.43 |
| B | Std Error | Flood | B | 0.1 | 0.03 | 3.4 | 0.08 | 0.40 | 0.10 | 0.60 | 0.13 | 0.03 | 0.00 | 0.48 | 1.30 |
| C | Mean | Flood | B | 5.4 | 24.50 | 196.7 | 2.35 | 5.02 | 24.73 | 17.62 | 3.68 | 0.15 | 0.00 | 1.32 | 71.79 |
| C | Std Error | Flood | B | 0.0 | 0.06 | 7.2 | 0.53 | 0.61 | 1.93 | 0.40 | 0.23 | 0.03 | 0.00 | 0.09 | 3.32 |
| D | Mean | Flood | B | 5.4 | 23.03 | 225.0 | 4.95 | 7.26 | 19.81 | 16.37 | 4.43 | 0.10 | 0.00 | 1.47 | 84.98 |
| D | Std Error | Flood | B | 0.0 | 0.03 | 10.6 | 1.02 | 0.74 | 0.82 | 0.58 | 0.33 | 0.01 | 0.00 | 0.09 | 4.25 |
| E | Mean | Flood | B | 5.5 | 22.00 | 243.7 | 6.60 | 9.03 | 9.59 | 15.17 | 3.92 | 0.00 | 0.00 | 1.63 | 96.98 |
| E | Std Error | Flood | B | 0.1 | 0.00 | 12.1 | 1.41 | 0.74 | 0.14 | 0.28 | 0.27 | 0.00 | 0.00 | 0.13 | 5.88 |
| F | Mean | Flood | B | 5.5 | 24.97 | 261.3 | 8.53 | 11.42 | 9.18 | 19.59 | 4.19 | 0.00 | 0.00 | 2.50 | 105.65 |
| F | Std Error | Flood | B | 0.1 | 0.03 | 17.1 | 1.78 | 1.29 | 0.43 | 0.46 | 0.35 | 0.00 | 0.00 | 0.11 | 7.62 |
| G | Mean | Flood | B | 5.7 | 23.33 | 281.7 | 10.81 | 12.27 | 8.59 | 19.68 | 3.91 | 0.00 | 0.00 | 2.69 | 141.26 |
| G | Std Error | Flood | B | 0.1 | 0.03 | 18.5 | 1.91 | 1.27 | 0.50 | 0.54 | 0.36 | 0.00 | 0.00 | 0.11 | 9.64 |
| H | Mean | Flood | B | 5.4 | 23.17 | 287.3 | 13.02 | 13.73 | 7.50 | 20.43 | 4.94 | 0.00 | 0.00 | 1.77 | 122.27 |
| H | Std Error | Flood | B | 0.1 | 0.03 | 21.7 | 2.84 | 1.32 | 0.49 | 0.49 | 0.44 | 0.00 | 0.00 | 0.06 | 11.82 |
| I | Mean | Flood | B | 5.5 | 20.93 | 299.7 | 13.55 | 14.16 | 5.99 | 20.02 | 5.78 | 0.00 | 0.00 | 2.01 | 139.49 |
| I | Std Error | Flood | B | 0.1 | 0.03 | 18.2 | 2.87 | 1.26 | 0.61 | 0.54 | 0.51 | 0.00 | 0.00 | 0.09 | 11.79 |
| J | Mean | Flood | B | 5.4 | 22.07 | 284.3 | 13.51 | 12.49 | 5.91 | 16.94 | 4.97 | 0.00 | 0.00 | 2.87 | 176.59 |
| J | Std Error | Flood | B | 0.1 | 0.03 | 17.6 | 3.15 | 0.96 | 0.70 | 0.36 | 0.41 | 0.00 | 0.00 | 0.52 | 18.13 |
| K | Mean | Flood | B | 5.6 | 23.33 | 293.3 | 16.96 | 13.15 | 5.69 | 16.10 | 4.96 | 0.00 | 0.00 | 2.20 | 226.82 |
| K | Std Error | Flood | B | 0.1 | 0.07 | 21.9 | 4.66 | 1.19 | 0.66 | 0.40 | 0.42 | 0.00 | 0.00 | 0.16 | 27.46 |
| L | Mean | Flood | B | 5.6 | 22.27 | 292.3 | 16.24 | 14.24 | 5.09 | 15.92 | 5.23 | 0.00 | 0.00 | 1.66 | 155.10 |
| L | Std Error | Flood | B | 0.1 | 0.03 | 26.3 | 5.74 | 1.50 | 0.71 | 0.31 | 0.41 | 0.00 | 0.00 | 0.19 | 17.77 |

| Week | Sample | Cycle No | Loc | pH | Temp | Cond | Fe | Mn | Pb | Zn | Ca | Ni | NO$_3^-$ | Cl$^-$ | SO$_4^{2-}$ |
|---|---|---|---|---|---|---|---|---|---|---|---|---|---|---|---|
| | | | | | $^0$C | μS/s | mg/L | mg/L | mg/L | mg/L | mg/L | mg/L | mg/L | mg/L | mg/L |
| A | Mean | F/C | B | 5.3 | 23.73 | 81.7 | 0.00 | 0.09 | 9.34 | 4.29 | 2.21 | 0.18 | 3.47 | 1.34 | 19.52 |
| A | Std Error | F/C | B | 0.0 | 0.09 | 24.3 | 0.00 | 0.05 | 1.99 | 0.64 | 0.32 | 0.03 | 0.38 | 0.17 | 2.04 |
| B | Mean | F/C | B | 5.3 | 23.70 | 69.3 | 0.00 | 0.32 | 11.45 | 5.36 | 1.49 | 0.22 | 3.16 | 1.05 | 22.74 |
| B | Std Error | F/C | B | 0.0 | 0.00 | 5.0 | 0.00 | 0.05 | 0.25 | 0.42 | 0.12 | 0.03 | 0.46 | 0.11 | 1.14 |
| C | Mean | F/C | B | 5.2 | 24.30 | 93.3 | 0.00 | 0.29 | 22.78 | 8.63 | 1.98 | 0.00 | 3.15 | 0.65 | 22.74 |
| C | Std Error | F/C | B | 0.0 | 0.10 | 9.5 | 0.00 | 0.08 | 0.57 | 0.14 | 0.36 | 0.00 | 0.33 | 0.41 | 2.59 |
| D | Mean | F/C | B | 5.3 | 23.67 | 76.3 | 0.00 | 0.38 | 18.72 | 6.69 | 1.91 | 0.06 | 2.49 | 0.64 | 23.62 |
| D | Std Error | F/C | B | 0.0 | 0.12 | 9.1 | 0.00 | 0.15 | 0.58 | 0.76 | 0.18 | 0.01 | 0.61 | 0.23 | 3.53 |
| E | Mean | F/C | B | 5.3 | 21.67 | 77.0 | 0.19 | 0.50 | 6.73 | 5.11 | 1.76 | 0.00 | 2.57 | 1.00 | 32.55 |
| E | Std Error | F/C | B | 0.0 | 0.09 | 6.7 | 0.16 | 0.18 | 0.58 | 0.54 | 0.16 | 0.00 | 0.38 | 0.23 | 1.00 |
| F | Mean | F/C | B | 5.3 | 24.93 | 86.7 | 0.00 | 0.59 | 9.96 | 11.87 | 2.08 | 0.00 | 3.27 | 1.76 | 38.32 |
| F | Std Error | F/C | B | 0.0 | 0.03 | 9.1 | 0.00 | 0.21 | 0.10 | 1.32 | 0.14 | 0.00 | 0.27 | 0.09 | 3.44 |
| G | Mean | F/C | B | 5.2 | 22.63 | 77.3 | 0.00 | 0.40 | 7.61 | 7.94 | 1.79 | 0.00 | 2.34 | 2.54 | 34.00 |
| G | Std Error | F/C | B | 0.0 | 0.13 | 7.8 | 0.00 | 0.16 | 1.16 | 1.06 | 0.27 | 0.00 | 0.30 | 0.62 | 3.78 |
| H | Mean | F/C | B | 5.3 | 21.73 | 74.7 | 0.00 | 0.41 | 6.71 | 8.65 | 1.74 | 0.00 | 1.77 | 3.58 | 26.07 |
| H | Std Error | F/C | B | 0.1 | 0.18 | 5.2 | 0.00 | 0.14 | 0.58 | 0.46 | 0.08 | 0.00 | 0.32 | 0.83 | 2.08 |
| I | Mean | F/C | B | 5.2 | 21.37 | 61.0 | 0.00 | 0.30 | 6.02 | 7.38 | 1.83 | 0.00 | 1.45 | 0.82 | 22.25 |
| I | Std Error | F/C | B | 0.0 | 0.12 | 7.0 | 0.00 | 0.11 | 0.90 | 1.13 | 0.20 | 0.00 | 0.28 | 0.05 | 3.21 |
| J | Mean | F/C | B | 5.1 | 22.10 | 74.3 | 0.12 | 0.27 | 7.19 | 8.30 | 1.80 | 0.00 | 1.80 | 1.09 | 55.63 |
| J | Std Error | F/C | B | 0.0 | 0.06 | 10.4 | 0.12 | 0.09 | 1.67 | 1.58 | 0.22 | 0.00 | 0.47 | 0.14 | 9.33 |
| K | Mean | F/C | B | 5.3 | 23.23 | 78.7 | 0.05 | 0.37 | 7.94 | 8.05 | 1.80 | 0.00 | 1.61 | 0.66 | 72.31 |
| K | Std Error | F/C | B | 0.0 | 0.03 | 6.7 | 0.04 | 0.10 | 0.68 | 1.12 | 0.16 | 0.00 | 0.41 | 0.02 | 9.49 |
| L | Mean | F/C | B | 5.2 | 21.57 | 84.7 | 0.00 | 0.37 | 7.35 | 9.64 | 2.20 | 0.00 | 0.95 | 0.38 | 65.07 |
| L | Std Error | F/C | B | 0.0 | 0.03 | 5.6 | 0.00 | 0.09 | 0.46 | 0.44 | 0.17 | 0.00 | 0.15 | 0.11 | 3.95 |

# Appendix 4.3.1 Sequential extraction average Fe, Pb, Zn and Mn mg/kg with % standard error (n=3) by grain size, top and bottom of the mesocosm

Fe (mg/kg) with standard error % recovered from extraction A – D, by run, for < 2 mm and < 63 µm grain size sediment fractions at the top (T) and bottom (B) of the mesocosms.

| Fe | | | | < 2 mm > 63 µm | | | | | | < 63 µm | | | |
|----|-------|---------|---------|---------|---------|---------|---------|---------|---------|---------|---------|---------|---------|
| | Ext % | Initial | F/C | Flood | 1wwet | 3wdry | 3wwet | Initial | F/C | Flood | 1wwet | 3wdry | 3wwet |
| | A | 3198.7 | 1062.3 | 1869.8 | 25840.1 | 29380.1 | 2641.4 | 15520.0 | 15990.8 | 10513.6 | 7844.1 | 7538.9 | 6322.1 |
| | Err% | 43.8 | 57.5 | 87.0 | 18.4 | 10.2 | 87.0 | 18.2 | 12.2 | 21.8 | 9.5 | 9.9 | 4.3 |
| | B | 215.3 | 212.9 | 227.1 | 281.5 | 340.7 | 224.0 | 778.8 | 836.3 | 1087.5 | 1092.2 | 982.8 | 1110.0 |
| | Err% | 23.6 | 12.0 | 5.1 | 10.0 | 25.8 | 32.2 | 5.7 | 2.0 | 6.8 | 0.7 | 5.0 | 2.4 |
| T | C | 6309.8 | 8343.6 | 8763.1 | 5821.8 | 9901.7 | 7862.5 | 18247.9 | 22447.6 | 23183.2 | 19400.9 | 20459.2 | 22381.1 |
| | Err% | 12.0 | 12.0 | 7.4 | 9.8 | 21.4 | 26.5 | 10.1 | 3.4 | 0.7 | 2.0 | 3.4 | 5.2 |
| | D | 10373.0 | 12189.4 | 12282.8 | 12186.4 | 12664.6 | 10952.5 | 11988.9 | 13040.3 | 14910.9 | 15216.4 | 14290.1 | 12499.0 |
| | Err% | 9.6 | 7.4 | 3.8 | 2.5 | 8.6 | 7.5 | 7.7 | 2.8 | 0.5 | 3.9 | 5.6 | 5.0 |
| | Total | 20096.9 | 21808.2 | 23142.8 | 44129.9 | 52287.1 | 21680.4 | 46535.6 | 52315.0 | 49695.2 | 43553.6 | 43271.0 | 42312.2 |
| | A | 3198.7 | 1062.3 | 2378.4 | 24287.3 | 29204.8 | 17924.4 | 15520.0 | 15990.8 | 7628.4 | 7485.7 | 7512.6 | 7467.9 |
| | Err% | 43.8 | 57.5 | 12.5 | 0.2 | 9.6 | 49.4 | 18.2 | 12.2 | 5.9 | 2.0 | 3.5 | 17.4 |
| | B | 215.3 | 212.9 | 315.0 | 228.3 | 269.2 | 221.3 | 778.8 | 836.3 | 867.2 | 1095.9 | 1062.0 | 1068.6 |
| | Err% | 23.6 | 12.0 | 0.9 | 1.4 | 11.3 | 8.0 | 5.7 | 2.0 | 4.0 | 3.4 | 5.5 | 3.4 |
| B | C | 6309.8 | 8343.6 | 5371.2 | 5494.8 | 7320.2 | 5502.2 | 18247.9 | 22447.6 | 21819.6 | 20541.6 | 22360.4 | 21640.6 |
| | Err% | 12.0 | 12.0 | 2.9 | 27.4 | 6.5 | 18.3 | 10.1 | 3.4 | 5.1 | 2.9 | 3.1 | 6.7 |
| | D | 10373.0 | 12189.4 | 12540.3 | 13899.7 | 11089.0 | 10691.1 | 11988.9 | 13040.3 | 15878.4 | 14573.0 | 14769.8 | 14125.2 |
| | Err% | 9.6 | 7.4 | 3.2 | 11.4 | 13.1 | 19.0 | 7.7 | 2.8 | 4.7 | 0.7 | 2.7 | 2.9 |
| | Total | 20096.9 | 21808.2 | 20604.9 | 43910.1 | 47883.2 | 34339.0 | 46535.6 | 52315.0 | 46193.6 | 43696.3 | 45704.8 | 44302.2 |

Pb (mg/kg) with standard error % recovered from extraction A – D, by run, for < 2 mm and < 63 µm grain size sediment fractions at the top (T) and bottom (B) of the mesocosms.

| Pb | | | | < 2 mm > 63 µm | | | | | | < 63 µm | | | |
|----|-------|---------|---------|---------|---------|---------|---------|---------|---------|---------|---------|---------|---------|
| | Ext % | Initial | F/C | Flood | 1wwet | 3wdry | 3wwet | Initial | F/C | Flood | 1wwet | 3wdry | 3wwet |
| | A | 10776.3 | 10867.3 | 8737.4 | 12265.0 | 11750.7 | 8712.2 | 52914.2 | 45871.4 | 52189.5 | 50853.2 | 54391.4 | 37707.9 |
| | Err% | 14.2 | 13.9 | 12.4 | 33.8 | 6.4 | 25.6 | 7.3 | 7.2 | 8.1 | 2.2 | 16.7 | 9.3 |
| | B | 1462.0 | 2736.3 | 2366.0 | 3444.3 | 2727.2 | 3116.3 | 35768.2 | 38234.0 | 36067.8 | 44230.4 | 35598.7 | 41616.1 |
| | Err% | 9.4 | 35.2 | 18.3 | 46.0 | 3.2 | 25.5 | 6.3 | 6.4 | 6.5 | 3.2 | 1.6 | 12.6 |
| T | C | 2.8 | 50.4 | 2.1 | 6.1 | 33.5 | 21.4 | 362.5 | 173.2 | 320.7 | 443.7 | 430.2 | 396.4 |
| | Err% | 56.8 | 79.6 | 4.3 | 275.5 | 13.0 | 70.6 | 34.9 | 24.8 | 2.0 | 6.0 | 19.6 | 8.2 |
| | D | 1425.0 | 4718.7 | 2652.2 | 4813.8 | 3633.7 | 4977.3 | 2205.4 | 11363.8 | 7538.0 | 11622.3 | 11410.0 | 15960.1 |
| | Err% | 74.4 | 63.2 | 14.0 | 77.5 | 62.4 | 16.3 | 20.0 | 16.7 | 22.7 | 9.7 | 62.5 | 14.9 |
| | Total | 13666.1 | 18372.7 | 13757.8 | 20529.2 | 18145.1 | 16827.2 | 91250.3 | 95642.4 | 96116.0 | 107149.6 | 101830.3 | 95680.5 |
| | A | 10776.3 | 10867.3 | 13250.1 | 11673.8 | 11389.0 | 5334.8 | 52914.2 | 45871.4 | 49252.3 | 48802.3 | 46686.2 | 36678.4 |
| | Err% | 14.2 | 13.9 | 4.0 | 51.6 | 27.2 | 19.5 | 7.3 | 7.2 | 3.0 | 2.7 | 9.2 | 11.3 |
| | B | 1462.0 | 2736.3 | 1828.2 | 5776.7 | 1641.1 | 823.0 | 35768.2 | 38234.0 | 28220.8 | 28889.8 | 29265.7 | 30730.4 |
| | Err% | 9.4 | 35.2 | 39.7 | 94.5 | 37.2 | 25.1 | 6.3 | 6.4 | 10.3 | 6.4 | 4.2 | 9.9 |
| B | C | 2.8 | 50.4 | 24.9 | 24.3 | 41.4 | 23.7 | 362.5 | 173.2 | 429.5 | 282.9 | 342.5 | 419.1 |
| | Err% | 56.8 | 79.6 | 53.1 | 99.3 | 3.3 | 10.3 | 34.9 | 24.8 | 2.6 | 1.7 | 18.0 | 9.7 |
| | D | 1425.0 | 4718.7 | 1757.7 | 11470.8 | 779.7 | 540.6 | 2205.4 | 11363.8 | 5929.6 | 4899.3 | 4676.9 | 4358.4 |
| | Err% | 74.4 | 63.2 | 67.0 | 99.0 | 102.1 | 53.0 | 20.0 | 16.7 | 10.4 | 19.3 | 4.1 | 28.8 |
| | Total | 13666.1 | 18372.7 | 16860.9 | 28945.6 | 13851.2 | 6722.1 | 91250.3 | 95642.4 | 83832.3 | 82874.4 | 80971.2 | 72186.3 |

**Zn (mg/kg) with standard error % recovered from extraction A – D, by run, for < 2 mm and < 63 µm grain size sediment fractions at the top (T) and bottom (B) of the mesocosms.**

| Zn | | <2 mm > 63 µm | | | | | | < 63 µm | | | | | |
|---|---|---|---|---|---|---|---|---|---|---|---|---|---|
| | Ext % | Initial | F/C | Flood | 1wwet | 3wdry | 3wwet | Initial | F/C | Flood | 1wwet | 3wdry | 3wwet |
| | A | 413.7 | 291.5 | 197.2 | 293.6 | 300.4 | 333.7 | 585.4 | 521.6 | 469.7 | 548.5 | 496.3 | 519.3 |
| | Err% | 23.9 | 15.2 | 2.6 | 6.4 | 15.2 | 26.2 | 11.0 | 2.9 | 6.5 | 0.9 | 3.8 | 2.7 |
| | B | 151.3 | 108.3 | 155.7 | 165.1 | 173.4 | 144.4 | 155.4 | 151.4 | 176.9 | 221.6 | 218.6 | 208.8 |
| | Err% | 3.3 | 7.3 | 17.1 | 19.1 | 8.6 | 16.1 | 10.1 | 9.2 | 1.9 | 7.6 | 6.4 | 6.8 |
| T | C | 262.2 | 229.9 | 88.8 | 155.1 | 176.8 | 122.4 | 440.5 | 472.5 | 519.9 | 421.6 | 393.6 | 477.5 |
| | Err% | 34.7 | 44.1 | 7.3 | 7.1 | 24.7 | 24.0 | 14.1 | 2.0 | 0.5 | 7.6 | 2.2 | 9.5 |
| | D | 1639.3 | 976.3 | 1036.4 | 1156.7 | 2659.0 | 735.5 | 710.0 | 565.6 | 669.2 | 510.4 | 629.5 | 581.3 |
| | Err% | 45.0 | 51.5 | 40.3 | 40.3 | 32.6 | 37.5 | 11.0 | 3.0 | 2.6 | 1.2 | 15.6 | 2.8 |
| | Total | 2466.5 | 1606.1 | 1478.1 | 1770.4 | 3309.7 | 1336.0 | 1891.3 | 1711.1 | 1835.7 | 1702.1 | 1737.9 | 1786.9 |
| | A | 413.7 | 291.5 | 281.2 | 267.5 | 308.0 | 277.1 | 585.4 | 521.6 | 569.7 | 639.1 | 690.5 | 607.4 |
| | Err% | 23.9 | 15.2 | 5.1 | 6.8 | 5.5 | 9.8 | 11.0 | 2.9 | 1.4 | 1.0 | 5.6 | 2.9 |
| | B | 151.3 | 108.3 | 150.5 | 212.3 | 148.0 | 178.5 | 155.4 | 151.4 | 206.6 | 223.6 | 245.6 | 228.5 |
| | Err% | 3.3 | 7.3 | 14.0 | 15.2 | 4.7 | 5.6 | 10.1 | 9.2 | 9.9 | 10.3 | 16.6 | 4.1 |
| B | C | 262.2 | 229.9 | 69.5 | 55.6 | 104.3 | 51.3 | 440.5 | 472.5 | 507.5 | 449.2 | 496.9 | 498.9 |
| | Err% | 34.7 | 44.1 | 22.9 | 41.3 | 24.2 | 29.2 | 14.1 | 2.0 | 4.4 | 3.1 | 4.0 | 7.7 |
| | D | 1639.3 | 976.3 | 235.5 | 323.2 | 509.8 | 1434.0 | 710.0 | 565.6 | 560.5 | 460.4 | 426.9 | 534.4 |
| | Err% | 45.0 | 51.5 | 34.8 | 45.7 | 43.1 | 74.5 | 11.0 | 3.0 | 2.1 | 3.9 | 4.1 | 2.8 |
| | Total | 2466.5 | 1606.1 | 736.6 | 858.6 | 1070.1 | 1940.9 | 1891.3 | 1711.1 | 1844.3 | 1772.2 | 1859.9 | 1869.1 |

**Mn (mg/kg) with standard error % recovered from extraction A – D, by run, for < 2 mm and < 63 µm grain size sediment fractions at the top (T) and bottom (B) of the mesocosms.**

| Mn | | <2 mm > 63 µm | | | | | | < 63 µm | | | | | |
|---|---|---|---|---|---|---|---|---|---|---|---|---|---|
| | Ext % | Initial | F/C | Flood | 1wwet | 3wdry | 3wwet | Initial | F/C | Flood | 1wwet | 3wdry | 3wwet |
| | A | 32.3 | 8.0 | 11.4 | 25.8 | 21.5 | 14.1 | 159.4 | 201.3 | 107.2 | 135.5 | 124.0 | 86.1 |
| | Err% | 24.3 | 18.4 | 7.5 | 22.2 | 46.1 | 53.0 | 9.7 | 28.0 | 3.9 | 2.5 | 9.3 | 4.5 |
| | B | 53.3 | 50.9 | 109.2 | 29.9 | 73.0 | 73.9 | 108.6 | 60.7 | 199.6 | 182.1 | 185.4 | 159.8 |
| | Err% | 68.8 | 24.8 | 35.6 | 31.6 | 43.9 | 80.3 | 7.6 | 96.6 | 6.0 | 8.8 | 8.7 | 0.7 |
| T | C | 6.7 | 3.4 | 12.4 | 2.7 | 0.2 | 9.8 | 0.0 | 11.5 | 14.5 | 6.2 | 10.4 | 17.7 |
| | Err% | 86.7 | 100.0 | 60.6 | 100.0 | 100.0 | 50.0 | | 23.3 | 10.1 | 11.2 | 38.1 | 14.2 |
| | D | 143.1 | 190.9 | 200.1 | 171.3 | 184.7 | 190.5 | 157.4 | 180.1 | 213.9 | 202.2 | 179.7 | 194.0 |
| | Err% | 11.2 | 2.7 | 4.6 | 8.4 | 8.0 | 13.1 | 8.6 | 4.5 | 2.1 | 2.0 | 9.2 | 3.7 |
| | Total | 235.5 | 253.2 | 333.2 | 229.7 | 279.4 | 288.4 | 425.5 | 453.6 | 535.0 | 525.9 | 499.6 | 457.6 |
| | A | 32.3 | 8.0 | 27.3 | 17.3 | 8.8 | 16.5 | 159.4 | 201.3 | 75.9 | 113.9 | 93.2 | 64.2 |
| | Err% | 24.3 | 18.4 | 5.9 | 31.4 | 67.6 | 36.0 | 9.7 | 28.0 | 5.2 | 1.2 | 3.1 | 5.0 |
| | B | 53.3 | 50.9 | 0.0 | 0.0 | 21.7 | 0.0 | 108.6 | 60.7 | 0.0 | 32.2 | 68.7 | 5.4 |
| | Err% | 68.8 | 24.8 | | | 34.2 | | 7.6 | 96.6 | | 5.6 | 3.6 | 100.0 |
| B | C | 6.7 | 3.4 | 0.0 | 0.0 | 1.0 | 0.0 | 0.0 | 11.5 | 1.4 | 5.9 | 12.1 | 10.6 |
| | Err% | 86.7 | 100.0 | | | 100.0 | | | 23.3 | 50.2 | 23.7 | 14.6 | 14.5 |
| | D | 143.1 | 190.9 | 177.1 | 196.5 | 145.8 | 162.6 | 157.4 | 180.1 | 226.9 | 209.7 | 208.5 | 196.8 |
| | Err% | 11.2 | 2.7 | 1.3 | 17.3 | 20.4 | 17.8 | 8.6 | 4.5 | 1.6 | 1.5 | 3.0 | 2.2 |
| | Total | 235.5 | 253.2 | 204.4 | 213.9 | 177.3 | 179.1 | 425.5 | 453.6 | 304.2 | 361.7 | 382.5 | 276.9 |

## Appendix 4.3.2 X-Ray diffraction for Identification of Galena and Sphalerite standards



### Raw data

| | | | | | | | |
|---|---|---|---|---|---|---|---|
| Sample | : galena | X-ray | : Cu / 30 kV / 15 mA | Counter | : Miniflex counter | | |
| File | : SL_2705H.RAW | Goniometer | : Miniflex goniometer | | | | |
| Comment | : | Attachment | : Standard sample holder | | | | |
| Date | : May-27-14 15:40:24 | Filter | : Kb filter | Scan mode | : Continuous | | |
| Operator | : Sarah L | I.Monochro | : Not used | Scan speed | : 2.000 deg./min. | | |
| | | C.Monochro | : Not used | Sampling width | : 0.010 deg. | | |
| | | Divergence slit | : Variable | Scan axis | : 2theta/theta | | |
| | | Scattering slit | : 4.2deg | Scan range | : 20.000 -> 85.000 deg. | | |
| | | Receiving slit | : 0.3mm | Theta offset | : 0.000 deg. | | |

Memo :

May-27-2014 17:11:19 Page-1

**X-ray diffraction pattern for a crystal standard of Galena (PbS) showing intensity maximas as a function of 2Θ angle. Maximas occur where Bragg's conditions is satisfied**



### Raw data

| | | | | | | | |
|---|---|---|---|---|---|---|---|
| Sample | : sphalerite | X-ray | : Cu / 30 kV / 15 mA | Counter | : Miniflex counter | | |
| File | : SL_2705G.RAW | Goniometer | : Miniflex goniometer | | | | |
| Comment | : | Attachment | : Standard sample holder | | | | |
| Date | : May-27-14 15:02:38 | Filter | : Kb filter | Scan mode | : Continuous | | |
| Operator | : Sarah L. | I.Monochro | : Not used | Scan speed | : 2.000 deg./min. | | |
| | | C.Monochro | : Not used | Sampling width | : 0.010 deg. | | |
| | | Divergence slit | : Variable | Scan axis | : 2theta/theta | | |
| | | Scattering slit | : 4.2deg | Scan range | : 5.000 -> 85.000 deg. | | |
| | | Receiving slit | : 0.3mm | Theta offset | : 0.000 deg. | | |

Memo :

May-27-2014 17:10:35 Page-1

**X-ray diffraction pattern for a crystal standard of sphalerite (ZnS) showing intensity maximas as a function of 2Θ angle. Maximas occur where Bragg's conditions is satisfied**

284

## Appendix 4.3.4

## Results from ANOVA  Post Hoc Tukey Tests Fe (bottom)

**Multiple Comparisons**

Dependent Variable: mgkg

Tukey HSD

| (I) Group | (J) Group | Mean Difference (I-J) | Std. Error | Sig. | 95% Confidence Interval Lower Bound | Upper Bound |
|---|---|---|---|---|---|---|
| 1 | 2 | -57.510 | 56.589 | .904 | -247.59 | 132.57 |
|  | 3 | -88.350 | 56.589 | .636 | -278.43 | 101.73 |
|  | 4 | -317.120* | 56.589 | .001 | -507.20 | -127.04 |
|  | 5 | -283.120* | 56.589 | .003 | -473.20 | -93.04 |
|  | 6 | -289.730* | 56.589 | .003 | -479.81 | -99.65 |
| 2 | 1 | 57.510 | 56.589 | .904 | -132.57 | 247.59 |
|  | 3 | -30.840 | 56.589 | .993 | -220.92 | 159.24 |
|  | 4 | -259.610* | 56.589 | .006 | -449.69 | -69.53 |
|  | 5 | -225.610* | 56.589 | .017 | -415.69 | -35.53 |
|  | 6 | -232.220* | 56.589 | .014 | -422.30 | -42.14 |
| 3 | 1 | 88.350 | 56.589 | .636 | -101.73 | 278.43 |
|  | 2 | 30.840 | 56.589 | .993 | -159.24 | 220.92 |
|  | 4 | -228.770* | 56.589 | .016 | -418.85 | -38.69 |
|  | 5 | -194.770* | 56.589 | .044 | -384.85 | -4.69 |
|  | 6 | -201.380* | 56.589 | .036 | -391.46 | -11.30 |
| 4 | 1 | 317.120* | 56.589 | .001 | 127.04 | 507.20 |
|  | 2 | 259.610* | 56.589 | .006 | 69.53 | 449.69 |
|  | 3 | 228.770* | 56.589 | .016 | 38.69 | 418.85 |
|  | 5 | 34.000 | 56.589 | .989 | -156.08 | 224.08 |
|  | 6 | 27.390 | 56.589 | .996 | -162.69 | 217.47 |
| 5 | 1 | 283.120* | 56.589 | .003 | 93.04 | 473.20 |
|  | 2 | 225.610* | 56.589 | .017 | 35.53 | 415.69 |
|  | 3 | 194.770* | 56.589 | .044 | 4.69 | 384.85 |
|  | 4 | -34.000 | 56.589 | .989 | -224.08 | 156.08 |
|  | 6 | -6.610 | 56.589 | 1.000 | -196.69 | 183.47 |
| 6 | 1 | 289.730* | 56.589 | .003 | 99.65 | 479.81 |
|  | 2 | 232.220* | 56.589 | .014 | 42.14 | 422.30 |
|  | 3 | 201.380* | 56.589 | .036 | 11.30 | 391.46 |
|  | 4 | -27.390 | 56.589 | .996 | -217.47 | 162.69 |
|  | 5 | 6.610 | 56.589 | 1.000 | -183.47 | 196.69 |

*. The mean difference is significant at the 0.05 level.

**Appendix 4.3.4 cont.**

**Results from ANOVA Post Hoc Tukey Tests Zn (bottom)**

**Multiple Comparisons**

Dependent Variable: mgkg

Tukey HSD

| (I) Group | (J) Group | Mean Difference (I-J) | Std. Error | Sig. | 95% Confidence Interval | |
|---|---|---|---|---|---|---|
| | | | | | Lower Bound | Upper Bound |
| 1 | 2 | 3.973 | 23.089 | .998 | -69.97 | 77.91 |
| | 4 | -68.183 | 23.089 | .071 | -142.12 | 5.76 |
| | 6 | -73.090 | 23.089 | .053 | -147.03 | .85 |
| 2 | 1 | -3.973 | 23.089 | .998 | -77.91 | 69.97 |
| | 4 | -72.157 | 23.089 | .056 | -146.10 | 1.78 |
| | 6 | -77.063$^{*}$ | 23.089 | .041 | -151.00 | -3.12 |
| 4 | 1 | 68.183 | 23.089 | .071 | -5.76 | 142.12 |
| | 2 | 72.157 | 23.089 | .056 | -1.78 | 146.10 |
| | 6 | -4.907 | 23.089 | .996 | -78.85 | 69.03 |
| 6 | 1 | 73.090 | 23.089 | .053 | -.85 | 147.03 |
| | 2 | 77.063$^{*}$ | 23.089 | .041 | 3.12 | 151.00 |
| | 4 | 4.907 | 23.089 | .996 | -69.03 | 78.85 |

*. The mean difference is significant at the 0.05 level.

286

**Appendix 4.3.4 cont.**

**Results from ANOVA  Post Hoc Tukey Tests Fe (top)**

**Multiple Comparisons**

Dependent Variable: mgkg

Tukey HSD

| (I) Group | (J) Group | Mean Difference (I-J) | Std. Error | Sig. | 95% Confidence Interval | |
|---|---|---|---|---|---|---|
| | | | | | Lower Bound | Upper Bound |
| 1 | 2 | -57.510 | 60.431 | .925 | -260.49 | 145.47 |
| | 3 | -308.677* | 60.431 | .003 | -511.66 | -105.69 |
| | 4 | -313.370* | 60.431 | .002 | -516.35 | -110.39 |
| | 5 | -203.987* | 60.431 | .049 | -406.97 | -1.00 |
| | 6 | -331.217* | 60.431 | .002 | -534.20 | -128.23 |
| 2 | 1 | 57.510 | 60.431 | .925 | -145.47 | 260.49 |
| | 3 | -251.167* | 60.431 | .013 | -454.15 | -48.18 |
| | 4 | -255.860* | 60.431 | .011 | -458.84 | -52.88 |
| | 5 | -146.477 | 60.431 | .222 | -349.46 | 56.51 |
| | 6 | -273.707* | 60.431 | .007 | -476.69 | -70.72 |
| 3 | 1 | 308.677* | 60.431 | .003 | 105.69 | 511.66 |
| | 2 | 251.167* | 60.431 | .013 | 48.18 | 454.15 |
| | 4 | -4.693 | 60.431 | 1.000 | -207.68 | 198.29 |
| | 5 | 104.690 | 60.431 | .538 | -98.29 | 307.67 |
| | 6 | -22.540 | 60.431 | .999 | -225.52 | 180.44 |
| 4 | 1 | 313.370* | 60.431 | .002 | 110.39 | 516.35 |
| | 2 | 255.860* | 60.431 | .011 | 52.88 | 458.84 |
| | 3 | 4.693 | 60.431 | 1.000 | -198.29 | 207.68 |
| | 5 | 109.383 | 60.431 | .495 | -93.60 | 312.37 |
| | 6 | -17.847 | 60.431 | 1.000 | -220.83 | 185.14 |
| 5 | 1 | 203.987* | 60.431 | .049 | 1.00 | 406.97 |
| | 2 | 146.477 | 60.431 | .222 | -56.51 | 349.46 |
| | 3 | -104.690 | 60.431 | .538 | -307.67 | 98.29 |
| | 4 | -109.383 | 60.431 | .495 | -312.37 | 93.60 |
| | 6 | -127.230 | 60.431 | .346 | -330.21 | 75.75 |
| 6 | 1 | 331.217* | 60.431 | .002 | 128.23 | 534.20 |
| | 2 | 273.707* | 60.431 | .007 | 70.72 | 476.69 |
| | 3 | 22.540 | 60.431 | .999 | -180.44 | 225.52 |
| | 4 | 17.847 | 60.431 | 1.000 | -185.14 | 220.83 |
| | 5 | 127.230 | 60.431 | .346 | -75.75 | 330.21 |

*. The mean difference is significant at the 0.05 level.

## Appendix 4.3.4 cont.

## Results from ANOVA  Post Hoc Tukey Tests Zn (top)

**Multiple Comparisons**

Dependent Variable: mgkg

Tukey HSD

| (I) Group | (J) Group | Mean Difference (I-J) | Std. Error | Sig. | 95% Confidence Interval | |
|-----------|-----------|-----------------------|------------|------|-------------|-------------|
|           |           |                       |            |      | Lower Bound | Upper Bound |
|           | 2 | 3.973 | 19.473 | 1.000 | -61.43 | 69.38 |
|           | 3 | -21.473 | 19.473 | .871 | -86.88 | 43.93 |
| 1         | 4 | -66.220* | 19.473 | .047 | -131.63 | -.81 |
|           | 5 | -63.173 | 19.473 | .061 | -128.58 | 2.23 |
|           | 6 | -53.440 | 19.473 | .136 | -118.85 | 11.97 |
|           | 1 | -3.973 | 19.473 | 1.000 | -69.38 | 61.43 |
|           | 3 | -25.447 | 19.473 | .776 | -90.85 | 39.96 |
| 2         | 4 | -70.193* | 19.473 | .033 | -135.60 | -4.79 |
|           | 5 | -67.147* | 19.473 | .043 | -132.55 | -1.74 |
|           | 6 | -57.413 | 19.473 | .098 | -122.82 | 7.99 |
|           | 1 | 21.473 | 19.473 | .871 | -43.93 | 86.88 |
|           | 2 | 25.447 | 19.473 | .776 | -39.96 | 90.85 |
| 3         | 4 | -44.747 | 19.473 | .266 | -110.15 | 20.66 |
|           | 5 | -41.700 | 19.473 | .330 | -107.11 | 23.71 |
|           | 6 | -31.967 | 19.473 | .590 | -97.37 | 33.44 |
|           | 1 | 66.220* | 19.473 | .047 | .81 | 131.63 |
|           | 2 | 70.193* | 19.473 | .033 | 4.79 | 135.60 |
| 4         | 3 | 44.747 | 19.473 | .266 | -20.66 | 110.15 |
|           | 5 | 3.047 | 19.473 | 1.000 | -62.36 | 68.45 |
|           | 6 | 12.780 | 19.473 | .984 | -52.63 | 78.19 |
|           | 1 | 63.173 | 19.473 | .061 | -2.23 | 128.58 |
|           | 2 | 67.147* | 19.473 | .043 | 1.74 | 132.55 |
| 5         | 3 | 41.700 | 19.473 | .330 | -23.71 | 107.11 |
|           | 4 | -3.047 | 19.473 | 1.000 | -68.45 | 62.36 |
|           | 6 | 9.733 | 19.473 | .995 | -55.67 | 75.14 |
|           | 1 | 53.440 | 19.473 | .136 | -11.97 | 118.85 |
|           | 2 | 57.413 | 19.473 | .098 | -7.99 | 122.82 |
| 6         | 3 | 31.967 | 19.473 | .590 | -33.44 | 97.37 |
|           | 4 | -12.780 | 19.473 | .984 | -78.19 | 52.63 |
|           | 5 | -9.733 | 19.473 | .995 | -75.14 | 55.67 |

*. The mean difference is significant at the 0.05 level.

**Appendix 4.3.4 cont.**

**Results from ANOVA  Post Hoc Tukey Tests Mn (top)**

**Multiple Comparisons**

Dependent Variable: mgkg

Tukey HSD

| (I) Group | (J) Group | Mean Difference (I-J) | Std. Error | Sig. | 95% Confidence Interval | |
|---|---|---|---|---|---|---|
| | | | | | Lower Bound | Upper Bound |
| 1 | 4 | -73.403$^*$ | 17.191 | .012 | -128.45 | -18.35 |
| | 5 | -76.797$^*$ | 17.191 | .009 | -131.85 | -21.75 |
| | 6 | -51.167 | 17.191 | .069 | -106.22 | 3.88 |
| 4 | 1 | 73.403$^*$ | 17.191 | .012 | 18.35 | 128.45 |
| | 5 | -3.393 | 17.191 | .997 | -58.44 | 51.66 |
| | 6 | 22.237 | 17.191 | .591 | -32.81 | 77.29 |
| 5 | 1 | 76.797$^*$ | 17.191 | .009 | 21.75 | 131.85 |
| | 4 | 3.393 | 17.191 | .997 | -51.66 | 58.44 |
| | 6 | 25.630 | 17.191 | .485 | -29.42 | 80.68 |
| 6 | 1 | 51.167 | 17.191 | .069 | -3.88 | 106.22 |
| | 4 | -22.237 | 17.191 | .591 | -77.29 | 32.81 |
| | 5 | -25.630 | 17.191 | .485 | -80.68 | 29.42 |

*. The mean difference is significant at the 0.05 level.

**Appendix 4.3.4 cont. Results from ANOVA post hoc Tukey test for Pb, variable runs top and bottom of the mesocosm (1, 2, 3) 1 week wet, 3 week dry, 3 week wet, respectively at the bottom (4, 5, 6) 1 week wet, 3 week dry, 3 week wet at the top.**

**Multiple Comparisons**

Dependent Variable: mgkg

Tukey HSD

| (I) Group | (J) Group | Mean Difference (I-J) | Std. Error | Sig. | 95% Confidence Interval | |
|---|---|---|---|---|---|---|
| | | | | | Lower Bound | Upper Bound |
| 1 | 2 | -375.909 | 3824.425 | 1.000 | -13221.85 | 12470.03 |
| | 3 | -1840.611 | 3824.425 | .996 | -14686.55 | 11005.33 |
| | 4 | -15340.613* | 3824.425 | .017 | -28186.55 | -2494.67 |
| | 5 | -6708.905 | 3824.425 | .526 | -19554.85 | 6137.04 |
| | 6 | -12726.344 | 3824.425 | .053 | -25572.28 | 119.60 |
| 2 | 1 | 375.909 | 3824.425 | 1.000 | -12470.03 | 13221.85 |
| | 3 | -1464.702 | 3824.425 | .999 | -14310.64 | 11381.24 |
| | 4 | -14964.704* | 3824.425 | .020 | -27810.64 | -2118.76 |
| | 5 | -6332.996 | 3824.425 | .581 | -19178.94 | 6512.95 |
| | 6 | -12350.435 | 3824.425 | .062 | -25196.38 | 495.51 |
| 3 | 1 | 1840.611 | 3824.425 | .996 | -11005.33 | 14686.55 |
| | 2 | 1464.702 | 3824.425 | .999 | -11381.24 | 14310.64 |
| | 4 | -13500.001* | 3824.425 | .038 | -26345.94 | -654.06 |
| | 5 | -4868.294 | 3824.425 | .794 | -17714.23 | 7977.65 |
| | 6 | -10885.732 | 3824.425 | .116 | -23731.67 | 1960.21 |
| 4 | 1 | 15340.613* | 3824.425 | .017 | 2494.67 | 28186.55 |
| | 2 | 14964.704* | 3824.425 | .020 | 2118.76 | 27810.64 |
| | 3 | 13500.001* | 3824.425 | .038 | 654.06 | 26345.94 |
| | 5 | 8631.708 | 3824.425 | .282 | -4214.23 | 21477.65 |
| | 6 | 2614.269 | 3824.425 | .980 | -10231.67 | 15460.21 |
| 5 | 1 | 6708.905 | 3824.425 | .526 | -6137.04 | 19554.85 |
| | 2 | 6332.996 | 3824.425 | .581 | -6512.95 | 19178.94 |
| | 3 | 4868.294 | 3824.425 | .794 | -7977.65 | 17714.23 |
| | 4 | -8631.708 | 3824.425 | .282 | -21477.65 | 4214.23 |
| | 6 | -6017.439 | 3824.425 | .629 | -18863.38 | 6828.50 |
| 6 | 1 | 12726.344 | 3824.425 | .053 | -119.60 | 25572.28 |
| | 2 | 12350.435 | 3824.425 | .062 | -495.51 | 25196.38 |
| | 3 | 10885.732 | 3824.425 | .116 | -1960.21 | 23731.67 |
| | 4 | -2614.269 | 3824.425 | .980 | -15460.21 | 10231.67 |
| | 5 | 6017.439 | 3824.425 | .629 | -6828.50 | 18863.38 |

*. The mean difference is significant at the 0.05 level.

**Appendix 4.3.4 cont. Results from ANOVA post hoc Tukey test for Mn, variable runs top and bottom of the mesocosm (1, 2) 1 week wet, 3 week dry respectively at the bottom (3, 4) 1 week wet, 3 week dry at the top.**

**Multiple Comparisons**

Dependent Variable: Run_analysed

Tukey HSD

| (I) VAR00001 | (J) VAR00001 | Mean Difference (I-J) | Std. Error | Sig. | 95% Confidence Interval | |
|---|---|---|---|---|---|---|
| | | | | | Lower Bound | Upper Bound |
| 1.00 | 2.00 | -36.4500 | 16.2952 | .193 | -88.633 | 15.733 |
| | 3.00 | -149.8367* | 16.2952 | .000 | -202.020 | -97.654 |
| | 4.00 | -153.2300* | 16.2952 | .000 | -205.413 | -101.047 |
| 2.00 | 1.00 | 36.4500 | 16.2952 | .193 | -15.733 | 88.633 |
| | 3.00 | -113.3867* | 16.2952 | .001 | -165.570 | -61.204 |
| | 4.00 | -116.7800* | 16.2952 | .000 | -168.963 | -64.597 |
| 3.00 | 1.00 | 149.8367* | 16.2952 | .000 | 97.654 | 202.020 |
| | 2.00 | 113.3867* | 16.2952 | .001 | 61.204 | 165.570 |
| | 4.00 | -3.3933 | 16.2952 | .997 | -55.576 | 48.790 |
| 4.00 | 1.00 | 153.2300* | 16.2952 | .000 | 101.047 | 205.413 |
| | 2.00 | 116.7800* | 16.2952 | .000 | 64.597 | 168.963 |
| | 3.00 | 3.3933 | 16.2952 | .997 | -48.790 | 55.576 |

*. The mean difference is significant at the 0.05 level.

## Appendix 5.2.3 Spectroquant sulphide test (1.14779.0001) titration method

Reagents purchased from Merck as described below:

Iodine Solution ($I_2$)  0.05 mol/L  solution
approx. 1000 ppm sodium sulphide hydrate 60% for analysis
Sodium thiosulfate solution 0.1 mol/L solution
Sulphuric acid 25% for analysis
Zinc iodide-starch solution for analysis


In a fume cupboard in a nitrogen bag

0.5 g of 60% $Na_2S.H_2O$ was weighed out and added to a 100 ml deoxygenated DIW in a glass volumetric – to make up approximately 1000 ppm standard of aqueous sulphide (Merck, 2013).

100 ml DIW and 5 ml 25 % sulphuric acid were added to a 500 ml glass volumetric.
Add 25 ml of 1000 ppm sulphide stock to the volumetric followed by
25 ml of 0.05 mol/L iodine solution. Mix the contents of volumetric for 1 minute.

Titrate with 0.1 mol/L sodium thiosulfate solution until the yellow iodine colour disappeared.

Add 1 ml zinc iodide-starch solution and then continue to titrate until a milky, pure white colour emerges.

Calculation of exact concentration of the sulphide stock :

C1 = consumption of sodium thiosulfate 0.1 mol/L via titration

C2 = quantity of iodine solution 0.05 mol/L (25 ml)

mg/L sulphide = C2 – C1 x 64.13 (dilution factor)

Further quality standards were then calculated once the exact concentration of the sulphide stock was known. All standards were considered acceptable if within 5%.

## Appendix 5.3 Raw pore water data for Top (T) and (B) Bottom of the mesocosm

| Loc | Sample# | Week | pH | Cond | Temp | D.O. | Redox | Cl | Nitrate | Sulphate | Na | K | Ca | TIC | DOC | Pb | Zn | Mn | Fe |
|-----|---------|------|-----|------|------|------|-------|--------|---------|----------|----|----|----|------|-------|-------|-------|------|------|
| T | 1 | A | 5.65 | 148 | 18.2 | 113 | 517 | 1.98 | 1.65 | 4.93 | 1 | 1 | 0 | 1.00 | 2.63 | 2.32 | 4.97 | 0.02 | 0.06 |
| T | 4 | A | 5.63 | 125 | 18.6 | 114 | 519 | 2.92 | 2.58 | 13.29 | 2 | 0 | 3 | 1.28 | 2.67 | 2.01 | 4.88 | 0.01 | 0.02 |
| T | 7 | A | 5.65 | 117 | 18.3 | 114 | 526 | 3.84 | 2.23 | 13.32 | 3 | 1 | 4 | | 1.77 | 2.07 | 4.23 | 0.02 | 0.03 |
| T | 10 | A | 5.78 | 86 | 18.6 | 112 | 526 | 3.32 | 1.35 | 13.21 | 3 | 0 | 1 | 0.67 | 2.43 | 2.51 | 4.79 | 0.01 | 0.02 |
| T | 1 | B | 5.54 | 258 | 15.7 | 109 | 527 | 7.67 | 2.53 | 19.28 | 2 | 4 | 1 | 0.37 | 2.70 | 7.99 | 14.32 | 0.07 | 0.02 |
| T | 4 | B | | | | | | | | | | | | | | | | | |
| T | 7 | B | 5.71 | 186 | 16.2 | 105 | 492 | 1.27 | 1.20 | 9.15 | 1 | 0 | 2 | 0.33 | 1.94 | 6.70 | 13.12 | 0.04 | 0.02 |
| T | 10 | B | 5.77 | 162 | 16.2 | 106 | 497 | 1.85 | 1.08 | 14.10 | 1 | 0 | 1 | 0.62 | 2.21 | 7.20 | 14.16 | 0.03 | 0.02 |
| T | 1 | C | 5.6 | 665 | 17.9 | 113 | 453 | 193.48 | 0.77 | 8.40 | 11 | 1 | 3 | 4.22 | 12.79 | 0.09 | 3.17 | 0.01 | 0.03 |
| T | 4 | C | | | | | | | | | | | | | | | | | |
| T | 7 | C | | | | | | | | | | | | | | | | | |
| T | 10 | C | 5.66 | 365 | 18.2 | 111 | 485 | 27.58 | 1.07 | 34.76 | 12 | 25 | 7 | 1.41 | 4.91 | 5.00 | 18.49 | 0.03 | 0.00 |
| T | 1 | D | 5.56 | 373 | 17.5 | 79 | 481 | 6.53 | 2.77 | 63.92 | 0 | 0 | 8 | 1.11 | 2.75 | 8.34 | 29.22 | 0.07 | 0.00 |
| T | 4 | D | 5.73 | 210 | 17.1 | 81 | 468 | 4.02 | 1.19 | 52.86 | 7 | 1 | 7 | 1.11 | 2.78 | 7.51 | 27.04 | 0.05 | 0.09 |
| T | 7 | D | | | | | | | | | | | | | | | | | |
| T | 10 | D | 5.75 | 187 | 17.5 | 99 | 468 | 2.33 | 0.63 | 22.50 | 3 | 0 | 1 | 0.93 | 2.61 | 6.93 | 21.50 | 0.03 | 0.05 |
| T | 1 | E | 5.7 | 71 | 16.1 | 93 | 455 | 2.01 | 0.52 | 4.94 | 2 | 0 | 0 | 0.82 | 2.35 | 3.55 | 3.92 | 0.01 | 0.04 |
| T | 4 | E | 5.8 | 90 | 16.8 | 101 | 475 | 2.61 | 0.56 | 4.08 | 4 | 0 | 0 | 1.70 | 2.53 | 1.24 | 2.59 | 0.01 | 0.07 |
| T | 7 | E | 5.76 | 85 | 17 | 108 | 482 | 3.14 | 0.57 | 6.42 | 3 | 0 | 0 | 0.67 | 2.64 | 2.25 | 2.88 | 0.01 | 0.05 |
| T | 10 | E | 5.41 | 176 | 16.5 | 102 | 472 | 2.10 | 0.29 | 8.74 | 3 | 0 | 0 | 0.62 | 2.44 | 7.18 | 9.61 | 0.02 | 0.17 |
| T | 1 | F | 5.7 | 173 | 16.3 | 102 | 459 | 2.43 | 1.19 | 9.31 | 2 | 0 | 1 | 0.63 | 1.86 | 8.14 | 12.40 | 0.04 | 0.05 |
| T | 4 | F | | | | | | | | | | | | | | | | | |
| T | 7 | F | 5.67 | 170 | 16.5 | 99 | 479 | 1.37 | 0.08 | 8.75 | 2 | 0 | 0 | 0.50 | 1.86 | 6.50 | 15.04 | 0.03 | 0.05 |
| T | 10 | F | 5.7 | 180 | 16.1 | 103 | 476 | 1.48 | 0.00 | 7.00 | 2 | 0 | 1 | 0.50 | 1.86 | 7.26 | 13.02 | 0.03 | 0.09 |
| T | 1 | G | 5.3 | 103 | 18.2 | 108 | 565 | 1.01 | 0.14 | 3.08 | 1 | 0 | 2 | 0.46 | 1.89 | 3.48 | 3.58 | 0.01 | 0.04 |
| T | 4 | G | | | | | | | | | | | | | | | | | |
| T | 7 | G | | | | | | | | | | | | | | | | | |
| T | 10 | G | 5.5 | 254 | 17.7 | 106 | 555 | 2.64 | 0.18 | 15.23 | 3 | 0 | 0 | 0.19 | 2.05 | 8.02 | 24.47 | 0.20 | 0.03 |
| T | 1 | H | 5.39 | 174 | 18 | 106 | 473 | 23.45 | 1.12 | 8.45 | 3 | 1 | 0 | 0.93 | 3.15 | 9.17 | 12.00 | 0.08 | 0.00 |
| T | 4 | H | 5.58 | 276 | 18.4 | 101 | 477 | 1.62 | 1.71 | 19.34 | 4 | 0 | 4 | 0.70 | 3.00 | 14.23 | 23.79 | 0.08 | 2.05 |
| T | 7 | H | | | | | | | | | | | | | | | | | |
| T | 10 | H | 5.8 | 385 | 19 | 95 | 446 | 1.62 | 0.70 | 42.83 | 13 | 1 | 14 | 0.98 | 3.13 | 13.18 | 42.24 | 0.36 | 0.00 |
| T | 1 | I | 5.24 | 44 | 17.9 | 103 | 545 | 2.02 | 0.00 | 3.27 | 4 | 0 | 1 | 0.78 | 1.81 | 2.33 | 1.37 | 0.01 | 0.03 |
| T | 4 | I | 5.52 | 43 | 17.9 | 100 | 534 | 2.27 | 0.05 | 4.24 | 5 | 0 | 1 | 1.03 | 1.70 | 1.10 | 2.00 | 0.01 | 0.05 |
| T | 7 | I | 5.18 | 35 | 18 | 100 | 534 | 1.07 | 0.06 | 1.88 | 2 | 0 | 1 | 0.91 | 1.52 | 0.51 | 1.53 | 0.01 | 0.00 |
| T | 10 | I | 5.65 | 336 | 17.3 | 100 | 503 | 8.91 | 2.09 | 59.45 | 8 | 1 | 10 | 0.25 | 1.92 | 15.02 | 39.76 | 0.46 | 0.00 |
| T | 1 | J | 5.1 | 148 | 20.1 | 106 | 603 | 2.26 | 0.15 | 25.33 | 4 | 1 | 2 | 1.01 | 2.06 | 7.96 | 10.06 | 0.01 | 0.00 |
| T | 4 | J | | | | | | | | | | | | | | | | | |
| T | 7 | J | 5.5 | 170 | 20.3 | 101 | 525 | 2.48 | 0.57 | 35.18 | 6 | 0 | 4 | 0.90 | 2.02 | 5.00 | 16.27 | 0.02 | 0.00 |
| T | 10 | J | 5.64 | 416 | 20.3 | 98 | 492 | 25.26 | 1.04 | 115.27 | 22 | 1 | 18 | 1.00 | 2.66 | 9.46 | 47.18 | 0.71 | 0.00 |
| T | 1 | L | | | | | | | | | | | | | | | | | |
| T | 4 | L | 5.38 | 206 | 19.6 | 101 | 504 | 6.37 | 0.43 | 35.78 | 5 | 0 | 3 | 0.70 | 1.90 | 8.20 | 17.68 | 0.03 | 0.00 |

| Loc | Sample# | Week | pH | Cond | Temp | D.O. | Redox | Cl | Nitrate | Sulphate | Na | K | Ca | TIC | DOC | Pb | Zn | Mn | Fe |
|---|---|---|---|---|---|---|---|---|---|---|---|---|---|---|---|---|---|---|---|
| B | 3 | A | 5.8 | 327 | 18.7 | 108 | 530 | 3.82 | 6.17 | 155.53 | 3 | 1 | 12 | 0.80 | 3.15 | 4.34 | 39.39 | 0.12 | 0.05 |
| B | 6 | A | 5.82 | 310 | 18.6 | 89 | 510 | 1.08 | 1.81 | 52.65 | 2 | 0 | 8 | 0.40 | 4.76 | 4.78 | 40.47 | 1.00 | 0.05 |
| B | 9 | A | 5.83 | 274 | 19 | 99 | 506 | 0.86 | 1.48 | 44.72 | 1 | 0 | 2 | 0.56 | 2.63 | 4.88 | 42.36 | 0.11 | 0.02 |
| B | 12 | A | 5.77 | 299 | 19.2 | 89 | 522 | 2.75 | 3.72 | 123.87 | 3 | 1 | 10 | 0.42 | 2.83 | 4.91 | 43.26 | 1.00 | 0.04 |
| B | 3 | B | 5.73 | 362 | 16.4 | 10 | 483 | 2.78 | 2.29 | 113.79 | 3 | 1 | 12 | 0.60 | 3.33 | 5.57 | 50.04 | 0.23 | 0.05 |
| B | 6 | B | | | | | | | | | | | | | | | | | |
| B | 9 | B | 5.73 | 338 | 16.3 | 13 | 486 | 3.41 | 2.26 | 125.93 | 4 | 1 | 13 | 0.97 | 3.83 | 4.27 | 47.46 | 0.23 | 0.08 |
| B | 12 | B | 5.73 | 342 | 16.5 | 11 | 482 | 3.06 | 0.47 | 116.75 | 4 | 1 | 14 | 1.06 | 3.33 | 4.76 | 49.17 | 1.00 | 0.05 |
| B | 3 | C | 5.65 | 410 | 18 | 110 | 498 | 6.47 | 2.24 | 90.71 | 9 | 2 | 13 | 0.93 | 3.93 | 2.28 | 40.83 | 0.13 | 0.02 |
| B | 6 | C | | | | | | | | | | | | | | | | | |
| B | 9 | C | | | | | | | | | | | | | | | | | |
| B | 12 | C | 5.64 | 438 | 18.3 | 14 | 485 | 5.25 | 0.00 | 126.97 | 15 | 1 | 17 | 3.80 | 4.80 | 4.08 | 45.65 | 1.57 | 0.58 |
| B | 3 | D | 5.81 | 435 | 17.6 | 43 | 457 | 4.84 | 2.07 | 114.01 | 7 | 1 | 14 | 1.77 | 3.15 | 3.78 | 51.97 | 0.21 | 0.05 |
| B | 6 | D | 5.79 | 359 | 17.5 | 8 | 436 | 3.96 | 0.20 | 116.55 | 9 | 1 | 14 | 2.29 | 4.23 | 2.29 | 49.26 | 2.20 | 0.11 |
| B | 9 | D | | | | | | | | | | | | | | | | | |
| B | 12 | D | 5.77 | 354 | 17.8 | 12 | 435 | 1.83 | 0.00 | 63.51 | 5 | 0 | 9 | 2.06 | 3.17 | 2.82 | 57.64 | 2.96 | 0.13 |
| B | 3 | E | 5.8 | 256 | 17.2 | 100 | 474 | 2.62 | 1.25 | 53.64 | 4 | 1 | 7 | 1.05 | 3.06 | 2.49 | 38.14 | 0.05 | 0.08 |
| B | 6 | E | 5.84 | 278 | 17.3 | 105 | 482 | 2.83 | 2.29 | 75.70 | 5 | 1 | 10 | 0.69 | 3.17 | 2.55 | 41.42 | 1.00 | 0.06 |
| B | 9 | E | 5.74 | 297 | 17.4 | 110 | 487 | 2.61 | 2.05 | 76.84 | 5 | 0 | 11 | 0.94 | 3.61 | 3.12 | 45.69 | 0.06 | 0.05 |
| B | 12 | E | 5.76 | 434 | 17.1 | 8 | 422 | 1.80 | 0.00 | 81.09 | 4 | 0 | 13 | 2.18 | 3.78 | 3.81 | 52.95 | 3.84 | 0.24 |
| B | 3 | F | 5.7 | 336 | 16.5 | 43 | 469 | 2.57 | 1.13 | 78.66 | 4 | 1 | 8 | 0.93 | 2.40 | 4.74 | 57.70 | 0.09 | 0.08 |
| B | 6 | F | | | | | | | | | | | | | | | | | |
| B | 9 | F | 5.69 | 393 | 16.5 | 46 | 479 | 1.44 | 1.03 | 90.00 | 3 | 0 | 12 | 0.75 | 2.55 | 6.95 | 67.63 | 0.05 | 0.16 |
| B | 12 | F | 5.78 | 470 | 16.5 | 10 | 396 | 17.46 | 0.00 | 75.56 | 17 | 1 | 13 | 2.13 | 3.67 | 3.51 | 50.76 | 4.49 | 0.23 |
| B | 3 | G | 5.6 | 259 | 18.5 | 106 | 512 | 1.85 | 0.54 | 40.01 | 3 | 1 | 3 | 0.59 | 2.30 | 2.85 | 41.46 | 0.05 | 0.08 |
| B | 6 | G | | | | | | | | | | | | | | | | | |
| B | 9 | G | | | | | | | | | | | | | | | | | |
| B | 12 | G | 5.75 | 395 | 18.3 | 7 | 425 | 1.24 | 0.00 | 45.99 | 2 | 0 | 4 | 1.30 | 2.53 | 4.71 | 62.67 | 7.00 | 0.41 |
| B | 3 | H | 5.71 | 418 | 18.5 | 35 | 469 | 3.63 | 1.20 | 47.68 | 4 | 1 | 11 | 0.94 | 3.48 | 5.36 | 54.63 | 0.09 | 0.04 |
| B | 6 | H | 5.78 | 436 | 19.1 | 28 | 413 | 1.10 | 0.00 | 66.62 | 19 | 1 | 16 | 2.56 | 4.88 | 6.93 | 59.00 | 5.33 | 0.20 |
| B | 9 | H | | | | | | | | | | | | | | | | | |
| B | 12 | H | 5.82 | 411 | 19.4 | 8 | 381 | 0.73 | 0.00 | 75.40 | 7 | 1 | 16 | 2.25 | 3.84 | 4.01 | 45.53 | 7.17 | 0.33 |
| B | 3 | I | 5.72 | 229 | 17.7 | 101 | 552 | 2.03 | 0.55 | 56.19 | 5 | 1 | 6 | 0.61 | 2.41 | 3.71 | 35.65 | 0.05 | 0.05 |
| B | 6 | I | 5.82 | 276 | 17.6 | 97 | 520 | 3.34 | 0.67 | 93.90 | 8 | 1 | 13 | 1.11 | 2.97 | 3.31 | 43.67 | 1.18 | 0.03 |
| B | 9 | I | 5.74 | 305 | 17.6 | 101 | 515 | 2.01 | 1.57 | 67.46 | 4 | 0 | 10 | 0.78 | 2.24 | 4.41 | 41.69 | 0.03 | 0.04 |
| B | 12 | I | 5.83 | 377 | 17.4 | 13 | 407 | 4.39 | 0.00 | 99.41 | 6 | 1 | 14 | 2.56 | 3.24 | 4.83 | 53.79 | 9.97 | 0.38 |
| B | 3 | J | 5.6 | 409 | 20.1 | 37 | 530 | 2.66 | 0.55 | 121.90 | 6 | 1 | 14 | 1.67 | 3.20 | 5.23 | 55.37 | 0.13 | 0.05 |
| B | 6 | J | | | | | | | | | | | | | | | | | |
| B | 9 | J | 5.64 | 415 | 20.3 | 53 | 509 | 2.88 | 2.47 | 145.00 | 7 | 1 | 16 | 1.55 | 2.94 | 6.15 | 68.18 | 0.04 | 0.00 |
| B | 12 | J | 5.78 | 452 | 20.3 | 23 | 413 | 9.94 | 0.00 | 123.45 | 10 | 1 | 17 | 3.23 | 3.86 | 3.65 | 55.44 | 9.87 | 0.19 |
| B | 3 | L | | | | | | | | | | | | | | | | | |
| B | 6 | L | 5.7 | 420 | 20 | 19 | 436 | 5.50 | 0.00 | 147.70 | 15 | 1 | 17 | 3.41 | 3.70 | 5.58 | 68.51 | 3.00 | 0.05 |

**Appendix 5.3.4 Summary of results from Wilcoxon rank sum test to determine whether there was a significant increase in Pb and Zn from sediment to pore and surface water over flooded periods**

| Element | Run | Loc | Median strt | Std err | Median end | Std err | Test statistic Calc W | Calc W2 | Calc Z | P | (n) | If Z <-1.96 Reject Null H. |
|---------|------|-----|-------------|---------|------------|---------|------------------------|---------|--------|------|-----|------------------------------|
| Pb | 1wwet | B | 2.9 | 0.4 | 5.2 | 0.3 | 16 | 39 | -2.4 | .05 | 5 | Y |
| Pb | 1wwet | T | 2.3 | 0.6 | 8.1 | 0.2 | 15 | 40 | -2.61 | .05 | 5 | Y |
| Zn | 1wwet | B | 39.4 | 1.0 | 54.6 | 1.3 | 15 | 40 | -2.61 | .05 | 5 | Y |
| Zn | 1wwet | T | 3.6 | 0.6 | 12.4 | 3.5 | 15 | 40 | -2.61 | .05 | 5 | Y |
| Pb | 3wwet | B | 3.3 | 0.7 | 5.6 | 1.4 | 9 | 12 | -0.66 | .51 | 3 | N |
| Pb | 3wwet | T | 1.2 | 0.3 | 8.2 | 2.1 | 6 | 15 | -1.964 | .05 | 3 | Y |
| Zn | 3wwet | B | 41.4 | 0.9 | 59.0 | 5.6 | 6 | 15 | -1.964 | .05 | 3 | Y |
| Zn | 3wwet | T | 2.6 | 0.9 | 23.8 | 2.7 | 6 | 15 | -1.964 | .05 | 3 | Y |
| Pb | 3wdry | B | 4.4 | 0.5 | 6.1 | 0.8 | 8 | 13 | -1.09 | .275 | 3 | N |
| Pb | 3wdry | T | 2.1 | 0.6 | 6.5 | 0.5 | 6 | 15 | -1.964 | .05 | 3 | Y |
| Zn | 3wdry | B | 42.4 | 1.2 | 67.6 | 6.8 | 6 | 15 | -1.964 | .05 | 3 | Y |
| Zn | 3wdry | T | 2.9 | 0.8 | 15.0 | 0.9 | 6 | 15 | -1.964 | .05 | 3 | Y |
| Pb | Flood | B | 3.7 | 0.3 | 4.1 | 0.6 | 24.5 | 30.5 | -0.63 | .53 | 5 | N |
| Pb | Flood | T | 7.3 | 1.2 | 7.2 | 1.7 | 24 | 31 | -0.73 | .465 | 5 | N |
| Zn | Flood | B | 50.8 | 2.2 | 53.0 | 3.1 | 27 | 28 | -0.1 | .917 | 5 | N |
| Zn | Flood | T | 21.5 | 7.2 | 18.5 | 5.2 | 25 | 30 | -0.52 | .602 | 5 | N |

**Appendix 5.3.6 Summary of results from Wilcoxon rank sum test to determine whether there was a significant difference in average dissolved Pb and Zn at the end of a flood for 2014 mesocosm runs compared to 2012 mesocosm runs**

| Element | Run | Loc | Test statistic Calc W | Calc W2 | Calc Z | P | If Z <- 1.96 Reject Null H. | (n) 2012 | (n) 2014 |
|---------|-----|-----|------------------------|---------|--------|------|------------------------------|----------|----------|
| Pb | 1wwet | B | 15 | 261 | -3.354 | .001 | Y | 18 | 5 |
| Pb | 3wdry | B | 6 | 72 | -2.496 | .05 | Y | 9 | 3 |
| Pb | 3wwet | B | 6 | 72 | -2.496 | .05 | Y | 9 | 3 |
| Pb | Flood | B | 20 | 256 | -2.981 | .01 | Y | 18 | 5 |
| Pb | 1wwet | T | 15 | 261 | -3.354 | .001 | Y | 18 | 5 |
| Pb | 3wdry | T | 6 | 72 | -2.496 | .05 | Y | 9 | 3 |
| Pb | 3wwet | T | 6 | 72 | -2.496 | .05 | Y | 9 | 3 |
| Pb | Flood | T | 21 | 255 | -2.907 | .01 | Y | 18 | 5 |
| Zn | 1wwet | B | 105 | 171 | -3.354 | .001 | Y | 18 | 5 |
| Zn | 3wdry | B | 33 | 45 | -2.496 | .05 | Y | 9 | 3 |
| Zn | 3wwet | B | 33 | 45 | -2.496 | .05 | Y | 9 | 3 |
| Zn | Flood | B | 105 | 171 | -3.354 | .001 | Y | 18 | 5 |
| Zn | 1wwet | T | 79 | 197 | -1.416 | .157 | N | 18 | 5 |
| Zn | 3wdry | T | 26 | 52 | -1.200 | .229 | N | 9 | 3 |
| Zn | 3wwet | T | 31 | 47 | -2.126 | .05 | Y | 9 | 3 |
| Zn | Flood | T | 92 | 184 | -2.385 | .05 | Y | 18 | 5 |

**Appendix 5.3.7 Re-run of sequential extraction on sediment (< 63 μm) using sediment from 2012, and 2014. Table showing Fe, Mn, Zn, Pb (mg/kg) recovered from the sediment with standard errors and total difference (more or less recovered)**

| Elem | | 2012 Average mg/kg | 2012 stderr | 2014 average mg/kg | 2014 stderr |
|------|-------|------------|------------|------------|------------|
| Fe | A | 2905.44 | 242.25 | 4721.70 | 49.21 |
| Fe | B | 1183.78 | 76.66 | 1255.53 | 111.32 |
| Fe | C | 22973.33 | 1596.42 | 13812.56 | 248.13 |
| Fe | D | 19260.56 | 1452.82 | 24078.46 | 990.63 |
| | total | **46323.11** | | **43868.26** | |
| | | | difference | 2454.85 | less |
| Mn | A | 146.92 | 13.50 | 361.31 | 2.34 |
| Mn | B | 59.86 | 9.24 | 105.45 | 10.75 |
| Mn | C | 68.81 | 3.56 | 64.54 | 0.84 |
| Mn | D | 330.86 | 24.17 | 386.43 | 15.14 |
| | total | **606.44** | | **917.73** | |
| | | | difference | 311.29 | more |
| Pb | A | 59463.89 | 8589.64 | 59807.23 | 2015.06 |
| Pb | B | 25306.39 | 3940.23 | 16276.89 | 911.92 |
| Pb | C | 0.00 | 0.00 | | |
| Pb | D | 2952.89 | 1436.24 | | |
| | total | **87723.17** | | **76084.11** | |
| | | | difference | 11639.05 | Less |
| Zn | A | 997.72 | 69.28 | 2928.30 | 27.62 |
| Zn | B | 136.28 | 4.00 | 268.09 | 46.00 |
| Zn | C | 769.06 | 47.34 | 540.88 | 10.98 |
| Zn | D | 642.58 | 33.07 | 999.34 | 39.98 |
| | total | **2545.64** | | **4736.61** | |
| | | | difference | 2190.97 | More |

## Appendix 5.3.8. Spearmans Rho correlation coefficient matrices for pore water samples

### 1 week wet (top) n = 10, correlation coefficient sig. 2-tailed

|  | pH | Sulphate | Pb | Zn | Mn | Fe | Redox |
|---|---|---|---|---|---|---|---|
| pH | 1.000 | .012 | -.036 | .188 | .284 | .556 | -.802** |
|  | . | .973 | .920 | .602 | .426 | .095 | .005 |
| Sulphate | .012 | 1.000 | **.661*** | **.818*** | .439 | -.652* | -.067 |
|  | .973 | . | .038 | .004 | .204 | .041 | .855 |
| Pb | -.036 | .661* | 1.000 | .818** | .750* | -.535 | -.018 |
|  | .920 | .038 | . | .004 | .012 | .111 | .960 |
| Zn | .188 | .818** | .818** | 1.000 | .817** | -.369 | -.030 |
|  | .602 | .004 | .004 | . | .004 | .294 | .934 |
| Mn | .284 | .439 | **.750*** | **.817*** | 1.000 | -.195 | -.213 |
|  | .426 | .204 | .012 | .004 | . | .589 | .554 |
| Fe | .556 | -.652* | -.535 | -.369 | -.195 | 1.000 | -.172 |
|  | .095 | .041 | .111 | .294 | .589 | . | .634 |
| Redox | -.802** | -.067 | -.018 | -.030 | -.213 | -.172 | 1.000 |
|  | .005 | .855 | .960 | .934 | .554 | .634 | . |

\*. Correlation is significant at the 0.05 level (2-tailed).

\*\*. Correlation is significant at the 0.01 level (2-tailed).

### 3 week wet (top) n = 6, correlation coefficient sig. 2-tailed

**Correlations**

|  | pH | Sulphate | Pb | Zn | Mn | Fe | Redox |
|---|---|---|---|---|---|---|---|
| pH | 1.000 | -.257 | -.257 | .086 | -.029 | .486 | -.657 |
|  | . | .623 | .623 | .872 | .957 | .329 | .156 |
| Sulphate | -.257 | 1.000 | .714 | **.886*** | .771 | .086 | -.371 |
|  | .623 | . | .111 | .019 | .072 | .872 | .468 |
| Pb | -.257 | .714 | 1.000 | .829* | .943** | .257 | -.371 |
|  | .623 | .111 | . | .042 | .005 | .623 | .468 |
| Zn | .086 | .886* | .829* | 1.000 | .943** | .429 | -.657 |
|  | .872 | .019 | .042 | . | .005 | .397 | .156 |
| Mn | -.029 | .771 | **.943*** | **.943*** | 1.000 | .486 | -.543 |
|  | .957 | .072 | .005 | .005 | . | .329 | .266 |
| Fe | .486 | .086 | .257 | .429 | .486 | 1.000 | -.600 |
|  | .329 | .872 | .623 | .397 | .329 | . | .208 |
| Redox | -.657 | -.371 | -.371 | -.657 | -.543 | -.600 | 1.000 |
|  | .156 | .468 | .468 | .156 | .266 | .208 | . |

**3 week dry (top) n = 6, Spearman rho correlation coefficient sig. 2-tailed**

**Correlations**

| | pH | Sulphate | Pb | Zn | Mn | Fe | Redox |
|---|---|---|---|---|---|---|---|
| pH | 1.000 | -.086 | .543 | .029 | .371 | .696 | -.771 |
| | . | .872 | .266 | .957 | .468 | .125 | .072 |
| Sulphate | -.086 | 1.000 | .371 | .771 | .543 | -.174 | .029 |
| | .872 | . | .468 | .072 | .266 | .742 | .957 |
| Pb | .543 | .371 | 1.000 | .714 | .943** | .290 | -.714 |
| | .266 | .468 | . | .111 | .005 | .577 | .111 |
| Zn | .029 | .771 | .714 | 1.000 | .771 | .058 | -.429 |
| | .957 | .072 | .111 | . | .072 | .913 | .397 |
| Mn | .371 | .543 | .943** | .771 | 1.000 | .232 | -.543 |
| | .468 | .266 | .005 | .072 | . | .658 | .266 |
| Fe | .696 | -.174 | .290 | .058 | .232 | 1.000 | -.783 |
| | .125 | .742 | .577 | .913 | .658 | . | .066 |
| Redox | -.771 | .029 | -.714 | -.429 | -.543 | -.783 | 1.000 |
| | .072 | .957 | .111 | .397 | .266 | .066 | . |

*. Correlation is significant at the 0.05 level (2-tailed).

**. Correlation is significant at the 0.01 level (2-tailed).

**Flood (top) n = 10, Spearman rho correlation coefficient sig. 2-tailed**

**Correlations**

| | pH | Sulphate | Pb | Zn | Mn | Fe | Redox |
|---|---|---|---|---|---|---|---|
| pH | 1.000 | -.009 | -.227 | -.127 | -.137 | -.229 | -.291 |
| | . | .979 | .502 | .709 | .689 | .499 | .385 |
| Sulphate | -.009 | 1.000 | .445 | .864** | .834** | -.849** | -.127 |
| | .979 | . | .170 | .001 | .001 | .001 | .709 |
| Pb | -.227 | .445 | 1.000 | .700* | .738** | -.172 | .064 |
| | .502 | .170 | . | .016 | .010 | .614 | .853 |
| Zn | -.127 | .864** | .700* | 1.000 | .893** | -.572 | -.073 |
| | .709 | .001 | .016 | . | .000 | .066 | .832 |
| Mn | -.137 | .834** | .738** | .893** | 1.000 | -.564 | -.155 |
| | .689 | .001 | .010 | .000 | . | .071 | .649 |
| Fe | -.229 | -.849** | -.172 | -.572 | -.564 | 1.000 | .038 |
| | .499 | .001 | .614 | .066 | .071 | . | .911 |
| Redox | -.291 | -.127 | .064 | -.073 | -.155 | .038 | 1.000 |
| | .385 | .709 | .853 | .832 | .649 | .911 | . |

## 1 week wet (bottom) n = 10, correlation coefficient sig. 2-tailed

**Correlations**

|  | pH | Sulphate | Pb | Zn | Mn | Fe | Redox |
|---|---|---|---|---|---|---|---|
| **pH** | 1.000 | .293 | .024 | -.354 | .250 | .138 | -.379 |
|  | . | .412 | .947 | .316 | .486 | .705 | .280 |
| **Sulphate** | .293 | 1.000 | .285 | .139 | .782** | -.304 | .170 |
|  | .412 | . | .425 | .701 | .008 | .393 | .638 |
| **Pb** | .024 | .285 | 1.000 | .624 | .455 | -.109 | -.152 |
|  | .947 | .425 | . | .054 | .187 | .763 | .675 |
| **Zn** | -.354 | .139 | .624 | 1.000 | .406 | -.201 | -.468 |
|  | .316 | .701 | .054 | . | .244 | .578 | .172 |
| **Mn** | .250 | .782** | .455 | .406 | 1.000 | -.401 | -.243 |
|  | .486 | .008 | .187 | .244 | . | .250 | .498 |
| **Fe** | .138 | -.304 | -.109 | -.201 | -.401 | 1.000 | -.006 |
|  | .705 | .393 | .763 | .578 | .250 | . | .987 |
| **Redox** | -.379 | .170 | -.152 | -.468 | -.243 | -.006 | 1.000 |
|  | .280 | .638 | .675 | .172 | .498 | .987 | . |

## 3 week wet (bottom) n = 6, correlation coefficient sig. 2-tailed

**Correlations**

|  | pH | Sulphate | Pb | Zn | Mn | Fe | Redox |
|---|---|---|---|---|---|---|---|
| **pH** | 1.000 | -.464 | -.580 | -.899* | -.897* | -.250 | .638 |
|  | . | .354 | .228 | .015 | .015 | .633 | .173 |
| **Sulphate** | -.464 | 1.000 | -.257 | .657 | .377 | -.174 | -.143 |
|  | .354 | . | .623 | .156 | .461 | .742 | .787 |
| **Pb** | -.580 | -.257 | 1.000 | .429 | .551 | .058 | -.257 |
|  | .228 | .623 | . | .397 | .257 | .913 | .623 |
| **Zn** | -.899* | .657 | .429 | 1.000 | .928** | .290 | -.657 |
|  | .015 | .156 | .397 | . | .008 | .577 | .156 |
| **Mn** | -.897* | .377 | .551 | .928** | 1.000 | .456 | -.754 |
|  | .015 | .461 | .257 | .008 | . | .364 | .084 |
| **Fe** | -.250 | -.174 | .058 | .290 | .456 | 1.000 | -.899* |
|  | .633 | .742 | .913 | .577 | .364 | . | .015 |
| **Redox** | .638 | -.143 | -.257 | -.657 | -.754 | -.899* | 1.000 |
|  | .173 | .787 | .623 | .156 | .084 | .015 | . |

*. Correlation is significant at the 0.05 level (2-tailed).

**. Correlation is significant at the 0.01 level (2-tailed).

## 3 week dry (bottom) n = 6, correlation coefficient sig. 2-tailed

**Correlations**

|  | pH | Sulphate | Pb | Zn | Mn | Fe | Redox |
|---|---|---|---|---|---|---|---|
| **pH** | 1.000 | -.928** | -.493 | -.899* | .290 | -.116 | .232 |
|  | . | .008 | .321 | .015 | .577 | .827 | .658 |
| **Sulphate** | -.928** | 1.000 | .200 | .886* | -.029 | .086 | -.257 |
|  | .008 | . | .704 | .019 | .957 | .872 | .623 |
| **Pb** | -.493 | .200 | 1.000 | .486 | -.371 | -.086 | -.086 |
|  | .321 | .704 | . | .329 | .468 | .872 | .872 |
| **Zn** | -.899* | .886* | .486 | 1.000 | .029 | .086 | -.429 |
|  | .015 | .019 | .329 | . | .957 | .872 | .397 |
| **Mn** | .290 | -.029 | -.371 | .029 | 1.000 | .314 | -.600 |
|  | .577 | .957 | .468 | .957 | . | .544 | .208 |
| **Fe** | -.116 | .086 | -.086 | .086 | .314 | 1.000 | -.829* |
|  | .827 | .872 | .872 | .872 | .544 | . | .042 |
| **Redox** | .232 | -.257 | -.086 | -.429 | -.600 | -.829* | 1.000 |
|  | .658 | .623 | .872 | .397 | .208 | .042 | . |

## Flood (bottom) n = 10, correlation coefficient sig. 2-tailed

**Correlations**

|  | pH | Sulphate | Pb | Zn | Mn | Fe | Redox |
|---|---|---|---|---|---|---|---|
| **pH** | 1.000 | -.032 | -.219 | -.046 | .757** | .014 | -.790** |
|  | . | .926 | .517 | .894 | .007 | .968 | .004 |
| **Sulphate** | -.032 | 1.000 | .055 | -.564 | -.009 | .027 | .182 |
|  | .926 | . | .873 | .071 | .979 | .937 | .593 |
| **Pb** | -.219 | .055 | 1.000 | -.236 | -.392 | -.109 | .500 |
|  | .517 | .873 | . | .484 | .233 | .750 | .117 |
| **Zn** | -.046 | -.564 | -.236 | 1.000 | .282 | .091 | -.055 |
|  | .894 | .071 | .484 | . | .400 | .790 | .873 |
| **Mn** | .757** | -.009 | -.392 | .282 | 1.000 | .497 | -.838** |
|  | .007 | .979 | .233 | .400 | . | .120 | .001 |
| **Fe** | .014 | .027 | -.109 | .091 | .497 | 1.000 | -.318 |
|  | .968 | .937 | .750 | .790 | .120 | . | .340 |
| **Redox** | -.790** | .182 | .500 | -.055 | -.838** | -.318 | 1.000 |
|  | .004 | .593 | .117 | .873 | .001 | .340 | . |

# 8. LIST OF REFERENCES

Alastuey, A., Garcia-Sanchez, A. and Lopez, F. et al. (1999) Evolution of pyrite mud weathering and mobility of heavy metals in the Guadiamar Valley after the Aznalcollar spill, South-West Spain. **Science of the Total Environment**, 242: 41-55

Alpers, C.N., Nordstrom, D.K. and Thompson, J.M. (1993) Seasonal Variations of Zn/Cu Ratios in Acid Mine Water from Iron Mountain, California. **American Chemical Society**, 550: 324-344

Andrews, J.E., Brimblecombe, P. and Jickells, T.D. et al. (2008) **An Introduction to Environmental Chemistry**. 2$^{nd}$ ed. Oxford, UK: Blackwell Publishing

Appelo, C.A.J. and Postma, D. (2010) **Geochemistry, groundwater and pollution**. 3nd ed. Leiden, The Netherlands: A.A. Balkema Publishers

Aquaread (2014) **Instruction manual for the Aquaprobe Multiparameter Water quality probe** [online].Available from: http://www.aquaread.co.uk/downloads/manuals/Aquaread-AP700-AP800-Aquaprobe-Manual.pdf  [Accessed 01/10/14]

Astilleros, J.M., Godelitsas, A., Rodriguez-Blanco, J.D., et al. (2010) Interaction of gypsum with lead in aqueous solutions. **Applied Geochemistry**, 25: 1008-1016

Axe, L. and Trivedi, P. (2002) Intraparticle surface diffusion of metal contaminants and their attenuation in microporous amorphous Al, Fe, and Mn oxides. **Journal of Colloid and Interface Science**, 247 (2): 259-265

Baba, A.A., Adekola, F.A. and Fapojuwo, D.P.T. et al. (2011) Dissolution kinetics and solvent extraction of lead from anglesite ore. **Journal of the Chemical Society of Nigeria**, 36 (1): 157-164

Ball, J. and Nordstrom, D.K. (2001) **User's Manual for WATEQ4F. with revised thermodynamic database and test cases for calculating speciation of major, trace and redox elements in natural waters** [online]. Available from: http://wwwbrr.cr.usgs.gov/projects/GWC_chemtherm/pubs/wq4fdoc.pdf [Accessed 06/01/15]

Baltpurvins, K.A., Burns, R.C. and Lawrance, G.A. et al. (1996) Effect of pH and anion type on the aging of freshly precipitated iron(III) hydroxide sludges. **Environmental Science and Technology**, 30 (3): 939-944

Banks, V.J. and Palumbo-Roe, B. (2010) Synoptic monitoring as an approach to discriminating between point and diffuse source contributions to zinc loads in mining impacted catchments. **Journal of Environmental Monitoring**, 12: 1684

Barrett, J.E.S., Taylor, K.G. and Hudson-Edwards, K.A. et al. (2010) Solid-Phase Speciation of Pb in Urban Road Dust Sediment: A XANES and EXAFS Study. **Environmental Science and Technology**, 44 (8): 2940-2946

Bartlett, R.J. (1999) "Characterizing soil redox behaviour". In Sparks, D.L. (Ed.) **Soil Physical Chemistry**. 2nd ed. Boca Raton, FL., CRC Press 371-397.

Baskerville, S. and Evans, W. (2006) **Acid Mine Drainage – A Legacy of Industrial Past** [online]. Available from: http://www.rsc.org/Education/EiC/Restricted/2006/Mar/AcidMineDrainage.asp [Accessed 24/03/2010]

Batty, L.C. (2003) Wetland plants - more than just a pretty face? **Land Contamination & Reclamation**, 11 (2): 173-180

Bennett, W.W., Teasdale, P.R. and Panther, J.G., et al. (2012) Investigating arsenic speciation and mobilization in sediments with DGT and DET: A mesocosm evaluation of oxic-anoxic transitions. **American Chemical Society**, 46: 3981-3989

Berner, R.A. (1981) A new geochemical classification of sedimentary environments. **Journal of sedimentary Petrology**, 51: 359-365

Bick, D.E. (1976) **The Old Metal Mines of Mid-Wales. Part 1 Cardiganshire - South of Devil's Bridge**. Newent, Glos.: The Pound House.

Billon, G., Ouddane, B. and Laureyns, J. et al. (2001) Chemistry of Metal Sulfides in Anoxic Sediments. **Physical Chemistry**, 3: 3586-3592

Boult, S., Collins, D.N. and White, K.N. et al. (1994) Metal Transport in a Stream Polluted by Acid Mine Drainage - The Afon Goch, Anglesey, UK. **Environmental Pollution**, 84: 279-284

Bradley, S.B. and Lewin, J. (1982) Transport of Heavy-Metals on suspended sediments under high flow conditions in a mineralized region of Wales. **Environmental Pollution Ser. B**, 4 (4): 257-267

Bradley, S.B. (1995) "Long-term Dispersal of Metals in Mineralised Catchment by Fluvial Processes". In Foster, I.D.L.; Gurnell, A.M. & Webb, B.W. (ed.) **Sediment and Water Quality in River Catchments** John Wiley & Sons Ltd. pp. 161-177

British Geological Survey (2007) **British Regional Geology: Wales**. Nottingham: British Geological Survey.

Buckby, T., Black, S. and Coleman, M.L. et al. (2003) Fe-sulphate-rich evaporative mineral precipitates from the Rio Tinto, southwest Spain. **Mineralogical Magazine**, 67 (2): 263-278

Buekers, J., Amery, F. and Maes, A. et al. (2008) Long-term reactions of Ni, Zn and Cd with iron oxyhydroxides depend on crystallinity and structure and on metal concentrations. **European Journal of Soil Science**, 59 (4): 706-715

Burton, E.D., Phillips, I.R. and Hawker, D.W. (2005) Geochemical Partitioning of Copper, Lead and Zinc in Benthic, Estuarine Sediment Profiles. **Journal of Environmental Quality**, 34: 263-273

Butler, B.A. (2009) Effect of pH, ionic strength, dissolved organic carbon, time, and particle size on metals release from mine drainage impacted streambed sediments. **Water Research**, 43: 1392-1402

BWB Technologies (2012) **A guide to Flame Photometer analysis** [online]. Available from: http://bwbtech.com/pdfs/flame_photometery_guide.pdf  BWB Technologies [Accessed 2014]

Byrne, P., Reid, I. and Wood, P.J. (2009) "Short-Term Fluctuations in Heavy Metal Concentrations during Flood Events through Abandoned Metal Mines, With Implications for Aquatic Ecology and Mine Water Treament". **International Mine Water Conference (IMWC). South Africa, 19-23 October 2009.** Pretoria.

Byrne, P., Reid, I. and Wood, P.J. (2010) Sediment geochemistry of streams draining abandoned lead/zinc mines in central Wales: the Afon Twymyn. **Journal of Soils and Sediments**, 10 (4): 683-697

Byrne, P., Reid, I. and Wood, P.J. (2013) Stormflow hydrochemistry of a river draining an abandoned metal mine: the Afon Twymyn, central Wales. **Environmental Monitoring & Assessment**, 185: 2817–2832

Byrne, P., Zhang, H. and Ullah, S. et al. (2014) Diffusive equilibrium in thin films provides evidence of suppression of hyporheic exchange and larte-scale nitrate transformation in a groundwater-fed river. **Hydrological Processes**

Caetano, M., Madureira, M.J. and Vale, C. (2003) Metal remobilisation during resuspension of anoxic contaminated sediment: short-term laboratory study. **Water, Air, and Soil Pollution**, 143 (1-4): 23-40

Caille, N., Tiffreau, C. and Leyval, C. et al. (2003) Solubility of metals in an anoxic sediment during prolonged aeration. **Science of the Total Environment**, 301 (1-3): 239-250

Cama, J., Acero, P. and Ayora, C. et al. (2005) Galena surface reactivity at acidic pH and 25$^o$C based on flow-through and in situ AFM experiments. **Chemical Geology**, 214: 309-330

Carroll, S.A., O'Day, P.A. and Piechowski, M. (1998) Rock-water interactions controlling zinc, cadmium, and lead concentrations in surface waters and sediments, US Tri-State Mining District. 2. Geochemical interpretation. **Environmental Science & Technology**, 32 (7): 956-965

Caruso, B.S. and Bishop, M. (2009) Seasonal and Spatial Variation of Metal Loads from Natural Flows in the Upper Tenmile Creek Watershed, Montana. **Mine Water Environment**, 28 (3): 166-181

Cave, R.R., Andrews, J.E. and Jickells, T.D. et al. (2005) A review of sediment contamination by trace metals in the Humber catchment and estuary, and the implications for future estuary water quality **Estuarine, Coastal and Shelf Science**, 62: 547-557

Chapman, P.M., Wang, F.Y. and Janssen, C.R. et al. (2003) Conducting ecological risk assessments of inorganic metals and metalloids: Current status. **Human and Ecological Risk Assessment**, 9 (4): 641-697


Charlatchka, R. and Cambier, P. (2000) Influence of reducing conditions on solubility of trace metals in contaminated soils. **Water, Air and Soil Pollution**, 118 (1-2): 143-167


Centre for Ecology and Hydrology (2014) **National River Flow Archive** [online]. Available from: http://www.ceh.ac.uk/data/nrfa/data/station.html?63004 [Accessed 101014]


Clarke, C., Tourney, J. and Johnson, K. (2012) Oxidation of anthracene using waste Mn oxide minerals: The importance of wetting and drying sequences. **Journal of Hazardous Materials**, 205-206: 126-130


Collins, A., Ohandja, D. and Hoare, D. et al. (2012) Implementing the Water Framework Directive: a transition from established monitoring networks in England and Wales. **Environmental Science & Policy**, 17: 49-61


Coulthard, T.J. and Macklin, M.G. (2003) Modeling long-term contamination in river systems from historical metal mining. **Geology**, 31 (5): 451-454


Cravotta, C.A. (2008) Dissolved metals and associated constituents in abandoned coal-mine discharges, Pennsylvania, USA. Part 2: Geochemical controls on constituent concentrations. **Applied Geochemistry**, 23: 203-226


Cravotta, C.A. and Bilger, M.D. (2001) Water-Quality trends for a Stream Draining the Southern n Anthracite Field, Pennsylvania. **Geochemistry: Exploration, Environment, Analysis**, 1: 33-50


Crawford, R.J., Harding, I.H. and Mainwaring, D.E. (1993) Adsorption and coprecipitation of single heavy metal ions onto the hydrated oxides of iron and chromium. **Langmuir**, 9 (11): 3050-3056


Davis, J.A. and Kent, D.B. (1990) Surface Complexation modeling in aqueous geochemistry **Reviews in Mineralogy and Geochemistry**, 23: 177-260

Davison, W., Grime, G.W. and Morgan, J.W., et al. (1991) Distribution of dissolved iron in sediment pore waters at submillimetre resolution. **Nature***,* 352: 323-325

Davison, W., Fones, G. and Harper, M., et al. (2000) "Dialysis, DET and DGT: In situ diffusional techniques for studying water, sediments and soils". In Buffle, J. & Horvai, G. (Eds.) **In situ monitoring of aquatic systems - chemical analysis and speciation***.* Chichester, UIPAC, John Wiley & Sons Ltd 495-569

DEFRA (2012a) **Climate Change Risk Assessment for the water sector. Project Code GA0204** [online]. Available from: http://randd.defra.gov.uk/Default.aspx?Module=More&Location=None&ProjectID= 15747  Crown [Accessed 10102014]

DEFRA (2012b) "Climate Change Risk Assessment for the Floods and Coastal Erosion Sector Project code GA0204". Wallingford.

Dennis, I.A., Macklin, M.G. and Coulthard, T.J. et al. (2003) The impact of the October-November 2000 floods on contaminant metal dispersal in the River Swale catchment, North Yorkshire, UK. **Hydrological Processes***,* 17 (8): 1641-1657

Dennis, I.A., Coulthard, T.J. and Brewer, P. et al. (2009) The Role of Floodplains in Attenuating Contaminated Sediment Fluxes in Formerly Mined Drainage Basins. **Earth Surface Processes and Landforms***,* 34 (3): 453-466

Desbarats, A.J. and Dirom, G.C. (2005) Temporal Variation in Discharge Chemistry and Portal Flow from the 8-level adit, lynx Mine, Myra Falls Operations, Vancouver island, British Colombia. **Environmental Geology***,* 47: 445-456

Desbarats, A.J. and Dirom, G.C. (2007) Temporal Variationsin the Chemistry of Circum-neutral drainage from the 10-level portal, Myra Mine, Vancouver island, British Columbia. **Applied Geochemistry***,* 22: 415-435

Docekalova, H., Clarisse, O. and Salomon, S. et al. (2002) Use of constrained DET probe for a high-resolution determination of metals and anions distribution in the sediment pore water. **Talanta***,* 57: 145-155

Domenech, C., Pablo, J. and Ayora, C. (2002) Oxidative dissolution of pyritic sludge from the Azanlcollar mine (SW Spain). **Chemical Geology***,* 190: 339-353

Du Laing, G., Vanthuyne, D.R. and Vandecasteele, B. et al. (2007) Influence of hydrological regime on pore water metal concentrations in a contaminated sediment-derived soil. **Environmental Pollution**, 147 (3): 615-625

Du Laing, G., Rinklebe, J. and Vandecasteele, B. et al. (2009) Trace metal behaviour in estuarine and riverine floodplain soils and sediments: A review. **Science of the Total Environment**, 407: 3972-3985

Durham County Council (2013) **Durham Heritage Coast: turning the tide** [online]. Available from: http://www.durhamheritagecoast.org/Pages/TurningtheTide.aspx Durham_County_Council [Accessed 09/02/15]

Dzombak, D.A. and Morel, F.M.M. (1987) Adsorption of inorganic pollutants in aquatic systems. **Journal of Hydraulic Engineering-Asce**, 113 (4): 430-475

Eggleton, J. and Thomas, K.V. (2004) A Review of Factors Affecting the Release and Bioavailability of contaminants during Sediment Distrubance Events. **Environment International**, 30: 973-980

Emerson, S., Cranston, R.E. and Liss, P.S. (1979) Redox species in a reducing fjord: equilibrium and kinetic considerations. **Deep Sea Research Part A. Oceanographic Research Papers**, 26A: 859-878.

Environment Agency (2008a) "Abandoned Mines and the Water Environment. Science Report SC030136-41". Environment Agency, Bristol.

Environment Agency (2008b) "Assessment of metal mining contaminated river sediments in England and Wales. Science Report SC030136.SR4". Environment Agency, Bristol.

Environment Agency (2009) "Updated technical background to CLEA model. Science Report SC050021/SR3". Bristol.

Environment Agency (2010a) "The River Basin Districts Typology, Standards and Groundwater threshold values (Water Framework Directive) (England and Wales) Directions 2010". Environment Agency

Environment Agency (2011) **Chemical Standards** [online]. Available from: http://evidence.environment-agency.gov.uk/ChemicalStandards/Home.aspx [Accessed 23/01/15]


Environment Agency (2012a) "Prioritisation of abandoned non-coal mine impacts on the environment. Science Report SC030136/R2 The national Picture". Environment Agency, Bristol


Environment Agency (2012b) "Prioritisation of abandoned non-coal mine impacts on the environment. SC030136/R6 The Western Wales River Basin District.".


Environment Agency (2012c) "Prioritisation of abandoned non-coal mine impacts on the environment. SC030136/R12 Future management of abandoned non-coal mine water discharges".


Environment Agency (2014) "Mitigation of pollution from abandoned metal mines. Investigation of passive compost bioreactor systems for treatment of abandoned metal mine discharges. Science Report SC090024/R1". Environment Agency. Bristol.


Evans Analytical Group (2007) **ICP OES and ICP MS detection limit guidance** [online]. Available from: http://www.nanoscience.co.jp/surface_analysis/pdf/icp-oes-ms-detection-limit-guidance-BR023.pdf  [Accessed 010614]


Evans, D. (1991) Chemical and physical partitioning in contaminated stream sediments in the River Ystwyth, Mid-Wales. **Environmental Geochemistry & Health**, 13 (2): 84-92


Evans, K.A., Watkins, D.C. and Banwart, S.A. (2006) Rate controls on the chemical weathering of natural polymineralic material. II. Rate-controlling mechanisms and mineral sources and sinks for element release from four UK mine sites, and implications for comparison of laboratory and field scale weathering studies. **Applied Geochemistry**, 21 (2): 377-403


Fairchild, I.J., Spotl, C. and Frisia, S. et al. (2010) Petrology and geochemistry of annually laminated stalagmites from an Alpine cave (Obir, Austria): seasonal cave physiology. **Geological Society, London, Special Publications**, 336: 295-321

Farnsworth, C.E. and Hering, J.G. (2011) Inorganic Geochemistry and Redox Dynamics in Bank Filtration Settings. **Environmental Science & Technology***,* 45 (12): 5079-5087


Fernandez Albores, A., Perez Cid, B. and Fernandez Gomez, E. et al. (2000) Comparison between sequential extraction procedures and single extractions for metal partitioning in sewage sludge samples. **The Analyst***,* 125: 1353-1357


Field, A. (2009) **Discovering Statistics Using SPSS**. 3$^{rd}$ ed. London: SAGE Publications Ltd.


Ford, R.G., Bertsch, P.M. and Farley, K.J. (1997) Changes in transition and heavy metal partitioning during hydrous iron oxide aging. **Environmental Science & Technology***,* 31 (7): 2028-2033


Foulds, S.A., Brewer, P.A. and Macklin, M.G. et al. (2014) Flood-related contamination in catchments affected by historical metal mining: An unexpected and emerging hazard of climate change. **Science of the Total Environment***,* 476-477


Fruh, A. (2006) **Pourbaix diagram for Manganese; c(Mn) = 1 mol/l, T = 25 °C** [online]. Available from: https://commons.wikimedia.org/wiki/File:Pourbaix_diagram_for_Manganese.svg Western Oregon University [Accessed 18/09/2015]


Fuge, R., Laidlaw, I.M.S., Perkins, W.T., et al. (1991) The influence of acidic mine and spoil drainage on water quality in the mid-Wales area. **Environmental Geochemistry and Health***,* 13 (2): 70-75.


Fuller, C.C. and Bargar, J.R. (2014) Processes of zinc attenuation by biogenic manganese oxides forming in the hyporheic zone of Pinal Creek, Arizona. **Environmental Science & Technology***,* 48: 2165-2172


Fuller, C.C. and Harvey, J.W. (2000) Reactive uptake of trace metals in the hyporheic zone of a mining-contaminated stream, Pinal Creek, Arizona. **Environmental Science & Technology***,* 34: 1150-1155

Galan, E., Gomex-Ariza, J.L. and Gonzalez, I. et al. (2003) Heavy metal partitioning in river sediments severely polluted by acid mine drainage in the Iberian Pyrite Belt. **Applied Geochemistry**, 18: 409-421

Gambrell., Delaune, R.D. and Patrick, J.R.W. (1991) "Redox Processes in Soils following Oxygen Depletion". <u>In</u> Jackson, M.B., Davies, D.D., Lambers, H. (Ed.) **Plant Life Under Oxygen Depriviation**. The Hague, SPB Academic Publishing 101-117.

Gambrell, R.P. (1994) Trace and toxic metals in Wetlands - A review. **Journal of Environmental Quality**, 23 (5): 883-891

Gandy, C.J., Smith, J.W.N. and Jarvis, A.P. (2007) Attenuation of mining-derived pollutants in the hyporheic zone: a review. **Science of the Total Environment**, 373 (2-3): 435-446

Gao, Y., Leermakers, M., Gabelle, C., et al. (2006) High-resolution profiles of trace metals in the pore waters of riverine sediment assessed by DET and DGT. **Science of the Total Environment**, 362: 266-277.

Garmo, O.A., Davison, W. and Zhang, H. (2008) Interactions of Trace Metals with Hydrogels and Filter Membranes Used in DET and DGT Techniques. **Environmental Science & Technology**, 42: 5682-5687

Gill, R. (1997) **Modern Analytical Geochemistry**. Addison Wesley Longman Limited.

Gotoh, S. and Patrick, W.H. (1974) Transformation of iron in a waterlogged soil as influenced by redox potential and pH. **Soil Science Society of America Journal**, 38 (1): 66-71

Gozzard, E., Mayes, W.M. and Potter, H.A. et al. (2011) Seasonal and spatial variation of diffuse (non-point) source zinc pollution in a historically metal mined river catchment, UK. **Environmental Pollution**, 159 (10): 3113-3122

Grundl, T. and Delwiche, J. (1993) Kinetics of Ferric Oxyhydrixide precipitation. **Journal of Contaminant Hydrology**, 14: 71-97.

Hamilton-Taylor, J., Giusti, L. and Davison, W. et al. (1997) Sorption of trace metals (Cu, Pb, Zn) by suspended lake particles in artificial (0.005 M NaNO3) and natural (Esthwaite Water) freshwaters. **Colloids and Surfaces A: Physicochemical and Engineering Aspects**, 120 (1-3): 205-219

Hannaford, J. and Marsh, T.J. (2008) High flow and flood trends in a network of undisturbed catchments in the UK. **International Journal of Climatology**, 28 (10): 1325-1338

Harper, M., Davison, W. and Tych, W. (1997) Temporal, Spatial, and Resolution Constraints for in Situ Sampling Devices Using Diffusional Equilibration: Dialysis and DET. **Environmental Science & Technology**, 31: 3110-3119

Harris, D.L., Lottermoser, B.G. and Duchesne, J. (2003) Ephemeral acid mine drainage at the Montalbion silver mine, north Queensland. **Australian Journal of Earth Sciences**, 50: 797 – 809

Hayes, S.M., Webb, S.M., Bargar, J.R., et al. (2012) Geochemical weathering increases lead bioaccessibility in semi-arid mine tailings. **Environmental Science & Technology**, 46: 5834-5841.

Heidel, C. and Tichomirowa, M. (2011) Galena oxidation investigations on oxygen and sulphur isotopes. **Isotope in Environmental and Health Studies**, 47: 169-188

Heidel, C., Tichomirowa, M. and Junghans, M. (2013) Oxygen and sulfur isotope investigations of the oxidation of sulfide mixtures containing pyrite, galena, and sphalerite. **Chemical Geology**, 342: 29-43

Heron, G., Crouzet, C. and Bourg, A.C.M. et al. (1994) Speciation of Fe(II) and Fe(III) in contaminated aquifer sediments using chemical extraction techniques. **Environmental Science & Technology**, 28: 1698-1705

Hofmann, T. and Schuwirth, N. (2008) Zn and Pb release of sphalerite (ZnS)-bearing mine waste tailings **Journal of Soils Sediments**, 8 (6): 433-441

Horowitz, A.J. and Elrick, K.A. (1987) The relation of stream sediment surface area, grain size and composition to trace element chemistry. **Applied Geochemistry**, 2: 437-451

Hughes, S.J.S. (1981) **The Cwmystwyth Mines**. Northern Mine Research Society.


Hürkamp, K., Raab, T. and Völkel, J. (2009) Lead Pollution of Floodplain Soils in a Historic Mining Area—Age, Distribution and Binding Forms. **Water, Air, and Soil Pollution**, 201 (1-4): 331-345


Hudson-Edwards, K.A. (2003) Sources, mineralogy, chemistry and fate of heavy metal-bearing particles in mining-affected river systems. **Mineralogical Magazine**, 67 (2): 205-217

Hudson-Edwards, K.A., Macklin, M.G. and Taylor, M.P. (1999a) 2000 years of sediment-borne heavy metal storage in the Yorkshire Ouse basin, NE England, UK. **Hydrological Processes**, 13 (7): 1087-1102


Hudson-Edwards, K.A., Schell, C. and Macklin, M.G. (1999b) Mineralogy and geochemistry of alluvium contaminated by metal mining in the Rio Tinto area, southwest Spain. **Applied Geochemistry**, 14: 1015-1030


Hudson-Edwards, K.A., Macklin, M.G. and Jamieson, H.E. et al. (2003) The impact of tailings dam spills and clean-up operations on sediment and water quality in river systems: The Rios Agrio-Guadiamar, Aznalcollar, Spain. **Applied Geochemistry**, 18: 221-239


Hudson-Edwards, K.A., Jamieson, H.E., Charnock, J.M., et al. (2005) Arsenic speciation in waters and sediment of ephemeral floodplain pools, Rios Agrio-Guadiamar, Aznalcollar, Spain. **Chem. Geol.**, 219: (1-4): 175-192.


I.C.D.D. (2008) **How to analyse minerals: Fundamentals** [online]. Available from: http://www.icdd.com/resources/tutorials/pdf/HowtoAnalyzeMinerals-Fundamentals.pdf  I.C.D.D. [10102014]


Ixer, R.A. and Budd, P. (1998) The Mineralogy of Bronze Age Copper Ores from the British Isles: Implications for the Composition of Early Metal Work. **Oxford Journal of Archaeology**, 17 (1): 15 – 41


James, R.O. and MacNaughton, M.G. (1977) The Adsorption of Aqueous heavy metals on Inorganic Minerals. **Geochimica et Cosmochimica Acta**, 41: 1549-1555.

Jeffries, M. and Mills, D. (1990) **Freshwater Ecology: Principles and Applications.** London: Wiley-Blackwell.

Johnston, D. and Rolley, S. (2008)  **Abandoned Mines and the Water Framework Directive in the United Kingdom**. Environment Agency

Karthikeyan, K.G., Elliott, H.A. and Cannon, F.S. (1997) Adsorption and Coprecipitation of Copper with the Hydrous Oxides of Iron and Aluminum. **Environmental Science & Technology***,* 31 (10): 2721-2725

Khodaverdiloo, H., Rahmanian, M. and Rezapour, S. et al. (2012) Effect of Wetting-Drying Cycles on Redistribution of Lead in Some Semi-Arid Zone Soils Spiked with a Lead Salt. **Pedosphere***,* 22 (3): 304-313

Komárek, M. and Zeman, J. (2004) Dynamics of Cu, Zn, Cd, and Hg release from sediments at surface conditions. **Bulletin of Geosciences***,* 79: (2)

Krause, S., Hannah, D.M. and Fleckenstein, J.H. et al. (2010) Inter-disciplinary perspectives on processes in the hyporheic zone. **Ecohydrology***,* 4 (4): 481-499

Ku Leuven (2010) **X-ray diffraction – Bruker D8 Discover** [online]. Available from: https://fys.kuleuven.be/iks/nvsf/experimental-facilities/x-ray-diffraction-2013-bruker-d8-discover  Ku Leuven [Accessed 101014]

Ku, T.C.W., Kay, J. and Browne, E. et al. (2008) Pyritization of iron in tropical coastal sediments: Implications for the development of iron, sulfur, and carbon diagenetic properties, Saint Lucia, Lesser Antilles. **Marine Geology***,* 249: 184-205

Kuechler, R., Klause, N. and Zorn, T. (2004) Investigation of gypsum dissolution under saturated and unsaturated water conditions. **Ecological Modelling***,* 176: 1-14

Laine, D.M. (1999) The treatment of pumped minewater at Woolley colliery, West Yorkshire. **Journal of the Chartered Institution of Water and Environmental Management***,* 13 (2): 127-130

Larsen, D. and Mann, R. (2005) Origin of high manganese concentrations in coal mine drainage, eastern Tennessee. **Journal of Geochemical Exploration***,* 86 (3): 143-163

Lee, G., Bigham, J.M. and Faure, G. (2002) Removal of trace metals by coprecipitation with Fe, Al and Mn from natural waters contaminated with acid mine drainage in the Ducktown Mining District, Tennessee. **Applied Geochemistry***,* 17 (5): 569-581

Leermakers, M., Gao, Y. and Gabelle, C. et al. (2005) Determination of high resolution pore water profiles of trace metals in sediments of the Rupel River (Belgium) using DET (Diffusive Equilibirum in Thin films) and DGT (Diffusive Gradients in Thin films) techniques. **Water, Air, and Soil Pollution***,* 166: 265-286

Leinz, R.W., Sutley, S.J. and Desborough, G.A. et al. (2000) "An Investigation of the Partitioning of Metals in Mine Wastes Using Sequential Extractions". **ICARD 2000: Proceedings from the Fifth International Conference on Acid Rock Drainage** Denver, Colorado, U.S. Geological Survey.

Lesven, L., Lourino-Cabana, B. and Billon, G. et al. (2010) On metal diagenesis in contaminated sediments of the Deule river (northern France). **Applied Geochemistry***,* 25 (9): 1361-1373

Lewin, J. and Macklin, M.G. (1987) Metal Mining and Floodplain Sedimentation in Britian. **International Geomorphology***,* 1009-1027

Li, X.D., Shen, Z.G. and Wai, O.W.H. et al. (2001) Chemical forms of Pb, Zn and Cu in the sediment profiles of the Pearl River Estuary. **Marine Pollution Bulletin***,* 42 (3): 215-223

Licheng, Z. and Guijiu, Z. (1996) The species and geochemical characteristics of heavy metals in the sediments of Kangjiaxi River in the Shuikoushan Mine Area, China. **Applied Geochemistry***,* 11: 217-222.

Linge, K.L. (2008) Methods for Investigating Trace Element Binding in Sediments. **Critical Reviews in Environmental Science & Technology***,* 38: 165-196

Lovley, D.R. (1991) Dissimilatory Fe(III) and Mn(IV) Reduction. **Microbiological Reviews***,* 55 (2): 259-287

Lovley, D.R. and Klug, M.J. (1986) Model for the distribution of sulfate reduction and methanogenesis in freshwater sediments. **Geochimica Cosmochimica Acta**, 50 (1): 11-18

Lovley, D.R. and Phillips, E.J.P. (1986) Availability of Ferric Iron for Microbial Reduction in Bottom Sediments of the Freshwater Tidal Potomac River. **Applied and Environmental Microbiology**, 52: 751-757

Lovley, D.R. and Phillips, E.J.P. (1987) Competitive Mechanisms for Inhibition of Sulfate Reduction and Methane Production in the Zone of Ferric Iron Reduction in Sediments. **Applied Environmental Microbiology**, 53: 2636-2641

Lovley, D.R. and Phillips, E.J.P. (1989) Manganese inhibition of microbial iron reduction in anaerobic sediments. **Geomicrobiology Journal**, 6 (3-4): 145-155

Lu, X. and Wang, H. (2012) Microbial oxidation of Sulfide Tailings and the Environmental consequences. **Elements**, 8: 119-124

Luo, L., Chu, B., Liu, Y., et al. (2014) Distribution, origin, and transformation of metal andmetallod pollution in vegetable fields, irrigation water, and aerosols near a Pb-Zn mine. **Environmental Science & Pollution Research**, 21: 8242-8260

Lynch, S.F.L., Batty, L.C. and Byrne, P. (2014) Environmental risk of metal mining contaminated river bank sediment at redox-transitional zones. **Minerals**, 4: 52-73

Macklin, M.G., Brewer, P.A., Hudson-Edwards, K.A., et al. (2006) A geomorphological approach to the management of rivers contaminated by metal mining. **Geomorphology**, 79 (3-4): 423-447

Macklin, M.G. and Dowsett, R.B. (1989) The Chemical and Physical Speciation of Trace-Metals in fine-grained overbank flood sediments in the Tyne basin, Northeast England. **CATENA**, 16 (2): 135-151

Macklin, M.G. and Lewin, J. (1989) Sediment Transfer and Transformation of an alluvial valley floor: the River South Tyne, Northumbria, U.K.. **Earth Surface Processes and Landforms**, 14: 233-246

Macklin, M.G. and Lewin, J. (2008) Alluvial responses to the changing Earth system. **Earth Surface Processes and Landforms**, 33 (9): 1374-1395

Matsuda, I. (2004) **River Morphology and Channel Processes** [online]. Available from: http://www.eolss.net/ebooks/Sample%20Chapters/C07/E2-07-02-01.pdf [Accessed 12012012]

Mayanna, S., Peacock, C.L., Schaffner, F., et al. (2015) Biogenic precipitation of manganese oxides and enrichment of heavy metals at acidic soil pH. **Chemical Geology***, 402: 6-17

Mayes, W.M., Potter, H.A.B. and Jarvis, A.P. (2013) Riverine Flux of Metals from Historically Mined Orefields in England and Wales. **Water, Air, Soil Pollut.***, 224: 1425.

Merck (2013) **Analytical Quality Assurance Standard for Sulfide** [online]. Available from: http://www.merckmillipore.com/INTERSHOP/web/WFS/Merck-GB-Site/en_US/-/GBP/ViewParametricSearch-Browse?SynchronizerToken=4a9f8d318a9c639404fa7f882e3ecdc82a9c367e1ba2c7873bdf1eb0c8b9d152&TrackingSearchType=filter&SearchTerm=analytical+quality+assurance+standard+for+sulfide&SelectedSearchResult=SFDocumentSearch&SearchContextPageletUUID=&SearchParameter=%26%40QueryTerm%3Danalytical%2Bquality%2Bassurance%2Bstandard%2Bfor%2Bsulfide%26channels%3DGB_or_GLOBAL%26display_in_internet%3DY%26MERCK_FF.defaultSimilarity%3D9000&PageNumber=0&SortingAttribute=&PageSize=20 Merck Millipore [Accessed 2013]

Merinero, R., Lunar, R. and Somoza, L. et al. (2009) Nucleation, growth and oxidation of framboidal pyrite associated with hydrocarbon-derived submarine chimneys: lessons learned from the Gulf of Cadiz. **European Journal of Mineralogy***, 21 (5): 947-961

Merrington, G. and Alloway, B.J. (1994) The transfer and fate of Cd, Cu, Pb, and Zn from two historic metalliferous mine sites in the U.K. **Applied Geochemistry***, 9: 677-687

Meybeck, M. (1982) Carbon, Nitrogen and Phosphorus Transport by World Rivers. **American Journal of Science***, 282: 401-450.

Mindat.org (2014) **Cwmystwyth Mine, Cwmystwyth, Upper Llanfihangell-y-Creuddyn, Ceredigion (Dyfed; Cardiganshire), Wales, UK** [online]. Available from: http://www.mindat.org/loc-4257.html [Accessed 100814]

Montserrat, A.M. (2010) **Environmental impact of mine drainage and its treatment on aquatic communities.** PhD, University of Birmingham.

Morrison, M.I. and Aplin, A.C. (2009) Redox geochemistry in organic-rich sediments of a constructed wetland treating colliery spoil leachate. **Applied Geochemistry***,* 24 (1): 44-51

Morse, J.W., Gledhill, D.K. and Sell, K.S. et al. (2002) Pyritization of Iron in Sediments from the Continental Slope of the Northern Gulf of Mexico.

**Aquatic Geochemistry***,* 8: 3-13

Mortimer, R.J.G., Krom, M.D. and Hall, P.O.J. et al. (1998) Use of gel probes for the determination of high resolution solute distributions in marine and estuarine pore waters. **Marine Chemistry***,* 63: 119-129

Najafpour, M.M., Hotynska, M., Shamkhili, A.N., et al. (2014) The role of nano-sized manganese oxides in the oxygen-evolution reactions by manganese complexes: towards a complete picture. **Dalton Transactions***,* 43: 13122 – 13135

Nakayama, S.M.M., Ikenaka, Y. and Hamada, K. et al. (2011) Metal and metalloid contamination in roadside soil and wild rats around a Pb-Zn mine in Kabwe, Zambia. **Environmental Pollution***,* 159: 175-181

Natural Resources Wales (2004) **A Metal Mines Strategy for Wales** [online]. Available from: http://imwa.de/docs/imwa_2004/IMWA2004_03_Johnston.pdf Natural Resources Wales [Accessed 02/12/2011]

Natural Resources Wales (2000) **Mwyngloddfa Cwmystwyth Site of Special Scientific Interest** [online]. Available from: http://www.ccgc.gov.uk/landscape--wildlife/protecting-our-landscape/special-landscapes--sites/protected-landscapes-and-sites/sssis/sssi-sites/mwyngloddfa-cwmystwyth.aspx [Accessed 09/02/15]

Neal, C., Reynolds, B., Neal, M., et al. (2001) Long-term changes in the water quality of rainfall, cloud water and stream water for moorland, forested and clear-felled catchments at Plynlimon, mid-Wales. **Hydrology and Earth System Sciences***,* 5 (3): 459-476

NERC (2015) **National River Flow Archive** [online]. Available from: http://www.ceh.ac.uk/data/nrfa/data/station.html?63004 [Accessed 25/02/15]

Nordstrom, D.K. (2011) Hydrogeochemical processes governing the origin, transport and fate of major and trace elements from mine wastes and mineralized rock to surface waters. **Applied Geochemistry**, 26: 1777-1791

Nordstrom, D.K. (2009) Acid rock drainage and climate change. **Journal of Geochemical Exploration**, 100 (2-3): 97-104

Nordstrom, D.K. and Alpers, C.N. (1999) "Geochemistry of Acid Mine Waters". In Plumlee, G.S.a.L., M.J. (Ed.) **The Environmental Geochemistry of Mineral Deposits. Part A: Processes, Techniques, and Health Issues**. Colorado, USA, Society of Economic Geologists, Inc. 133-160

Oxford Instruments (2008) **INCAEnergy Applications training notes**. Bucks: Oxford Instruments.

Palmer, M. (1992) **Standard Operating Procedure for GLNPO Total Alkalinity Titration** [online]. http://www.epa.gov/greatlakes/lmmb/methods/alkali.pdf United States Environmental Protection Agency [Accessed 10102013]

Palumbo-Roe, B., Klinck, B. and Banks, V. et al. (2009) Prediction of the long-term performance of abandoned lead zinc mine tailings in a Welsh catchment. **Journal of Geochemical Exploration**, 100 (2-3): 169–181

Palumbo-Roe, B., Wragg, J. and Banks, V.J. (2012) Lead mobilisation in the hyporheic zone and river bank sediments of a contaminated stream: contribution to diffuse pollution. **Journal of Soils & Sediments**, 12: 1633-1640

Palumbo-Roe, B., Wragg, J. and Cave, M. et al. (2013) Effect of weathering product assemblages on Pb bioaccessibility in mine waste: implications for risk management. **Environmental Science & Pollution Research**, 20 (11): 7699 – 7710

Parbhakar-Fox, A., Lottermoser, B.G. and Bradshaw, D. (2013) Evaluating waste rock mineralogy and microtexture during kinetic testing for improved acid rock drainage prediction. **Minerals Engineering**, 52: 111-124

Parkman, R.H., Curtis, C.D. and Vaughan, D.J. et al. (1996) Metal fixation and mobilisation in the sediments of the Afon Goch estuary - Dulas bay, Anglesey. **Applied Geochemistry**, 11 (1-2): 203-210

Patrick, W.H. and Delaune, R.D. (1972) Characterization of oxidized and reduced zones in flooded soil. **Soil Science Society of America Journal**, 36 (4): 573

Patrick, W.H. and Henderson, R.E. (1981) Reduction and Reoxidation cycles of manganese and iron in flooded soil and in water solution. **Soil Science Society of America Journal**, 45 (5): 855-859

Ponnamperuma, F.N., Estrella, M.T. and Teresita, L. (1967) Redox Equilibria in Flooded soils: I. the Iron Hydroxide Systems. **Soil Science**, 103: (6)

Poulton, S.W. and Canfield, D.E. (2005) Development of a sequential extraction procedure for iron: implications for iron partitioning in continentally derived particulates. **Chemical Geology**, 214 (3–4): 209-221

Pradit, S., Gao, Y. and Faiboon, A. et al. (2013) Application of DET (diffusive equilibrium in thin films) and DGT (diffusive gradients in thin filesm) techniques in the study of the mobility of sediment-bound metals in the outer section of Songkhla Lake, Southern Thailand. **Environmental Monitoring  and Assessment**, 185: 4207-4220

Ross, S. (1989) **Soil Processes**. New York: Routledge.

Salomons, W., de Rooij, N.M. and Kerdijk, H. et al. (1987) Sediments as a Source for Contaminants? **Hydrobiologia**, 149: 13-30

Shimadzu Scientific Instruments (2014) **List of Shimadzu Application Notes** [online]. Available from: https://www.ssi.shimadzu.com/literature/litSearchResults.cfm  [Accessed 01052014]

Shope, C.L., Xie, Y. and Gammons, C.H. (2006) The influence of hydrous Mn-Zn oxides on diel cycling of Zn in an alkaline stream draining abandoned mine lands. **Applied Geochemistry**, 21: 476-491

Shuman, L.M. (1977) Adsorption of Zn by Fe and Al hydrous Oxides as Influenced by aging and pH. **Soil Science Society of America Journal**, 41 (4): 703-706

Smith, K. (1999) "Metal Sorption on Mineral Surfaces: An Overview with Examples Relating to Mineral Deposits". In Plumlee, G.S.A.L., M.J. (Ed.) **The Environmental Geochemistry of Mineral Deposits Part A: Processes, Techniques and Health Issues**. Colorado, USA, Society of Economic Geologists.

Spectroquant (2010) "Sulphide Test". Merck.

Stanton, M.R., Taylor, C.D. and Gemery-Hill, P.A. et al. (2006) "Laboratory studies of sphalerite decomposition: applications to the weathering of mine wastes and potential effects on water quality". **7th International conference on Acid Rock Drainage (ICARD)**. St. Louis MO., USA, American Society of Mining and Reclamation (ASMR).

Stone, M. and Droppo, I.G. (1996) Distribution of lead, copper and zinc in size-fractionated river bed sediment in two agricultural catchments of southern Ontario, Canada. **Environmental Pollution**, 93 (3): 353

Stumm, W. and Sulzberger, B. (1992) The Cycling of Iron in Natural Environments: considerations based on labroatory studies of heterogeneous redox processes. **Geochimica Et Cosmochimica Acta**, 56: 3233-3257

Tack, F.M. and Verloo, M.G. (1995) Chemical speciation and fractionation in soil and sediment heavy metal analysis: A review. **International Journal of Environmental Analytical Chemistry**, 59: 225-238

Tankere-Muller, S., Zhang, H. and Davison, W., et al. (2007) Fine scale remobilisation of Fe, Mn, Co, Ni, Cu and Cd in contaminated marine sediment. **Marine Chemistry**, 106: 192-207

Taylor, M.P. and Hudson-Edwards, K.A. (2008) The dispersal and storage of sediment-associated metals in an arid river system: the Leichhardt River, Mount Isa, Queensland, Australia. **Environmental Pollution**, 152 (1): 193-204

Tessier, A., Campbell, P.G.C. and Bisson, M. (1979) Sequential Extraction Procedure for the speciation of particulate trace metals. **Analytical Chemistry**, 51: 844-851

Thamdrup, B., Fossing, H. and Jorgensen, B.B. (1994) Manganese, Iron and Sulphur Cycling in a coastal marine sediment, Aarhus Bay, Denmark. **Geochimica Et Cosmochimica Acta**, 58 (23): 5115-5129


Torres, E., Ayora, C. and Canovas, C.R. et al. (2013) Metal cycling during sediment early diagenesis in a water reservoir affected by acid mine drainage. **Science of the Total Environment**, 461-462: 416-429


Tripole, S., Gonzalez, P. and Vallania, A. et al. (2006) Evaluation of the impact of acid mine drainage on the chemistry and the macrobenthos in the Carolina Stream (San Luis-Argentina). **Environmental Monitoring & Assessment**, 114 (1-3): 377-389


Twardowska, I., Allen, H.E. and Stefaniak, S. (2006) **Soil and Water Pollution Monitoring, Protection and Remediation** [online]. Available from: http://books.google.co.uk/books?id=0v6Tu4kI7s8C&pg=PA53&lpg=PA53&dq=Twardowska+et+al+2006&source=bl&ots=HHjDWDbOaI&sig=lXg6gCMyBhtePD3kIx-C8aYrPpo&hl=en&sa=X&ei=SeCXT9atI6Oi0QXPhuWRBg&ved=0CCAQ6AEwAA#v=onepage&q=Twardowska%20et%20al%202006&f=false  Springer [Accessed 24042012]


Ullah, S., Zhang, H. and Heathwaite, A.L. et al. (2012) In situ measurement of redox sensitive solutes at high spatial resolution in a riverbed using Diffusive Equilibrium in Thin Films (DET). **Ecological Engineering**, 49: 18-26


Ullah, S., Zhang, H. and Heathwaite, A.L. et al. (2013) Influence of emergent vegetation on nitrate cycling in sediments of a groundwater-fed river. **Biogeochemistry**, 1-14


USGS (2001) **Lead-Rich Sediments, Coeur d'Alene River Valley, Idaho: Area, Volume, Tonnage and Lead Content** [online]. Available from: http://pubs.usgs.gov/of/2001/of01-140/of01-140.pdf  [Accessed 121014]

USGS (2008) **Water Chemistry 2: Sampling and Presenting Water Analysis** [online]. Available from: http://inside.mines.edu/~epoeter/_GW/18WaterChem2/WaterChem2pdf.pdf [Accessed 2014]

USGS (2013) **Natural processes of ground-water and surface-water interaction** [online]. Available from: http://pubs.usgs.gov/circ/circ1139/htdocs/natural_processes_of_ground.htm [Accessed 15/01/15]


van der Geest, H.G. and Paumen, M.L. (2008) Dynamics of metal availability and toxicity in historically polluted floodplain sediments. **Science of the Total Environment***, 406 (3): 419-425


vanLoon, G.W. and Duffy, S.J. (2011) **Environmental Chemistry**. 3$^{rd}$ ed. Oxford, UK: Oxford University Press.


Walling, D.E., Owens, P.N. and Carter, J. et al. (2003) Storage of sediment-associated nutrients and contaminants in river channel and floodplain systems. **Applied Geochemistry***, 18 (2): 195-220


Wang, L., Yu, R. and Hu, G. et al. (2010) Speciation and assessment of heavy metals in surface sediments of JinJiang River Tidal Reach, Southeast of China. **Environmental Monitoring Assessment***, 165: 491-499


Weber, F., Voegelin, A. and Kretzschmar, R. (2009) Multi-metal contaminant dynamics in temporarily flooded soil under sulphate limitation. **Geochimica Et Cosmochimica Acta***, 73: 5513-5527


Webster, J.G., Swedlund, P.J. and Webster, K.S. (1998) Trace metal adsorption onto an acid mine drainage iron(III) oxyhydroxy sulfate. **Environmental Science & Technology***, 32: 1361-1368


Wen, X.H. and Allen, H.E. (1999) Mobilization of heavy metals from Le An River sediment. **Science of the Total Environment***, 227 (2-3): 101-108

Whitehead, P.G., Cosby, B.J. and Prior, H. (2005) The Wheal Jane wetlands model for bioremediation of acid mine drainage. **Science of the Total Environment***, 338 (1-2): 125-135


Wilson, B. and Pyatt, F.B. (2007) Heavy metal dispersion, persistance, and bioccumulation around an ancient copper mine situated in Anglesey, UK. **Ecotoxicology and environmental safety***, 66: 224-231

Wolfenden, P.J. and Lewin, J. (1977) Distribution of Metal Pollutants in Floodplain Sediments. **CATENA**, 4: 309-317

Wragg, J. and Palumbo-Roe, B. (2011) "Contaminant mobility as a result of sediment inundation: Literature review and laboratory scale pilot study on mining contaminated sediments". British Geological Survey Open Report.

Yeh, T.Y. (2008) Removal of Metals in Constructed Wetlands: Review. **Practice Periodical of Hazardous, Toxic, and Radioactive Waste Management**, 12 (2): 96

Young, E.A., Dawson, E.J., Macklin, M.G., et al. (2007) **Mobilisation and Deposition of Metal Contaminated Sediments in the River Swale, North Yorkshire, UK** [online].  Available from: http://meetings.copernicus.org/www.cosis.net/abstracts/EGU2007/03971/EGU2007-J-03971-1.pdf  European Geosciences Union [Accessed 120114]

Younger, P.L. (1995) Hydrogeochemistry of minewaters flowing from abandoned coal workings in County Durham. **Quarterly Journal of Engineering Geology**, 28: S101-S113

Younger, P.L. (1998) "Coalfield Abandonment: Geochemical processes and hydrochemical products". In Nicholson, K. (Ed.) **Energy and the Environment: Geochemistry of fossil, nuclear and renewable resources.** MacGregor Science, 1-29

Younger, P.L. (2000) Predicting temporal changes in total iron concentrations in groundwaters flowing from abandoned deep mines: a first approximation. **Journal of Contaminant Hydrology**, 44: 4 –69

Younger, P.L., Banwart, S.A. and Hedin, R.S. (2002) **Mine Water: Hydrology, Pollution, Remediation**. London: Kluwer Academic Publishers.

Zakir, H.M., Shikazono, N. and Otomo, K. (2008) Geochemical Distribution of Trace Metals and Assessment of Anthropogenic Pollution in Sediment of Old Nakagawa River, Tokyo, Japan. **American Journal of Environmental Sciences**, 4 (6): 654-665

Zhang, H. and Davison, W. (1999) Diffusional characteristics of hydrogels used in DGT and DET techniques. **Analytica Chimica Acta**, 398: 329-340

Zhao, Y. and Marriott, S.B. (2013) Dispersion and remobilisation of heavy metals in the River Severn system, UK. **Procedia Environmental Sciences**, 18: 167-173